

On-load Tap Changer Diagnosis on High-Voltage Power Transformers using Dynamic Resistance Measurements

On-load Tap Changer Diagnosis on High-Voltage Power Transformers using Dynamic Resistance Measurements

Proefschrift

ter verkrijging van de graad van doctor
aan de Technische Universiteit Delft,
op gezag van de Rector Magnificus prof. ir. K.C.A.M. Luyben,
voorzitter van het College voor Promoties,
in het openbaar te verdedigen op maandag 28 maart 2011 om 12:30 uur
door Juriaan Jonathan ERBRINK
elektrotechnisch ingenieur
geboren te Arnhem

Dit proefschrift is goedgekeurd door de promotor:

Prof. dr. J.J. Smit

Samenstelling promotiecommissie:

Rector Magnificus,
Prof. dr. J.J. Smit,
Prof. ir. L. van der Sluis,
Prof. dr. hab. ir. E. Gulski,
Prof. dr. hab. inz. R.A. Malewski,
Prof. dr. ing. S. Tenbohlen,
Prof. dr.-ing. E. Gockenbach,
Dr. ir. B. Quak,
Prof. dr. ir. J. Biemond,

Voorzitter
Technische Universiteit Delft, promotor
Technische Universiteit Delft
Poznan University of Technology
Instytut Elektrotechniki w Warszawie
Universität Stuttgart
University of Hannover
Seitz Instruments AG
Technische Universiteit Delft, reservelid

The investigations for this thesis were financially and technically supported by Seitz Instruments AG in Switzerland and by Alliander in the Netherlands.

ISBN: 978-94-6169-042-5

Summary

On-load Tap Changer Diagnosis on High-Voltage Power Transformers using Dynamic Resistance Measurements

It is a modern tendency to perform condition-based rather than time-based maintenance. In this way, utilities attempt to reduce maintenance costs, extend the service-life of equipment and prevent possible catastrophic failures. Condition-based tap changer maintenance requires diagnostic measurements to identify the condition of the on-load tap changer (OLTC) in order to determine when and what maintenance is necessary. In addition, diagnostic measurements can be used for the pre-failure detection of defects not seen during maintenance and to assess the condition of parts that are not easily accessible for visual inspection. Although many service-aged OLTCs are in service and although literature shows that it is responsible for a major part of transformer failures, it is not common to assess the condition before returning the power transformer to operation after maintenance. Maintenance errors, contact degradation and mechanical defects can thus remain undetected.

This thesis elaborates on the condition diagnosis of the electrical contacts of in-tank high-speed resistor tap changers using dynamic resistance measurement (DRM). While originally used to diagnose circuit breakers, it is also suitable for measuring the resistance while the tap changer is in operation. This study describes how to perform DRM on tap changers and how to interpret the results.

Following the introduction, an overview of tap changer technology, degradation and failure is given in Chapter 2. Several contact resistance models from literature are discussed and the applicability to DRM is clarified. Subsequently, Chapter 3 discusses the possible methods available to diagnose the OLTC's technical condition. The connection between dissolved gas analysis (DGA) and contact resistance is studied in more depth to determine whether there is a correlation in the methods. A statistical analysis of DGA and DRM results of a population of transformers was undertaken but no relationship was found for the dataset selected.

Chapter 4 shows that contact diagnosis can be applied to different types of tap changers in service and that DRM can detect a large variety of defects and degradation mechanisms using a low measurement current. Its results provide more information about the tap changer condition than static resistance measurement and important information about the significance and location of several aging mechanisms can be extracted from the results. The dynamic

measurements are discussed in detail, including the effect of the measurement current and circuit resistance.

Because each diagnostic method is sensitive to certain defects, a set of methods is selected and implemented (Chapter 5), creating a diagnostic system. The building blocks of the diagnostic system are discussed and hardware demands were determined for each block. The chapter discusses which results should be clearly presented after a measurement, so that a power transformer can be re-energised without the risk of failure.

The aging mechanisms revealed through DRM are addressed in Chapter 6. The different degradation mechanisms examined are: film formation on the contact surface, coking at high-temperature spots caused by the load current flow, and pitting and contact erosion due to arcing. DRM results from approximately 450 OLTCs were examined during this project and measurement data from a number of these tap changers was compared with findings based on visual inspections. A substantial number within this population were shown to have degraded contacts. Chapter 6 proves that dynamic resistance measurement is an effective tool for assessing the technical condition of tap changers, proving to be highly sensitive to dominant defects, in particular contacts affected by the long-term aging effect on the change-over selector or the tap selector, as well as defects that compromise the main function of the OLTC (switching between taps without interrupting the load current). Typical DRM plots which reveal these various defects are presented with an explanation of how these defects can be recognised in different types of tap changers, in particular in relation to transformer subcomponents that are not accessible for visual inspection during regular maintenance because they are enclosed in the transformer tank.

Laboratory experiments (Chapter 7) and several test cases were then used to verify the aging mechanisms to which DRM is sensitive. In addition to a DC current of 1 A, other measurement current levels were used during the experiments (Appendix C). The effect of artificially degraded contacts on measurement results was studied using a test model. The study shows that the surface film on contacts is measurable. Contact resistance was shown to increase significantly when contacts move over a surface film, which can conceal more significant contact degradation. Arcing contact wear influences the contact timing, thereby changing the shape and amplitude of the resistance graphs. Interruptions of the current can appear in the graphs when excessively worn contacts are tested.

This thesis also demonstrates how DRM results can be represented as condition indices using an interpretation flowchart that categorises them using boundary values (Chapter 8). Complex diagnostic information is converted into simple condition indices. This process is dependent on the type of tap changer being measured. Irregularities can be attributed to the arcing switch, the tap selector or the change-over selector, and to the drive system. On the basis of the DRM results, quantities which can be used to reveal the most common defects were determined. Basically six situations are distinguished: Contacts in good condition, contacts with an increased contact resistance, tap changers with open contacts, transition time deviations, worn contacts or phase synchronisation problems. An example of a flowchart to be used for decision support was developed and its practical applicability to a large population of OLTCs was

verified. The deviation of the measurement current with respect to the expected value was used and limits were determined for decision-making. The technical condition can thereby be determined, allowing the selection of a set of critical tap changers that will benefit from failure-reduction efforts.

Table of contents

SUMMARY.....	VII
TABLE OF CONTENTS.....	XI
1 INTRODUCTION	1
1.1 On-load tap changers in power transformers	1
1.2 Failure aspects of on-load tap changers	3
1.3 Tap changer diagnostics.....	5
1.4 Objectives of this thesis	5
1.5 Approach.....	6
1.6 Outline of this thesis	7
2 OLTC TECHNOLOGY AND DEGRADATION	9
2.1 OLTC technology overview.....	9
2.1.1 Selector switch type tap changer	10
2.1.2 Diverter switch type tap changer.....	11
2.2 OLTC degradation mechanisms.....	12
2.3 Contact degradation	12
2.3.1 Clean contacts	13
2.3.2 Contacts with a surface film.....	17
2.3.3 Contacts with high local temperatures	23
2.3.4 Contact failure due to overheating.....	24
2.3.5 Corrected model of tap changer resistance	27
2.4 Conclusions.....	30
3 ON-LOAD TAP CHANGER DIAGNOSIS	31
3.1 Oil and insulation diagnosis	32
3.1.1 Dissolved gas analysis	32
3.1.2 Study of the agreement between DGA and DRM results	34
3.2 Mechanical diagnosis	37
3.2.1 Acoustic and vibration signature.....	37
3.2.2 Motor power measurement.....	38
3.2.3 Position measurement.....	39
3.3 Contact status diagnosis.....	39
3.3.1 Temperature difference measurement.....	40
3.3.2 Static resistance measurement	41
3.3.3 Dynamic resistance measurement (DRM)	43

3.4 Discussion	43
3.5 Conclusions.....	48
4 DYNAMIC RESISTANCE OF ON-LOAD TAP CHANGERS.....	49
4.1 Measurement setup.....	50
4.1.1 Indirect measurement of the OLTC.....	50
4.1.2 Direct measurement of the OLTC	51
4.2 Measurement current	55
4.2.1 Winding configuration	55
4.2.2 Amplitude of the measurement current.....	56
4.2.3 Sensitivity	61
4.3 Circuit resistance	62
4.4 Secondary short circuit.....	66
4.5 Determination of the contact resistance	69
4.6 Conclusions.....	69
5 POWER TRANSFORMER DIAGNOSTIC SYSTEM.....	71
5.1 International standards for power transformer testing.....	73
5.2 Transformer diagnostic system.....	75
5.3 Measurement procedure	77
5.3.1 Dynamic resistance of the OLTC	77
5.4 OLTC drive system condition	81
5.5 Hardware and data processing.....	83
5.6 Conclusions.....	84
6 EVALUATION OF TYPICAL DRM DIAGNOSTIC DATA	85
6.1 Regular DRM plots.....	86
6.2 Irregular DRM plots.....	93
6.3 Irregularities in the change-over selector	95
6.3.1 Long-term aging in selector switch type OLTCs	95
6.3.2 Current interruptions due to the change-over selector	104
6.4 Irregularities in the arcing switch	106
6.4.1 Long-term aging in the arcing switch.....	107
6.4.2 Contact wear of the arcing switch.....	109
6.4.3 Timing difference between phases.....	110
6.4.4 Maintenance errors	110
6.4.5 Current interruptions due to the arcing switch.....	112
6.4.6 OLTC transition times.....	113
6.5 Defects in both parts of the OLTC.....	115
6.6 Conclusions.....	116
7 LABORATORY VERIFICATION OF SELECTED FAILURE MECHANISMS	119
7.1 Measurability of the surface film using DRM	119
7.1.1 Correlation between DRM and contact degradation.....	119
7.1.2 Effect of the surface film on DRM	123
7.1.3 Accelerated degradation tests.....	124
7.2 Arcing contact wear.....	128

7.2.1 Arcing contact dimensions.....	128
7.2.2 Arcing contact timing.....	131
7.3 Conclusions.....	134
8 DRM KNOWLEDGE RULES FOR DECISION SUPPORT	137
8.1 Condition assessment.....	137
8.2 DRM knowledge rules.....	138
8.3 Quantities reflecting the OLTC condition.....	141
8.4 Condition indexing	143
8.5 Application example	146
8.5.1 Open contacts	147
8.5.2 Contact resistance	148
8.5.3 Flowchart verification	152
8.6 Conclusions.....	155
9 CONCLUSIONS & RECOMMENDATIONS.....	157
9.1 Conclusions.....	157
9.2 Suggestions for future work	160
REFERENCES.....	163
APPENDIX A - OLTC TECHNOLOGY, DEGRADATION AND PROTECTION....	173
APPENDIX B - INDIRECT MEASUREMENT OF THE OLTC DYNAMIC RESISTANCE	189
APPENDIX C - EXAMPLES OF STATIC RESISTANCE MEASUREMENTS WITH INCREASING CURRENT ON SERVICE-AGED OLTC CONTACTS.....	195
APPENDIX D - DESIGN CONSIDERATIONS OF A TRANSFORMER DIAGNOSTIC SYSTEM.....	203
LISTS	217
ACKNOWLEDGEMENTS	225
SAMENVATTING	227
CURRICULUM VITAE.....	231

1

Introduction

1.1 On-load tap changers in power transformers

Large amounts of electrical power are transported and distributed by the electricity grid. In addition, long distances have to be bridged between the generation and consumption of electrical power and high voltages are used to reduce the power losses during this transport. Different voltage levels are used in the grid and these voltages are linked using power transformers.

A power transformer basically has two functions:

- To link different voltage levels in the high-voltage power grid in such a way that electrical power can be exchanged.
- To keep the voltage at an acceptable level when the load changes.

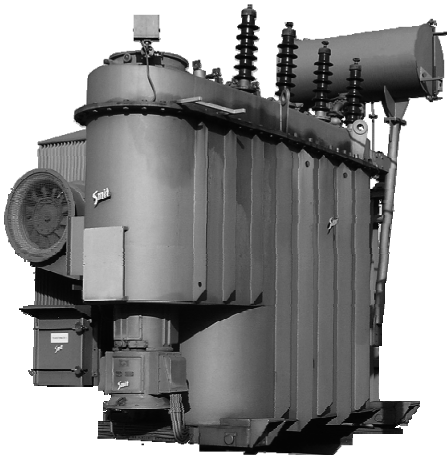


Figure 1.1 Example of a 50/10 kV (14 MVA) power transformer with on-load tap changer.

The second function, voltage regulation, is accomplished by adjusting the transformation ratio of the power transformer. For that purpose, the transformer winding is equipped with tapped windings that can be selected by an on-load tap changer. The active and reactive power flow can be controlled by the tap changer. On-load tap changers are also used for phase regulation in phase shifter transformers. In general, it can be said that on-load tap changers are used to select tapped windings along the main transformer windings. The function of an on-load tap changer can therefore be described as:

To select another transformer tapped winding without interrupting the load current

An on-load tap changer is driven by a complex drive mechanism for which timing is an important issue. The OLTC can easily switch 100,000 times during its lifetime, depending on the function and location of the transformer. The operation of the on-load tap changer is usually performed by an autonomous control system, but an on-load tap changer can also be operated from a control room or manually at the transformer. Different types of tap changers are in service worldwide. These types can be grouped according to:

- The physical location of the tap changer: tap changers that are installed inside the transformer ('in-tank type') or tap changers that are bolted onto the transformer ('compartment type').
- The electrical location, resulting in types that are installed on the high-voltage side of the transformer and tap changers that are installed on the low-voltage side.
- The transition impedance that is used: reactor type or high-speed resistor-type tap changers.
- The number of contacts available for load switching: diverter or selector switch type tap changers.
- The winding configuration in which the tap changer is incorporated: wye or delta connected.
- The switching cycle of the transition contacts: flag-cycle or pennant-cycle operation (symmetrical and asymmetrical).
- The capabilities of switching load: on-load tap changers (OLTCs) or de-energised tap changers (DETCs).
- The contact material of the change-over selector, for example copper or silver-plated contacts.

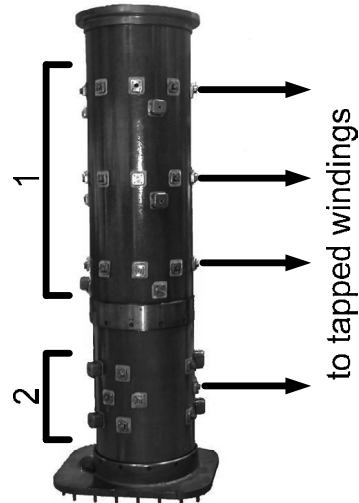


Figure 1.2 Example of an in-tank selector switch type on-load tap changer; 1) selector switch, 2) coarse tap-selector.

Diversity can also be seen in the switching technology of OLTCs. Tap changers having their arcing contacts submerged in insulating oil are already in use for many decades. This type of on-load tap changer dominates the market and, due to the long lifetime of power transformers, degradation of this oldest design is of concern nowadays.

New developments, like vacuum switching or solid state (thyristor) technology, are being developed and implemented with the purpose to prolong the maintenance interval. Solid state tap changers, mostly found in transformers with a low power rating, are expensive, have high no-load losses and have difficulties with handling high short circuit currents. Vacuum tap changers (see Figure 1.3) transfer the load current using vacuum bottle switches and can handle high power ratings, but are also relatively new and therefore not yet widely implemented. The application of vacuum switching technology reduces the need for maintenance and diagnosis.

Besides these newly installed technologies, manufacturers continuously improve the design of oil type OLTCs. For example, experience with tap changer degradation led to design improvements using new contact materials, higher contact pressure or wiping contacts. OLTCs that use oil as arc quenching medium are still the most frequently installed type due to their cheap and improved design. Therefore, this type will still be in service for at least 50 years and it is expected that condition assessment of OLTCs will still be beneficial in the future, although the future population will face different problems.

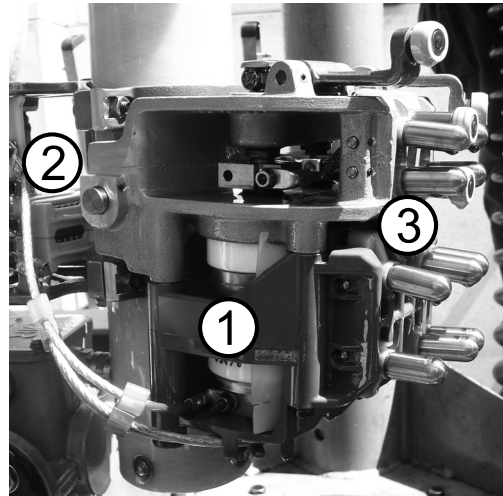


Figure 1.3 Example of an on-load tap changer using vacuum switching technology (one phase of the switch is shown); 1) Vacuum switch bottle, 2) transition resistor, 3) connections to tapped windings.

1.2 Failure aspects of on-load tap changers

Tap changers, like transformers, have a long lifetime and a high level of reliability. However, the average age of the total transformer population is also high [1]. Therefore, degraded transformers remain in service and failures occur regularly [2]. The on-load tap changers are responsible for the major part of the unplanned transformer unavailability, as follows from power transformer failure studies [3-12]. This makes the OLTC the most vulnerable part of a power transformer [13]. Its failure can result in unavailability of the power transformer, damage to the tap changer and surrounding transformer and even the total loss of the power transformer. A catastrophic failure of a power transformer not only involves

replacement costs, but safety, environmental issues and, in case a spare transformer is not directly available, additional costs for not delivered power and penalty costs should also be considered.

In general, it is the quality of the paper winding insulation that mainly determines the transformer's lifetime; repairing relatively small parts like degenerated contacts is still considered worthwhile as long as the transformer had yet not reached the end of its life. For example, if the degree of polymerisation of the cellulose insulation indicates that the paper still has 50% of its life left but the tap changer is in a critical condition, the tap changer can be given an extensive overhaul (costing for example €70,000-€150,000) to prolong the transformer's life. A new transformer (costing for example between €500,000 for a 40 MVA unit and €2,500,000 for a 500 MVA unit) will not be needed for at least another 10-15 years. Diagnostic measurements (costing relatively little and requiring relatively few man-hours, for example 2 maintenance engineers working for 8 hours each for a resistance measurement) can be used to determine when such maintenance work can be cost-effective.

Figure 1.4 shows two examples of such failure studies: 41% of the transformer failures were related to the on-load tap changer according to an international study [4] and 56% according to a Dutch study [6].

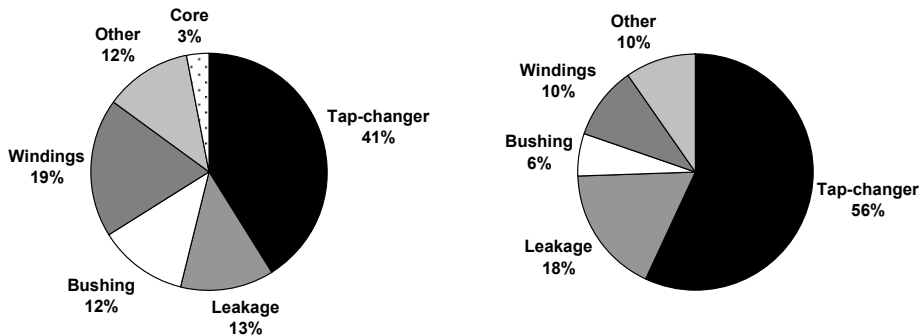


Figure 1.4 Failure distribution of an international population [4] and a population of Dutch 50-150 kV power transformers [6].

Dutch failure studies come with higher OLTC failure percentages compared to other studies and those percentages are lower in the US than in Europe [14]. These differences can be explained by the difference of types that are in service. The Dutch on-load tap changer population contains a considerable number of old tap changers, the design of which makes them more prone to degradation mechanisms than modern designs by tap changer manufacturers which incorporate design improvements. Old tap changers are clearly also more service-aged than the modern types of tap changers. Therefore the current population of OLTCs could benefit from tap changer diagnosis. In addition, service-aged tap changers provide interesting case studies that can be used to show the effect of aging on diagnostic parameters.

1.3 Tap changer diagnostics

Maintenance is normally recommended by the supplier after a fixed time interval or a fixed number of operations. A modern tendency is to perform condition-based rather than time-based maintenance. In this way, utilities try to reduce maintenance costs, extend the service-life of equipment and prevent possible catastrophic failures. Condition-based maintenance requires diagnostic measurements: one needs to know the condition of the tap changer to determine when and what maintenance is necessary.

In addition, diagnostic measurements on OLTCs can be used for the pre-failure detection of defects not seen during maintenance and to assess the condition of parts that are not easily accessible. Although many service-aged OLTCs are in service and the literature shows that it is responsible for the majority of transformer failures, it is not yet common to assess the condition before returning the power transformer to operation after maintenance. Maintenance errors, contact degradation and mechanical defects can remain undiscovered. A number of diagnostic tests can be performed and utilities combine different tests to determine its need for maintenance. A few utilities apply dynamic resistance measurement (DRM) to OLTCs during regular maintenance. Preliminary results showed that it is sensitive to major degradation mechanisms in on-load tap changers.

However, few scientific studies of the dynamic resistance of OLTCs have been performed: most research has focused on the contact degradation process. This thesis investigates the suitability of dynamic resistance measurements as a simple, direct means of detecting defects and degradation mechanisms in OLTCs and hence of checking the main functions of the tap changer. In particular, underlying knowledge about how to perform DRM on tap changers and how to interpret the results obtained in this way requires more scientific research.

Diagnostic measurements, including DRM, result in a large amount of raw measurement data. The structured interpretation of these results can be helpful in drawing conclusions about the tap changer condition. Interpretative support that relates the DRM results to the actual condition of the tap changer is important.

1.4 Objectives of this thesis

This thesis elaborates on the condition diagnosis of high-speed resistor-type tap changers for the pre-failure detection of frequently occurring defects. The aim is to establish the sensitivity of dynamic resistance measurements and to provide interpretation support.

The specific research objectives of this thesis are to:

1. Assess the prioritisation of tap changer degradation mechanisms and defects, thereby including the application of existing contact resistance models to tap changers.

2. Derive a diagnostic methodology which can be used to detect and localise the dominant electrical and mechanical degradation mechanisms of an on-load tap changer without opening the transformer tank.
3. Perform a sensitivity verification of dynamic resistance measurements for pre-failure phenomena in OLTCs.
4. Determine the measurement parameters that are most suitable for detecting these defects, such as the presence of a contact film or pyrolytic carbon, contact wear and pitting.
5. Propose a systematic method of interpreting the dynamic resistance curves of OLTCs, using concise evidence-based rules, which can be used to support strategic decisions about the maintenance or overhaul.

1.5 Approach

Firstly, after introducing OLTC technology, an overview of dominant defects and degradation mechanisms is set up. Several contact resistance models from literature are discussed and their applicability to DRM is explained. Based on the dominant failure modes, existing diagnostic methods will be evaluated. The sensitivity, suitability for the early detection of aging, their limitations and their mutual relationship will be discussed.

Secondly, dynamic resistance measurements will be discussed in more detail, in particular the important topics that should be considered when performing dynamic resistance measurements, such as the effect of the measurement current amplitude, a short circuit on the secondary side of the transformer and the reproducibility of the measurements.

Thirdly, the sensitivity of dynamic resistance measurement to defective and degraded tap changer contacts is verified using field measurements, visual inspection results, laboratory experiments and transformer failure data. The sensitivity of DRM to the dominant degradation mechanisms is verified using artificial defects and accelerated degradation. In total, 20 laboratory experiments are performed, each consisting of 3-16 measurements. These experiments use a test model that was developed for this project.

Several methods are selected to assess the dominant failure modes of an OLTC, and an off-line solution for condition diagnosis is proposed. Up until now, about 700 post-maintenance measurements have been performed with this system, of which 95% have been measured with a prototype of the proposed system. The results of these field measurements are used to demonstrate the defects and degradation mechanisms that can be found using DRM and to discuss their significance, in order to determine a suitable corrective action. In addition, the additional value of performing dynamic resistance measurements after tap changer maintenance is investigated.

Concise rules are formulated based on the knowledge gained from the experience of field and laboratory measurements. These knowledge rules can be arranged in such a way to create a decision-support flowchart. In addition, an example will be worked through.

1.6 Outline of this thesis

Following this introduction:

- **Chapter 2** introduces the reader to the subject by explaining the operation of some common types of on-load tap changers. An overview of tap changer degradation mechanisms is discussed and a model for tap changer contact degradation is derived.
- **Chapter 3** describes the possible options for on-load tap changer diagnosis to assess the condition of the tap changer, including the mechanical drive mechanism and contact degradation.
- **Chapter 4** provides more detail on dynamic resistance measurements (for example the measurement setup, circuit resistance, measurement current amplitude and short circuit on the secondary transformer side).
- **Chapter 5** presents a measurement device for transformer diagnosis based on dynamic resistance measurements, OLTC drive motor power measurements, position measurements on the drive shaft of the on-load tap changer, transformer turn ratio measurements and DC winding resistance measurements.
- **Chapter 6** discusses the possible irregularities of the dynamic resistance measurement data.
- **Chapter 7** deals with the measurability of a surface film that is formed on the tap changer contacts in the early stage of the long-term aging effect. Experiments with worn arcing contacts are also discussed.
- **Chapter 8** presents the main issues related to the assessment of the condition of on-load tap changers and explains the advantages of condition indexing. Decision-support for dynamic resistance measurements is provided, based on the knowledge rules derived in previous chapters. An example of the application is given.
- **Chapter 9** presents conclusions and recommendations for future research.

2

OLTC Technology and Degradation

The primary function of an on-load tap changer is to select another tap without interrupting the load current. This can be accomplished in many ways, resulting in a considerable diversity of tap changer designs [15-16]. This chapter will first provide an overview of OLTC technology. The terminology used throughout this thesis follows that given in [17].

2.1 OLTC technology overview

All on-load tap changer designs must transfer the load current and are therefore equipped with an arcing switch. Two different arcing switch principles are in use, namely a diverter switch and a selector switch. The main difference between these designs is that a diverter switch type OLTC uses a tap selector to pre-select taps without switching current, in combination with a diverter switch to switch the load from the selected to the pre-selected tap. A selector switch type OLTC combines the selection of fine tap windings with the switching of the load current. To expand the regulating range of the arcing switch, the design can be extended by a change-over selector. The change-over selector can be implemented as a reversing change-over selector, a coarse change-over selector or a combination of both.

Another difference in design principles is the transition impedance that is used to control the circulating current that exists when two taps are selected during the transfer of the load current from one tap to another. A reactor type OLTC, which uses a reactor as transition impedance, is mainly used in the US. The reactor type OLTC normally consists of a diverter switch designed as a compartment type OLTC and can be found on the low-voltage side of the transformer. Most OLTCs in Europe are in-tank high-speed OLTCs which use a transition resistor during the transfer of the load current. These tap changers are normally located in the high-voltage transformer windings. Finally, tap changers using vacuum switches have

been developed and installed in several hundred transformers. Operational experience of the vacuum type OLTC has been gathered for a few years and indicates satisfactory performance.

2.1.1 Selector switch type tap changer

Selector switch type OLTCs combine the switching of the load current with the selection of fine winding taps. Selector switches can be used in a stand-alone manner but their voltage regulating range can also be extended with a (multiple) coarse change-over selector. When all of the fine tap windings are selected by the selector switch, a coarse tap winding can then be inserted before the selector switch can continue.

An example of a selector switch type OLTC is shown in Figure 2.1, with its selector switch on top of the coarse change-over selector. The selector switch is accessible at the top of the transformer, while the coarse change-over selector is mounted deeper within the transformer tank, underneath the selector switch. As a result, the selector switch can be checked during regular maintenance by removing the rotor insert, the dirty oil can be replaced, the selector switch inspected and its arcing contacts renewed when necessary.

The selector switch and the coarse change-over selector both consist of a stator on which the static contacts are mounted. These contacts are connected to the taps on the transformer windings, shown on the left of Figure 2.1. The rotor is located inside the stator and rotated by the drive system. The rotor makes a connection between the stator contacts. When switching the load current the selector switch will cause arcs; therefore, its insulation oil is separated from the main transformer tank and the arcing contacts are made of tungsten. The entire selector switch movement will take about 30-200 ms.

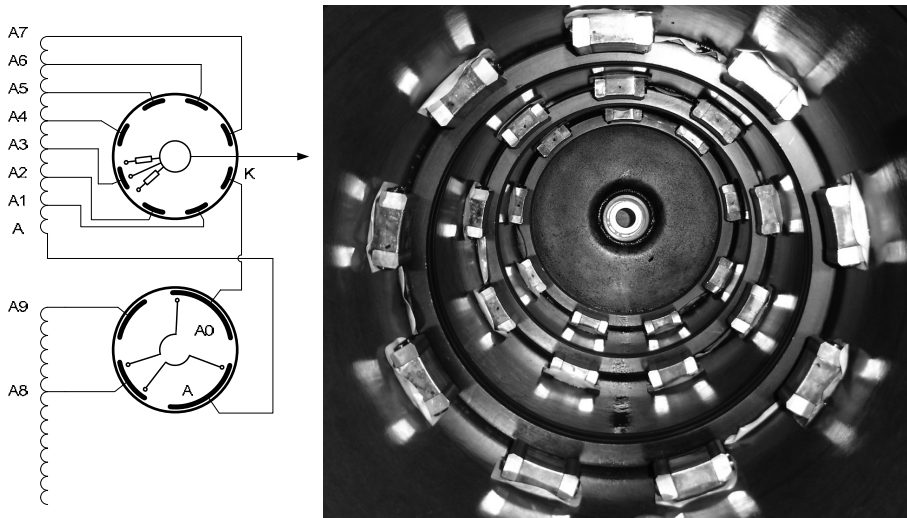


Figure 2.1 Selector switch type OLTC with coarse change-over selector (left). Right: picture of the stator contacts of a selector switch when the rotor and insulation oil are removed.

The selector switch changes the voltage ratio with one voltage step at a time. The coarse change-over selector depicted in this figure makes a voltage change of 8 steps when switching from coarse tap A8 to A9 (Figure 2.1). The tap changer as depicted in Figure 2.1 has now selected the main winding on tap A8. The current is brought to the selector switch stator by the rotor of the coarse change-over selector (using contact A in Figure 2.1). The selector switch has selected three fine tap windings using tap A3. The current leaves the tap changer using a slip ring. Appendix A describes the switching cycle of a selector switch type OLTC in more detail.

The transition resistors are necessary to prevent the short circuit of adjacent fine tapped windings and to provide a non-interrupted current path for the load current during the switching operation. The resulting circulating current is determined by the step voltage and the resistance of the selector switch.

2.1.2 Diverter switch type tap changer

A diverter switch type OLTC combines a diverter switch and a tap selector. The tap selector has two sets of contacts available for tap selection. One of the two contacts is selected by the diverter switch and is under load. The other contact selects the next tap (pre-selected tap) without switching current. The diverter switch then switches from the selected to the pre-selected tap. Diverter switch type OLTCs use transition resistors to limit the circulating current in the diverter switch. Figure 2.2 shows a schematic overview of a tap selector and a diverter switch. The tap selector can be combined with a change-over selector to expand the range of the tap changer, see appendix A. By switching the reversing change-over selector one can add or subtract the selected transformer windings, thus doubling its range. A coarse change-over selector can add a section of the regulating winding to the main winding, in this way changing the voltage of all tap selector contacts.

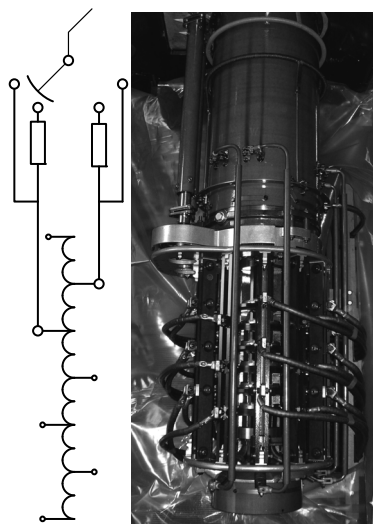


Figure 2.2 Diverter switch with transition resistors (top) and a tap selector (bottom).

In contrast to the selector switch type tap changer, most diverter switch type OLTCs have no rotor inside the arcing switch. A stationary insert is used instead. The diverter switch can easily be maintained by removing the diverter switch insert. The dirty oil can be replaced, the diverter switch inspected and its arcing contacts replaced.

2.2 OLTC degradation mechanisms

The high failure rate of OLTCs [14] emphasises the need to understand tap changer degradation. Figure 2.3 provides an overview of the different degradation mechanisms (electrical, mechanical, thermal and chemical) that are discussed in appendix A, the overview is based on literature, observations during overhaul and post-mortem investigation. The arrows indicate the location at which the degradation mechanisms act and some properties of the subcomponents (as discussed above) are also summarised. Contact degradation is described in this chapter, more information about other degradation mechanisms can be found in appendix A.

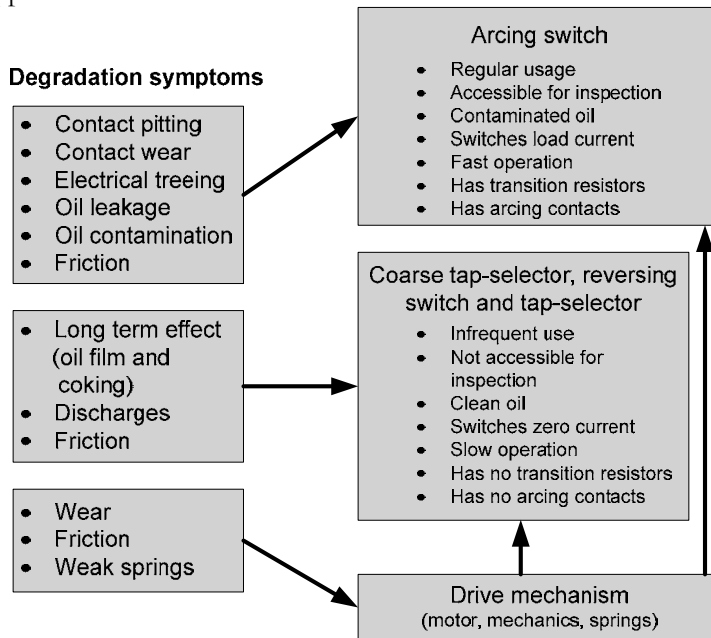


Figure 2.3 Overview of the different degradation mechanisms. The arrows indicate the location at which the mechanisms act. Important features of the OLTC parts are listed.

2.3 Contact degradation

An OLTC has sets of contacts that switch different currents at different recovery voltages. For example, the main contacts of the arcing switch are designed to transfer the load current to the transition contacts. The arcing contacts of the arcing switch are designed to break the load current and the circulating current. In contrast, the contacts of the tap selector and the change-over selector are not designed to switch current. Therefore these sets of contacts wear differently.

Change-over selector contacts (including tap selector contacts) do not wear as fast as arcing switch contacts that wear due to the switching of load currents. These contacts will not switch significant currents, but can show pitting of the

contacts and the development of pyrolytic carbon [18-19]. This contact degradation is not due to the arcs caused by switching the current but by a long term overheating process.

Usually, the contacts of the change-over selector are infrequently used and can be motionless for long periods. This activates the second degradation mechanism of change-over selector contacts: a long-term aging effect on contacts under oil, henceforth referred to as the 'long-term effect'. The long-term effect is the most common degradation mechanism on the change-over selector in the Netherlands and causes most change-over selector failures.

Three basic stages of the long-term effect can be distinguished and are shown in Figure 2.4. This section deals with these degradation stages. Formulae for contact resistance found in literature will be explained. Finally, in Section 2.3.5, the formulae will be completed using experimentally derived correction factors, which correct for OLTC operation and for the measurement current amplitude.

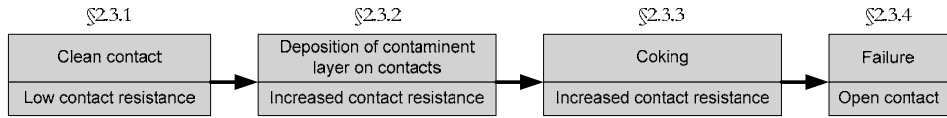


Figure 2.4 The long-term effect starts with the formation of a surface film on the contacts. The increased resistance can cause coking. Thermal runaway can finally cause failure of the OLTC due to open contacts.

2.3.1 Clean contacts

A clean contact involves a metal-to-metal connection between two contacts. The resistance of this contact material can be described as:

$$R_B = \rho \frac{X'}{A} \quad 2-1$$

where R_B is the bulk resistance of the material in Ω , ρ the specific resistivity of the contact material in Ωm , X' the contact thickness in meter and A the contact cross-sectional area in square meter. Since the contact material is deformable, contact between the two surfaces is made over a small contact area, not at a single point.

For example, let us consider the cross-sectional contact area between an ideal pair of radial contacts (two contacting hemispheres, see Figure 2.5) of diameter D . Due to the contact force, a contact area A is created a distance $D/2 - C$ from the centre of each hemisphere, which may be written:

$$A = \pi \left[\left(\frac{D}{2} \right)^2 - X^2 \right] \quad [20] \quad 2-2$$

over the range $X = 0$ to $D/2 - C$, so that two contacting hemispheres have a bulk material resistance of:

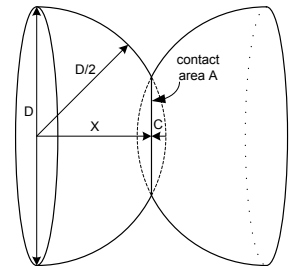


Figure 2.5 Two contacting hemispheres create a contact area A a distance $D/2 - C$ from the sphere's centre.

$$R_c = 2 \int_0^{D/2-C} \frac{\rho}{\pi} \left[\left(\frac{D}{2} \right)^2 - X^2 \right]^{-1} dX = \frac{-2\rho}{\pi D} \left[\ln \left| \frac{\frac{D}{2} - X}{\frac{D}{2} + X} \right| \right]_0^{D/2-C} \quad [20] \quad 2-3$$

where C is the part of the radius of each hemisphere involved in the contact. For example, a 200 amp tap changer with 22 N contact force will have $D = 8$ mm and $C = 4$ μm , so that $R_c = 10.5$ $\mu\Omega$ for copper contacts at 20 °C [20]. This theoretical resistance would exist if there was no contaminant film between the contact surfaces and perfect contact was made over the entire contact area. Practical experience of copper contacts indicates an as-built resistance closer to 50 or 60 $\mu\Omega$, suggesting that true contact is not achieved uniformly over the whole surface [20].

The small contact area constricts the current from flowing uniformly: the current lines are bunched near the micro contact. This gives rise to an additional resistance, the constriction resistance (often called the contact resistance). Assuming an infinite volume of bulk material above and below the circular contact spot, we can calculate the constriction resistance to be:

$$R = \frac{\rho}{2a} \quad [21] \quad 2-4$$

where a is the radius of the circular contact spot in meter and assuming that a is much smaller than the apparent contact area.

In practice, electrical contact will be made at more than one spot due to the roughness of the material. It follows that parallel metal-to-metal micro contacts must be assumed to be present in OLTCs. In addition to the total cross-sectional area of the contact spots (R_{parallel}), there will then be an additional resistance due to interaction between the spots ($R_{\text{interaction}}$). Ref. [22] describes this effect on the assumption of n circular spots on clean contact surfaces, where the contact resistance of a circular clean contact is given by:

$$R_c = R_{\text{parallel}} + R_{\text{interaction}} = \frac{\rho}{2 \sum_{i=1}^n a_i} + \frac{\rho}{\pi} \frac{\sum_{i=1, i \neq j}^n \sum_{j=1}^n \frac{a_i a_j}{d_{ij}}}{\left(\sum_{i=1}^n a_i \right)^2} \quad 2-5$$

which can be approximated as:

$$R_c \approx \frac{\rho}{2 \sum_{i=1}^n a_i} + \frac{\rho}{\pi n^2} \sum_{i=1, i \neq j}^n \sum_{j=1}^n \frac{1}{d_{ij}} \quad [22] \quad 2-6$$

where a_i and a_j are the radii of contact spot i and j in meter, and d_{ij} is the distance between the centres of spot i and j in meter. The approximation of Equation 2-6 assumes that there is no correlation between the size of the contact spot and its position, so only the mean radius is considered in the second term ($a_i = a_j = a$). Hence, the number of contact spots and the distance between them determine the ratio of the parallel to the interaction resistance; see Figure 2.6. When the number

of contact spots is low, the contact resistance is mainly determined by the parallel resistance of the spots, while with a large number of spots the resistance is mainly determined by the interaction between the spots.

The voltage drop over this cluster of clean circular spots may be written [22]:

$$U = \frac{\rho}{2} \left(\frac{I_i}{a_i} + \frac{2}{\pi} \sum_{j \neq i} \frac{I_j}{d_{ij}} \right) \quad 2-7$$

where U is the voltage over the contact interface in Volts and I_i and I_j are the currents through contact spot i and j in Amperes.

Ref. [21] describes the effect of parallel contact spots by the equation:

$$R_c = \rho \left(\frac{1}{2na} + \frac{1}{2\alpha} \right) \quad 2-8$$

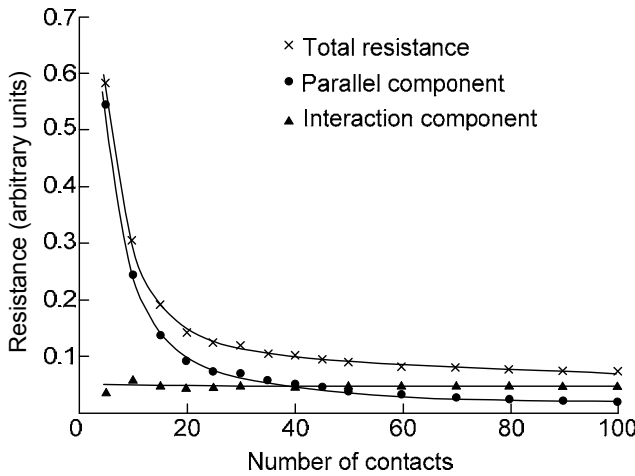


Figure 2.6 The number of micro-spot contacts determines the ratio of the parallel resistance of all micro-spots to the resistance due to the interaction between the contact spots [22].

where n is the number of contact spots with radius a uniformly distributed in a circular area of radius α (see Figure 2.7).

A higher contact pressure lowers the resistance of such a clean circular contact spot by increasing the contact area due to plastic deformation of the metal. OLTC contacts are therefore designed to ensure that the contact pressure is high and the surface film is wiped off each time the contacts are operated.

By way of example, Figure 2.8 shows the effect of temperature and contact force on the contact area of a cluster of circular contact spots of equal radius (see [23]). The numerical simulation performed by [23] employs a finite element model to calculate the material deformation due to mechanical and thermal stress near an aluminium contact

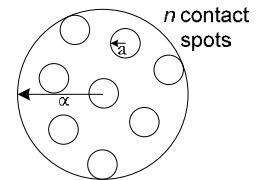


Figure 2.7 n contacts with radius a are distributed over an apparent contact area α .

boundary (similar to that shown in Figure 2.5). It may be seen from Figure 2.8 that higher contact forces and contact temperatures yield a larger contact area. The best-fit relation between the temperature T in degree Celsius and the contact area A_c in square metre for contacts with a high contact load (2.3 kN and 4 kN) can be found from Figure 2.8 [23] to be the exponential function:

$$A_c = 5.16 \cdot 10^{-6} + 7.27 \cdot 10^{-7} e^{1.05 \cdot 10^{-2} T / T_0} \quad 2-9$$

with $T_0 = 1^\circ\text{C}$.

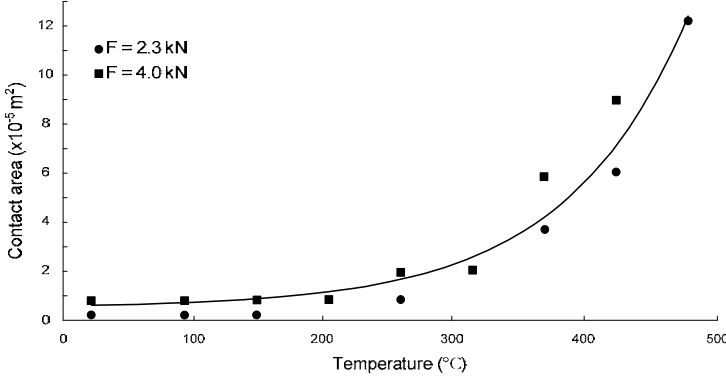


Figure 2.8 Example of a numerical simulation performed by [23], in which the contact area increases with higher temperature and contact force.

Ref. [23] gives the relationship between the resistivity and the contact temperature as:

$$\rho_c = \frac{\rho_0}{T_0} \beta T e^{-C\gamma(T-T_0)} \quad [23] \quad 2-10$$

where $\frac{\rho_0}{T_0} \beta T$ is the bulk resistance, ρ_0 and T_0 are reference values, β is the bulk contact resistivity factor (related to the applied load and surface condition), T is the temperature, $e^{-C\gamma(T-T_0)}$ is the softening effect factor reflecting the increase in contact area at high temperatures (as a function of the softening point of the contact material, which is about 200 °C for pure copper), and γ is the contact area correction factor. The change in contact resistance with temperature according to Equation 2-10 (adapted for degree Celsius, for $\beta = 1000$ and $\gamma = 1$) is plotted in Figure 2.9. It will be seen that the resistance initially increases with temperature, due to the bulk resistivity effect [23]. When the temperature rises above the softening point, the exponential term of Equation 2-10 causes the resistance to fall as the contact area increases due to the softening of the material [23].

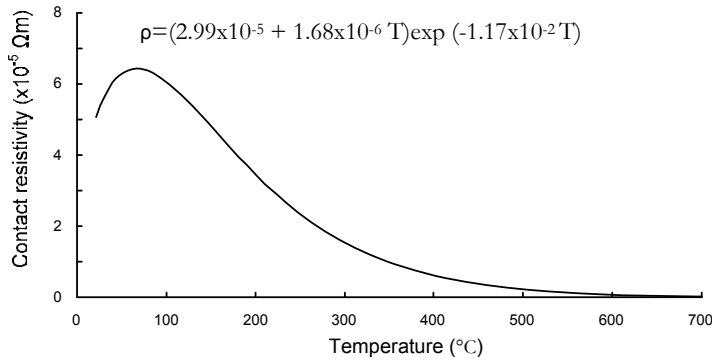


Figure 2.9 Relationship between the contact temperature and resistivity. The resistivity first rises with temperature due to the bulk resistivity effect, and then falls again as the contact material softens [23].

2.3.2 Contacts with a surface film

The resistance of a contact will gradually increase during its lifetime. There is empirical evidence [20][24-26] that this long-term effect starts with surface oxidation and the formation of organic polymers [19]; these effects reduce the conductivity. Anorganic layers consisting of tenorite (CuO), cuprite (Cu₂O) and sulfides (CuS and Cu₂S) form on copper contacts [19]. Ref. [26] found that the oxide and sulfide layers always formed in the same sequence; a thin sulphide layer followed by the cuprite later, then the tenorite, see Figure 2.10.

At higher temperatures an organic film is also formed [26]. It follows from [25] that the organic film is composed of organic compounds in the transformer oil and consists of polyacrylates and polyfurans [19], giving a red-orange color to the contact [26]. This layer bonds to the oxide layer formed on the contacts to give a stable film of low conductivity.

The formation of this surface film is referred to as the early stage of the long-term aging effect.

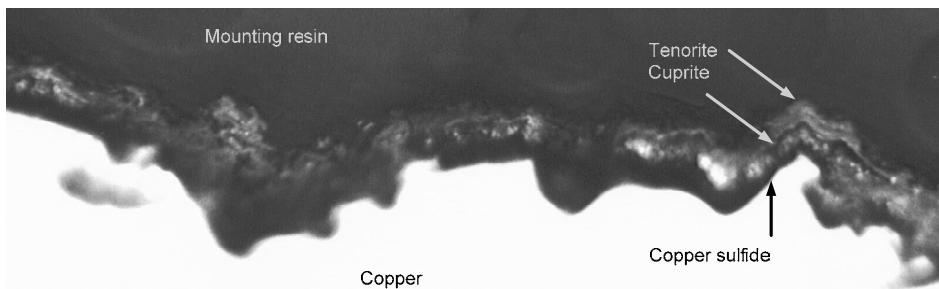


Figure 2.10 1600x magnification of a service-aged tap changer contact surface. The contact was mounted in resin to make this cross-sectional picture. A thin copper sulphide layer forms on the copper contact, followed by a cuprite and a tenorite layer. [26]

Experiments described in the literature [18][27] show that the surface film grows thicker as the contacts age, and that the growth rate of this layer is strongly dependent on the surface temperature of the contacts. Ref. [18] gives an expression for this process as a function of time, based on the endurance testing of OLTC contacts:

$$s = k_1 * \theta_0^{k_2} * t^{k_3} \quad 2-11$$

where s is the thickness of the film layer in Å, θ_0 is the surface temperature in °C at which the surface film grows on the contacts and t is the duration of the aging test in hours. k_1 , k_2 and k_3 are coefficients that depend on the contact material and oil composition [18]. For copper contacts immersed in Shell Diala insulating oil, this expression becomes:

$$s = k_0 * \theta_0^{3.862} * t^{0.3559} \quad [27] \quad 2-12$$

with $k_0 = 1.883 \cdot 10^{-6}$ with an appropriate unit to balance the equation.

Figure 2.11 shows the growth of this surface film as a function of time at different temperatures for copper and brass contacts. It may be seen from this figure that the film grows faster on copper than on brass, which means that copper contacts are more liable to this long-term aging effect. OLTC manufacturers therefore select the contact material carefully in order to slow the development of the resistive contact film.

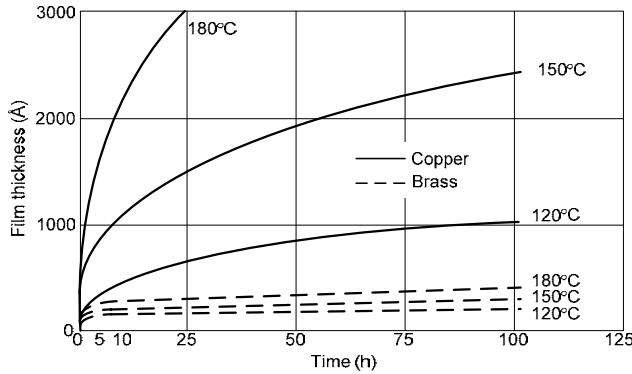


Figure 2.11 Regression lines of the surface film growth on copper and brass contacts at different surface temperatures in Shell Diala D insulating oil [24].

The contact resistance and the power losses at the contact increase as the surface film grows. Figure 2.12 gives an example of how the contact resistance increases as a function of thickness when an oxidation film develops on a copper contact in air. The contact first shows a low contact resistance when the film is relatively thin, but above film thickness of 1000 Å the resistance increases sharply leading to contact failure [28]. This is due to changes in the conduction mechanism: tunnelling effects are found in thin films (thinner than 50 – 100 Å), while the bulk resistivity of the film dominates in thick films [28]. Thick surface films of tens of micrometers have been found on tap changer contacts [26].

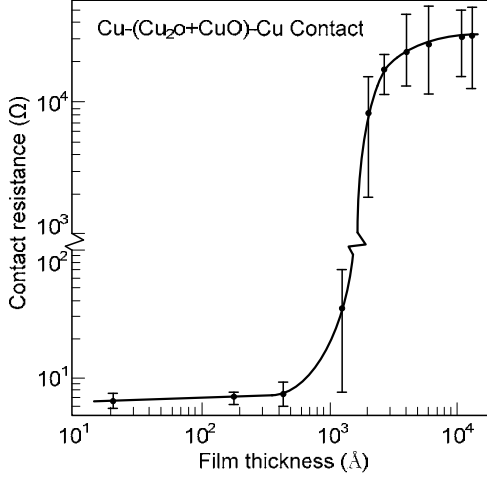


Figure 2.12 Resistance of an oxidation film on copper contacts in air, as a function of film thickness [28].

The contact resistance can now be written:

$$R_c = R_{clean} + R_{tunnel} + R_{FILM} \quad 2-13$$

where R_{clean} is the so called constriction resistance of the metal-to-metal contact, R_{tunnel} is the tunnelling resistance for thin films (creating a quasimetallic contact) and R_{FILM} the resistance of the thick film. Due to the thick film on degraded OLTC contacts, R_{FILM} can be high compared to R_{tunnel} and R_{clean} , as in the example of Figure 2.12, so R_{tunnel} and R_{clean} can be neglected during DRM on degraded OLTC contacts [29].

Ref. [30] describes the contact resistance for one circular contact spot of contact radius a and film resistivity λ as:

$$R_c = R_{clean} + R_{film} = \frac{\rho}{2a} + \frac{\lambda}{\pi a^2} \quad 2-14$$

where the film surface resistivity λ is calculated by multiplying the film resistivity ρ_f by the film thickness σ_f .

For multiple parallel contact spots with a resistive film, the resistance according to Equation 2-5 becomes:

$$R_c = \frac{1}{2\pi \sum \frac{a_i^2}{\rho\pi a_i + 2\lambda_i}} + \frac{\rho}{\pi} \frac{\sum_{i \neq j} \sum \frac{a_i^2 a_j^2}{d_{ij} (\rho\pi a_i + 2\lambda_i) (\rho\pi a_j + 2\lambda_j)}}{(\sum \frac{a_i^2}{\rho\pi a_i + 2\lambda_i})^2} \quad [30] \quad 2-15$$

If the contact force increases, the number of contact spots and the contact area increase. This causes both the film resistance and the constriction resistance to fall, as shown in Figure 2.13. When the contact pressure is released, the material

remains deformed so the radius of the contact spots remains large. As a result, the contact resistance will only increase slightly when the contact pressure is released [31]. The bulk resistance is independent of the contact force [31].

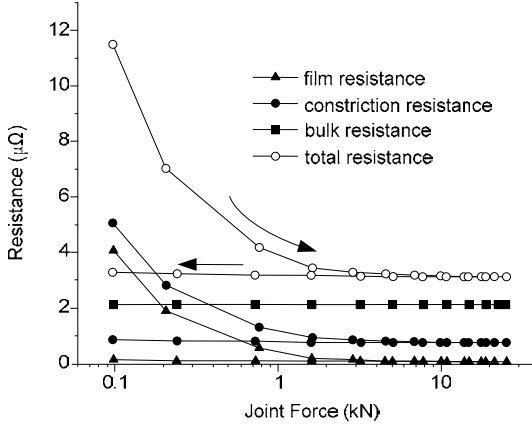


Figure 2.13 Increasing the contact force has no effect on the bulk resistance, but the film resistance and constriction resistance both fall because the number of contact spots and the contact area increase [31].

The resistive behaviour of the film can be simplified by assuming that the film is conducting when the thickness $\delta < \delta_c$ and insulating when $\delta > \delta_c$ [32], which simplifies the behaviour of the film shown in Figure 2.12. The growth of the layer can thus be described as a process that reduces the effective contact area. If we assume that the effective contact radius r is reduced to $r \leq a$, the contact area of one circular spot can be described as a function of time by the expression:

$$\frac{r}{a} = \left[1 - \sqrt{K_\delta} \sqrt{\frac{Dt}{a^2}} \right] \left[1 + K_\delta \frac{Dt}{a^2} \right] \quad [32] \quad 2-16$$

where the diffusion coefficient of the oxidation layer D (which describes the speed at which the layer grows into the contact area) can be written:

$$D = D_0 e^{-\frac{B}{\theta}} \quad [32] \quad 2-17$$

where D_0 is the frequency factor, B the temperature-dependent diffusion parameter and θ the homologous temperature (the temperature in relation to the melting point T_m):

$$\theta = \frac{T}{T_m} \quad 2-18$$

Ref. [32] determined contact lifetime of copper contacts using a coefficient K_δ :

$$K_\delta = 2.2 - 4 \ln \frac{\delta_c}{\delta_m} \quad 2-19$$

The contact resistance of this model can then be written:

$$R_{c(t)} = \frac{\rho}{2r_{(t)}} = \frac{R_0}{\left[1 - \sqrt{K_\delta} \sqrt{\frac{Dt}{a^2}}\right] \left[1 + K_\delta \frac{Dt}{a^2}\right]} \quad [32] \quad 2-20$$

where

$$R_0 = \frac{\rho}{2a} \quad 2-21$$

It follows from this model [32] that $R_c \rightarrow \infty$ when

$$t = t_m = \frac{a^2}{K_\delta D} \quad [32] \quad 2-22$$

This is the life of the contact under the assumptions used for Equation 2-20. It corresponds to the time at which the thickness of the film is $\delta > \delta_c$ everywhere, so that the contact can be considered to have failed. This contact life depends on a and is thus related to the initial contact resistance by $(1/R_0)^2$. It follows that a large initial contact radius a results in a long contact life.

The simplified model can be extended by considering parallel circular contact spots and a film on the contact surface. The average spot radius $r_{(t)}$ and the number of spots $n_{(t)}$ can be used to derive the following expression for the resistance:

$$R = \frac{\rho}{2n_{(t)}r_{(t)}} \quad [32] \quad 2-23$$

Equation 2-16 then becomes:

$$r_{(t)} = a \left[1 - \sqrt{K_\delta} \sqrt{\frac{Dt}{a_m^2}}\right] \left[1 + K_\delta \frac{Dt}{a_m^2}\right] \quad [32] \quad 2-24$$

where a is the initial value of the mean radius and a_m is the initial value of the maximum spot radius. The number of contact spots falls as the film thickness grows. At time t , all contact spots with initial radius $a < a_c$ disappear, where:

$$a_c = \sqrt{K_\delta Dt} \quad [32] \quad 2-25$$

so that the number of contact spots can be written:

$$n_{(t)} = n_0 \left(1 - \int_0^{x_c} f_{(x)} dx\right) \quad [32] \quad 2-26$$

where $x = a/a_m$ (the mean divided by the maximum radius), $x_c = a_c/a_m$ and $f_{(x)}$ describes the contact spot radius distribution. The rise in contact resistance calculated by [24] and experimentally determined by [33] resembles the calculated contact resistance of Equation 2-24 (evaluated by [32]) when $f_{(x)}$ is a beta distribution with $\alpha = 1$ and $\beta = 1$, for which we can use the expression:

$$f_{(x)} = 6x(1-x) \quad [32] \quad 2-27$$

This distribution describes an electrical contact with large contact spots in the middle and smaller ones on the outside. The contact resistance can then be written:

$$R_{(t)} = \frac{R_0}{\left[1 - \sqrt{K_\delta} \sqrt{\frac{Dt}{a_m^2}}\right]^3 \left[1 + 2\sqrt{K_\delta} \sqrt{\frac{Dt}{a_m^2}}\right] \left[1 + K_\delta \frac{Dt}{a_m^2}\right]} \quad [32] \quad 2-28$$

In reality, contacts fail before $R_c \rightarrow \infty$ (Equation 2-22), at the point where the resistance increases by a factor k relative to its initial value [32]. The life of a multipoint contact with a beta distribution of the contact radii can then be approximated as:

$$t_l = 0.56 t_m \left(1 - \frac{1}{k}\right)^2 \quad [32] \quad 2-29$$

where t_m is calculated from the maximum radius a_m . Equation 2-28 can be corrected for this effect by reducing the maximum life (when $k=\infty$) by a factor 0.56 (i.e. $t \rightarrow t/0.56$):

$$R = \frac{R_0}{\left[1 - \sqrt{K_\delta} \sqrt{\frac{D \cdot 1.79 \cdot t}{a_m^2}}\right]^3 \left[1 + 2\sqrt{K_\delta} \sqrt{\frac{D \cdot 1.79 \cdot t}{a_m^2}}\right] \left[1 + K_\delta \frac{D \cdot 1.79 \cdot t}{a_m^2}\right]} \quad 2-30$$

For example, the data from Table 2.1 can be used to calculate $R_{(t)}$. Figure 2.14a shows this curve for $0 \leq t < t_m$. It can be seen that the resistance goes to infinity as the contact approaches the end of its life. However, contact failure can already be expected earlier as described by Equation 2-29. In practice, the contact resistance will not go to infinity because the thin film will be disrupted due to the applied voltage, the contact will heat and high hotspot temperatures may arise. It is therefore assumed here that the calculation of $R_{(t)}$ is valid up to $k=10$ (i.e. up to $10 \cdot R_0$). This part of the calculated $R(t)$ curve is displayed in Figure 2.14b. A model that can be used for OLTC contacts at a more advanced stage of contact degradation will be discussed in the next section.

Table 2.1 Overview of simulation parameters used to plot $R(t)$ of Figure 2.14.

Parameter		Value	Reference
Bulk temperature	T_B	50 °C = 323 °K	assumption
Hotspot temperature	T	$T_B + 1 = 324$ °K	[32]
Melting point of copper	T_m	1356 °K	
Resistivity of copper	ρ	$1.7241 \cdot 10^{-8}$ Ωm	
Average contact spot radius	a	10 μm	[24][32]
Maximum contact spot radius	a_m	30 μm	assumption
Number of micro contact spots	n	45	[24]
Critical film thickness ratio	δ_c/δ_m	0.04	[32]
Diffusion coefficient	D_0	$1 \cdot 10^{-5}$ m ² /s	[32]
Diffusion parameter	B	7	[32]
Coefficient used by [32]	K_δ	15	[32]
Initial contact resistance	R_0	10 μΩ	assumption
Critical contact resistance increment	k	10	[32]

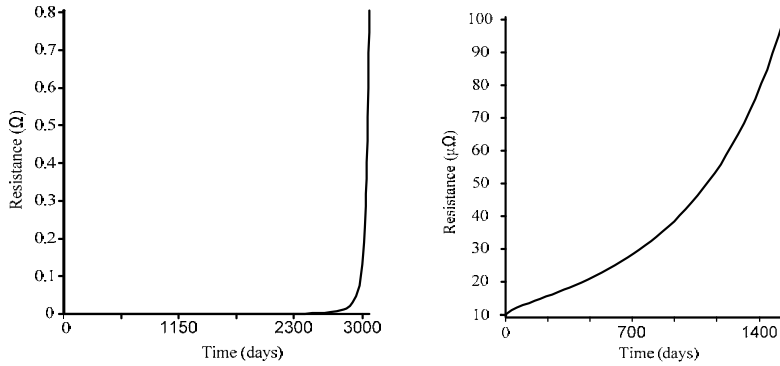


Figure 2.14 Simulation of resistance-time curve according to Equation 2-28 using the parameters from Table 2.1. Left: the variation of contact resistance up to the end of contact life. Right: close-up view of resistance variation up to $R(t)=10 \cdot R_0$.

At early stages of the long-term aging effect, the film can be wiped off by switching the OLTC through its cycle of operation. The motion of the contacts during this cycle partially breaks down the surface contamination [20][34-35], thus delaying the long-term aging effect.

2.3.3 Contacts with high local temperatures

Section 2.3.2 dealt with a mathematical model that described the early stage of contact degradation. Another model is needed to describe the advanced degradation stage, where long-term aging accelerates due to the temperature dependence of the surface film growth rate. The contact resistance can also fall during the long-term aging, as the surface film breaks down due to discharges [20] or contact wiping. Small discharges can restore a better current path by disrupting the surface film, but the contact resistance can increase by several orders of magnitude before the contact improves again [20]. These discharges become worse as degradation proceeds [20], and the oil dissociates due to these discharges and the high contact temperatures. It is these effects together that constitute advanced long-term aging.

Breakdown due to the applied measurement voltage can also indicate the stage reached by the surface film. Under normal conditions, the film has a breakdown voltage of 0.2-0.6 V, which increases to 1-4 V in the defective condition [36]. The accompanying electric field over thin films results in high field strengths.

The decomposition of transformer insulation oil leads to the deposition of carbon between the contacts (Figure 2.4B, [20][37]). This formation of pyrolytic carbon is called coking [19]. Oil cracking occurs at local temperatures above 300 °C [20]. Catastrophic conditions can thus be produced when the contact temperature rises above 300 °C [38], but even a rise in oil temperature near the contact to above 100-105 °C can be enough to cause serious defects [36]. Precise measurement of the hotspot temperature is a complicated procedure, but the

voltage drop over the contact can be used to calculate the temperature rise from the expression:

$$V^2 = 4L(T_C^2 - T_B^2) \quad [20] \quad 2-31$$

where L is the Lorenz constant, T_C the temperature increment over the bulk temperature in degree Kelvin and T_B the bulk temperature of the contact in degree Kelvin.

The highest local temperature at the contact interface can also be calculated based on the I^2R losses in the contact area:

$$T = T_B + \frac{I^2 \varphi_{eff}}{8\lambda_{eff}} \left(\frac{\delta}{S}\right)^2 \quad [9] \quad 2-32$$

where φ_{eff} is the effective electrical resistivity of the contact layer, λ_{eff} the thermal conductivity of the contact layer, δ the film thickness and S the surface area. Using this relation, [39] derived the following expression for the film thickness δ on OLTC contacts in oil:

$$\frac{d\delta}{dt} = \frac{K \cdot a \cdot t}{\rho} e^{-\frac{E_a}{R \cdot T}} = \frac{K \cdot a \cdot t}{\rho} e^{-\frac{\frac{E_a}{R}}{T_B + \frac{I^2 \varphi_{eff}}{8\lambda_{eff}} \left(\frac{\delta}{S}\right)^2}} \quad 2-33$$

where K is the coke deposition rate in cm/day, a the amount of coke precursor (g/cm³) generated in the oil every day due to OLTC operation, ρ the density of the coke, E_a the activation energy of the deposition process in Joule/mol and R the gas constant in Joule/(mol·Kelvin). Experiments conducted to determine the parameters [39] led to the values $K a / \rho = 0.13$ cm/day, $\varphi_{eff} = 0.0082$ Ω·cm and $E_a/R = 4730$ K. Furthermore, [39] used $\lambda_{eff} = 0.4$ W/mK, $I = 900$ A, $T_B = 300$ °K and $S = 2$ mm². These parameters can be used to calculate the life of OLTCs, although the high load current assumed by [39] is not common for the tap changers considered in this thesis; the calculations performed by [39] may thus be considered to correspond to an accelerated endurance test at heavy load. Equation 2-33 was evaluated numerically by [39] using these parameters, see Figure 2.15 and Figure 2.16. Film growth and power losses increase gradually, which causes a rising super temperature, until the contacts get overheated and failure occurs.

2.3.4 Contact failure due to overheating

In addition to coking, the contact material wears off locally and pitted spots become visible on the contacts. The contacts are now irreversibly damaged, and cannot be repaired by switching the OLTC through all its tap positions. An overhaul is needed to undo the pitting of the contacts. Because of the infrequent movement of the change-over selector, coking can occur on all stator contacts, rotor contacts and other movable parts that carry the load current.

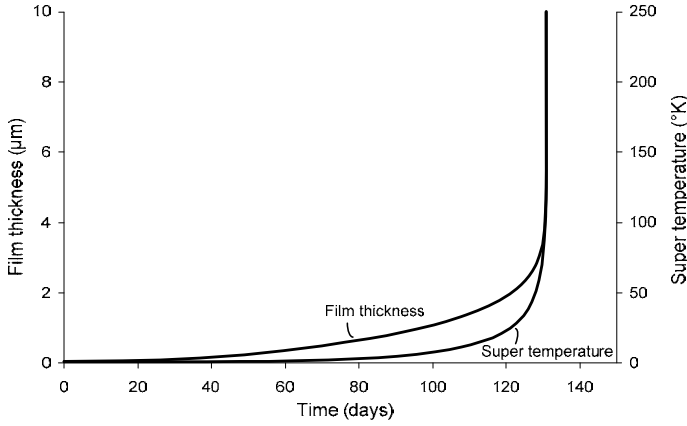


Figure 2.15 Film growth on OLTC contacts loaded at 900 A, as described by Equation 2-33, which results in a rising super temperature and finally in contact failure [39].

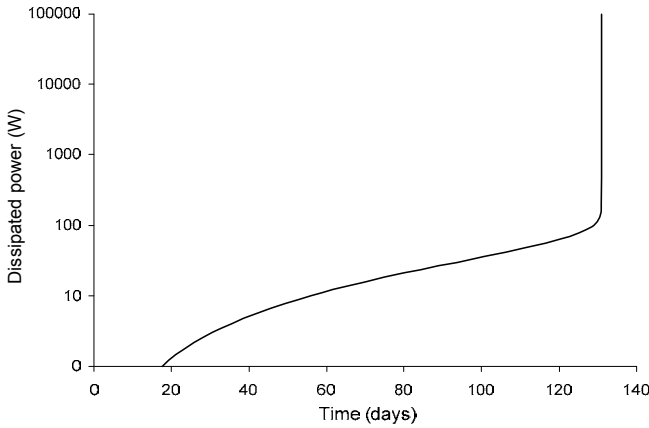


Figure 2.16 Power loss on OLTC contacts at a heavy load of 900 A due to the film described by Equation 2-33. The power losses increase gradually until contact failure occurs [39].

The final stage of the long-term aging effect is thermal runaway. The coking accelerates due to increased contact resistance and the thermal resistance characteristics of the carbon [9]. Coking between moving parts of the contacts and around the springs that provide the contact pressure can cause the contacts to lose pressure. Finally, a considerable amount of contact material disappears and excessive arcing activates the tap changer protection mechanisms. Figure 2.15 shows that film growth and super temperature increase gradually until thermal runaway occurs. Figure 2.16 shows how the corresponding power dissipation increases when the system exceeds the design limitations and the cooling capacity of the OLTC, leading to failure. Examples of failed contacts due to overheating are shown in Appendix A.

Figure 2.17 shows the effect of the current on the contact life (characterised by the moment at which the resistance increases to $k \cdot R_0$) of a copper-copper contact

in oil, as determined by numerical simulation [24]. It may be seen that a low current gives a longer life. Coking is likely to occur when the resistance is rising rapidly [24]. Figure 2.18 shows the simulated relationship between oil temperature and contact life; these curves have the same general form as those of Figure 2.17.

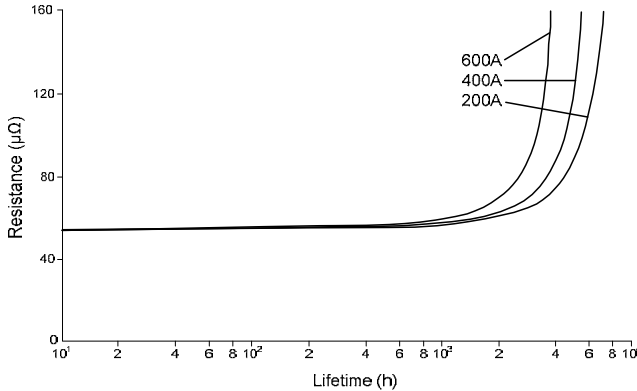


Figure 2.17 Simulated relationship between contact resistance and contact life for a copper-copper contact in oil at various load current [24]. A higher load gives a shorter contact life.

According to [24], the long-term aging effect is accelerated by:

- Infrequent movement of the contacts
 - The surface film is not wiped off the contacts when the change-over selector is not operated.
- High temperatures
 - The formation of the surface film is highly temperature-dependent.
- High load current
 - Power losses at the contact interface increase exponentially with the load current and lead to correspondingly greater heating of the contacts.
- Low contact pressure
 - Coking and pitting of the contacts are more likely to lead to contact jamming when the contact pressure is low. The layer of contamination on the contact surface, which can lead to contact malfunction or failure, is also more easily disrupted at high contact pressure.
- Copper or brass contacts
 - The growth rate of the surface film is higher on copper and brass contacts than on silver contacts [24]. Pitting and coking are reduced by silver-coating of the contact surface; however, older OLTC designs may use bare copper contacts.

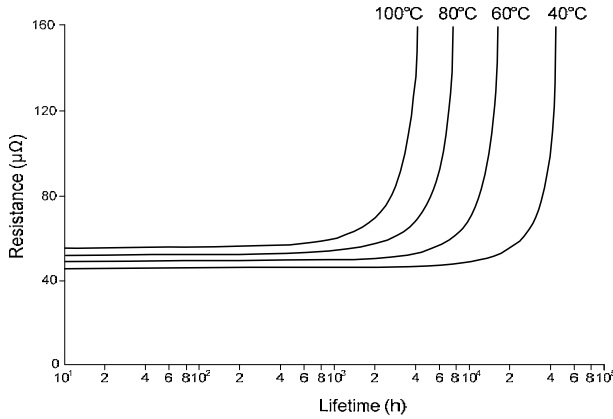


Figure 2.18 Simulated relationship between contact resistance and contact life for a copper-copper contact in oil at various load current [24]. A higher oil temperature gives a shorter contact life.

2.3.5 Corrected model of tap changer resistance

We describe the long-term variation of OLTC resistance $R_{(t)}$ by Equation 2-30 for slightly degraded contacts and the film thickness by Equation 2-33 for severely degraded contacts, on the basis of the following assumptions:

1. The early stage of contact degradation can be modelled by parallel circular metal-to-metal micro-contacts, as described in Section 2.3.2 The film is assumed to be conducting when its thickness $\delta < \delta_c$ and insulating when $\delta > \delta_c$. The effective contact radius r is therefore reduced to $r \leq a$
2. The radii of the contact spots are distributed according to a beta distribution
3. A constant contact force is applied
4. A constant current is applied
5. The on-load tap changer is not operated during its life
6. The contact film remains undisrupted

As indicated above, the model for $R_{(t)}$ is based on the assumptions that the OLTC is not operated during its life and that the contact film is not damaged. These assumptions are unrealistic, but can be corrected for with the aid of experimentally fitted parameters. Switching the tap changer will slow down the development of the contact film and reduce contact resistance. Moreover, differences in the measured resistance occur at different measurement current amplitudes due to damage to the film caused by the measurement current; this also needs to be corrected for. These corrections are illustrated in Figure 2.19. The corrected value of $R_{(t)}$ can be represented by the expression:

$$R_{(t)} = R_{(t)} \cdot C_{DRM} \cdot C_{OLTC} \quad 2-34$$

where C_{OLTC} represents the wiping effect due to operation of the OLTC, and C_{DRM} the correction for differences in the measurement current during the dynamic resistance measurement.

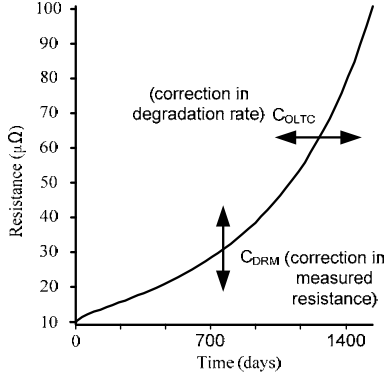


Figure 2.19 The calculated resistance $R(t)$ can be corrected for wiping action of the contact film caused by OLTC operation (C_{OLTC}) and for the damage to the film caused by the measurement current during the resistance measurement (C_{DRM}).

The correction factor C_{OLTC} is a number between 0 and 1, where 0 represents a wiping action that totally cleans the contacts and 1 represents the complete absence of wiping action. The actual value of C_{OLTC} depends on the contact design, contact pressure and the mechanical resistance of the film to the wiping action. Figure 2.20 presents typical experimental data that were used as a basis for the determination of the value of C_{OLTC} . A set of degraded OLTCs, all of the same type, was selected and the number of operations during a year was plotted against the contact resistance (estimated on the basis of the assumption that each dynamic resistance measurement was performed with 1 A and a constant voltage of 2 V, thus neglecting the change in resistance during the measurement). When multiple measurements were performed on a given OLTC, the results were averaged. A trend line was determined from the data points of Figure 2.20 using the least square method, resulting in the weak relationship:

$$R = R_0 \cdot (2144 - 0.32 \cdot n_y) \quad 2-35$$

where R is the resistance in $m\Omega$, R_0 is the reference resistance of $1m\Omega$ and n_y is the average number of operations during a year ($500 < n_y < 4500$). It follows that the correction factor C_{OLTC} can be written:

$$C_{OLTC} = \frac{R}{R_{n_y=0}} = 1 - 1.49 \cdot 10^{-4} \cdot n_y \quad 2-36$$

The data set shown in Figure 2.20 gives a (Pearson) correlation of -0.52, which indicates that there is a weak relation between the number of operations and the

contact resistance. We refrain from using this relation for predicting the resistance, due to the low correlation involved.

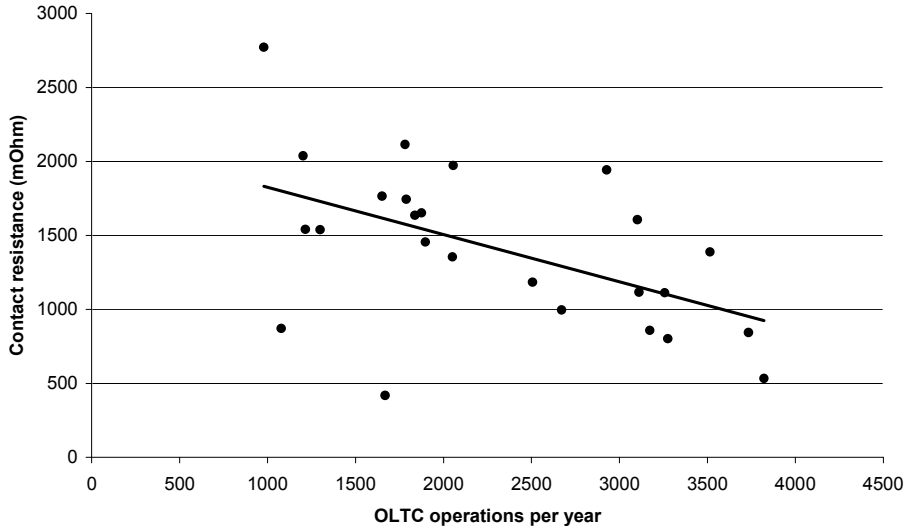


Figure 2.20 Contact resistance as measured by DRM plotted against the number of operations per year for a set of degraded OLTCs, all of the same type.

C_{DRM} is the ratio of the measured and calculated resistance. The difference between the two is due to damage to the film caused by the measurement current. This correction factor thus describes the effect of the measuring procedure on the results, not related to the degradation produced when the OLTC is in service. C_{DRM} depends on the measurement current; and is introduced to give a measure of the degradation process that is independent of the measurement parameters. It is assumed that the circuit resistance and inductance are kept constant during the measurement, so that the measurement voltage varies with the current i . Hence, C_{DRM} is a function of i :

$$C_{DRM} = \frac{R_{2,5}}{R_i} \quad 2-37$$

where $R_{2,5}$ is the resistance measured at 2.5 A. Experimental results show that C_{DRM} can be written in terms of two exponential functions:

$$C_{DRM} = \frac{R_{2,5}}{R_i} = \frac{R_{2,5}}{k_0 + k_{dyn1} \cdot e^{\frac{-(i-i_{offset})}{\tau_{i1}}} + k_{dyn2} \cdot e^{\frac{-(i-i_{offset})}{\tau_{i2}}}} \quad 2-38$$

where i is the amplitude of the measurement current, τ_{i1} and τ_{i2} the rate at which the resistance decreases when the current is increased, and I_{offset} , k_0 , k_{dyn1} and k_{dyn2} are constants used to fit the expression to the experimental results. Figure 2.21 shows the result of a set of resistance measurements performed on OLTCs suffering from advanced long-term aging, using currents from 2.5 to 100 A. The trend line giving the best fit with these results is represented by the expression:

$$C_{DRM} = k \cdot \frac{230}{10 + 220 \cdot e^{\frac{-(i-19)}{22}} + 30000 \cdot e^{\frac{-(i-19)}{4}}} \quad 2-39$$

where i is the amplitude of the current in the range $2.5 \text{ A} \leq I \leq 100 \text{ A}$ and k is a constant that is used to make the units of the equation equal. Since the scatter of the measured data is acceptably low and the (Spearman) correlation is high (-0.95), we conclude that Equation 2-39 can be used to describe the contact resistance of degraded OLTC contacts at different measurement current levels.

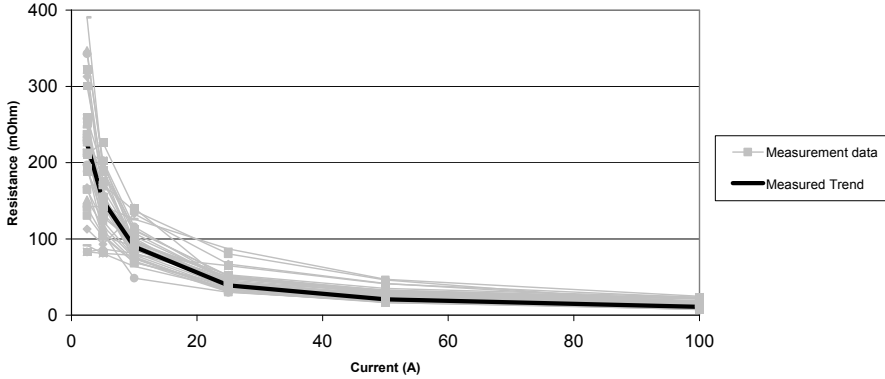


Figure 2.21 The black curve is the trend line determined on the basis of a set of resistance measurements using currents in the range $2.5 \text{ A} \leq i \leq 100 \text{ A}$.

2.4 Conclusions

This chapter gave an introductory explanation of the operation of common types of on-load tap changers, namely selector and diverter switch type OLTCs, including a coarse tap-selector, reversing switch and tap selector. It discussed the way in which degradation mechanisms can lead to failure of the tap changer. In this context, failure was defined as the situation in which the OLTC cannot perform its primary task, i.e. to select another tap without interrupting the load current. Contact degradation was modelled using equations taken from the literature and corrected with the aid of experimentally fitted correction parameters to match the results of dynamic resistance measurements on tap changers. OLTC condition diagnosis is discussed in the next chapter.

3

On-Load tap changer diagnosis

The previous chapter discussed the way on-load tap changers degrade, which affects the transformer reliability. However, what are the possible options for an early detection of these irregularities, and what are their limitations? This chapter considers possible methods employed to assess the condition of an OLTC. There are two basic kinds of methods which can be used: applying on-line monitoring or performing off-line diagnosis.

On-load tap changer monitoring entails the continuous checking of parameters that can be acquired on-line by a fixed, mounted monitoring device. A monitoring system logs operation parameters and safeguards the normal operation of the tap changer. Monitoring devices can generate alarms directly when a defect arises. Most on-line OLTC monitoring systems also generate maintenance advice based on the total switched current, the tap position history and operation temperatures.

In contrast to on-line monitoring, off-line diagnosis is characterised by periodic rather than continuous measurements. In this way, more accurate condition information can be obtained because more advanced measurement systems are normally used. Diagnostic measurements can be used to supplement on-line monitoring, for instance when the monitoring system indicates a defect, but can also be applied separately. The focus of condition assessment techniques is to identify defects at the earliest stage, before significant damage is caused. Early discovery and remedy of defects avoids expensive consequences [40].

Table 3.1 shows which of the OLTC diagnostic measurements discussed in this chapter can be applied on-line. The tap changer is subdivided into the oil / insulation and the mechanical part. The applicability of the diagnostic methods to these subsystems is also shown in Table 3.1. The methods that are suitable for those parts will be discussed separately in Sections 3.1-3.3.

Table 3.1 Overview of OLTC diagnostic measurements discussed in this thesis and their applicability to five subsystems.

	mechanical		electrical contacts		dielectric
	before springs	after springs	arcing switch	change-over selector	
Inspection / functional check offline	3	2	3	0	2 ^V
Dissolved gas analysis online offline	0	0	1	1 ^{III}	1 ^{VI}
Vibration / Acoustic fingerprint online offline	2	2	1 ^I	1 ^I	0
Temperature measurement online	0	0	1	2 ^{IV}	0
Motor power measurement online offline	3	0	0	1 ^I	0
Axis position measurement offline	0	1	1 ^I	0	0
Static resistance measurement offline	0	0	2 ^{II}	3	0
Dynamic resistance measurement offline	1	1	3	3	0
Transformer turn ratio test offline	0	0	1	1	0

0	not suitable
1	suitable as a functional check for a part of the subsystem or for some defects
2	suitable for a part of the subsystem or very suitable for some defects
3	very suitable

I	Diagnoses (excessive) friction
II	Only when the arcing switch insert is not removed
III	Rough diagnoses of coking
IV	Diagnoses only the current tap position
V	Only arcing switch accessible
VI	Diagnoses discharges and isolation aging

3.1 Oil and insulation diagnosis

3.1.1 Dissolved gas analysis

A frequently used method for transformer diagnosis is the analysis of transformer oil. This method is called dissolved gas analysis (DGA). A sample of oil is taken and the gasses which are dissolved in it are analysed, typically hydrogen, methane, ethane, ethylene, acetylene, carbon monoxide and carbon dioxide [37]. The method can be applied to oil from the arcing switch compartment [41] and to the oil of the (coarse) tap-selector. The method is based on the fact that oil decomposes into different gases depending on the temperature at the location of a defect (see Figure 3.1). A conclusion about the type of defect can thus be drawn. Detectable defects include contact coking, overheated contacts and insulation degradation. Duval [41-42] shows that gas development due to defects is temperature dependent (Figure 3.1 and Table 3.2). Some OLTC defects can also be found with DGA. The oil from the arcing switch compartment can provide valuable knowledge about the switching performance. [43] gives some examples of DGA results for an OLTC which suffers from coking, overheating or arcing. Specific gas concentrations can be used to draw global conclusions about the type of defect (Figure 3.2).

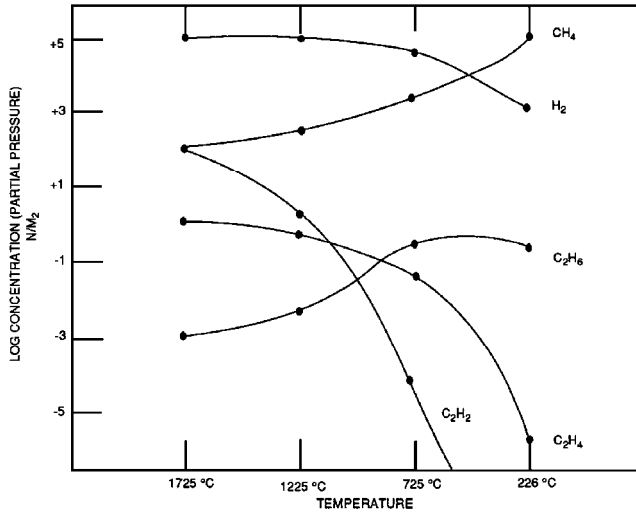


Figure 3.1 The concentration of dissolved gases is dependent on the fault temperature [44].

Table 3.2 Specific key gases are formed when transformer insulation oil decomposes into different gases. This process is dependent on the temperature at the location of a defect [45].

Key Gas	Characteristic Fault
H ₂	Partial Discharge
C ₂ H ₆	Thermal Fault <300 °C
C ₂ H ₄	Thermal fault 300 °C to <700 °C
C ₂ H ₂ , C ₂ H ₄	Thermal Fault >700 °C
C ₂ H ₂ , H ₂	Discharge of Energy

DGA provides on-line OLTC diagnosis. However, dissolved gas analysis does not offer precise information about change-over selector contact wear when it shares its oil with the transformer oil of the main tank. For example, DGA is effective when the contact temperature exceeds 400-500 °C due to a low rate of gas generation below the boiling point [36]. Due to the small heating surface (a few cm²) the rate of gas generation could be only a few ppm a month; gassing could be a symptom of severe contact deterioration [36]. Localisation of the defect is always difficult. In addition, looking at the trend in specific gases only provides a warning about failure in serious cases, such as overheating and thermal runaway [46]. Moreover, regular leakage of dirty oil from the arcing switch compartment to the change-over selector makes an unambiguous analysis of oil in the main tank difficult. To conclude, defects inside the OLTC take some time to show in a DGA.

Oil samples for DGA can be analysed in a laboratory, but on-site devices for DGA are also available, for example the ones described in [47-49].

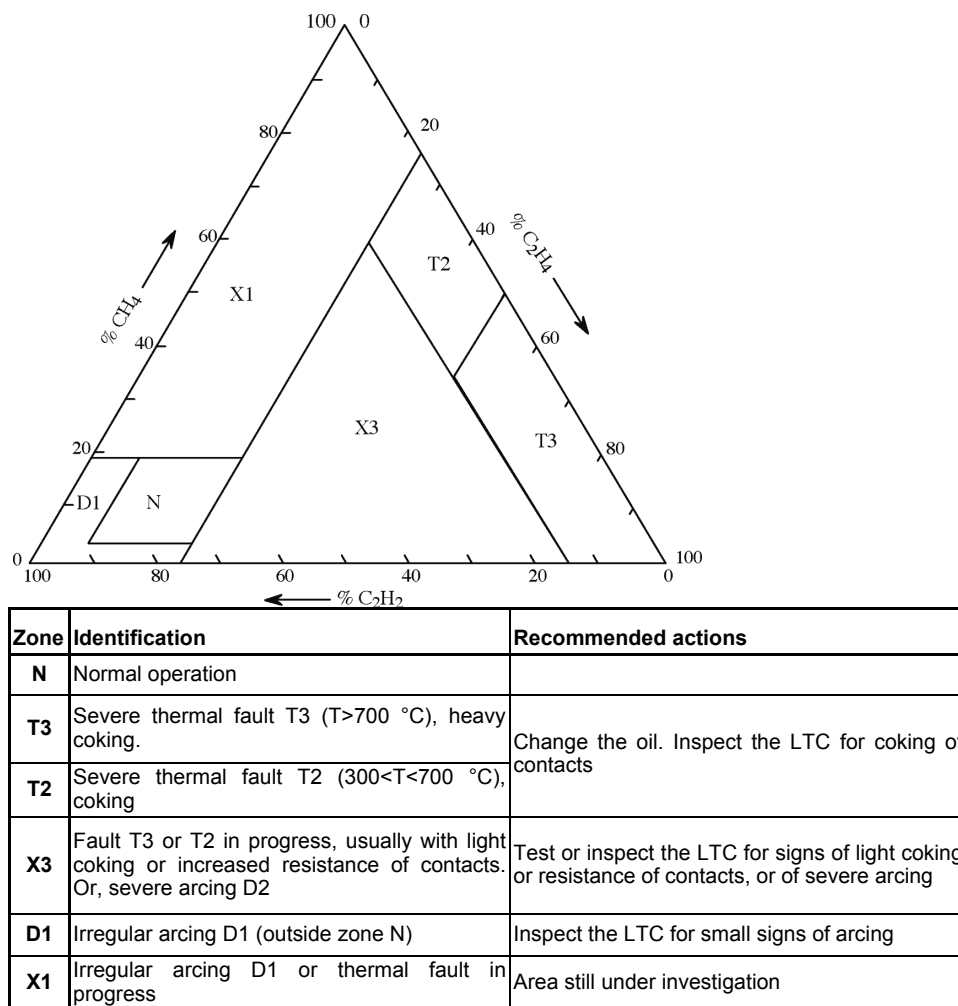


Figure 3.2 The Duval Triangle determines the source of the gas by looking at OLTC gas ratios [41].

3.1.2 Study of the agreement between DGA and DRM results

It is of interest to know if there is a relationship between the gases that are produced at degraded change-over selector contacts and the results of dynamic resistance measurements. Both methods are sensitive to coking [43], which occurs during the long-term aging effect on the OLTC contacts. In this situation, the gases CH_4 , C_2H_6 and C_2H_4 are formed. C_2H_2 and H_2 are expected to form in the advanced stages (at higher temperatures). In addition, the contact resistance will increase, and therefore a relationship with DRM is expected.

Figure 3.3 shows a possible relationship between DGA and DRM results. Increasing gas concentrations were measured in the transformer main tank oil, which triggered the Buchholz alarm three times (indicated with arrows in Figure 3.3). Analysis of the gas concentrations and ratios indicated a serious thermal fault with coking. DRM results showed increased contact resistance on a few tap positions, an indication of a tap-selector contact problem. Inspection of the tap-selector contacts indeed showed overheated contacts as predicted by DGA and DRM (the overheated and normal contacts are shown in Figure 3.3-inset).

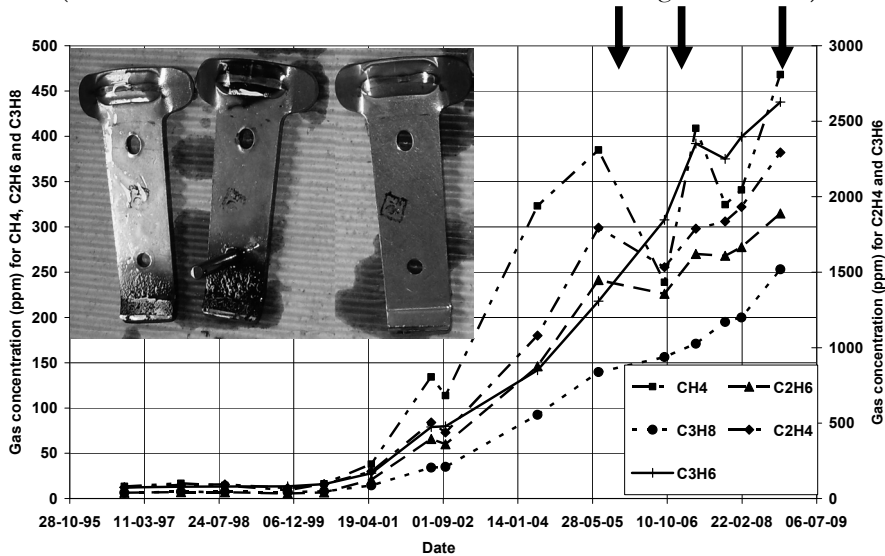


Figure 3.3 Example of DGA results for an OLTC with overheated tap-selector contacts (inset). Rising gas concentrations are visible, which caused Buchholz alarms at the dates indicated by an arrow.

To determine whether there is a general similarity between DRM and DGA results, a population of OLTCs was selected. Oil samples were taken from the main tank and a dynamic resistance measurement was performed on all transformers.

The dataset selected contained 72 transformers. The power rating of the transformers was between 18 MVA and 30 MVA. Most of the transformers had a voltage ratio of 50 kV/10 kV and have selector switch type tap changers with a change-over selector. Each change-over selector was measured with DRM:

- 31 were in good condition
- 26 were in moderate condition
- 15 were in severe condition

This information on the condition of the tap changer, together with the results of DGA tests, was used for statistical analysis.

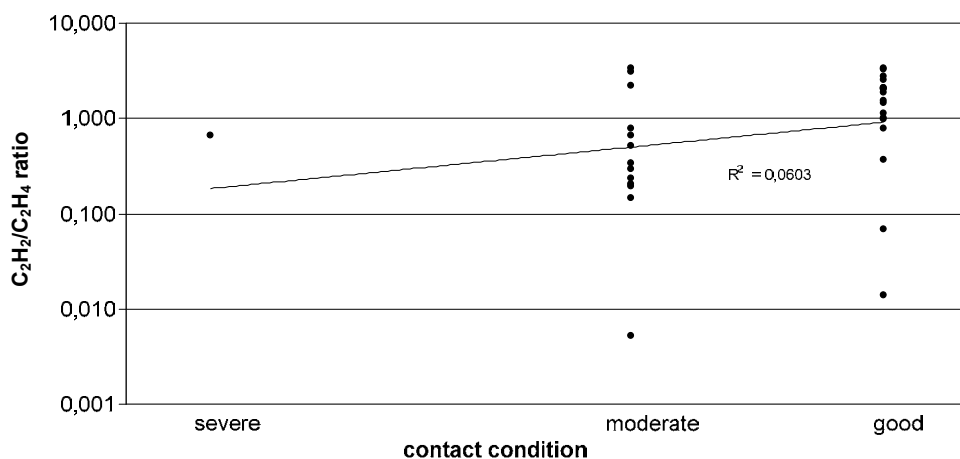
First, the correlation between the gas produced (or gas ratio) and the condition of the tap changer is calculated. The result reveals that C_2H_4 and C_3H_6 and the gas

ratios C_2H_4/T (where T represents $[CH_4 + C_2H_4 + C_2H_2]$) and C_2H_2/C_2H_4 have the best correlation with the information about the condition of the OLTC. Gas ratios were only calculated if one of the gases exceeds the Duval limits (for example 3 ppm for C_2H_2 and 75 ppm for C_2H_4). For example, C_2H_2/C_2H_4 has the highest correlation of 0.25 with the DRM results, which means that the gas ratio is expected to decrease as the condition of the contacts deteriorates.

Scatter plots of the gases which have the highest correlation have been made. Figure 3.4 shows this scatter plot for C_2H_2/C_2H_4 . There is a large correlation between the dissolved gases and the three contact conditions as determined by DRM (good, moderate and severe).

A probability density plot was then made to determine the best fit of the regression line onto the gases, using the Weibull distribution. Again, a large correlation was found between the probability density functions of the C_2H_2/C_2H_4 conditions, which was expected regarding the scatter plot.

Using this dataset, only a very weak relationship between the condition of the OLTC change-over selector contacts (as measured with DRM) and a certain gas amount or gas ratio was found. A C_2H_2/C_2H_4 ratio could not be related to the DRM results. This can be explained firstly by the large amount of oil in the main tank: different degradation mechanisms can produce various gases at the same time and distort the conclusions. Secondly, the main tank exchanges air with the surrounding environment through breathers, and thus gases formed by coking can be dissipated. Therefore, it is concluded that DRM can be used for finding contact problems that did not appear in DGA.



3.2 Mechanical diagnosis

3.2.1 Acoustic and vibration signature

The moving parts of the drive mechanism produce acoustic waves and vibrations when the OLTC is in operation. Tap changers with mechanical or electrical problems produce different signals compared to healthy tap changers. The number of bursts, the time between them [13], the main frequencies [50] and the strength of the signal can contain valuable information. Comparing the signal measured with a known signature will indicate these problems. For this comparison it is necessary to know the signature of a healthy tap change operation. A large number of measurements have been used to determine a normal operation for each type of tap changer. One can also compare the measurements with previous measurements to see if the tap changer is damaged or whether excessive arcing occurs. These measurements can be performed periodically or continuously and can be done on-line. Problems in the arcing switch and the change-over selector can be distinguished because they operate at another time. Monitoring devices [51] compare the signatures at every tap change, in this way looking at the development of wear.

Figure 3.5 shows an example of the acoustic waves that are recorded when an OLTC operates. Hilbert transform was used to present this envelope. The tap changer was measured when the transformer was in an energised and de-energised state. Comparing the recordings of an energised and de-energised transformer can separate the electrical (arcing) and mechanical sources.

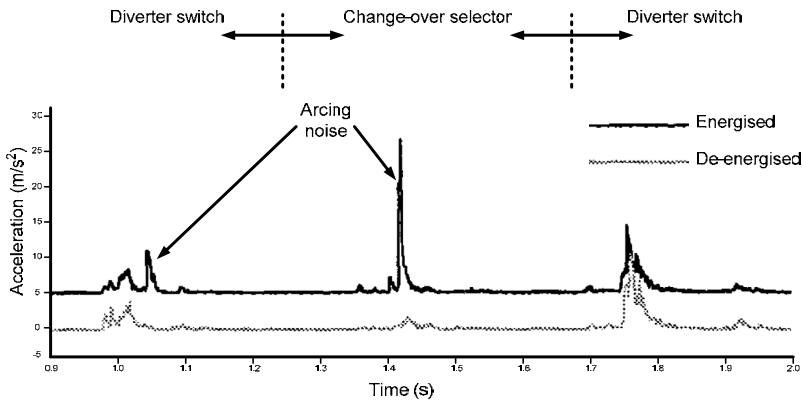


Figure 3.5 Example of acoustic waves that can be recorded on an energised and de-energised OLTC, after Hilbert transform [52].

To obtain the desired information from the complex measurement data, a transformation can be applied to the data, for instance a Fourier transform or continuous wavelet transform [53]. References [13],[51] and [54-56] discuss this

diagnostic method in-depth. An example of a method using acoustic and vibration signatures is given in [57].

3.2.2 Motor power measurement

Defects or friction in the drive mechanism and the OLTC can also be detected by the measurement of the active power consumption of the drive motor [58]. The active power consumption is proportional to the delivered torque of the motor. Irregularities in power consumption can therefore indicate defects in the mechanical system that is connected to the motor. The springs inside the drive mechanism act as an energy accumulator and separate the motor drive from the OLTC itself. Measuring motor power will therefore allow diagnosis of defects in the drive from the motor to the springs. This measurement can be done both on- and off-line.

Figure 3.6 provides an example of an off-line measurement of a motor power curve of an OLTC drive motor. Power variations can be caused by moving the selector contacts or by loading the springs.

Some tap changer monitoring devices use the motor operation time in combination with average or maximum active power consumption. The start-up time of the motor can also provide information about the status of the drive. The curve can also be compared with earlier measurements. The location and amplitude of the power peaks can indicate their cause.

Another example of a motor power measurement is described in Ref. [59].

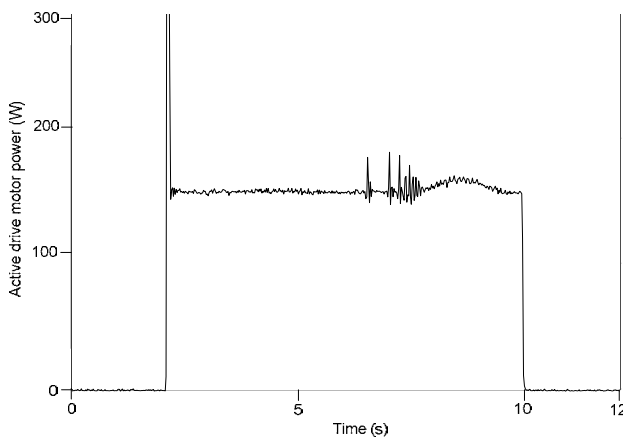


Figure 3.6 The motor power of a tap changer drive motor shows the inrush current followed by a stable operation. Power variations can be caused by moving the selector contacts or by loading the springs.

3.2.3 Position measurement

Section 3.2.2 showed that the active motor power consumption of the drive motor can reveal defects and friction in the mechanical system up to the spring system. Another method is necessary to diagnose that part of the drive mechanism and the tap changer that is operated after releasing the springs. Measuring the position of the remote end of the drive shaft is one way, although the drive shaft is not always accessible at the remote end. Each OLTC operation results in a movement of the shaft (see Figure 3.7, the DRM-current is also plotted). It can be clearly seen that the shaft oscillates at the end position.

A position measurement such as this can be used to derive the graphs of velocity and acceleration. Defects, friction, torsion or synchronisation problems between the phases alter these graphs, so a comparison with earlier measurements is indispensable.

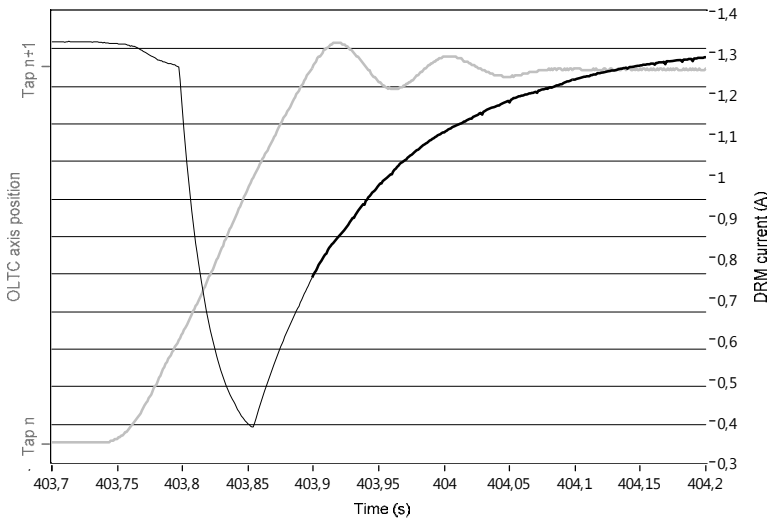


Figure 3.7 The movement of the remote end of the drive shaft can show defects or friction in the OLTC.

3.3 Contact status diagnosis

In addition to mechanical and insulation condition assessment, diagnosis of the contact status can be performed. Three methods for contact diagnosis will be discussed in this chapter. Apart from the methods discussed here, [60] mentions that the exciting current and power factor in a transformer turn ratio measurement and a sweep frequency response analysis can also indicate contact problems.

3.3.1 Temperature difference measurement

Damaged contacts inside the tap changer, for instance due to coking of the change-over selector contacts, can lead to increased contact resistance. This is accompanied by an increased power loss. These power losses may run up to hundreds of watts for each contact at a nominal current [11]. At OLTCs which are mounted against the transformer tank, the temperature of the oil can increase significantly due to power losses on the contact interface. A temperature difference between the tap changer oil and the main transformer oil will then develop [50]. A healthy tap changer will produce very little heat and its temperature will be lower than the main tank. Table 3.3 shows an example of how the temperature difference can be interpreted.

In the case of an external OLTC, temperature difference measurement can be used as a diagnostic or monitoring tool to detect bad contacts. This method has been applied to reactor type OLTCs. Resistor-type OLTCs may warm the oil in the external tap changer tank through the heat developed in the transition resistors. However, as only one tap position is measured, the problematic contacts that are not a part of the current circuit and do not produce heat will not be detected.

Table 3.3 Example of how the temperature difference between the tap changer and the main transformer tank can be used to diagnose the contacts [45].

CLASSIFICATION	TEMPERATURE EXCESS
Attention	0–9 °C
Intermediate	10–20 °C
Serious	21–49 °C
Critical	>50 °C

The monitoring of the temperature difference can be done on-line. Fixed sensors inside the transformer can be used and should be positioned on the same side at the same elevation [61]. Other heat sources such as sun or a changing load should not cause warning signals when the OLTC's oil heats faster than the oil in the main tank or vice versa [50]. The same problem can occur when the cooling fans switch on and off [50].

External tap changers can also be diagnosed by infrared thermography, see Figure 3.8.

Examples of tap changer diagnosis using temperature measurements include [62] and [63].

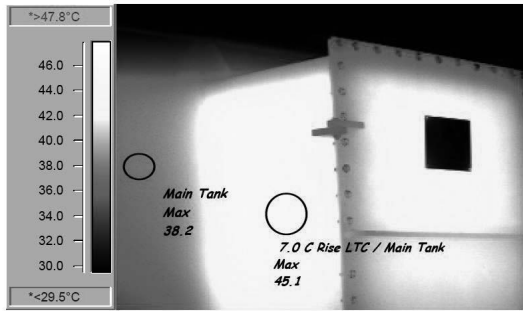


Figure 3.8 Infrared image of an OLTC, where the tap changer temperature is about 7 °C higher than the transformer main tank due to contact problems [64].

3.3.2 Static resistance measurement

OLTC contact degradation can be measured by means of a resistance measurement. Additional information is obtained compared to the temperature measurement because all tap positions are measured. These resistance measurements are performed when the tap changer is motionless and are therefore referred to as static resistance measurements.

Static resistance measurement can be performed using a simple DC power source or a dedicated measurement device. Static resistance measurements can be used to:

- Determine the resistance of each tap position, see Figure 3.9. A straight line is seen when the tap changer is in good condition. This method is also called a transformer DC winding resistance measurement because the tap changer is measured in series with the transformer windings. As the windings have a large inductance, this measurement takes a long time: the resistance is measured when the current through the winding is completely stable. Equation 3-1 shows this relationship. Resistance is measured when $dI/dt=0$.

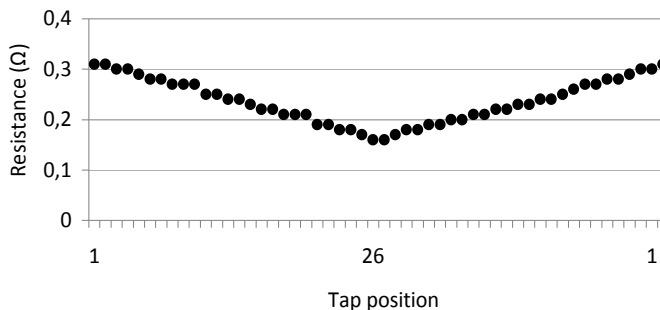


Figure 3.9 Graph of the static resistance measurement of all tap positions.

$$U = I * R + L * \frac{dI}{dt} \quad 3-1$$

The results obtained can be compared with earlier resistance measurements, but one should be careful to correct the readings for changes in the winding temperature because values depend on the latter, according to Equation 3-2.

$$R_S = R_M \frac{(T_S + T_K)}{(T_M + T_K)} [65] \quad 3-2$$

Where:

R_S = resistance at reference temperature T_S

R_M = measured resistance

T_S = reference temperature

T_M = temperature at which resistance was measured

T_K = Temperature coefficient, 234.5 for copper and 225 for aluminium

- Determine the resistance of one tap position when the current is increased and decreased. A considerable memory effect is measured when the contacts are degraded (see also Appendix C). New contacts barely show this effect. The resistance of the carbon and the surface film is highly dependent on the current [11]; therefore a resistance measurement with high measurement currents can diagnose the degradation at currents that resemble the operation conditions. In this case, the removable part of the arcing switch is taken out and the measurement current is directly applied to the change-over selector. In this way, the main transformer windings are not measured, so a higher current can easily be applied to the tap changer. A DC power source can be used to measure the resistance (for example up to 100 A). An example of such a measurement on degraded contacts is shown in Figure 3.10 [11]. The initial resistance can be in the range of 500 mΩ. When the current is increased, the resistance of the carbon usually decreases (for example to about 20 mΩ). A memory effect is present when the current is decreased, as the resistance does not rise to the initial value again. Section 4.2.2 will discuss this memory effect in more detail. A coarse tap winding can be located in series with the measurement in some tap positions. This value has to be subtracted from the measured contact resistance.
- Detect discontinuity of the OLTC. The tap changer can be operated between two static resistance measurements and some transformer ohmmeters can detect discontinuity in the measurement current.

Resistance measurements on tap changers can be performed using transformer ohmmeters such as [66] and [67].

3.3.3 Dynamic resistance measurement (DRM)

Dynamic resistance measurement is suitable for detecting irregularities in the OLTC contact resistance, as are static resistance measurements. The main difference between dynamic measurements and static measurements is that the tap changer is operated during the measurement. Important information about the importance and location of the long-term effect on the change-over selector contacts can be extracted from the measurement. The contacts do not remain at each position long enough to allow the measurement current to stabilise (stabilisation is attained after a relatively long time constant caused by a high inductance of transformer windings). Despite the fact that DRM can be considered less accurate than static resistance measurements, it may provide more information about the type and location of defects inside the OLTC. For example, a typical dynamic measurement does not allow enough time to stabilise the measurement current and cannot reveal contacts with resistance increased by $100\ \mu\Omega$, whereas static resistance measurement can do this, but cannot show irregularities in the transition time. Chapter 4 deals with DRM in more detail.

Examples of diagnostic instruments that are able to show the dynamic resistance during operation are [12] and [68-70].

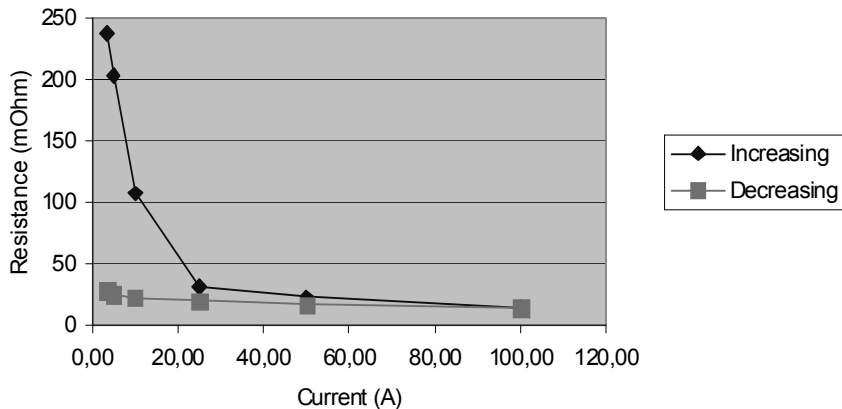


Figure 3.10 Typical resistance measurement example [11]. When the current increases, the resistance will decrease. In this example the resistance dropped from $237\ m\Omega$ to $14\ m\Omega$ when the current was increased from $3.5\ A$ to $100\ A$. At a decreasing current the memory effect means the resistance cannot rise.

3.4 Discussion

In Table 3.4 we give an overview of the diagnostic methods for OLTC as discussed in the previous sections. The following can be concluded:

- **Visual inspection** can be used to reveal degradation in the accessible parts of the OLTC and drive mechanism. Inspection intervals are determined by the number of operations or by time intervals, whichever comes first [71]. However, not all parts are accessible for inspection. Change-over selector contacts, for example, are not accessible in in-tank type OLTCs. Other diagnostic methods can be used to diagnose these parts and to detect maintenance errors.
- **Dissolved gas analysis** is in principle sensitive to the irregular operation of the contacts due to coking and overheating. However, oil samples taken from the main tank of two-compartment type OLTCs provides information about all components in the main tank, which masks the sought information about contact conditions. Other methods can be used to localise the defect. DGA is insensitive to mechanical defects.
- **Acoustic vibration measurements** on the OLTC are useful for detecting mechanical and electrical defects. Both types of defects can be distinguished by comparing measurements of an energised and a de-energised OLTC and by looking to dominant frequencies in the signal. On-line and off-line measurements can be performed: on-line measurements can be used to detect defects and degradation at an early stage, which can limit possible damage to the transformer.

Different types of OLTCs can produce different vibration signals, the interpretation of vibration signals can therefore be complex. The method is insensitive to dielectric degradation.

- **Temperature measurements** on the OLTC can also be useful to detect increased contact resistances. This measurement is performed on-line but does not diagnose the tap positions that have not been used. Defects that do not generate heat are not detected. This method is applicable to reactor type OLTCs installed in a separate tank.
- **Motor power and shaft rotation measurements** can be used to find problems in the drive mechanism: active motor power consumption in the mechanical system up to the spring system and drive shaft rotation for parts behind the springs.
- **Static and dynamic resistance measurements** can determine the condition of the contacts. For a dynamic measurement it must be possible to short circuit the transformers secondary windings, because the effect of the resistance changes can then be recorded with high time-accuracy. Both methods use off-line measurements. Section 3.3.3 concluded that dynamic resistance measurements provide more information about the condition than static measurements because a larger contact surface is measured. This is an added value of dynamic resistance measurements.

Other methods than resistance measurements must be used to obtain a full picture of the insulation condition and mechanical condition (although DRM is able to detect defects in the drive mechanism that affect the operation of the contacts).

DRM results were compared with the results of DGA in Section 3.1.2: statistical analysis showed that there is no significant correlation between defects that are detected with the DGA and the DRM method on the basis of the database and parameters used. Resistance measurements and DGA can be considered to supplement each other.

Resistance measurements and ratio measurements are common detection methods for power transformer defects [72-73] and these methods, together with inspection and gas analysis, account for 61% of the popular power transformer measurements [72]. These two methods are particularly suitable for detecting defective windings. In addition, resistance measurements are also suitable for detecting contact degradation, especially when applied while the OLTC is in operation.

Table 3.4 Overview of OLTC diagnostic measurements. Each method diagnoses particular areas of the OLTC: the practicability is indicated for each method.

Visual inspection		
Mechanical (drive)	Up to springs	The drive can be inspected for wear and defects
	Behind springs	The drive can be inspected for wear and defects
Electrical contacts	Arcing switch	Accessible for inspection: contact wear can be recognised, misaligned contacts could be visible.
	Change-over selector and tap-selector	In-tank contacts are not accessible for inspection
Dielectric		Arcing switch compartment is accessible for inspection

Dissolved gas analysis		
Mechanical (drive)	Up to springs	Mechanical defects usually do not influence DGA results
	Behind springs	Mechanical defects usually do not influence DGA results
Electrical contacts	Arcing switch	Contact coking, contact wear leading to excessive arcing or overheated contacts can be detected by DGA, but is not considered reliable since the products of oil decomposition by arcing masks the effect of contact degradation.
	Change-over selector and tap-selector	Contact coking, discharges or overheated contacts can be detected by DGA. In case of two compartment type OLTCs, the oil sample resembles the condition of all components in the main transformer tank and this method is not considered reliable since the products of oil decomposition by arcing may leak from the arcing switch compartment.
Dielectric		Insulation degradation due to high contamination and surface discharged (treeing) can be detected.

Acoustic vibration measurements		
Mechanical (drive)	Up to springs	Mechanical defects can cause deviations in the vibration signature compared to recordings from the same type of OLTC.
	Behind springs	Mechanical defects can cause deviations in the vibration signature compared to recordings from the same type of OLTC.
Electrical contacts	Arcing switch	Excessive arcing and friction can be visible in the vibration signature.
	Change-over selector and tap-selector	Excessive arcing and friction can be visible in the vibration signature.
Dielectric		Dielectric defects and degradation usually do not show in vibration signatures.

Temperature measurements		
Mechanical (drive)	Up to springs	Mechanical defects do usually not generate heat.
	Behind springs	Mechanical defects do usually not generate heat.
Electrical contacts	Arcing switch	Contact coking or overheated contacts that carry the load current can generate heat and can be detected.
	Change-over selector and tap-selector	Contact coking or overheated contacts that carry the load current can generate heat and can be detected.
Dielectric		Dielectric defects and degradation usually do not generate heat.

Motor power measurements		
Mechanical (drive)	Up to springs	Friction, contact binding and wear can change the active motor power needed for the OLTC operation.
	Behind springs	The drive mechanism behind the spring system is not powered by the drive motor but by the springs.
Electrical contacts	Arcing switch	The contacts after the spring system is not powered by the drive motor but by the springs.
	Change-over selector and tap-selector	Friction and contact binding can change the active motor power needed for the OLTC operation.
Dielectric		Dielectric defects and degradation usually do not affect the active motor power.

Shaft angular position measurement		
Mechanical (drive)	Up to springs	Defects and degradation in the drive system usually do not affect shaft rotation.
	After springs	The rotation of the remote end of the drive shaft can give condition information about the mechanical properties of the shaft, friction and synchronisation problems between phases.
Electrical contacts	Arcing switch	Friction of the contacts can influence the shaft rotation.
	Change-over selector and tap-selector	The change-over selector and tap-selector are usually not accessible for position measurements.
Dielectric		Dielectric defects and degradation usually do not affect the axis rotation.

Static resistance measurements		
Mechanical (drive)	Up to springs	Defects and degradation in the drive system usually do not affect contact resistance.
	After springs	Defects and degradation in the drive system usually do not affect contact resistance.
Electrical contacts	Arcing switch	One contact position is diagnosed, defects and degradation such as contact wear, coking and misalignment can be detected.
	Change-over selector and tap-selector	One contact position is diagnosed, defects and degradation such as contact wear, coking and misalignment can be detected.
Dielectric		Dielectric defects and degradation usually do not affect contact resistance.

Dynamic resistance measurements		
Mechanical (drive)	Up to springs	Defects and degradation in this part of the drive system usually do not affect dynamic resistance.
	After springs	Defects and degradation in the drive system can influence OLTC transition time and can be detected with DRM.
Electrical contacts	Arcing switch	All contact positions are diagnosed, defects and degradation such as contact wear, coking and misalignment can be detected.
	Change-over selector and tap-selector	All contact positions are diagnosed, defects and degradation such as contact wear, coking and misalignment can be detected.
Dielectric		Dielectric defects and degradation usually do not affect contact resistance.

The overview in Table 3.4 can be summarized, as in Table 3.5. From Table 3.5 it can be concluded that none of the methods provides a full OLTC diagnosis.

- **Mechanical** condition diagnosis can be obtained by:
 - Inspection
 - Acoustic/vibration measurements
 - A combination of:
 - Motor power measurement (for defects up to the spring system)
 - Position measurement on the remote end of the drive shaft (for defects behind the spring system)
- **Electrical contacts** that are not accessible for inspection may benefit from resistance measurements. Static and dynamic resistance measurements are both performed on all tap positions, but DRM provides more information about the condition of the contacts than static resistance measurements because the contact surface for the entire cycle of operation is measured. In addition, DRM can detect a wider variety of maintenance errors because contact timing is also checked.

Temperature measurements can reveal serious defects in the OLTC, but are less sensitive to increased contact resistances compared to resistance measurements. Defective contacts that are not selected are not recognised by temperature measurements.

In addition, DGA can also detect arcing and contact coking, but determining the location where coking occurred is more difficult compared to resistance measurements.
- **Dielectric** degradation can be detected by dissolved gas analysis. The arcing switch compartment insulation can be examined during inspection.

Table 3.5 Overview: suitability of OLTC diagnostic measurements as described in Table 3.4 for finding defects and degradation in particular parts of the OLTC.

Suitability of the discussed methods to diagnose specific OLTC parts		
Mechanical (drive)	Before springs	Inspection, acoustic vibration analysis, active motor power measurement.
	After springs	Inspection, acoustic vibration analysis, shaft rotation, dynamic resistance.
Electrical contacts	Arcing switch	Inspection, static and dynamic resistance, temperature measurements, acoustic vibration analysis.
	Change-over selector and tap-selector	Static and dynamic resistance, temperature measurements, DGA, acoustic vibration analysis.
Dielectric		DGA, Inspection.

3.5 Conclusions

This chapter evaluated the various methods that can be used to diagnose the condition of an OLTC, thereby detecting irregularities at an early stage, especially defects that are not seen during inspection and due to maintenance errors. The tap changer was first subdivided into three parts: oil and insulation, mechanics and the contacts. Arcing switch contacts were distinguished from change-over selector contacts (including tap-selector contacts).

Each diagnostic method was shown to be sensitive to defects in particular parts of the tap changer. Every method also proved to have its limitations. Table 3.4 provided an overview of the methods and their suitability to each of the OLTC parts. Table 3.5 showed that none of the methods provides a full OLTC condition diagnosis. Therefore, a combination of different methods would be worthwhile:

- Diagnosis of the mechanical system of the OLTC can be obtained by inspection, acoustic vibration measurements or through a combination of motor power and shaft position measurements.
- Electrical contacts that are not accessible for inspection may benefit from DRM. The following chapter will examine DRM in more detail.
- DGA is a popular method for diagnosing the OLTC dielectric.

Table 3.5 showed that parts of the tap changer can be diagnosed by more than one method because there is some correlation in their results. Section 3.1.2 elaborated on the relationship between DRM and DGA results; however, no relationship between the condition of the change-over selector contacts (as measured with DRM) and a certain gas amount or gas ratio was found for the dataset selected.

4

Dynamic resistance of on-load tap changers

As mentioned in the previous chapter, static resistance measurements on a transformer indicate increased contact resistances in the OLTC. These increased contact resistances can be measured by means of a dynamic resistance measurement (DRM). However, what is the additional value of this measurement and what are the important parameters that should be considered when performing dynamic resistance measurements? This chapter discusses the different aspects of dynamic resistance measurements, for example the measurement setup, the influence of the amplitude of the measurement current and voltage, the effect of circuit resistance and the secondary short circuit.

DRM runs a current through the OLTC to detect increased contact resistances and interruptions in the current while operating the contacts. The difference from static resistance measurements is that the tap changer is switched through all its tap positions during the measurement. The current has no chance to fully stabilise due to the inductance of the transformer windings. Dynamic resistance measurements are therefore less accurate in resistance value than static measurements but provide more information about the type and location of defects. This chapter will show that DRM finds more defects on OLTCs than can be found using static resistance measurements.

DRM was originally used for circuit breaker analysis, in which a high current, typically 100 A or higher, is applied to the closed circuit breaker and the voltage across the circuit breaker is measured. The circuit breaker is then opened. Valuable information about the arcing contacts inside the circuit breaker can be extracted from the contact resistance of the moving contacts and a high resolution can be obtained by the high measurement current.

4.1 Measurement setup

When DRM is applied to a power transformer, valuable information about the condition of the tap changer is obtained. Several options are possible:

- Send a measurement current through the transformer and measure the secondary voltage while the OLTC is in operation. The tap changer is measured indirectly by measuring the voltage induced on the side of the transformer without a tap changer (see Section 4.1.1).
- Send a measurement current through the transformer and measure the total current while the tap changer is in operation. The effect of irregularities in OLTC resistance is directly measured (see Section 4.1.2).
- Send a measurement current through the transformer and measure the impedance [74] while the tap changer is in operation (with or without extra resistance). The effect of irregularities in OLTC resistance is directly measured (see Section 4.1.2).
- Send a measurement current through the transformer and calculate the transformer resistance while the tap changer is in operation (compensate for the dynamic behaviour of the current). The effect of irregularities in OLTC resistance is directly measured (see Section 4.1.2).
- Use an oscilloscope to measure the measurement current or voltage, adjust the trigger level to trigger on the arcing switch operation.
- Use a dedicated recorder to measure both measurement voltage and current. Use these parameters to calculate impedance, transition times and to show close-up plots. A dedicated resistance recorder may be more user-friendly than an oscilloscope.

The accuracy of these options differs in terms of time and amplitude. However, the basic principle is the same: the measurement of electrical quantities that show the effect of irregularities in resistance while the tap changer is in operation.

4.1.1 Indirect measurement of the OLTC

Most listed measurement possibilities concern measurements on the windings that include the tap changer. Only the first option takes a measurement on the windings without the tap changer. In this case, the voltage induced in the secondary windings is measured while the tap changer is in operation on the primary side. The dynamic resistance of the tap changer is indirectly measured. Figure 4.1 shows an example of this secondary voltage during tap changer operation. The plot shows a fast response to the transition resistor inside the OLTC. It can be seen that the voltage decreases because DC does not pass through the transformer, which is a drawback of the indirect measurement method.

Information about the dynamic contact resistance can be obtained with better time accuracy compared to direct resistance measurements (as will be discussed in Section 4.1.2), especially when the effect of the transformer ratio is corrected. For example, Figure 4.1 shows details of the resistance at about 0.1ms, which would not be visible when the measurement is performed on the primary side, due to the slow effect of the transformer leakage inductance.

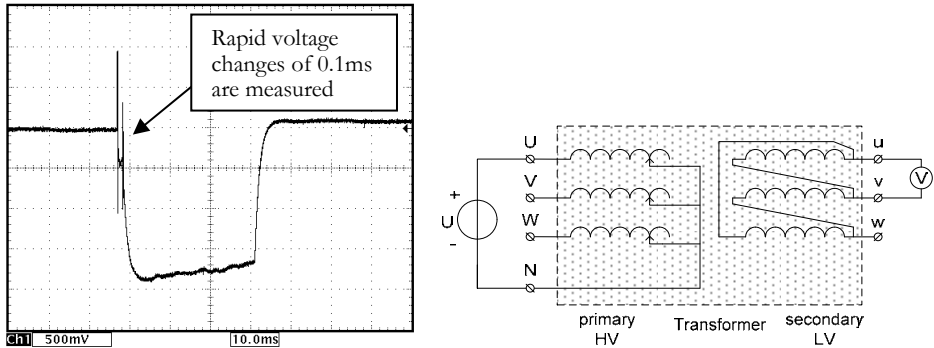


Figure 4.1 DRM applied to a transformer with OLTC. The secondary voltage is recorded while the OLTC switches.

Measurement of the secondary voltage is dealt with in Appendix B. The following section will elaborate on the options for the direct measurement of the effects of OLTC resistance. The effect of the transformer ratio is circumvented while the decreased time accuracy is acceptable. In addition, a secondary short circuit provides safety in the case of the primary measurement circuit being accidentally interrupted.

4.1.2 Direct measurement of the OLTC

Figure 4.2 shows a schematic representation of the setup for direct measurements of the OLTC. A DC test voltage is applied to the transformer and the voltage and current are measured while the transformer is switched through all of its tap positions. As the basic function of an OLTC is to change from one winding tap to another without interrupting the load current, DRM can therefore be considered a direct method of checking the basic functionality.

The resistance and inductance of a power transformer with a tap changer is significantly higher compared to a closed circuit breaker because of the presence of transformer windings. For example, transformer windings can have a resistance of 500 mΩ, while a closed circuit breaker may have a resistance of 100 μΩ. A dynamic measurement of transformer resistance always measures some of the transformer inductance because the current has no time to fully stabilise. The resistance measurement is performed while the tap changer is moving, so the inductance of the transformer still influences the impedance reading.

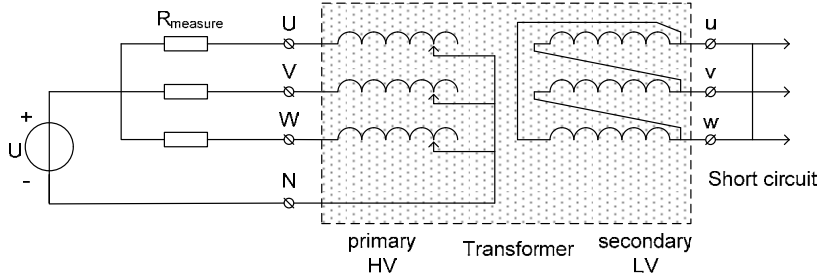


Figure 4.2 DRM applied to a transformer with OLTC. The voltage and current are measured while the OLTC switches through all its tap positions.

Due to the inductance of the transformer (for example, a leakage inductance of 50 mH), the current through the transformer cannot change quickly. The time constant of the changing current is given as:

$$\tau = \frac{L}{R} \quad 4-1$$

When the DC voltage is connected to the transformer, two effects occur. First, the current increases rapidly. The time constant can be calculated by entering the circuit parameters in Equation 4-1, resulting into Equation 4-2, where $R_{circuit}$ is the resistance of the measurement circuit, R_1 the resistance of the primary transformer windings, k the coupling factor between the windings, N the transformer ratio and L_1 the primary winding inductance. A current is induced in the short circuited secondary windings.

$$\tau_1 = \frac{2(1-k)L_1}{R_{circuit} + R_1 + N^2 R_2} \quad [75] \quad 4-2$$

As the current flows through the secondary short circuit the main inductance has no effect and the current is able to change relatively quickly. Figure 4.3 shows the voltage source connected to the transformer, represented as the T-equivalent circuit, with a short circuit on the secondary side. The time constant is in the order of tens of milliseconds. This rapid response is used during the measurement.

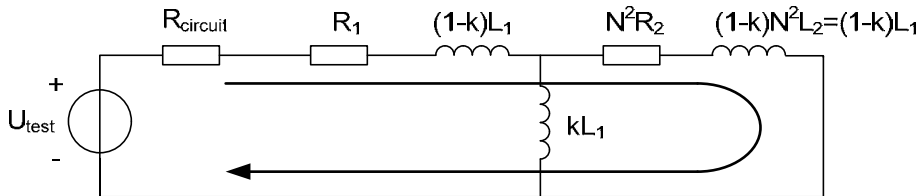


Figure 4.3 Schematic of a measurement voltage that is applied to a transformer, depicted as a T-equivalent circuit, with a secondary short circuit.

The rapid response is followed by a slower effect, with a time constant which is in the order of tens of seconds. The current now flows through the main inductance, while the current through the secondary windings decays to zero. The input impedance of the winding which is examined is then dominated by high magnetisation-inductance (for example 200 H). The energy stored in the magnetic field increases until the secondary current decays to zero, and then the measurement current stabilises. Equation 4-3 is valid after the first effect has disappeared (so the leakage inductance can be neglected). Figure 4.4 shows the path of this slowly varying current. This effect can be largely eliminated from the dynamic measurement by charging the main inductance before the measurement starts. The energy stored in the inductance slowly increases during this charging process, which uses a DC voltage source, and the dynamic measurement begins when the current through the transformer reaches its equilibrium [75].

$$\tau_2 = \frac{(R_{\text{circuit}} + R_1 + N^2 R_2) L_1}{(R_{\text{circuit}} + R_1) N^2 R_2} \quad [75] \quad 4-3$$

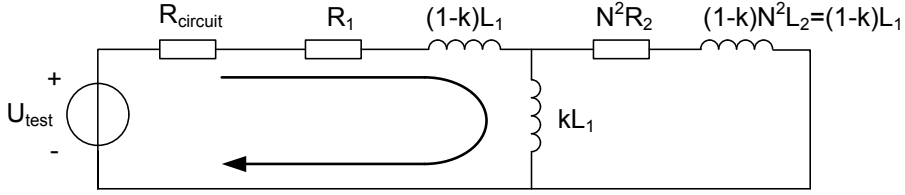


Figure 4.4 Schematic of a measurement voltage that is applied to a transformer, depicted as a T-equivalent circuit, with a secondary short circuit.

The current response when a stepwise change in the measurement voltage or in the circuit resistance is applied can therefore be written:

$$I = C_1 + C_2 e^{-\frac{t}{\tau_1}} + C_3 e^{-\frac{t}{\tau_2}} \quad [75] \quad 4-4$$

The constants C_1 - C_3 can be determined when the boundary conditions are known. For example, when a step voltage is applied to the transformer, $i_{(t=0)} = 0$ and $i_{(t=\infty)} = U_{\text{test}} / (R_{\text{circuit}} + R_1)$. Since $\tau_1 \ll \tau_2$, the current through the main inductance is still zero after a few periods of τ_1 , and therefore:

$$U_{\text{test}} = I(R_{\text{circuit}} + R_1 + N^2 R_2) \quad [75] \quad 4-5$$

Ref. [75] uses this effect to calculate the primary resistance and R_2 without a measurement on the secondary side of the transformer:

$$R_{\text{circuit}} + R_1 = \frac{U_{\text{test}}}{i_{(t=n*\tau_1)}} - N^2 R_2 \quad [75] \quad 4-6$$

$$R_2 = \frac{1}{N^2} \left(\frac{U_{test}}{i_{(t=n*\tau_1)}} - \frac{U_{test}}{i_{(t=\infty)}} \right) [75] \quad 4-7$$

Ref. [75] also uses the difference between the two time constants to calculate the value of an incremental resistance (dR) that exists in series with the primary windings to explain the change in the current (di) due to the fast effect (τ_1):

$$dR = \frac{di(R_{circuit} + R_1 + N^2 R_2)}{i_{(t=0)} + di} [75] \quad 4-8$$

Conversely, when dR is known di can be calculated from the expression:

$$di = \frac{I_{(t=0)} dR}{R_{circuit} + R_1 + dR + N^2 R_2} \quad 4-9$$

Since $\tau_1 \ll \tau_2$, Equation 4-4 can be simplified to:

$$I = C_1 + C_2 e^{-\frac{t}{\tau_1}} \quad 4-10$$

for fast changes in the OLTC resistance, so that adding a series resistor at $t=0$ results in a current response of:

$$I = I_{(t=0)} + di(1 - e^{-\frac{t}{\tau_1}}) \quad 4-11$$

In practice the measurement is performed on three-phase transformers. When the transformer windings with the OLTC are star-connected, the three phases can be measured simultaneously. Three currents are separately recorded and all three phases are short-circuited on the secondary side. Figure 4.5 shows the setup, consisting of three times the T-equivalent circuit of a transformer.

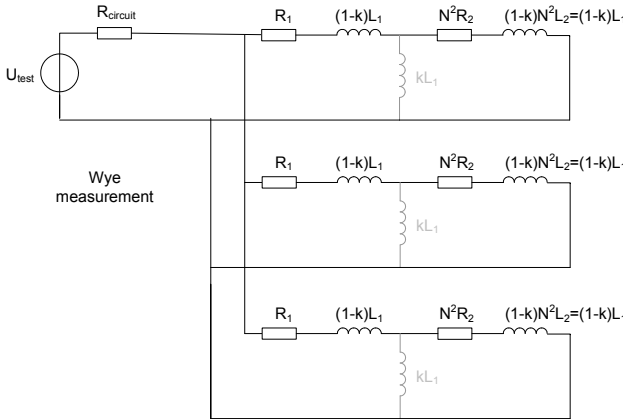


Figure 4.5 Dynamic resistance measurement on a star-connected transformer winding. Three phases can be measured simultaneously.

Transformers with the OLTC mounted in a delta-connected winding must be measured by means of three separate measurements. Only the phase that is measured needs a secondary short circuit (shown in Figure 4.7). This short circuit allows for the rapid response of the current. The other two phases lack this rapid response, so irregularities in these phases do not directly influence the current measured.

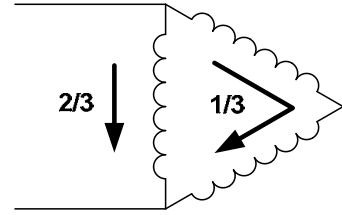


Figure 4.6 Only 2/3 of the current flows through the tested windings.

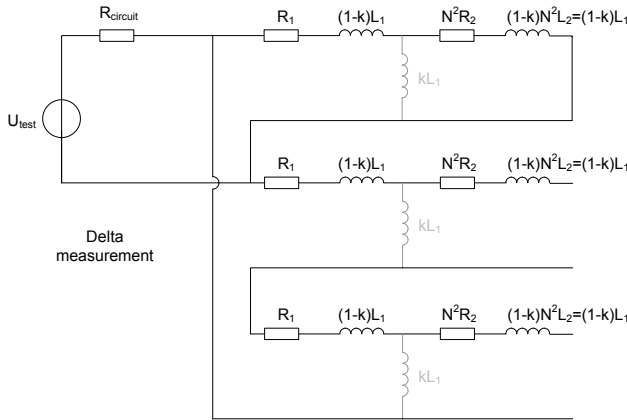


Figure 4.7 Dynamic resistance measurement on a delta-connected transformer winding. Each phase has to be measured individually.

4.2 Measurement current

4.2.1 Winding configuration

This section discusses the influence of the winding configuration on the measurement results. Chapter 4.1 already discussed the flow of the measurement current of star and delta-connected transformer windings. It was shown that the response of the current consists of a fast and a slow part in both cases. It can be seen that the fast response of the current is comparable in both configurations. However, there is a difference when the slow response is complete and the current is totally stable. Figure 4.6 shows the division of the current when the slow response takes over. The delta connection results in a division of the current. Only 2/3 of the total stabilised current flows through the OLTC phase that is diagnosed. Because of the lower measurement current, contact resistances will be higher and irregularities in this phase will be measured with a higher sensitivity.

The measurement current through the contacts should be equivalent when comparing the results. Therefore, the measurement current should be 50% higher

at delta-connected windings. For example, when charging the measurement current through a delta-connected *phase* to 1 A, the *total* current has to be stabilised to 1.5 A. In this case, the phase of the OLTC is diagnosed with the same current as a star-connected transformer winding, namely 1 A.

4.2.2 Amplitude of the measurement current

4.2.2.1 Non-linear effect during static resistance measurements

The effect of the measurement current is best demonstrated using static resistance measurements. Experiments show [11][76] that the resistance of degraded OLTC contacts is highly dependent on the measurement current and voltage that is used to determine the contact resistance. This section deals with the relationship between this effect and DRM.

Figure 3.10 showed a typical example of this current dependency on service-aged tap changer contacts: the resistance dropped from 237 mΩ to 14 mΩ when the current was increased from 3.5 A to 100 A. Figure 4.8, which shows more examples of the static resistance of a service-aged OLTC (the contacts are moved before but not during the measurement) when the current is increased to 100 A. Again, the contact resistance decreases when the measurement current is increased and even at 100 A resistance did not reach a stable reading. Section 2.3.5 already fitted a correction factor C_{DRM} on results from static resistance measurements, in order to correct measurement results for this effect. Ref. [77] comes with similar plots for the dynamic resistance of circuit breaker arcing contacts measured up to 875 A and shows that the contact resistance at 2800 A still decreases. Appendix C provides additional examples of static resistance measurements on service-aged contacts using increasing measurement currents.

Another example is shown in Figure 4.9. This figure shows typical results of static resistance measurements on clean and degraded OLTC contacts. Clean contacts can have contact resistances in the range of hundreds of micro ohms. The degraded contacts in this case had contact resistances in the range of hundreds of milliohms (measured at 2.5 A). As can be seen in the plots, it is easier to distinguish clean and degraded contacts from each other when the measurement is performed at low currents. The difference in contact resistance becomes smaller when the current is increased. However, contact degradation is measured with higher resolution when the measurement current is low, which makes it possible to distinguish contact resistance from winding resistance. Variations in the winding resistance (due to temperature variations) can be higher than the contact resistance at high currents, making it impossible to draw a conclusion about the contacts.

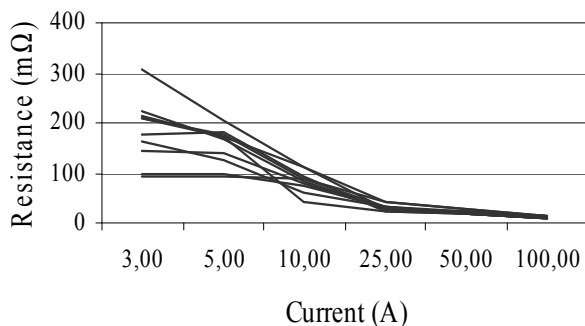


Figure 4.8 Static resistance measurements of service-aged OLTC contacts. The measurement current was increased to 100 A. A strong dependency of the contact resistance on the measurement current is revealed.

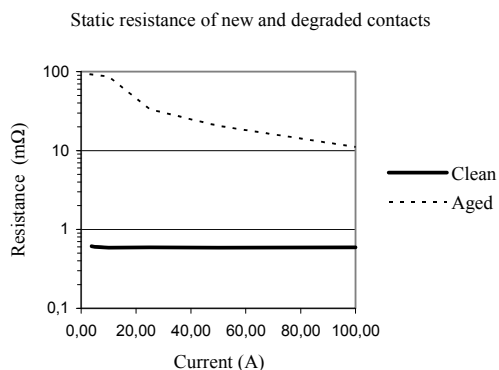


Figure 4.9 The contact resistance of clean and degraded contacts when the current is increased from 2.5 A to 100 A. Degraded contacts show high resistances at low currents, while the difference between clean and degraded contacts becomes smaller at higher currents.

The decreasing contact resistance at higher currents can be caused by several effects [34]. Firstly, the higher source voltage tends to break the thin insulating film on the contacts. Secondly, the high current can cause higher hotspot temperatures in the contact interface, melting the contact material locally. This improves the contact because the contact surface increases.

In general, it can be seen that the resistance measuring sensitivity to surface film on the contacts increases when the measurement current is decreased. This dependency can be a few decades in amplitude. A current that is too low (and therefore a low measurement voltage) might allow the thick surface film to interrupt the measurement current. The effect of the surface film decreases when the current or voltage is increased.

4.2.2.2 Non-linear effect during dynamic resistance measurements

The effect described above should also be kept in mind when one performs dynamic measurements: the magnitude of the measurement current influences the outcome directly. This effect can easily be demonstrated by performing the DRM on a service-aged OLTC using five different measurement current levels. Figure 4.10 shows the result. The current is plotted as a function of time at the moment the OLTC operates. The contact resistance may be larger when the current is low, in this example the current is almost interrupted at 200 mA, while the current profile looks undisrupted at 20 A. Chapter 7.1.2 explores the effect of the surface film in combination with low measurement currents in more depth using laboratory experiments.

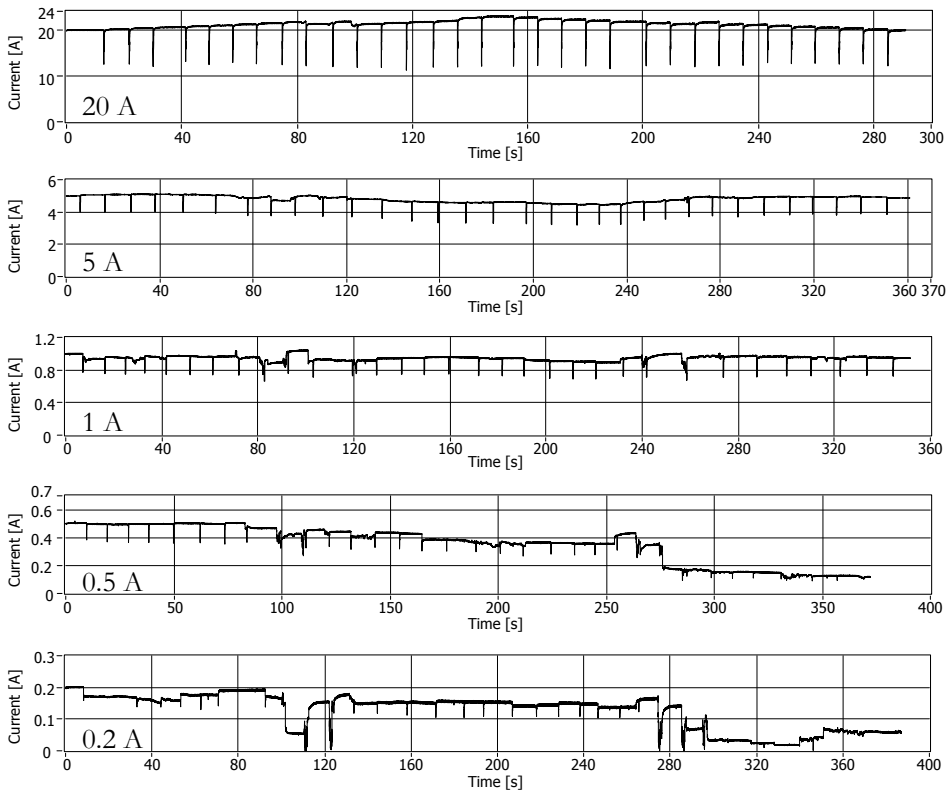


Figure 4.10 Dynamic resistance measurement on the same service-aged tap changer that suffers from the long-term effect on the change-over selector. Five different measurement current levels are used to demonstrate the influence of the amplitude.

Figure 4.11 shows an example of two dynamic resistance plots of the same service-aged change-over selector that moves over a surface film. The movement of the contact can be seen as spikes before the arcing switch operation. Two different source voltages are used. The higher voltage of 1.8 V will break the surface film, with only small irregularities being visible. The lower source voltage of 1 V is

obtained by removing the transformer windings from the measurement circuit. This results in frequent interruptions of the measurement current. This effect is also seen when the voltage is decreased by decreasing the measurement current.

This effect of the measurement current on degraded contacts is shown in Figure 4.12. OLTCs in three different aging stages were examined using DRM with five values for the measurement current and the deviation of the current from the expected value in each tap position was calculated. The expected value is the current that would be measured when there are no defects present in the tap changer. Two tap changers were measured in each category; Figure 4.12 shows the averaged maximum current deviation of those two OLTCs. A distinction between good, aged and bad contacts can be made at low measurement currents (<5 A), which is not possible at higher measurement current (e.g. 20 A). In addition, the correction factor C_{DRM} from Section 2.3.5 depends on the aging stage of the tap changer.

Transformer ohmmeters that perform static resistance measurements [67-68] also use low currents for resistance measurements. The ANSI/IEEE C57.12.90-1987 test code for power transformers advises that the current used should not exceed 15% of the rated current of the winding whose resistance is to be measured. Larger values may cause inaccuracy by heating the winding and thereby changing its temperature and resistance [65]. The selection of a suitable measurement current amplitude is complicated: on the one hand, sensitivity to surface film on the contacts increases when the measurement current is decreased, so a low measurement current, for instance below 10 A, may be desired if one wants to assess the importance of the long-term effect. On the other hand, interruptions of the measurement current due to the long-term effect may be considered undesirable because the surface film itself does not directly endanger proper OLTC operation and will not cause interruptions of the load current when the transformer is in service. The interpretation of DRM results may be simpler if only serious defects cause current interruptions. A current of at least a few hundred milliamps can be selected to prevent interruptions of the measurement current due to the thin film.

Within this margin, that is, a few hundred milliamps to 10 A, there will be large resolution differences in which the degradation can be measured. At low current, more false positive conclusions will be drawn from DRM. It will then indicate a defective situation, although no serious defect is confirmed by visual inspection or by additional measurements. Unnecessary time and money will then be spent on

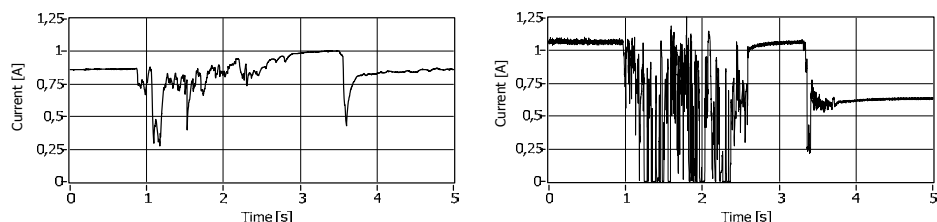


Figure 4.11 DRM of a change-over selector moving over a surface film. Left: standard DRM with a source voltage of 1.8 V. Right: The same movement when the OLTC is measured separately. The source voltage is only 1 V because the transformer windings are not in series.

the OLTC. On the other hand, a high current will result in more false negative conclusions, where a defective OLTC is not recognised by the DRM, which is a very undesirable situation. These two situations should be balanced carefully by choosing the optimal measurement current. However, the location where the degradation appears in the plots and the shape of the resistance irregularities will be the same. For that reason, this thesis discusses dynamic resistance measurements using a fixed measurement voltage with an amplitude such that the initial measurement current at the start of a measurement is 1 A. The current is not easily interrupted by the surface film at this amplitude, but the measurement is very sensitive to small defects and degradation. The chance of making false positive conclusions is then higher than of making false negative conclusions, which is desired because a transformer failure is more expensive than a diagnostic measurement.

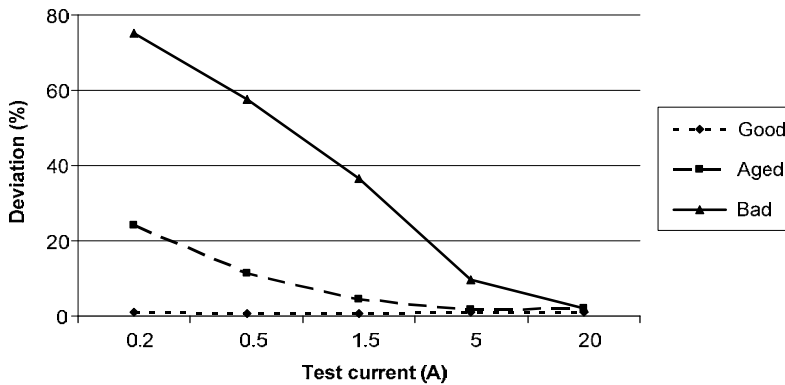


Figure 4.12 The deviation of the measurement current from the expected value decreases when the measurement current is increased. This plot shows averaged DRM results from two OLTCs with good contacts, two with aged contacts (a surface film) and two with bad contacts (with contact coking).

Due to this non-linear relationship between the current and the resistance, the resistance measured at low measurement currents does not resemble the contact resistance at nominal currents. Contact resistances measured at different current levels cannot be compared absolutely. When measuring with a low current, for example 1 A, it is unjustified to extrapolate the resistances measured to the load current level. For this reason dynamic resistance measurements at low current are considered less reliable [78]. The current level should be the same when comparing measurements (for example, from the same type of OLTC, between different winding configurations or with earlier measurements). Dynamic resistance measurements on high-voltage circuit breakers normally use currents of 100 A or higher [77-78]. Circuit breakers are designed to have a very low resistance, so a high measurement current is necessary to obtain an accurate voltage reading. A power transformer has a much higher resistance and a high current would result in a large power supply for the measurement device. The high inductance of the

transformer windings in combination with a high direct current would also make the measurement more risky.

However, the results can be very useful when the importance of the long-term effect on the change-over selector contacts is of interest. When taking the current dependency into consideration, the long-term effect can be measured with a higher sensitivity compared to measurements at currents of 100 A or higher. Again, the measured ohmic values do not resemble the contact resistance at operating currents.

4.2.3 Sensitivity

During a dynamic resistance measurement the contacts can move over degraded contact areas and it is possible that the measured resistance only deviates from normal values over a few milliseconds. The sensitivity of the dynamic resistance measurement to these brief irregularities in contact resistance is also influenced by the time that is needed for a defect to change the measurement current such that it exceeds the noise level. Defects with a high resistance force the measurement current to change rapidly. Therefore it is possible to detect defects that appear very briefly if they have a high resistance. Defects with a low resistance need much more time to change the measurement current more than the noise level. Therefore, contact degradation with a low resistance that is only measured briefly may remain below the detection limit of DRM. Figure 4.13 shows an example of the detection limit. This limit is dependent on the circuit parameters and the time constant of the transformer. Defects under the detection limit will not exceed the noise level during the dynamic resistance measurement.

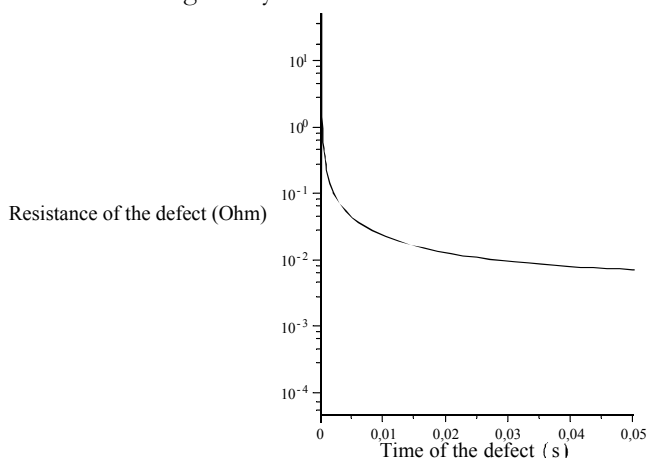


Figure 4.13 OLTC degradation that causes increased contact resistance needs time to influence the measurement current due to the circuit inductance. This graph gives an example of the detection limit of defects that appear over a certain time (x-axis) and have a specific amplitude (y-axis). Defects under this line lie below the noise level of this DRM setup. Simulation parameters: 1 Ω circuit resistance; 1 V test voltage; 20 mH leakage inductance; 5 mA noise on current measurement.

4.3 Circuit resistance

The measurement circuit also influences the sensitivity of the measurement [79]. Differences in circuit resistance have an effect on:

- 1) The time constant of the measurement circuit. Equation 4-1 shows that a higher circuit resistance allows for rapid changes in the current. This increases the accuracy for short irregularities and the influence of the inductance is less dominant in the plots (the current follows changes in the resistance more rapidly).
- 2) The drop in current in terms of percentage. An unwanted resistance in the circuit causes a smaller drop in current when the total resistance is larger.
- 3) The power supply that is needed.
- 4) The power losses in the circuit.

In relation to selecting measurement circuit parameters, the first effect is in conflict with the other three. On the one hand, a high resistance allows briefly registered defects to be detected; on the other hand, this results in a smaller signal that is barely distinguishable from the noise. Power losses in an additional resistor should also be considered.

A simulation has been carried out to obtain greater insight into these contradictory effects. The circuits shown in Figure 4.5 and Figure 4.7 are used for these simulations. The simulation parameters are based on a 50/10 kV 10 MVA transformer. A resistance measurement on the primary and secondary windings yields:

$$\begin{aligned} R_1 &= 0.45 \, \Omega \\ R_2 &= 0.0575 \, \Omega \\ N^2 R_2 &= 1.44 \, \Omega \end{aligned}$$

The inductances are based on the time constants of the measurement current measured:

$$(1-k)L_1 = 55 \, \text{mH}$$

The value of the main inductance could be calculated by the no load current and losses of the transformer and yielded:

$$L_1 = 197 \, \text{H (rounded to 200 H for the calculations)}$$

When the OLTC is in operation, the transition resistors are switched into the circuit for a short time. The four effects of the circuit resistance that were mentioned above are now explained by looking at the effect of the transition resistors.

A series of tap change operations were simulated on a delta-connected OLTC [80]. The transition resistor of $2 \, \Omega$ was in the circuit for 50 ms each time the OLTC was operated. An extra resistor was then added to the circuit. The effect of this extra resistor is listed in Table 4.1. It can be seen that the current drop due to

the transition resistor decreases from 25% to 2% when the resistance is increased to 64 Ω . A measurement voltage of about 100 V is needed in that case. The time constant of the circuit also changes, as is depicted in Figure 4.14.

Table 4.1 *The effect of an additional resistor on the current drop, response time and the measurement voltage.*

Ω	Current drop	τ (ms)	Utest
0	-25%	23.5	2.05
0.25	-24%	22.5	2.45
0.5	-23%	21	2.85
1	-21%	19.5	3.63
2	-19%	16.5	5.2
4	-15%	12.7	8.35
8	-11%	9.2	14.62
16	-6%	5.6	27.2
32	-4%	3.1	52.35
64	-2%	1.8	102.7

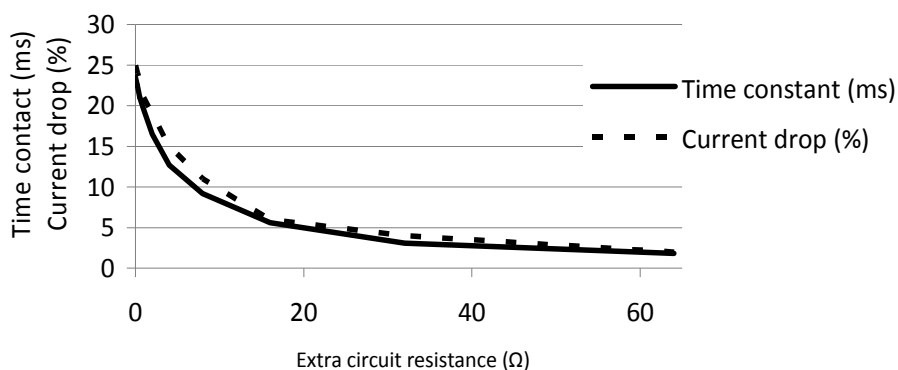


Figure 4.14 *The effect of the transition resistors on the DRM current decreases when the circuit resistance is increased, but the response also becomes faster (the time constant also decreases).*

A close-up view of the transition resistor operation is shown in Figure 4.15. A complete flag-cycle is simulated. Normally, the measurement circuit has a resistance of about 1 Ω . When an additional resistor is added to increase this value to 8 Ω , it can be seen that the response becomes faster but has a smaller amplitude. Figure 4.16 shows the effect of the transition resistors in the case of 64 Ω resistance in the measurement circuit. The response is almost direct.

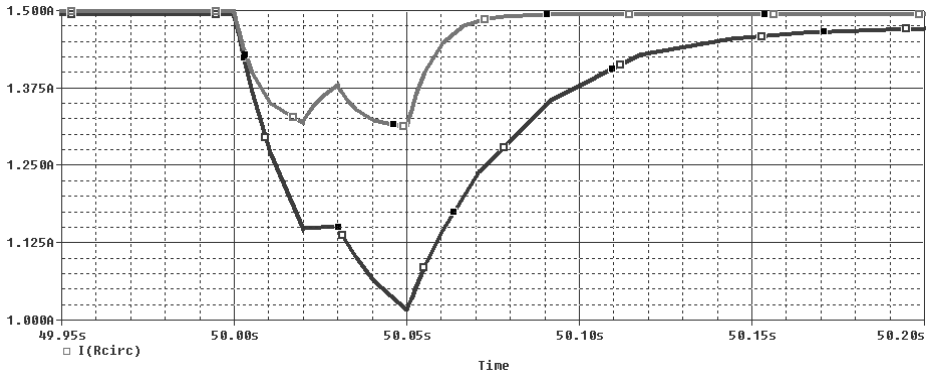


Figure 4.15 The response of the DRM current to the transition resistors. The amplitude of the response is larger at a circuit resistance of $1\ \Omega$ compared to $8\ \Omega$.

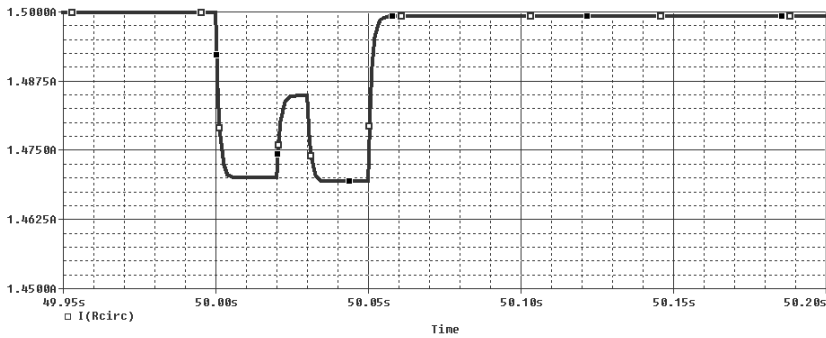


Figure 4.16 The response of the DRM current to the transition resistors at a circuit resistance of $64\ \Omega$. The current follows the resistance almost directly, so the effect of the inductance almost disappears.

When the circuit resistance is increased further, the current will directly react to changes in the contact resistance. However, the low amplitude will cause problems. Figure 4.17 shows a measurement with $75\ \Omega$ added resistance. It can be seen that the noise level is higher than the amplitude of the signal. It is impossible to detect defects in the OLTC when the signal is so small. The method discussed in Appendix B should be considered if a high level of time accuracy is desired.

The spikes in Figure 4.17 can be identified as noise because the current through the transformer is not able to change quickly. Peaks in the dynamic resistance can be identified as noise when they disappear much faster than the time constants of the transformer. Single peaks in the dynamic resistance are therefore caused by noise in the measurement circuit. The same effects can be measured or simulated in the case of the OLTC being applied to a star-connected winding.

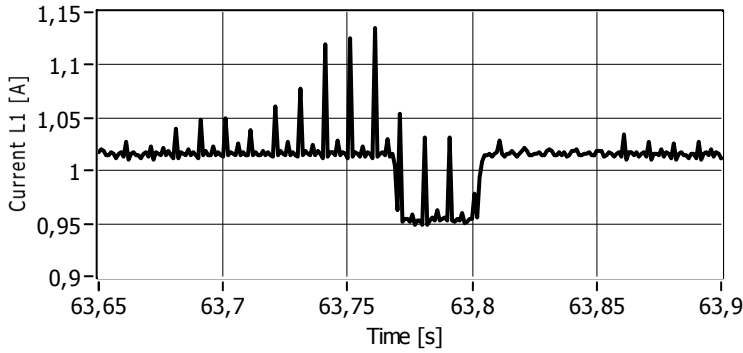


Figure 4.17 The response of the DRM current to the transition resistors at a circuit resistance of $75\ \Omega$. Noise on the measured signal makes it almost impossible to detect defects in the OLTC.

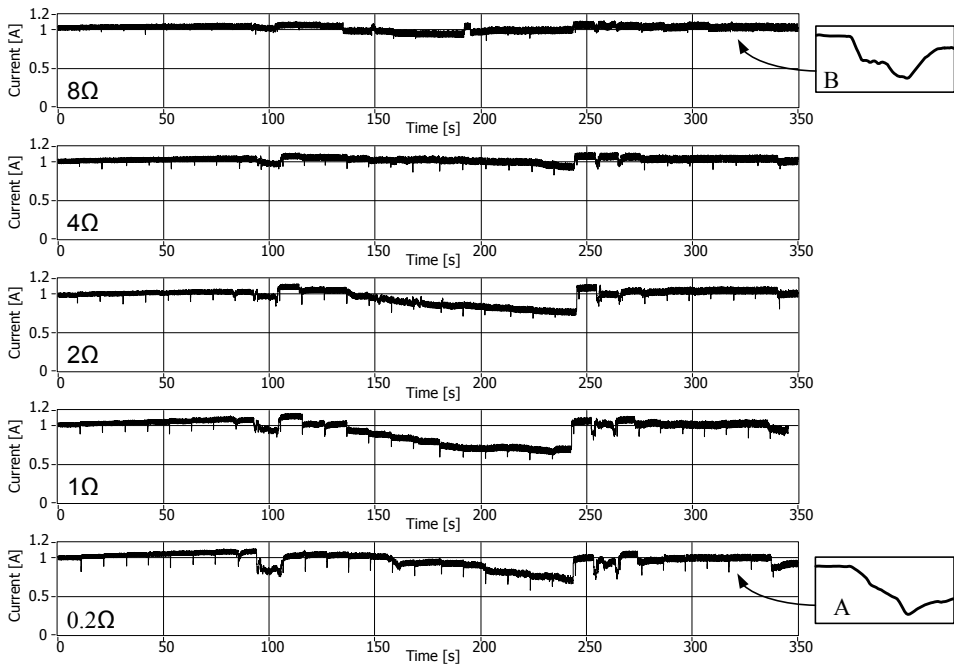


Figure 4.18 Dynamic resistance measurement on the same service-aged tap changer that suffers from the long-term effect on the change-over selector. Five different series resistors are used to demonstrate the influence of the circuit resistance.

Figure 4.18 shows an example of a DRM result of a service-aged OLTC with contact degradation using five different values of circuit resistance. A series resistance was added to the circuit for this purpose. It can be seen that the current deviates more from the expected value when a low circuit resistance is used. Inset A and B of Figure 4.18 show a close-up of the current when the tap changer

operates, from which it can be seen that the current reacts faster on changes in the resistance when a high circuit resistance is used ('B'), which corresponds with the simulations described in this section.

This effect can also be seen when the deviation of the current from the expected value is calculated for each tap position. DRM results from OLTCs in three different aging stages (good, aged and bad) were used, see Figure 4.19. Two tap changers were measured in each category; Figure 4.19 shows the averaged maximum current deviation of those two OLTCs. Five different series resistors were added to the measurement circuit. This example shows that the difference between the aging stages is higher at low series resistance ($<1\ \Omega$).

Another consequence of the circuit resistance dependency concerns the comparison of data between different DRM sets. Different measuring instruments can perform a dynamic resistance measurement [12][69][81-82], and may have other circuit resistances. Thus, the difference in the circuit resistance should be compensated for when comparing the resistances measured. An extra resistance can be introduced into the measurement circuit for this purpose.

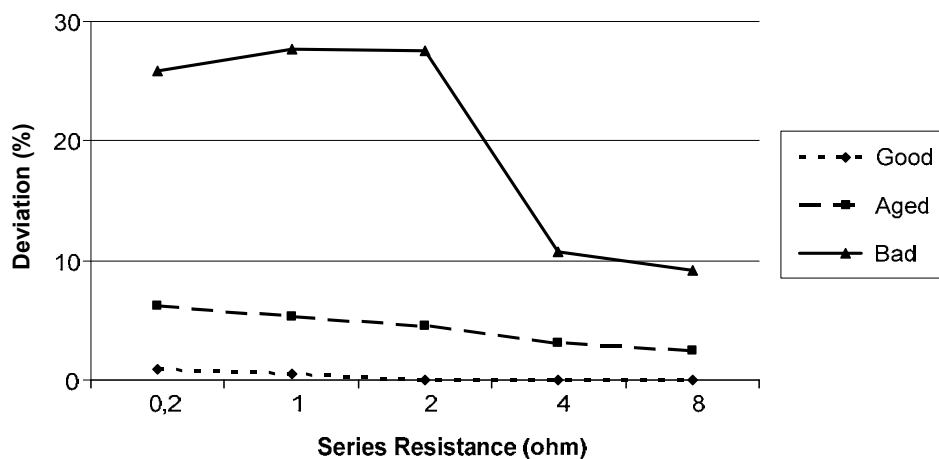


Figure 4.19 The deviation of the measurement current from the expected value decreases when the circuit resistance is increased. This plot shows averaged DRM results from two OLTCs with good contacts, two with aged contacts (a surface film) and two with bad contacts (with contact coking).

4.4 Secondary short circuit

Another issue concerns the effect of a secondary short circuit of the transformer when carrying out a dynamic resistance measurement. This short circuit has two functions. Firstly, safety is increased by the short circuit: the secondary short circuit provides a path for the current in the case of the primary side being interrupted. Without the short circuit, the current decreases and the steep dI/dt causes a high voltage over the inductance, causing an arc to occur.

More important is the second function of the secondary short circuit. It allows the measurement current to react quickly to changes in the supply voltage or in the circuit resistance. Without this fast time constant, short irregularities in the contact resistance cannot be measured. Section 4.1.2 elaborated on this time constant.

OLTCs in a delta-connected winding have to be measured three times, one measurement for each phase. In each case, the secondary short circuit is only applied to the phase(s) being measured (as depicted in Figure 4.20) and not to the other phases. In other words, the two phases which are not measured lack the secondary short circuit. In this way, the measurement current through the other phases is not able to change during the measurement and only a defect in the tested phase is measured and localisation possible. The secondary short circuit has to be changed for each measurement, which is a disadvantage (for example, due to safety).

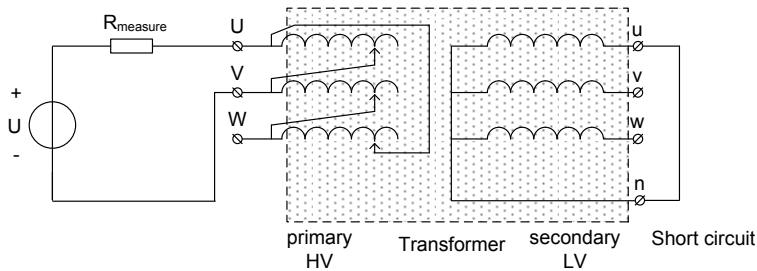


Figure 4.20 DRM setup for a transformer with the OLTC in a delta winding. The short circuit is applied to the measured phase only.

Another way to perform DRM is to apply a secondary short circuit to three phases at once. This situation is shown in Figure 4.21. However, the current through the two non-tested phases is also able to change quickly. A defect in the tested phase results in an increased current in the other two phases (due to current division on parallel paths). In such case, the measurement current supplied by the measurement system will not change as usual. Short irregularities in the contact resistance of other phases are also measured and crosstalk between the phases occurs.

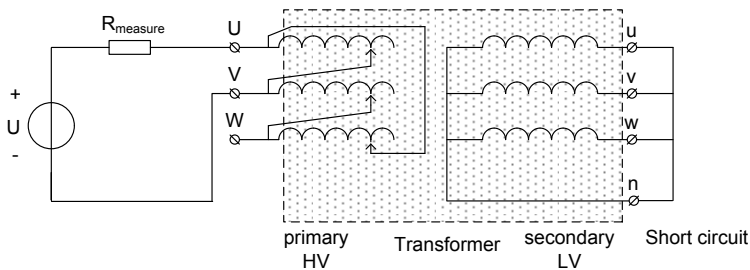


Figure 4.21 DRM setup for a transformer with the OLTC in a delta winding. The secondary short circuit is applied to all phases.

A simulation was used to investigate the effect of the secondary short circuit. An increased circuit resistance due to degradation causes an irregular current in the dynamic resistance measurement. To simulate this degradation, extra resistors can be introduced into the simulation. The irregularity can appear in one phase only or simultaneously in three phases. Therefore, three different resistances which create disturbance resistances are simulated:

- An increased resistance in the measured phase
- An increased resistance in one of the non-measured phases only
- An increased resistance in all three phases

Again, a 2 Ω resistor is switched in the circuit for 50 ms. The other circuit parameters are as described in Section 4.3. By doing so, the simulation gives the same time responses as a measurement on a real power transformer.

Table 4.2 gives an overview of the effect of these three irregularities on both short circuit conditions. The decrease in the measurement current is determined in terms of a percentage of the initial current. From the viewpoint of completeness, the effect of the irregularity in a star-connected measurement is added.

Table 4.2 Overview of simulation results. The change in current is presented for three types of irregularities and three measurement configurations. A resistance of 2 Ω was in the circuit for 50 ms.

Configuration	Winding configuration	No of sec. short circuits	Location of defect (50 ms, 2 Ω)		
			Three phase	Measured phase	Non-measured phase
Configuration	Δ	1	-24%	-24%	0%
	Δ	3	-33%	-22%	-11%
	Y	3	-28%	-38%	14%

From these simulations it can be concluded that a dynamic resistance measurement on a delta-connected transformer winding is best performed with one secondary phase short-circuited. In that case, a three-phase defect and a one-phase defect both give the same response (24% decline in the current), while a defect in a non-measured phase does not influence the measurement (0%). A three-phase short circuit would give an inferior result.

The current through one phase can rise at a star-connected tap changer when another phase has increased contact resistance (see Table 4.2). Figure 4.22 shows the simulation result in this situation, where the current rises 14%.

4.5 Determination of the contact resistance

DRM is a direct method for measuring defects on the OLTC contacts. The effect of variations in the contact resistance is measured quickly (by switching the OLTC through its cycle of operation). Corrections in the source current and voltage measured may be needed before the resistance can be displayed.

Section 4.1 discussed the time constants of a transformer in cases where the voltage and current measurements are performed on the same side of the transformer. Essentially, the impedance is measured because DRM does not provide long stabilisation times. Resistance can only be read after a long period. Corrections are needed in order to determine the real contact resistance. The same applies when the voltage response is measured on one side of the transformer and current is injected on the other side. A correction or calculation is needed to obtain the resistance values in both cases.

Firstly, the other circuit resistances need to be corrected, for instance the resistance of the measurement cables. A 4-point measurement makes this correction unnecessary. The resistance of the transformer windings should also be subtracted from the value measured in order to obtain the contact resistances (note that these values are temperature and frequency dependent).

Secondly, the time constant of the transformer windings to a DC voltage needs to be corrected. The response of the measurement current to a resistor with a known value is a way to avoid this: KEMA developed [68] and patented [83] this method. The resistance is calculated after the effect of the fast time constant disappears but before the slow response starts, as it is assumed that the current through the windings has not yet changed. The ohmic value obtained by this calculation is very close to the static resistance at that particular amplitude of the current. This value should not be compared to values obtained at other levels of the measurement current because the contact resistance can be strongly dependent on the current.

Finally, compensating for differences in the measurement setup could make the readings obtained less prone to variations in the setup, resulting in more readily reproducible readings.

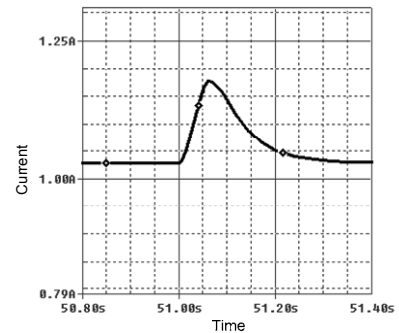


Figure 4.22 *Simulation of an OLTC with increased resistance in the adjacent phases.*

4.6 Conclusions

This chapter discussed aspects of dynamic resistance measurements, such as the effect of the secondary short circuit, circuit resistance and measurement current level. It was shown that a short circuit has to be applied to the secondary side of

the transformer (one short circuit at delta transformers). A four-wire resistance measurement directly on the transformer bushings can be used to compensate for the resistance of the test leads. We showed that a high circuit resistance results in smaller changes in the measurement current, making the readings more prone to noise, but the dynamic resistance that is measured shows fewer slow effects of the winding inductance (because $\tau = L/R$).

An important topic is the amplitude of the measurement current (and therefore also the measurement voltage). We showed that when the measurement current is decreased the sensitivity to surface film on the contact increases (see Figure 3.10). This variation in the resistance can be a few decades in amplitude. A current that is too low (and therefore a low measurement voltage) will allow the surface film to interrupt the measurement current. Because the formation of the surface film on the contacts is the first stage of the long-term aging effect that leads to coking, it is of interest to determine if this degradation mechanism has started. The dependency of the contact resistance and the amplitude of the measurement current on each other can be used to detect the long-term aging effect at an early stage. In addition, studying contact degradation by DRM at different current amplitudes provides information about both the very early stage of contact degradation (at low currents) and information about the behaviour of contact degradation at a nominal current during OLTC service (at high measurement current).

When doing so, a few issues have to be considered. Above all, it is impossible to determine the ‘real’ contact resistance of degraded contacts. Measurements at both high current and low current do not indicate a contact resistance that is independent of the measurement current. Results even fluctuate with the current when the measurement is performed with 100 A or higher. Examples were given in this chapter. This current dependency of the contact resistance during static resistance measurements should also be kept in mind when performing dynamic measurements as there was no stable reading of the resistance even at 100 A.

To conclude, performing a dynamic resistance measurement on an OLTC with a low measurement current has important advantages: it is able to detect a large variety of defects and degradation. The long-term aging effect can be discovered at an early stage when a low current is used for the measurement. The method provides more information about the tap changer condition than static resistance measurements because resistance can be measured at more contact locations.

Using DRM with low measurement current also has disadvantages: it is difficult to compare results with other measurement results (from other OLTCs or with earlier measurements on the same unit). Results measured at different currents should never be compared. One should be careful not to use a measurement current that is too low: extreme resistances can be measured in such cases, even causing total interruption of the current.

5

Power transformer diagnostic system

The diagnostic methods described in Chapter 3 do not cover all of the dominant degradation mechanisms when applied separately. Thus, in order to measure all of them, a combination of diagnostic measurements is recommended. This chapter proposes a power transformer diagnostic system that combines a set of diagnostic measurements which can diagnose the technical condition of the main power transformer subcomponents, focusing on the dominant failure modes. The diagnostic system discussed in this thesis focuses on condition assessment of power transformers with a high-speed resistor-type OLTC. No distinction is made between testing diverter and selector switch type OLTCs and between in-tank and compartment type OLTCs.

The subcomponents that are not accessible to visual inspection during regular maintenance, for example because they are enclosed in the transformer tank, are of particular interest. The diagnostic measurements used are therefore selected on the basis that they can reveal defects and degradation without disassembling the power transformer as they measure quantities that are accessible externally. Examples of such quantities include terminal voltage, excitation current, acoustic vibrations and drive motor power.

Certain aspects of two important power transformer subcomponents primarily determine the application of the transformer diagnostic system. First there is the OLTC, which is normally found in power transformers installed in transmission networks and in distribution networks, typically at voltages of 25 kV and above. The off-line measurements using the proposed diagnostic system are recommended on-site after regular tap changer maintenance or inspection. In this way, safe operation of the power transformer is guaranteed when it is re-energised. Contact degradation and defects that adversely affect the OLTC main function can be checked using the diagnostic system described in this chapter, which offers a direct way to detect whether the tap changer is able to select another winding tap without interrupting the load current.

The second important transformer subcomponent is the winding. Due to the diversity of transformer types, the winding configuration must be considered during diagnostic measurements. Common winding configurations (Figure 5.1) are:

- a. Delta-connected windings
- b. Star (Wye)-connected windings
- c. Autotransformers
- d. Zigzag-connected windings

Although the measurement of winding resistance and transformer turn ratio on these types of winding configurations are comparable, important differences exist:

1. The measurement voltage has to be applied on different terminals. Delta windings are measured phase-to-phase while star-connected windings and zigzag-connected windings with a neutral point can be tested phase-to-neutral (Figure 5.1, see also Section 4.1.2).
2. Current and voltage signals used for the ratio or resistance calculation must be measured on different terminals. The transformer vector group (e.g. Yd11) describes which windings are magnetically coupled and which windings are connected to which terminals. Therefore it determines which secondary terminals should be used for the measurement (Figure 5.1).
3. Resistance of the three transformer phases can be measured simultaneously at star and zigzag-connected windings with a neutral point (Figure 5.1). This not only affects the measurement circuit, but also the way results can be displayed (e.g. three phase results can be shown on the same timescale).
4. Section 4.4 described the secondary short circuit during a dynamic resistance measurement (DRM), which is dependent on the winding configuration.
5. Delta-connected windings offer an alternative path in the case of a single-phase interruption of the measurement current. This should be kept in mind when interpreting results.

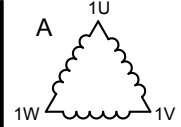
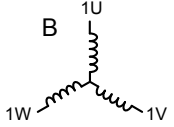
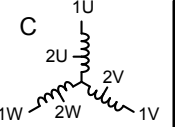
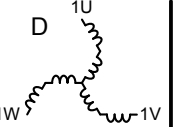
				
DC winding resistance measurement	Three separate measurements Correction factor needed	One measurement if neutral point accessible	One measurement if neutral point accessible	One measurement if neutral point accessible
Dynamic resistance measurement	See above and vector group determines secondary short circuit	See above and vector group determines secondary short circuit	See above and secondary short circuit on same phase	See above and vector group determines secondary short circuit
Transformer turn ratio measurement	Vector group determines secondary voltage reading	Vector group determines secondary voltage reading	Voltage reading on same phase	Vector group determines secondary voltage reading

Figure 5.1 Common three-phase transformer winding configurations include a) delta, b) star, c) auto and d) zigzag.

Taking the above considerations into account, a transformer diagnostic system that configures the measurement circuit according to the winding configuration can be beneficial.

This chapter firstly discusses the international testing standards that apply to power transformer testing (Section 5.1) and proposes a diagnostic system (Section 5.2). Secondly, the chapter elaborates on the aspects of this proposed diagnostic system by describing: 1) the typical measurement procedure, including practical aspects of using the diagnostic system (Section 5.3), 2) the hardware configuration of the proposed diagnostic device and data processing and analysis (Appendix D).

The measurement data from this diagnostic system contains condition information about the various transformer subsystems and requires interpretation by a transformer expert. The interpretation of typical diagnostic data will be discussed in Chapter 6.

5.1 International standards for power transformer testing

International standards are used to measurement different power transformer types in a consistent way. They advise several checks and measurements be performed on power transformers, but do not specify exactly how these checks should be performed. Relevant international standards for power transformer testing include:

1. ANSI/IEEE C57.12.90-1987: American national standard / IEEE Standard Test Code for Liquid-Immersed Distribution, Power, and Regulating Transformers.
2. IEC 60076-1: Power Transformers – Part 1: General.
3. IEEE Std 4-1995, IEEE Standard Techniques for High-Voltage Testing.
4. IEEE Std 62-1995: IEEE Guide for Diagnostic Field Testing of Electric Power Apparatus. Part 1: Oil Filled Power Transformers, Regulators, and Reactors.
5. IEEE Std C57.140-2006: IEEE Guide for the Evaluation and Reconditioning of Liquid-Immersed Power Transformers.
6. IEC 60214, Tap-changers – Performance requirements, test methods and application guide.
7. IEEE Std C57.131-1995: IEEE Standard Requirements for Load Tap Changers.

These standards require that the condition of the OLTC contacts and the drive mechanism, together with contact timing, are determined during regular maintenance, see Table 5.1. In particular, checking the contact alignment and film/carbon development is advised. Turn ratio measurements are also advised during regular maintenance.

Table 5.1 Summary of general test requirements of international standards for power transformer testing, describing which tests and checks should be performed during maintenance or inspection.

IEEE Std C57.140-2006 IEEE Guide for the Evaluation and Reconditioning of Liquid-Immersed Power Transformers	As part of a transformer upgrade and service life extension, the contact assemblies should be inspected for evidence of poor performance, such as discoloration and/or material flow (melting) of contacts and also film or carbon buildup (coking) in conducting contact area.
	The internal tap assemblies and their operating shafts/gears should be inspected carefully for alignment and physical condition.
	Contact alignment should be checked and corrected as needed.
IEEE Std 62-1995 IEEE Guide for Diagnostic Field Testing of Electric Power Apparatus. Part 1: Oil Filled Power Transformers, Regulators, and Reactors.	The ratio in particular is checked during regular (e.g. annual) inspections and it is recommended that it is also checked before returning the transformer to service if the unit has been subjected to a through-fault.

In addition to recommendations concerning what should be checked and measured, the standards also set general requirements on how to perform the measurements. The requirements for resistance measurements on power transformers must be considered in dynamic resistance measurements on OLTCs, which are summarized in Table 5.2. Transformer turn ratio measurement requirements are summarized in Table 5.3. It can be seen that these international standards do not specify precise measurement parameters for the advised measurements; the most practical parameters can be chosen within the boundaries described.

Table 5.2 Summary of test requirements of international standards for resistance measurements on power transformers, describing in general how these resistance measurements should be performed.

ANSI/IEEE C57.12.90-1987 American national standard / IEEE Standard Test Code for Liquid-Immersed Distribution, Power, and Regulating Transformers.	Measurement is made with direct current and simultaneous readings of current and voltage are taken.
	The voltmeter leads shall be independent of the current leads and shall be connected as closely as possible to the terminals of the winding to be measured.
	The current used shall not exceed 15% of the rated current of the winding whose resistance is to be measured. Larger values may cause inaccuracy by heating the winding and thereby changing its temperature and resistance.
IEC 60076-1 Power Transformers - Part 1: General.	Tests shall be made at any ambient temperature between 10°C and 40°C.

Table 5.3 Summary of test requirements of international standards for transformer turn ratio measurements, describing in general how these ratio measurements should be performed.

ANSI/IEEE C57.12.90-1987 American national standard / IEEE Standard Test Code for Liquid- Immersed Distribution, Power, and Regulating Transformers.	The ratio test shall be made at rated or lower voltage and rated or higher frequency. Transformers that have Y diametric connections but do not have the neutral of the Y brought out shall be tested for ratio with three-phase power.
IEEE Std 4-1995 IEEE Standard Techniques for High- Voltage Testing	The test voltage shall be an alternating voltage having a frequency in the range of 45-65 Hz. The voltage wave shape should approximate a sinusoid with both half cycles closely alike, and it should have a ratio of peak-to-rms values equal to the square root of 2 within +5%.
IEEE Std 62-1995 IEEE Guide for Diagnostic Field Testing of Electric Power Apparatus. Part 1: Oil Filled Power Transformers, Regulators, and Reactors.	If the transformer has load taps, the turn ratio should be determined for all of these taps. A meaningful ratio measurement may be made using only a few volts of excitation. The transformer should be excited from the highest voltage winding in order to avoid possibly unsafe high voltage. The voltmeters used should have accuracies commensurate with the requirements of a 0.5% ratio calculation.

5.2 Transformer diagnostic system

To obtain the desired information about the condition of the transformer subcomponents as mentioned in the previous section, the following off-line diagnostic methods are combined into a single diagnostic system:

- Resistance measurements (dynamic resistance of the OLTC and DC winding resistance)
- Transformer turn ratio
- Mechanical condition of the drive system

These measurements can be applied during regular tap changer maintenance and diagnose the contacts and mechanical drive system, see Table 3.1. Concerning the latter, to diagnose the mechanical condition and OLTC drive mechanism a selection of measurements can be made based on the considerations of Section 3.2. For example, information about the mechanical condition can be gained by measuring:

- a. The active drive motor power
- b. The remote end drive shaft rotation for rotor-type OLTCs with an accessible drive shaft (e.g. selector switch type tap changers)
- c. The timing of protective contactors, for example an excessive switch-time protective contact

Table 3.1 shows that these methods, in combination with a visual inspection, diagnose defects in all the OLTC subsystems from Table 3.1. Figure 5.2 illustrates the diagnostic methods selected for the proposed transformer diagnostic system. The condition of the power transformer subsystems, depicted left in Figure 5.2, is assessed using the four basic diagnostic measurements used in the diagnostic system (see also Chapter 3). In addition to the measurements included in the transformer diagnostic system, gas analysis of the transformer insulation oil, visual inspection of the transformer tank and accessories are also advised in order to determine the optimal maintenance strategy.

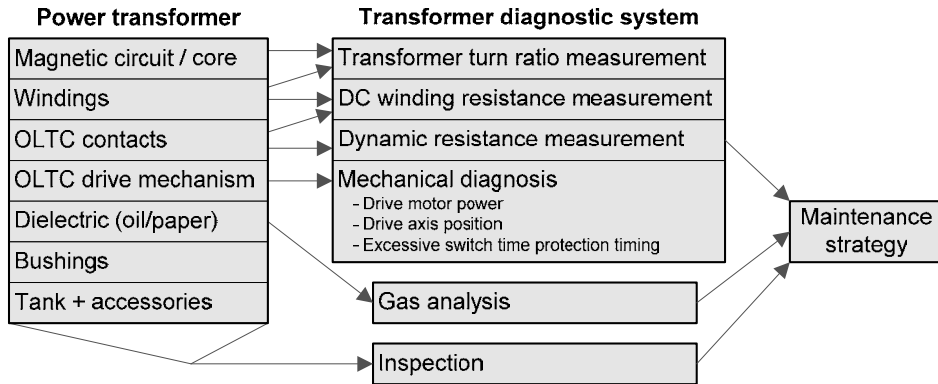


Figure 5.2 The transformer subsystems (left) are diagnosed by the transformer diagnostic system (centre). Additionally, gas analysis and inspection are advised. As a result, the optimal maintenance strategy can be determined.

The goal of applying this combination of diagnostic measurements is threefold:

- 1) To diagnose the power transformer windings and tap changer in cases where protective devices have switched off the transformer.
- 2) To assess the contact condition and contact timing after regular tap changer maintenance or repair, in particular for pre-failure detection of maintenance errors and to find defects and degradation that remained undiscovered during inspection.
- 3) To detect contact degradation at an early stage and thereby determine the optimal maintenance strategy.

In this thesis, the suitability of DRM on OLTCs is studied using the Transformer Diagnostic System described in [12][84] and as shown in Figure 5.3.



Figure 5.3 Transformer diagnostic system described by [12] during DRM field testing. The system is remotely controlled by a laptop.

5.3 Measurement procedure

Figure 5.4 shows the measurement procedure of the diagnostic system. Prior to the off-line measurements, the power transformer must first be prepared for the measurement. The transformer is de-energised, a safety ground is applied, the high-voltage

connections are uncoupled (Figure 5.4.1) and the clamps and sensors are connected (Figure 5.4.2). Figure 5.4.3a-e lists the general measurement procedure of the proposed diagnostic system, which applies for all diagnostic methods in the proposed diagnostic system. As a first step in the measurement, transformer parameters are entered (Figure 5.4.3a) in order to:

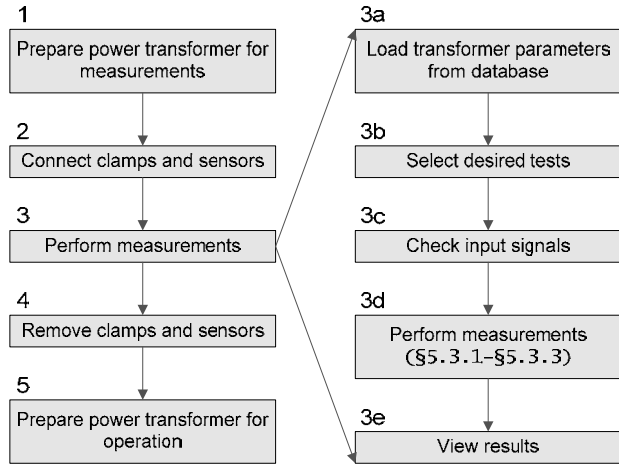


Figure 5.4 Measurement procedure for measuring power transformers with the proposed transformer diagnostic system.

- I. Store measurement data in a consistent way
- II. Define the transformer terminals that are used during the measurement and configure the relays in the output stage accordingly
- III. Make correct secondary short circuits during DRM
- IV. Correct the measured turn ratio

Subsequently, the desired measurement methods are selected (Figure 5.4.3b). The exact procedure involved in the measurement itself (Figure 5.4.3d) depends on the diagnostic method selected.

5.3.1 Dynamic resistance of the OLTC

Performing DRM with the proposed diagnostic system involves the setup of the measurement circuit, followed by charging, recording and discharging in succession, see Figure 5.5.

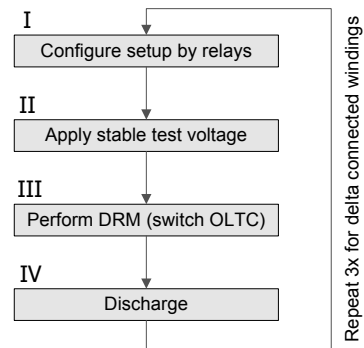


Figure 5.5 General measurement procedure for DRM.

Setup configuration

Configuration of the measurement circuit (Figure 5.5I) is done by connecting the DC power source to the transformer windings. Which transformer terminals are connected is determined by the winding configuration. The secondary short circuit is applied according to Sections 4.1.2 and 4.4 and also depends on the winding configuration. Figure 5.6 and Figure 5.7 give examples of a measurement circuit configuration for an YNd-connected winding. The proposed transformer diagnostic system has direct connections to all transformer terminals and configures the setup with relays.

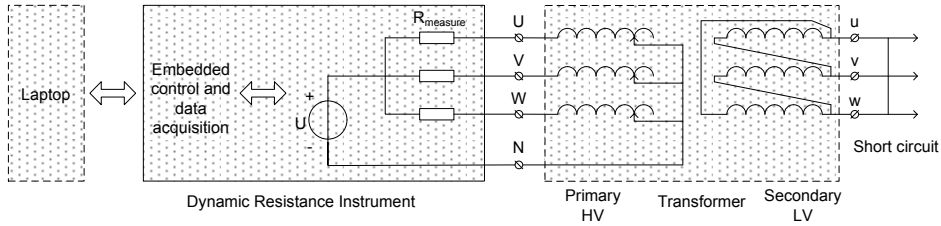


Figure 5.6 Dynamic resistance measurement applied to an YNd-connected power transformer. The diagnostic system is connected to the windings with the OLTC while the secondary side is short-circuited.

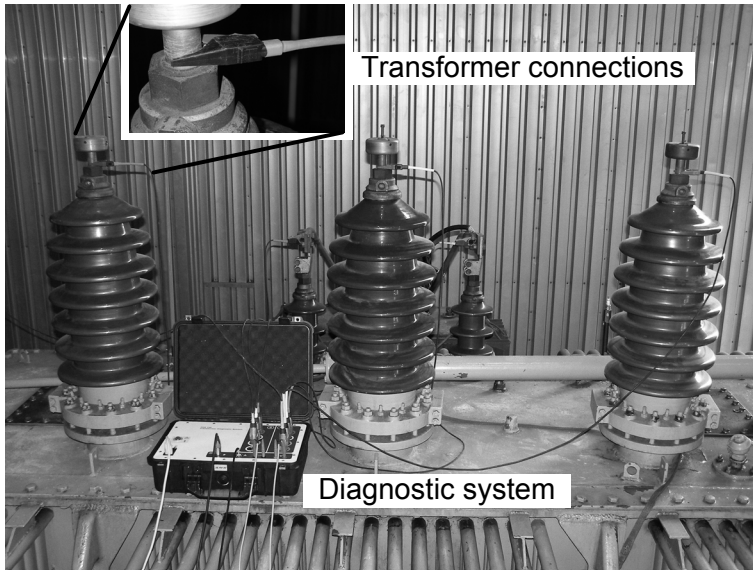


Figure 5.7 The transformer diagnostic system connected to the primary and secondary transformer terminals.

Charging

Firstly, during the charging process (Figure 5.5II) a DC voltage must be applied using a controllable DC voltage source. This voltage can be increased quickly (for example within 1 s) until the desired current is reached.

Secondly, the voltage needs to be regulated to a lower value to keep the measurement current at the desired level, due to the saturation of the transformer core and the effects discussed in Section 4.1.2. An example of a charging process is shown in Figure 5.8. During field measurements it was seen that, in general, a stable measurement current can be assumed when the voltage applied remains within 10% for 90 seconds. During this charging process, attention should be paid to the following:

1. Do not charge windings without a correct secondary short circuit, which can be recognized by a slowly rising current during the charging process.
2. Beware of an incorrect transformer connection, which can be recognized as a negative measurement current or zero current in some phases.
3. Beware of corrosion of the transformer terminals, which endangers a good electrical contact with the measurement clamps. This can be recognized by incorrect voltage readings.
4. Beware of saturation effects in the transformer core caused by the DC measurement current. If not eliminated during the charging process prior to the measurement, saturation might lead to overcurrent conditions during the measurement.

It should be kept in mind that transformer windings have a very high inductance (in the range of hundreds of Henry) and can therefore store a considerable amount

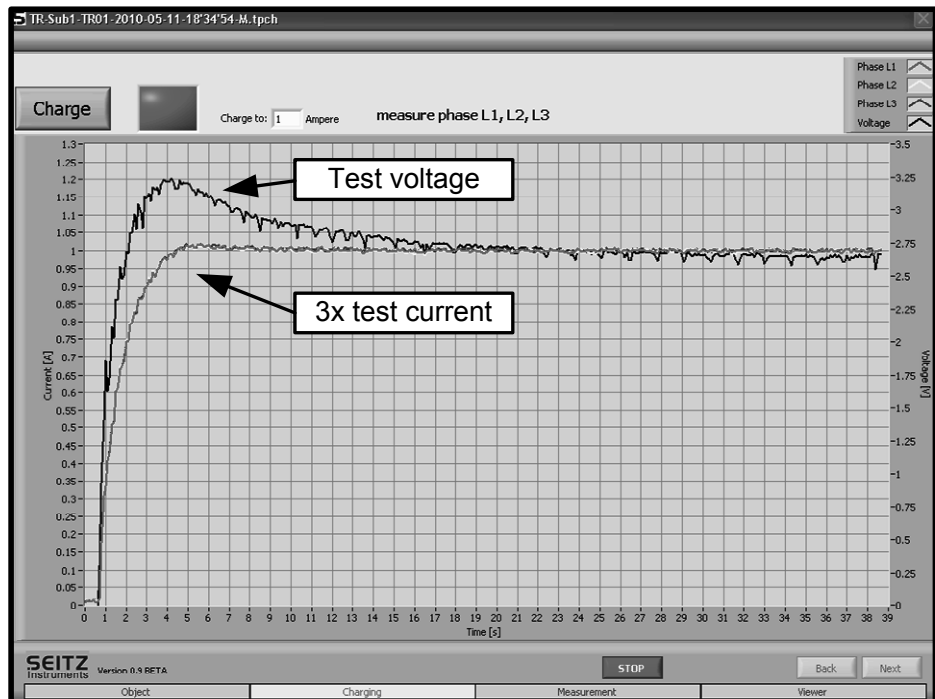


Figure 5.8 Charging the transformer windings with a DC current. Initially a higher source voltage is needed.

of magnetic energy. The diagnostic system charges and discharges the transformer windings safely and determines when the charging effect has disappeared and a stable reading is obtained. Attention should be paid to the current amplitude when testing delta-connected transformers, see Section 4.2.2.

Measurement

During the resistance measurement itself (Figure 5.5III) the source voltage is kept constant and the tap changer is operated. The current of the tested phases is stored together with the voltage difference of the corresponding transformer bushings. Again, attention should be paid to not overload the power supply, because the measurement current can increase due to changes in the winding resistance and contact resistance. During the recording phase, OLTC control can be applied by the transformer diagnostic system. Therefore the diagnostic system can be equipped with OLTC control contactors which are designed to control the drive mechanism. These contacts bridge the control buttons in the control box of the drive and this way the tap changer can be automatically switched through all its tap positions.

Discharge

During the discharge process (Figure 5.5IV) the DC power supply is switched off and a series resistor added to the circuit in order to dissipate the energy that is stored in the windings. Interrupting a small current through the transformer windings can still damage sensitive electronics inside the measurement system. Therefore, when the current reaches safe levels, a short circuit should be applied by the diagnostic system for safety reasons.

View results

When all phases are measured, results should be displayed in such a way that a decision about re-energising the transformer, without risk of failure, can be made on-site (Figure 5.4.3e). For that purpose, critical parameters from the DRM results should be clearly visible. The following results should be shown:

1. An overview of the measurement current or impedance during the complete cycle of operation. Its presentation depends on the winding configuration. Figure 5.9 provides an example of a DRM current overview graph for an OLTC in a Y-connected winding (the three phases are measured simultaneously) in good condition. Appendix D shows an example of an overview graph of a delta-connected OLTC with contact degradation (three phases are measured on a different timescale) and an example of the impedance overview graph.
2. Close-up view of the measurement current or impedance for each tap changer operation (see Appendix D).
3. Transition times of each operation (for example in a table or a graph, see the right side of Figure 5.9).
4. The voltage and current that were used for the measurement: to allow comparison of measurement results, which can be dependent on these measurement parameters (indicated in the right bottom side of Figure 5.9). It

can be seen that a decreasing current shows as an increasing impedance because the measurement voltage is fixed.

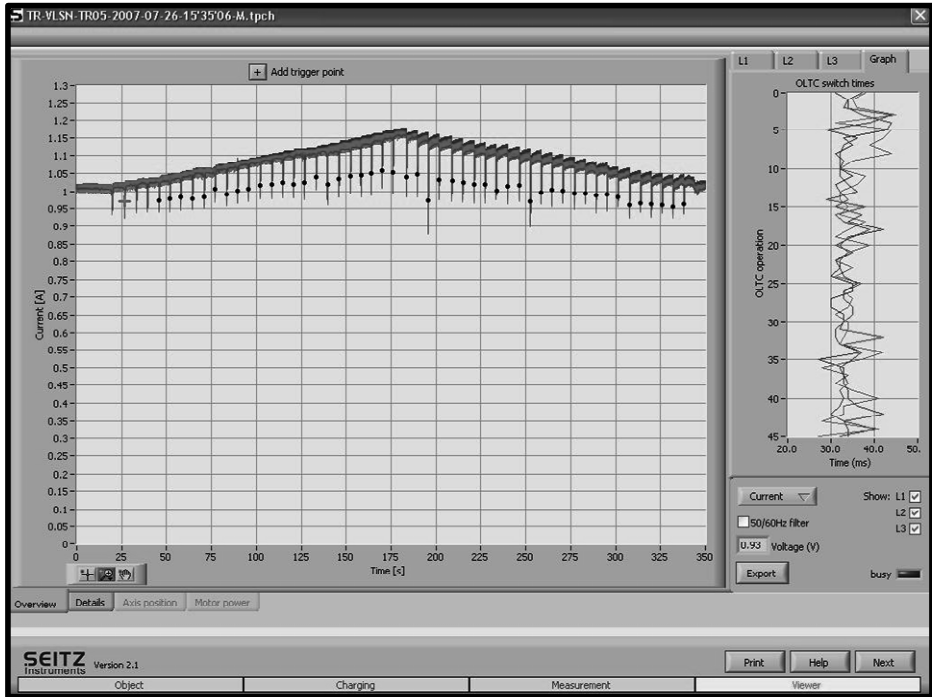


Figure 5.9 DRM results for OLTCs in star-connected windings can be displayed on the same timescale (A), results can be displayed as current.

5.4 OLTC drive system condition

Signals recorded for the mechanical diagnosis of the OLTC by the proposed diagnostic system can be displayed as in Figure 5.10. By default (see Section 5.2) these signals consists of drive motor voltage, drive motor current, drive shaft angular position and contact voltage of the excessive switch-time protective contact. Figure 5.10 shows the motor power results, consisting of an overview plot and a close-up plot. Graphic presentation of motor operation time and average motor power can give a clear indication of irregular taps. The close-up of the plots for each tap change operation reveal defects more readily.

In order to create the active motor power plots, the voltage and current recordings need to be processed. Instantaneous power $p_{3\phi(t)}$ of the three-phase drive motor is defined by:

$$p_{3\phi(t)} = v_{A(t)}i_{A(t)} + v_{B(t)}i_{B(t)} + v_{C(t)}i_{C(t)} \quad 5-1$$

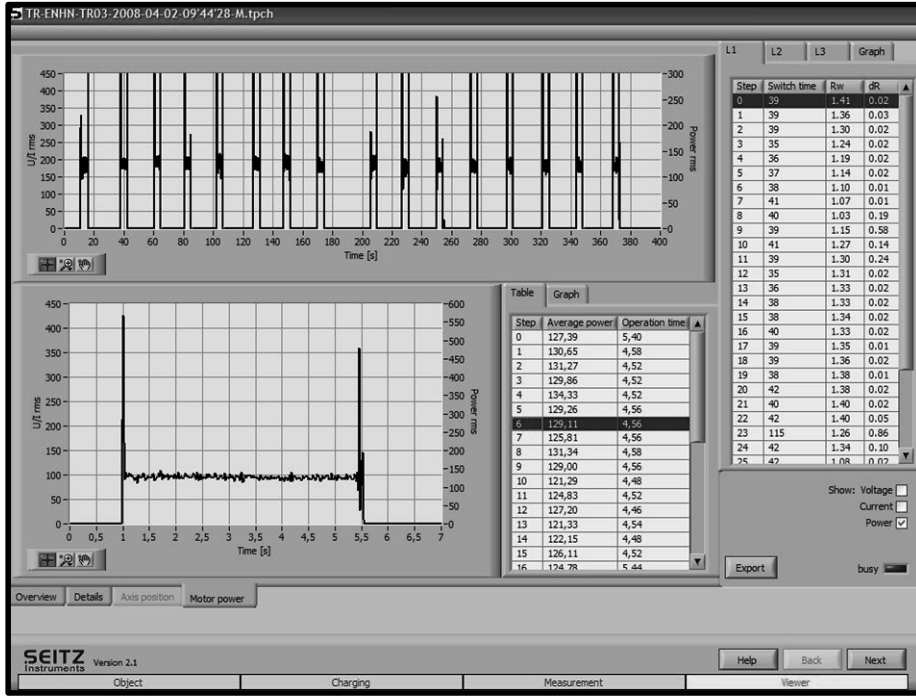


Figure 5.10 Example of active motor power results on an OLTC drive mechanism.

where $v_{A(t)}$, $v_{B(t)}$ and $v_{C(t)}$ are the line-to-neutral voltages of the three-phase drive motor and $i_{A(t)}$, $i_{B(t)}$ and $i_{C(t)}$ its three currents. Double net frequency components should be filtered out before results are analyzed. If RMS values are used, the power factor needs to be considered:

$$P_{3\phi} = V_A I_A \cos \varphi_A + V_B I_B \cos \varphi_B + V_C I_C \cos \varphi_C \quad 5-2$$

To reduce the number of measured signals, balanced operation of the drive motor can be assumed:

$$\begin{aligned} V_A &= V_B = V_C = V_{Phase} \\ I_A &= I_B = I_C = I_{Phase} \\ \cos \varphi_A &= \cos \varphi_B = \cos \varphi_C = \cos \varphi \end{aligned} \quad 5-3$$

The active power can then be calculated based on RMS values of the phase voltage and the measured single-phase current:

$$P_{3\phi} = 3V_{Phase} I_{Phase} \cos \varphi \quad 5-4$$

Figure 5.11 shows the OLTC drive shaft position results, where derivatives of the shaft rotation resulted in graphs of velocity and acceleration. Appropriate digital filters (e.g. low pass filters) are applied by the proposed diagnostic system to reduce noise on these signals. Irregularities in the shaft rotation, velocity and acceleration can be more readily detected when a graph is plotted with characteristic values for each tap changer operation. Therefore, the mechanical switching time, overshoot and maximum values of speed and acceleration are shown by the proposed diagnostic system. The close-up plots for each tap changer operation are useful to study faulty operations in more detail.

The timing of an excessive switch-time protective contact can be checked by plotting changes in the recorded contact voltage (AC or DC) in the dynamic resistance plots, see Appendix D. Incomplete or defective protection settings can then be recognized.

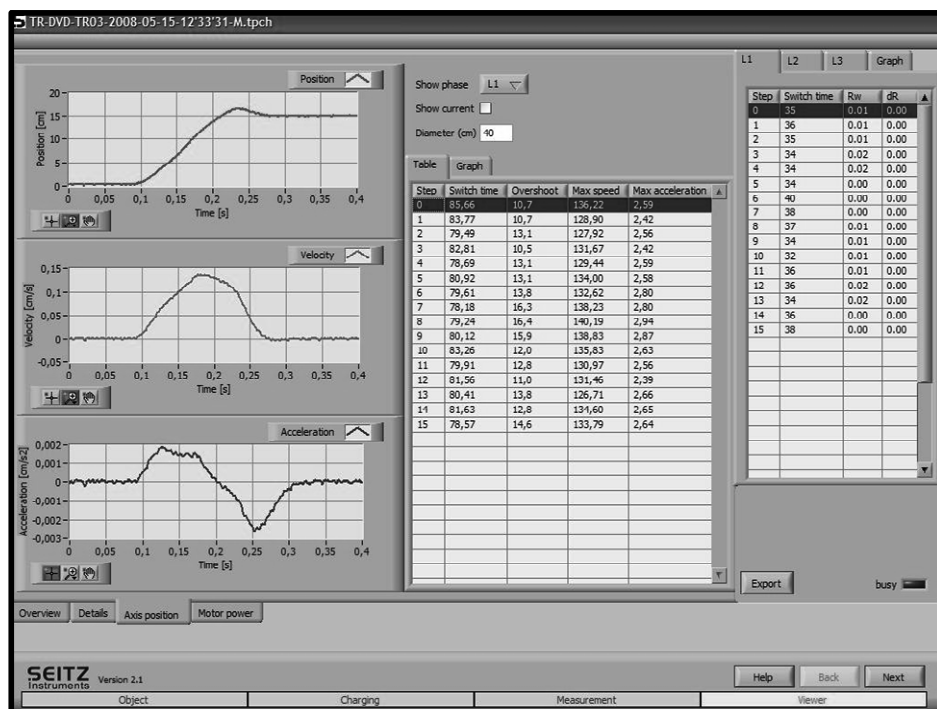


Figure 5.11 Example of drive shaft rotation results on an OLTC drive mechanism.

5.5 Hardware and data processing

Design considerations for such a diagnostic system are discussed in Appendix D. The diagnostic system is subdivided there into four basic units. The hardware demands are determined for each unit, on the assumption that the diagnostic system is designed to perform automated measurements. Appendix D also

discusses the data processing and analysis required as part of the embedded control of the diagnostic system. Examples of how the measurement results can be displayed are also given. Special emphasis is laid on the need to present DRM results clearly, for example by means of:

- a dynamic resistance overview plot covering all tap positions
- a dynamic resistance close-up plot for each operation
- details of the transition times for each operation
- values of the voltage and current used for the measurements

This should provide an adequate basis for the decision as to whether the power transformer can be re-energised without the risk of failure. Chapter 6 deals with the interpretation of the DRM results.

5.6 Conclusions

Firstly, this chapter explains the effect of the transformer winding configuration on different diagnostic measurements.

Secondly, it was shown in this chapter that international standards on power transformer testing do not specify precise measurement parameters for the advised measurements; the most practical parameters can be chosen.

Thirdly, this chapter discussed a combination of diagnostic measurements that is sensitive to assess the dominant OLTC degradation mechanisms and defective power transformer windings:

- Resistance measurements (dynamic and static)
- Turn ratio measurements
- Mechanical condition of the OLTC and drive

The condition of different transformer subsystems is evaluated using these proposed diagnostic measurements, after regular maintenance or after protective relays removed the transformer from service. In particular, the focus is on transformer subcomponents that are not accessible for visual inspection during regular maintenance because they are enclosed in the transformer tank. Practical aspects of using the proposed diagnostic system were discussed.

In the following chapters, the proposed diagnostic system will be used to show the suitability of DRM to detect the dominant OLTC degradation mechanisms. In particular, the following chapter will be concerned with the structured evaluation of the diagnostic data obtained by DRM on OLTCs.

6

Evaluation of typical DRM diagnostic data

Dynamic resistance plots obtained by measuring tap changers that are in good condition look similar. Many different kinds of irregularities in the results are expected when DRM is applied to defective or degraded OLTCs. This chapter presents an overview of possible measurement results and relates them to the physical condition of the tap changer. The variety of defects and degradation mechanisms that can be detected before failure occurs [85], shows that DRM is a valuable tool for the assessment of OLTC condition.

Four basic types of measurement results can be distinguished:

- a. DRM on OLTCs in good condition
- b. DRM on OLTCs with increased contact resistance
- c. DRM on OLTCs with open contacts (infinite resistance)
- d. DRM on OLTCs with contact timing problems (phase synchronism, contact wear and irregular transition times)

DRM results obtained in this project could all be assigned to one or more of these categories, which are discussed in turn below. This subdivision allows the different types of defects to be analyzed separately, as illustrated in Figure 6.1. The location where the defect shows in the current curve and the shape of this irregular current are used in this thesis to find the cause and importance of the defect. DRM plots can be compared with a reference graph, which may be a plot obtained from an OLTC without any defects or signs of contact degradation. Finally, a condition index may be determined as described in Chapter 8.

Most dynamic resistance plots presented in this chapter were recorded with the Transformer Diagnostic System described in the previous chapter and were obtained by measuring service-aged OLTCs in the Dutch utility grid. However some of the dynamic resistance plots were determined during experiments in a high-voltage laboratory.

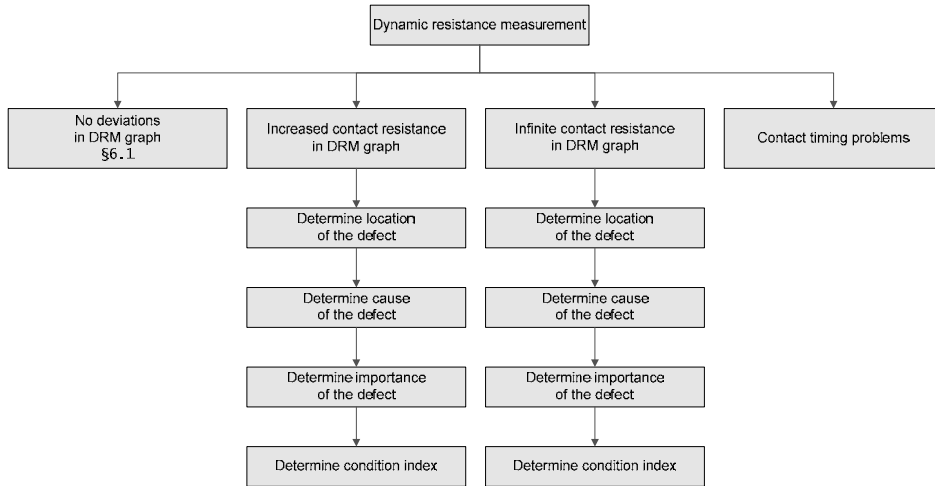


Figure 6.1 Condition assessment of an OLTC with the aid of DRM. Firstly, the results can be subdivided into:

- **no signs of defects or degradation**
- **increased contact resistance**
- **open contacts (infinite resistance)**
- **contact timing problems**

Secondly, the location and cause of the defect is determined, resulting in assessment of the importance of the defect (which can be summarized in terms of a condition index).

6.1 Regular DRM plots

If the DRM curve shows no signs of defects or degradation, only two sources of resistance variations are visible in the recorded measurement current:

- Transition resistors
- Resistance of the tapped windings

Figure 6.2 shows a typical example of the measurement current recorded on a healthy tap changer. The tap changer was switched through its cycle of operation (from the lowest to the highest tap position and back again) to obtain this recording. The effects of the two above-mentioned resistances may be clearly seen. The winding resistance changes when tapped windings are selected or deselected by the tap changer, resulting in a slope in the recorded current.

The close-up plot of Figure 6.2 reflects the operation of the transition resistors, while Figure 6.3 shows the relationship between the rotation of a selector switch (see Appendix A for a more extensive description) and the measurement current. The transition resistors cause the measurement current to decrease. This fast changing current is possible due to the short circuit on the secondary side of the transformer.

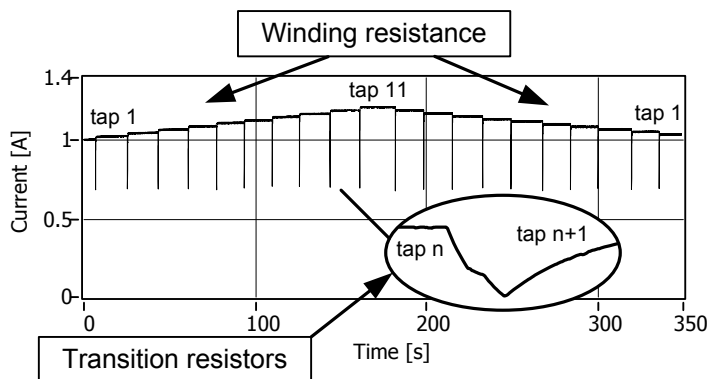


Figure 6.2 Typical DRM current in a healthy OLTC.

First, only one transition resistor is in the circuit and the current given by Equation 4-11. Only the fast response of the transformer, discussed in Section 4.1, is taken into account here.

Half-way through the OLTC operation, both the transition resistors are in parallel in the measurement circuit as shown in Figure 6.3. The resistance of the windings and the transition resistance may then be written:

$$R_w + \frac{R_t (R_t + R_{tw})}{2R_t + R_{tw}} \quad 6-1$$

where R_w is the winding resistance, R_t the transition resistance and R_{tw} the tapped winding resistance. This situation generally causes a less steep decrease in current (the current may also increase, depending on the contact timing and circuit

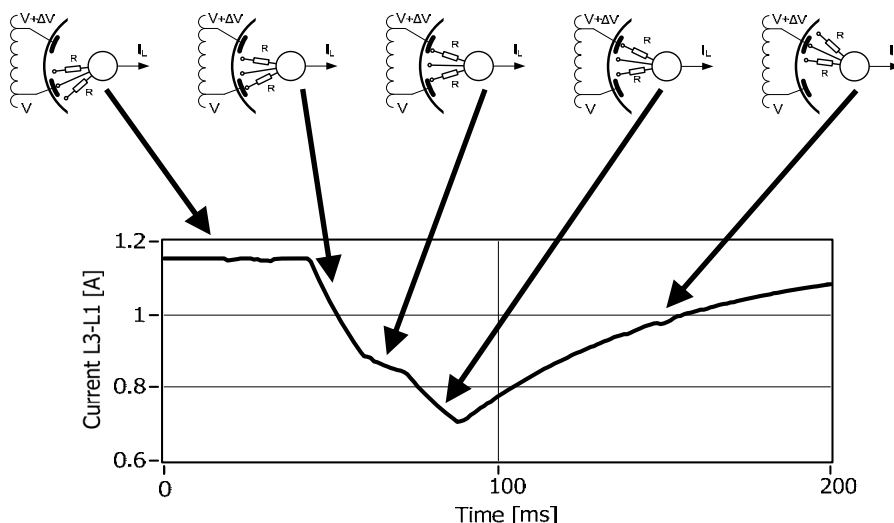


Figure 6.3 The relationship between the transition resistors and the DRM measurement current. The transformer windings are in series with the OLTC.

resistance). Finally, the transition resistor is removed and the measurement current stabilizes again. The current during OLTC operation can then be written as follows, using Equation 4-11 and the values of the different resistances in the circuit (see also Figure 6.4):

$$I_t = \begin{cases} I_0 & \text{for } t < 0 \\ I_0 - \frac{I_0 R_t}{R_{circuit} + R_1 + R_t + N^2 R_2} \left(1 - e^{-\frac{t(R_{circuit} + R_1 + R_t + N^2 R_2)}{2(1-k)L_1}} \right) & \text{for } 0 \leq t < t_1 \\ I_1 - \frac{I_1 \frac{R_t(R_t + R_{tw})}{2R_t + R_{tw}}}{R_{circuit} + R_1 + \frac{R_t(R_t + R_{tw})}{2R_t + R_{tw}} + N^2 R_2} \left(1 - e^{-\frac{(t-t_1)(R_{circuit} + R_1 + \frac{R_t(R_t + R_{tw})}{2R_t + R_{tw}} + N^2 R_2)}{2(1-k)L_1}} \right) & \text{for } t_1 \leq t < t_2 \\ I_2 - \frac{I_2 (R_{tw} + R_t)}{R_{circuit} + R_1 + R_{tw} + R_t + N^2 R_2} \left(1 - e^{-\frac{(t-t_2)(R_{circuit} + R_1 + R_{tw} + R_t + N^2 R_2)}{2(1-k)L_1}} \right) & \text{for } t_2 \leq t < t_3 \\ I_4 - (I_4 - I_3) e^{-\frac{(t-t_3)(R_{circuit} + R_1 + R_{tw} + N^2 R_2)}{2(1-k)L_1}} & \text{for } t \geq t_3 \end{cases} \quad 6-2$$

where:

$$\begin{aligned} I_0 &= \frac{U_{test}}{R_{circuit} + R_1} \\ I_1 &= I_0 - \frac{I_0 R_t}{R_{circuit} + R_1 + R_t + N^2 R_2} \left(1 - e^{-\frac{t_1(R_{circuit} + R_1 + R_t + N^2 R_2)}{2(1-k)L_1}} \right) \\ I_2 &= I_1 - \frac{I_1 \frac{R_t(R_t + R_{tw})}{2R_t + R_{tw}}}{R_{circuit} + R_1 + \frac{R_t(R_t + R_{tw})}{2R_t + R_{tw}} + N^2 R_2} \left(1 - e^{-\frac{(t_2-t_1)(R_{circuit} + R_1 + \frac{R_t(R_t + R_{tw})}{2R_t + R_{tw}} + N^2 R_2)}{2(1-k)L_1}} \right) \\ I_3 &= I_2 - \frac{I_2 (R_{tw} + R_t)}{R_{circuit} + R_1 + R_{tw} + R_t + N^2 R_2} \left(1 - e^{-\frac{(t_3-t_2)(R_{circuit} + R_1 + R_{tw} + R_t + N^2 R_2)}{2(1-k)L_1}} \right) \\ I_4 &= \frac{U_{test}}{R_{circuit} + R_1 + R_{tw}} \end{aligned}$$

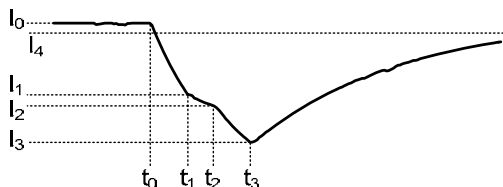


Figure 6.4 Definition of the times and currents used in Equation 6-2.

Diverter switch type OLTCs show DRM plots that are similar to those for selector switch type OLTCs; the plot of Figure 6.3 is typical for flag-cycle type OLTCs. The timing of the flag cycle (as shown appendix A) can be read off from the plot.

The effect of the transition resistors is made clearly visible when the tap changer is measured separately, without the effect of the transformer windings (Figure 6.5). The time constant of the current is no longer influenced by the leakage inductance of the transformer windings under these circumstances, and the current can change rapidly with circuit resistance changes.

Combining the results of Figure 6.3 and Figure 6.5 shows the effect of the leakage inductance clearly, see Figure 6.6. The current slowly changes towards the new equilibrium, but the transition resistors are operated again before the new equilibrium has been reached.

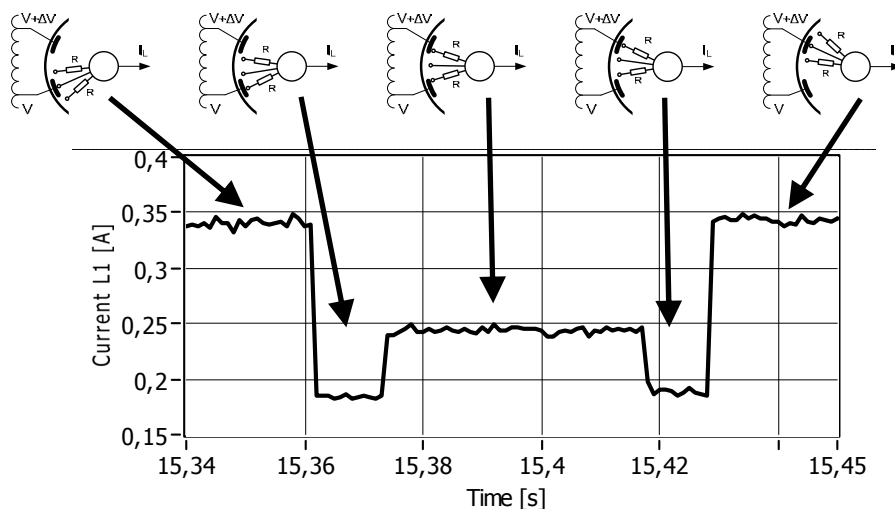


Figure 6.5 The relationship between the transition resistors and the DRM measurement current. The transformer windings are removed from the measurement circuit.

Various ways of performing DRM on a tap changer were explained in Section 4.1, where it was pointed out that defects appear in the measurement results in comparable ways. The present chapter discusses the recorded current flowing through the OLTC during the measurement in detail.

An impedance plot like that of Figure 6.7 is another way of displaying the results of a DRM. The voltage across the transformer bushings can be used to calculate the impedance. Impedance plots are mirror images of the current recordings, since the voltage is kept constant during the measurement.

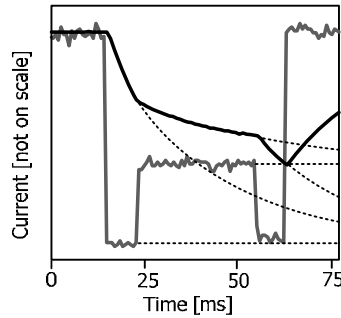


Figure 6.6 The DRM results of Figure 6.3 and Figure 6.5 are combined in this graph. The measurement current directly changes when the OLTC is measured separately, but slowly changes towards the equilibrium when the leakage inductance slows the current down.

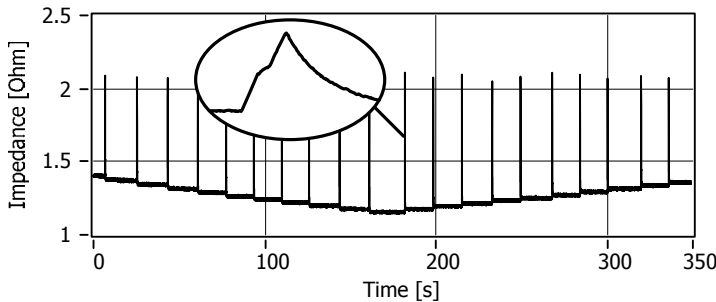


Figure 6.7 Impedance plot of a healthy OLTC. This plot corresponds to the current plot in Figure 6.2.

Another effect that can be found in normal dynamic resistance plots is related to the design of the change-over selector. Some OLTCs are designed in such a way that the arcing switch operates two times extra when the change-over selector is operated [86]. When operating the change-over selector, the arcing switch is operated twice to change one voltage step; the effect of the transition resistors can be seen in the plots at the moment when the change-over selector is operated (as indicated in Figure 6.8).

Figure 6.9 shows another effect that occurs at OLTC designs with a reversing switch: the tapped windings are reversed, allowing the tap changer to subtract the voltage of the tapped windings from that of the main windings. The polarity of the tapped windings is not measured with DRM, since the reversal does not affect the DC resistance. This gives the plot of Figure 6.9, where it looks as if the OLTC is switched through its cycle of operation twice – but this is the normal way this type of OLTC works.

The tapped winding that is reversed by the reversing change-over selector was charged in the opposite direction prior to the measurement. Reversal can result in a situation where the effect of the inductance is still measured. The central portion of the dynamic resistance plot may therefore look different from that shown in Figure 6.9. Figure 6.10 gives an example of a plot measured on a delta-connected OLTC with a reversing change-over selector showing this effect: the central portion of the plot is flat here, which is not caused by defects or contact degradation.

Measurement errors can also change the measurement plots, for example due to irregular switching, changing the measurement circuit or measurement voltage during the measurement, poor connections to the transformer terminals and starting the measurement before the current is stable. Figure 6.11 shows an example of a DRM result with a measurement error: the measurement was started before the charging phase had finished, resulting in an unstable current during the measurement. Such measurement errors typically lead to a higher current at the end of the measurement and a curved instead of a linear current pattern.

Irregularities in the plots due to measurement errors are not due to defects and degradation and the measurement can be redone to get better results.

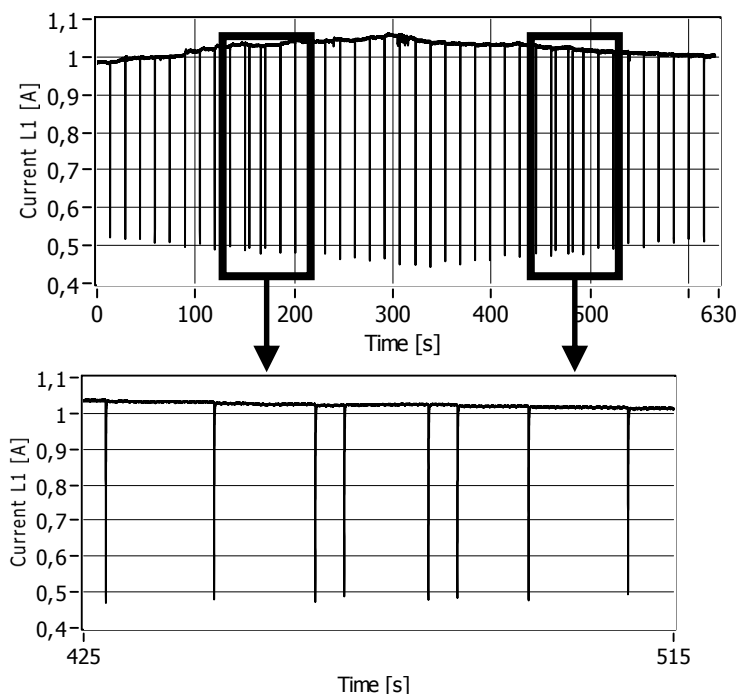


Figure 6.8 DRM results from an OLTC with three centre positions: two extra arcing switch operations are visible when the change-over selector operates (the arcing switch operates twice in succession to perform one voltage step).

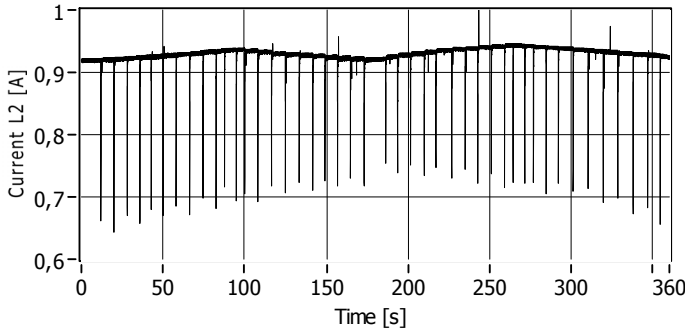


Figure 6.9 DRM plot of the cycle of operation of an OLTC with reversing switch.

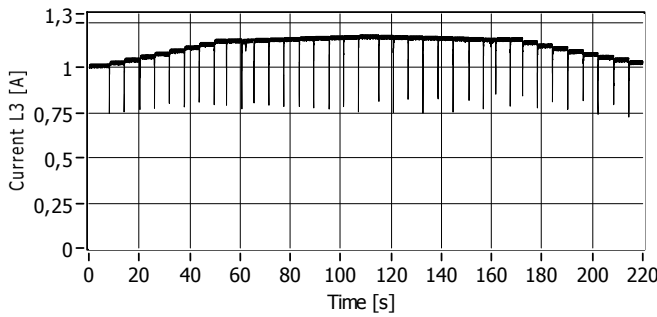


Figure 6.10 DRM plot of the cycle of operation of a delta-connected OLTC with reversing switch.

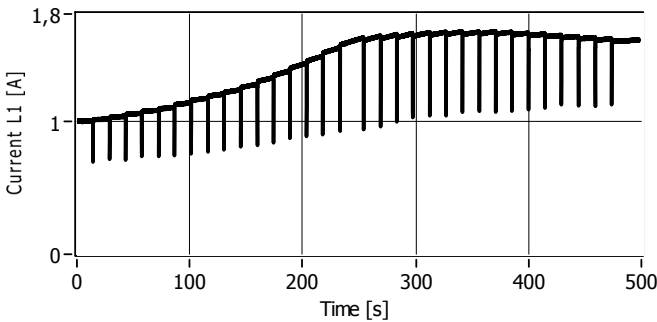


Figure 6.11 DRM plot of an OLTC affected by a measurement error: the measurement was started before the charging phase was completed. This caused the current to stabilize during the measurement instead of during the charging phase.

6.2 Irregular DRM plots

It is useful to interpret every deviation from the normal DRM plot (as discussed in the previous section) directly after the measurement, before taking the transformer back in operation again [87]. Plots with signs of defects or degradation can be resolved into different components [88], as illustrated in Figure 6.13:

Figure 6.13-A:	Measured plot, equal to the sum of components B+C+D+E
Figure 6.13-B:	Effect of winding resistance and measurement errors (this can be used as the ‘expected value’, see §6.1)
Figure 6.13-C:	Effect of the transition resistors (see §6.4.6)
Figure 6.13-D:	Effect of contact resistance
Figure 6.13-E:	Effect of open contacts (‘current interruptions’)

The first source of irregularities in dynamic resistance results which is related to degradation or defects (Figure 6.13D) is caused by increased contact resistance; this is not always a serious defect. In general, these irregularities can be caused by:

- 1 the change-over selector (discussed in Section 6.3), for example changes in contact resistance due to different stages of long-term aging
- 2 the arcing switch (discussed in Section 6.4), for example due to contact resistance or contact timing problems

During a DRM, the change-over selector is always measured in series with the arcing switch. Defects in both parts of the OLTC will show up in the results. These will be discussed in detail in the next two sections. First, Section 6.3 will give an overview of irregularities in the change-over selector. Section 6.4 will then review the effect of degradation and defects in the arcing switch.

Complete interruption of the measurement current due to open contacts is in general a more serious problem.

It is important to know the location of the defect when interpreting the measurement results. All the irregularities occur at specific locations on the current profile. Figure 6.12 gives a schematic representation of a typical measurement current recorded on a healthy tap changer as shown in Figure 6.2. This will be used as a basis for indicating where the defect is expected in DRM plots of the OLTC’s cycle of operation.

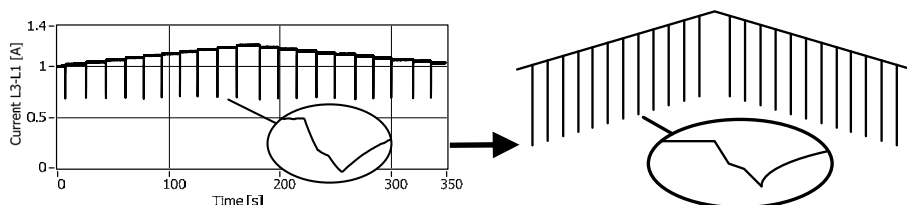


Figure 6.12 Schematic representation of a typical DRM current recorded on a healthy OLTC.

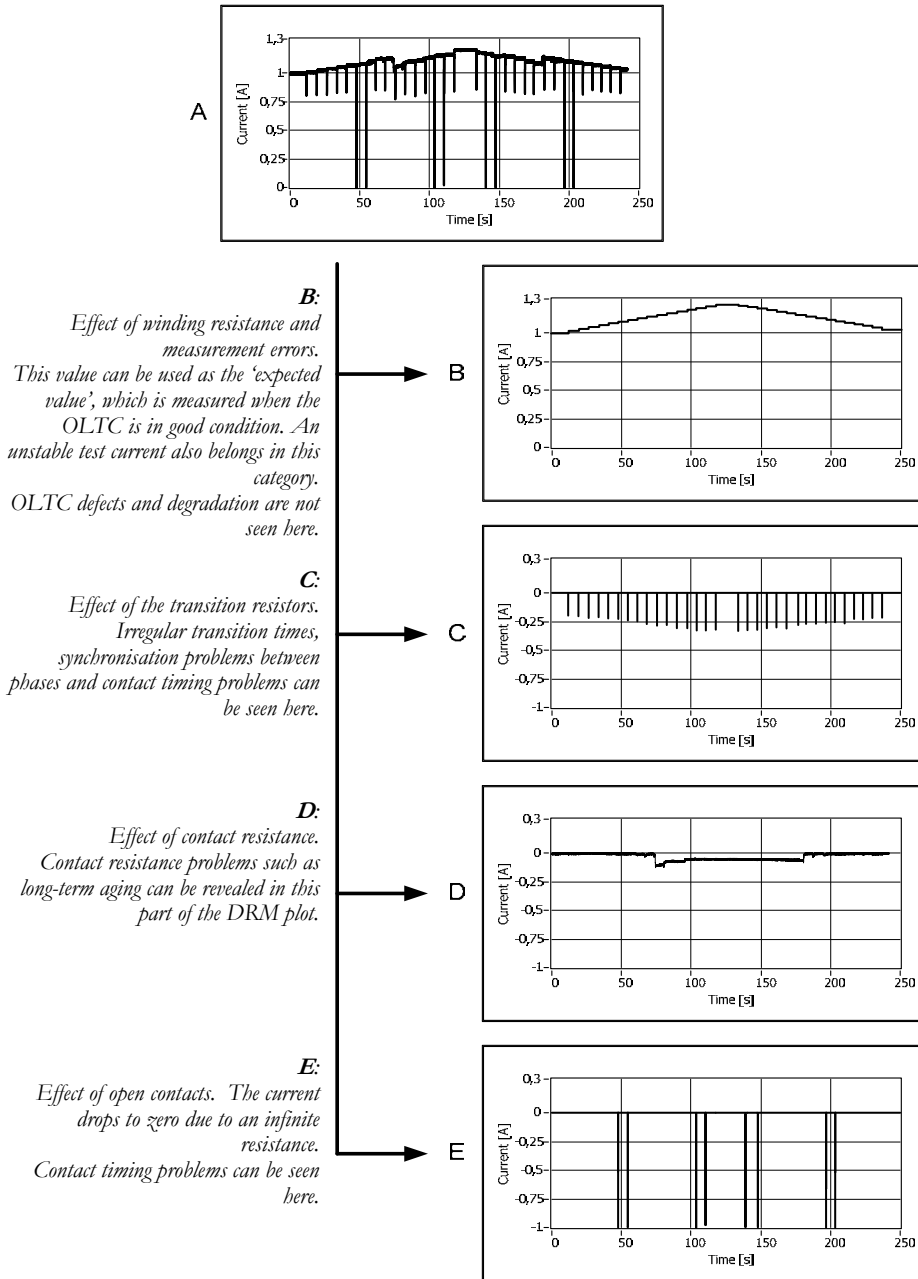


Figure 6.13 Example of a DRM plot of an OLTC (A) which can be separated into the effect of winding resistance (B), the effect of the transition resistors (C), the effect of contact resistance (D) and the effect of open contacts (E).

6.3 Irregularities in the change-over selector

More than 600 dynamic resistance measurements have been performed on OLTCs within the framework of this thesis project. Almost all change-over selector irregularities observed in the Dutch utility grid were due to the long-term aging effect discussed in Section 2.3. The present section deals with DRM where long-term aging is observed:

- 1) when the change-over selector selects another tap in combination with a selector switch (§6.3.1),
 - a) at an early stage (§6.3.1.2)
 - b) at an advanced stage (§6.3.1.3)
- 2) in the parking position and when the tap changer is at the end of its regulating range (§6.3.1.4)
- 3) in the change-over selector at the moment of operation of the arcing switch (§6.3.1.5)
- 4) in the tap selector when used in combination with a diverter switch (§6.3.1.6)

Irregularities in the measurement plots caused by the change-over selector appear, change or disappear while it is operated. A typical irregularity here is the surface film, which can be recognized when the change-over selector moves. An example is given in Figure 6.14, which shows a close-up view of the operation of an arcing switch preceded by spikes in the contact resistance due to contact movement in the change-over selector. To study this effect, it is necessary to determine when the change-over selector is moved by the drive mechanism.

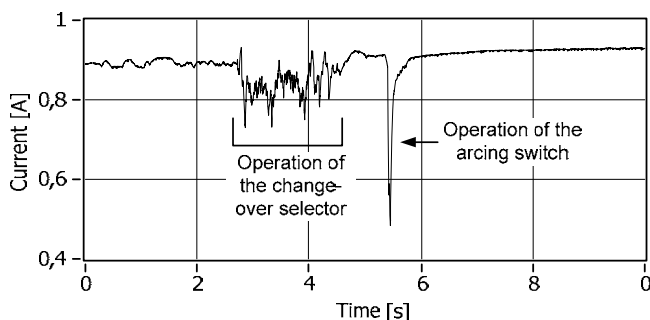


Figure 6.14 Moving change-over selector contacts cause spikes in the dynamic resistance just before the arcing switch is operated.

6.3.1 Long-term aging in selector switch type OLTCs

6.3.1.1 Movement of the coarse change-over selector

Depending on the number of fine taps and the desired number of tap positions, one or two coarse taps are used for expanding the regulating range. The coarse change-over selector only selects another coarse tap a few times during each cycle

of operation. This selection is much slower than the operation of the arcing switch. Figure 6.15 shows the corresponding locations in the recorded current for an OLTC with one (Figure 6.15A) or two (Figure 6.15B) coarse taps. The coarse change-over selection can cover two tap change operations of the selector switch. The contacts of the change-over selector typically move a few seconds before the operation of the selector switch. Valuable information about long-term aging can be extracted from the DRM results when the change-over selector contacts are carrying current when they move. This section takes this type of tap changer as an example to explain the movement of the change-over selector.

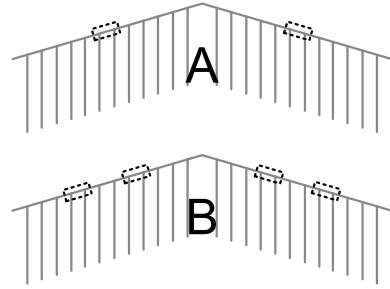


Figure 6.15 Positions where the coarse-tap selector moves its contacts to a next tap in an OLTC with one (A) or two (B) coarse taps.

The change-over selector contacts can move beyond these two tap positions due to the design of the drive mechanism. In the case that the drive is designed that way, the drive mechanism also causes the change-over selector to move a slightly outside the two positions of the coarse tap selection, to prepare for the coming coarse tap change. These small movements can occur two positions before and one position after the mid-position of the change-over selector, depending on the drive mechanism used. It follows that the total movement of the coarse change-over selector covers four tap change operations as indicated in Figure 6.16.

During the coarse tap change operations, the coarse change-over selector makes contact with both coarse taps, as already shown in Figure A.5C. This position will be called the mid-position of the coarse-tap selector. It does not always coincide with the parking position of the selector switch (the 'k' contact).

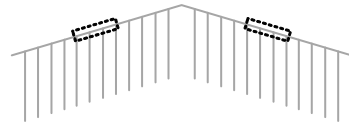
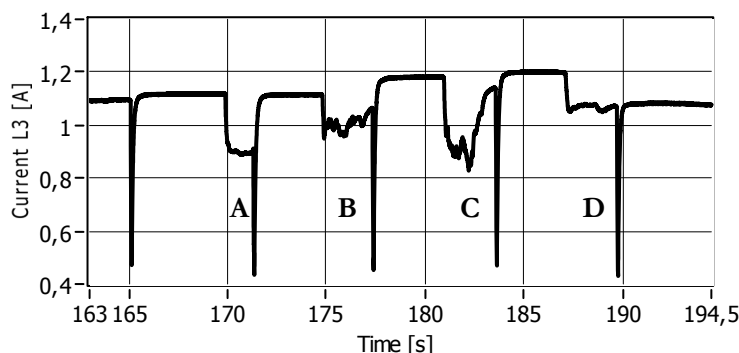


Figure 6.16 Positions where the coarse-tap selector moves its contacts to a next tap.

For example, Figure 6.17 shows the DRM plot of a service-aged coarse change-over selector. The contact resistance increases just before the operation of the arcing switch and lasts several seconds until the operation of the arcing switch. The Geneva wheel driver can cause a step in the measurement current, while the movement of the change-over selector to and from the mid-position gives rise to a spike, as can be seen in Figure 6.17. In general, moving contacts are visible as spikes in the contact resistance curve.

Figure 6.17 also shows the relative timing of the change-over selector and the arcing switch: the change-over selector (or tap-selector) starts to move a few seconds before the arcing switch operates. The tap change ends with the operation of the arcing switch, which is recognizable by the effect of the transition resistors. The OLTC and drive are motionless after the tap change, giving a constant resistance. This information can be used to recognize the operation of the arcing

switch in heavily distorted DRM plots. The plot can be read backwards to detect tap changes: the first resistance change then normally corresponds to operation of the arcing switch.



- A** Geneva wheel driver hooks into notch, causing a slight movement.
- B** Movement of coarse change-over selector to mid-position.
- C** Movement of coarse change-over selector to next stator block.
- D** Geneva wheel driver leaves the wheel, moving the tap-selector slightly.

Figure 6.17 Typical coarse change-over selection covering four tap positions. The contact resistance is measured during operation of the change-over selector. The driver of the Geneva wheel causes irregularities "A" and "D", while irregularities "B" and "C" originate in the movement of the change-over selector to and from the mid-position.

The movement of the change-over selector can depend on the direction the OLTC moves through all tap positions, making the range of motion of the change-over selector asymmetrical. This asymmetry is simply the result of the change-over selector design: no current switching is allowed. One set of contacts is without current and switches first, but this depends on the direction in which is switched. Figure 6.18 gives an example of this asymmetry for a design of selector switch type OLTC that is commonly used in the Netherlands. When the tap position is increasing, the irregularities are present at tap positions 8-11. The parking position (or 'k' contact) is used in tap position 9 (indicated by 'P'), while the mid-position of the change-over selector occurs at tap position 10 (indicated by 'M'). With a descending tap position (shown on the right), a higher contact resistance is also observed at tap positions 8-11 but the parking and mid-positions are both at tap position 9 in this case.

In general, these examples show that changes in the contact resistance caused by the change-over selector can be expected two positions before the mid-position and one position afterwards it.

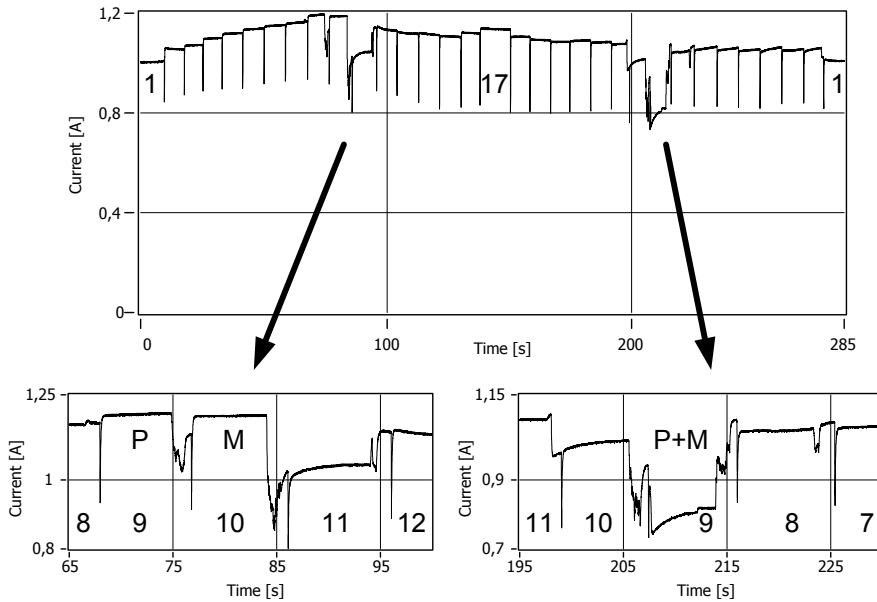


Figure 6.18 Example of DRM on a service-aged OLTC suffering from change-over selector contact degradation. Asymmetry in the change-over selector movement is observed. When the tap position is increasing (left), the irregularities are observed in tap positions 8-11. The parking position is at position 9 (indicated by 'P'), while the mid-position of the change-over selector occurs at position 10 (indicated by 'M'). With a descending tap position (right), the irregularities also occur at positions 8-11, but the parking and the mid-positions are both at position 9.

Finally, in some types of OLTCs the drive system can prepare for a coarse tap change at the end of the regulating range, but no coarse tap change is actually made because the end of the regulating range has been reached. The slight movement of the coarse change-over selector can be detected in dynamic resistance results as a rapid change in contact resistance, made visible as a stepwise change in the measurement current. This effect only shows up in measurement results in combination with long-term aging of the change-over selector contacts. To sum up, all places where the change-over selector can move are indicated in Figure 6.19.

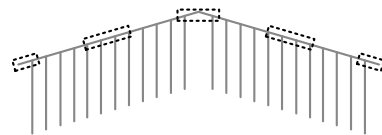


Figure 6.19 All positions where the coarse-tap selector can move its contacts.

6.3.1.2 The surface film layer

The surface film layer on change-over selector contacts, which is caused by long-term aging, results in increased contact resistance. This early stage of the long-term aging effect is measured when the contacts are moved over the film while the contacts carry the measurement current. This less conductive layer described in Section 2.3 grows slowly, so when DRM is performed during regular tap changer

maintenance – normally once every few years – the increase in contact resistance can be observed in different stages.

The early stage of long-term aging (i.e. the surface film) can be recognized by small changes in the contact resistance at the moment the change-over selector moves. Figure 6.20 shows an example. It is clearly visible here that the change-over selector is moved twice during the measurement. The recorded current curve remains linear after the coarse tap selection has been completed. The increased resistance is only observed in this example at tap positions which are infrequently used (no overheated contacts, as described in Section 2.3.2). It is clear that the irregularities originate in the change-over selector and not in the arcing switch.

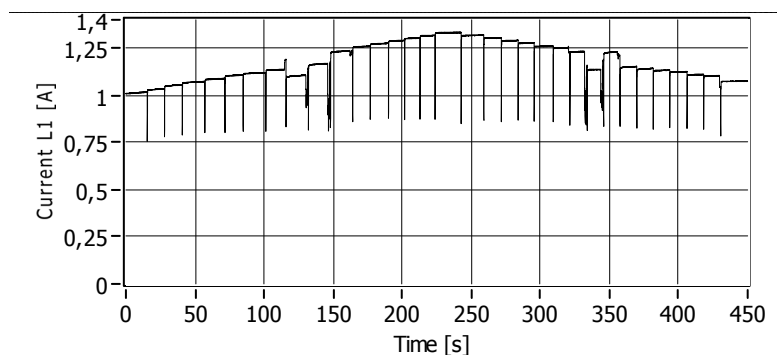


Figure 6.20 DRM diagnostic data showing contamination of the coarse change-over selector.

Figure 6.21 shows an example of a DRM plot of a service-aged OLTC with 8 fine windings and another plot for a tap changer with 5 fine windings. The latter makes two coarse tap changes instead of one to reach the same number of tap positions. The tap change operations indicated by rectangles involve the change-over selector. Both tap changers also show irregularities in contact resistance at the end of the regulating range. Once again, the arcing switch does not give rise to any irregularities in this example: contact degradation is only observed when the change-over selector moves, and thus only involves the contacts used at the few tap positions where the change-over selector operates. Since the change-over selector contacts in this example are infrequently used, they will be coated with a surface film (as discussed in Section 3.2.2.1). Several inspections reveal that these contacts are normally not degraded. As long as contact resistance is only present on change-over selector contact areas that are used briefly during OLTC operation, these contacts will not be pitted or covered with pyrolytic carbon. In general, this early stage of long-term aging should not be considered as critical, but the above-mentioned surface film could lead to coking in the long-term. It may be regarded as harmless in itself, in the absence of contact overheating leading to carbon formation.

It should be noted that this change-over selector contamination is only observed when the change-over selector contacts move to another position while carrying the measurement current, which is not always the case (as discussed in

appendix A). For example, small irregularities from normality will remain undiscovered in most diverter switch type OLTCs.

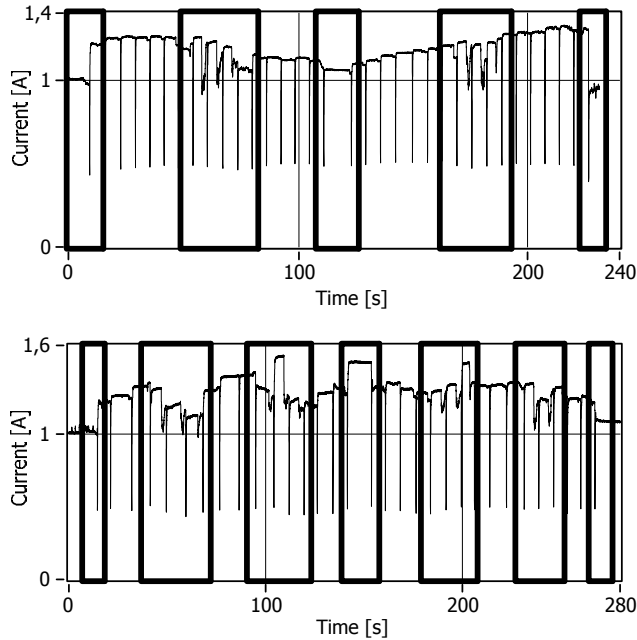


Figure 6.21 Typical irregularities caused by a moving coarse change-over selector. Top: DRM plot for a tap changer with 8 fine windings, using one coarse winding. Bottom: DRM plot for a tap changer with 5 fine windings, using two coarse windings.

6.3.1.3 Contact coking

When long-term aging develops further, the early change-over selector degradation discussed in the previous section will also lead to higher contact resistances when the change-over selector is motionless. The advanced long-term aging is defined as a state where a higher contact resistance is also present in tap positions where the change-over selector is motionless. This situation allows contact coking to occur. High contact temperatures are expected, as described in Section 2.3.3. The tap changer reached a part of its lifetime where the resistance increases rapidly and coking occurs, as shown in Figure 2.17 [24]. The measurement current will thus drop to lower values during significant parts of the regulating range. This stage of long-term aging can be recognized when the DRM diagnostic data shows stable changes in the contact resistance when the contacts are motionless. The high contact resistance leads to the deposition of low-conductivity carbon at the tap positions where the OLTC is

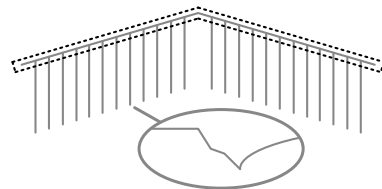


Figure 6.22 The positions where advanced long-term aging is observed.

often positioned when transformer is in service. We observed during overhaul that this phase of long-term aging is accompanied by the presence of a thick surface film, pyrolytic carbon and deep pitting of the contact surface.

A frequently observed irregularity of the recorded current plot is found when the change-over selector is moved and a stable resistance for that particular coarse tap is formed. Figure 6.23 shows two typical examples of measurement results from service-aged OLTCs. One of the coarse taps is in better condition, but extra resistance is introduced in the circuit when another coarse tap is selected. The extra resistance remains in the circuit until the change-over selector operates again. This is typical of change-over selector contact degradation.

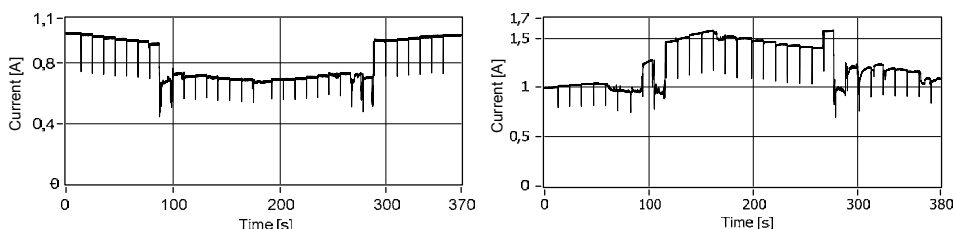


Figure 6.23 DRM diagnostic data showing increased contact resistance in one of the coarse change-over selector contacts.

6.3.1.4 The parking position

Another frequently observed irregularity of service-aged OLTCs with advanced long-term aging of the change-over selector is a rise or fall in the resistance when the change-over selector moves. We say that the parking position is visible, as illustrated in the DRM plot of Figure 6.25. The change-over selector now uses parts of the stator contact blocks without carbon formation or pitting. This contact area is not thermally degraded but a layer with low conductivity exists on the contact, as described in Section 2.3.2. The irregular contact resistance may also be observed away from the parking position, since the movement of the change-over selector can cover up to four tap positions (see Figure 6.24).

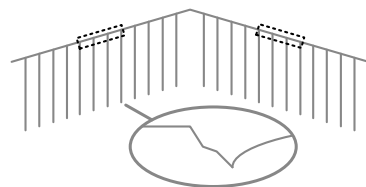


Figure 6.24 Typical location of the parking position.

Such defects look local, and hence not severe, at first sight but it should be borne in mind that the contacts at the parking position are usually in better condition than those at other tap positions, because they are only used at a few tap positions and are therefore not likely to suffer from severe contact coking. In this case, the other contacts of the change-over selector will be more liable to long-term aging.

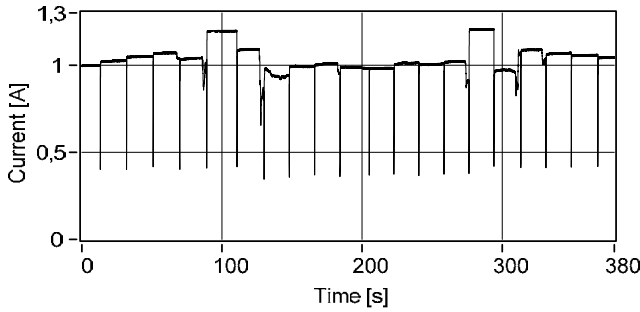


Figure 6.25 DRM diagnostic data showing a stable resistance in all positions, but less in the parking position.

6.3.1.5 Vibrations in the change-over selector due to operation of the arcing switch

Long-term aging of the change-over selector does not only show up when its contacts are moved by the drive mechanism. Small vibrations due to the arcing switch operation can also affect the contact resistance of heavily degraded change-over selector contacts. The change-over selector then causes changes in the contact resistance at points where it is normally motionless. This is the area where arcing switch defects are normally observed, giving the plot a chaotic appearance.

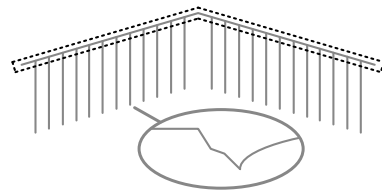


Figure 6.26 Locations where the effect of vibration of the change-over selector due to operation of the arcing switch can be observed.

A trial was performed to investigate the effect of arcing switch vibrations on long-term aging of a change-over selector. An OLTC with advanced long-term aging was removed from the transformer tank and mounted on a drive mechanism. A DRM plot was recorded for the change-over selector of this device without the arcing switch. Vibrations due to the mechanical operation of the drive mechanism and the arcing switch were found to have an effect on the contact resistance of the change-over selector. Figure 6.27 gives an example of the DRM plot of such a change-over selector, which is kept stationary. The contact resistance changes at the moment when the arcing switch is operated (indicated by * in the plot).

Irregularities in the change-over selector resistance due to operation of the arcing switch can be recognized by:

- 1 The presence of advanced long-term aging of the change-over selector contacts (see §6.3.16.3.1.3).
- 2 A time of inception that is related to operation of the arcing switch.
- 3 Contact resistance variations of an amplitude that is not related to the position of the arcing switch (see §6.4.1.2).
- 4 Irregularities in the current curve at points where the change-over selector is normally motionless.

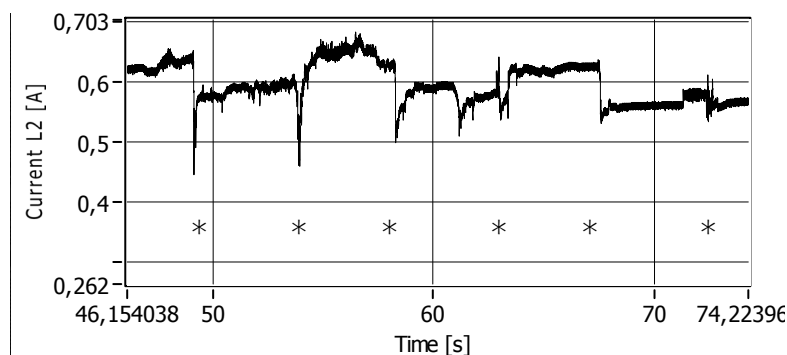


Figure 6.27 Close-up view of the DRM plot of a change-over selector. Vibrations in the drive mechanism and the arcing switch led to changes in the contact resistance.

These irregularities are easily confused with long-term aging of the arcing switch contacts themselves. In both cases, the resistance changes stepwise when the arcing switch operates. In general, the arcing switch is likely to cause irregularities in the dynamic resistance if the contact resistance when the change-over selector is motionless is out of proportion with the changes found when the change-over selector is operated. To put it the other way round, severe long-term aging of the change-over selector is likely to cause contact resistance changes when the OLTC operates. Contact degradation located in the arcing switch may hence remain undiscovered in this case.

6.3.1.6 Diverter switch type tap changers

The previous section considered a change-over selector design where the contacts were moved (not switched) while the measurement current flowed through them. The surface film on the contacts showed clearly in the DRM graphs at these types of OLTCs. However, diverter-switch type OLTCs normally move their tap-selector contacts without current. In that case, the surface film on the briefly-used contact area is not measured and only the stationary contact locations will be diagnosed. Early long-term aging of the change-over selector contacts may remain undiscovered. If the aging progresses further, a step change in the resistance can be observed when the diverter switch selects the next position of the coarse tap-selector (as shown in Figure 6.28). Diverter switch type tap changers normally use snap contacts (also called tap selector contact terminals, see Figure 6.29) to pre-select the next winding tap. These contacts have a strong mechanical wiping effect on the surface film and are thus less prone to long-term aging. An example of the DRM plot for such an OLTC is given in Figure 6.30.

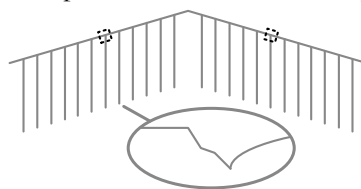


Figure 6.28 The locations where defects are observed in a coarse tap-selector in combination with a diverter switch.



Figure 6.29 Change-over selector contact of a diverter switch type tap changer. Two contact terminals for (pre) selecting a transformer winding are shown. The bottom terminal has been selected.

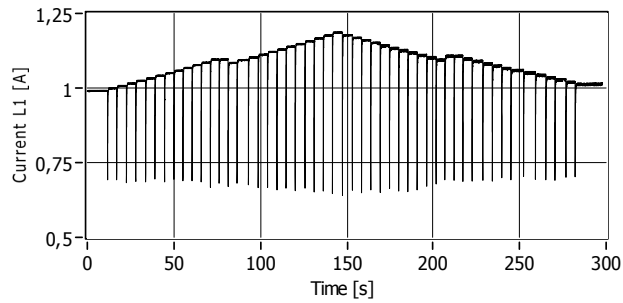


Figure 6.30 A typical current profile of a tap changer which moves its coarse tap-selector contacts at zero current. Only the stationary resistances are visible.

Another typical example is shown in Figure 6.31, which presents the plot of a diverter switch type OLTC with a number of overheated tap-selector contacts. Several tap positions show increased contact resistance. These tap-selector contacts did not have any surface film, and inspection showed that they were already heavily pitted.

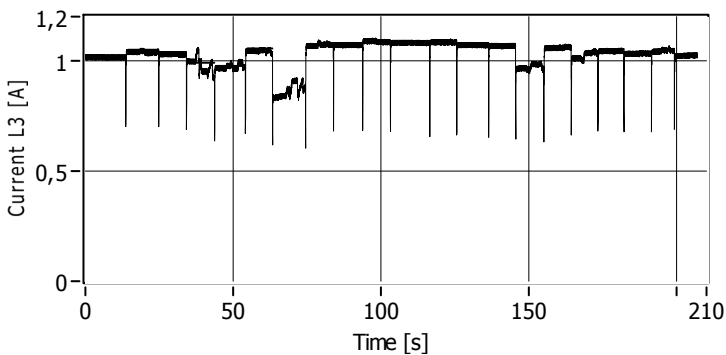


Figure 6.31 Example of a DRM plot of a service-aged OLTC with a tap-selector using snap contacts. Increased contact resistance was observed at several tap positions. Overheated tap-selector contacts were found during inspection.

6.3.2 Current interruptions due to the change-over selector

The second source of changes in the dynamic resistance measurement results that is related to degradation or defects (Figure 6.13E) occurs when the measurement current is completely interrupted by the tap changer. In that case, problems can be

expected when the OLTC is in service. The contacts are not designed to handle interruptions in the load current: the tap changer and the transformer surrounding it can be seriously damaged when the OLTC tries to interrupt the load current. Several factors can cause the measurement circuit to be totally interrupted during diagnostic measurements. These factors may be classified according to the location of the interruption (arcing switch or change-over selector).

The duration of the interruption and its location in the cycle of operation provide information about the site of the interruption. The influence of the amplitude of the measurement current can provide further information about the cause of the interruption.

Current interruptions caused by the change-over selector will appear and disappear when the change-over selector is operated, and typically last longer than the transition time of the arcing switch. Interruptions longer than 200 ms that appear in the area of the DRM plot where the change-over selector is moved are typically caused by the change-over selector. These interruptions may take place only when the change-over selector moves (Figure 6.32A) or may cover complete coarse taps (Figure 6.32B). Two examples of these defects as measured in the Dutch utility grid are shown in Figure 6.33 and Figure 6.34. The first concerns an OLTC with contact timing problems in the change-over selector due to a maintenance error. Wrong timing due to incorrect reassembly caused incorrect contact timing between the selector switch and the change-over selector. As a result, the change-over selector switched before the current was transferred to another contact. The interrupted current was recognized as a serious defect and the error was corrected before the transformer was re-energised. The example of Figure 6.34 concerns a change-over selector that did not establish a correct connection in one of its coarse taps due to advanced long-term aging. This transformer was damaged beyond repair when it was energized directly after the taking of the DRM of Figure 6.34 (note: this plot was recorded with the system described in [81]). Both cases involved complete interruption of the current: such current interruptions due to the change-over selector or tap-selector should be considered to be critical.

In general, interruptions of the current due to the change-over selector can be caused by:

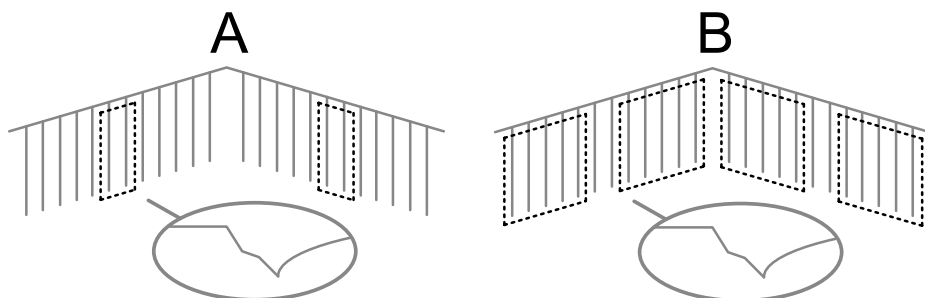


Figure 6.32 Current interruptions due to the change-over selector can occur when the change-over selector moves (A) or can cover larger parts of the cycle of operation (B).

- 1 Long-term aging (leading to a thick surface film or coking). DRM results recorded during previous OLTC maintenance will already show signs of long-term aging. The contact resistance will depend on the measurement voltage and current amplitude. Interruptions of the measurement current may disappear when the current amplitude is increased.
- 2 Wrong contact timing; such interruptions are independent of measurement voltage and current amplitude.
- 3 Mechanical damage to the OLTC; these interruptions are also independent of measurement voltage and current amplitude.

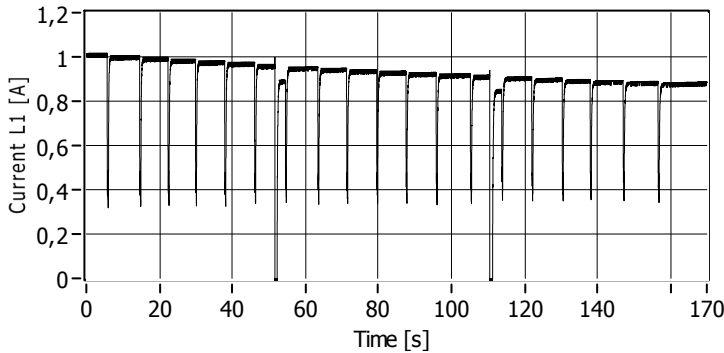


Figure 6.33 Dynamic resistance measurement on a tap changer with a change-over selector which interrupted the current due to incorrect contact timing.

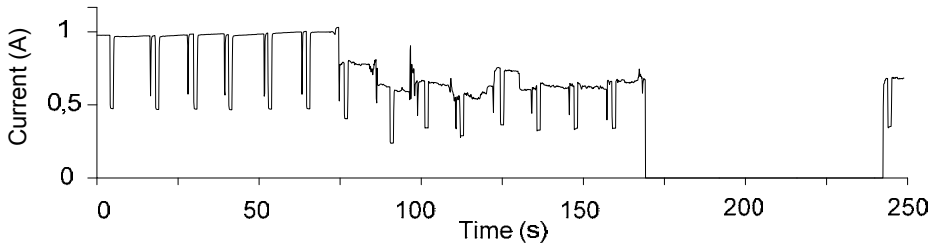


Figure 6.34 Dynamic resistance measurement on a service-aged tap changer with a change-over selector which interrupted the current due to long-term aging.

6.4 Irregularities in the arcing switch

It was demonstrated in the previous section that defects in the change-over selector show up when the change-over selector contacts move. In general, irregular values of the contact resistance appear, change and disappear when the contacts move. This also applies to the arcing switch: irregularities in the contact resistance caused by the arcing switch appear, change or disappear when it is operated. It should be noted that the arcing switch operates throughout the entire cycle of operation. Hence, the arcing switch can give rise to changes in the contact resistance that are more frequent but shorter-lived than those caused by the change-over selector.

The arcing switch is also operated more frequently during the service life of the power transformer than the change-over selector, typically 1-10 times a day. Long-term aging gets less chance to develop on the moving contacts under these conditions, because the surface film is wiped off during each operation of the arcing switch.

This section will elaborate on how defects in the arcing switch can lead to irregularities in the DRM plot. The following defects are considered:

- 1 Long-term aging (see §6.4.1)
- 2 Contact wear (see §6.4.2)
- 3 Timing difference between phases (see §6.4.3)
- 4 Maintenance errors (see §6.4.4)

Defects and contact degradation in the arcing switch can be checked during regular maintenance.

6.4.1 Long-term aging in the arcing switch

Despite the frequent movement of the moving contacts in the arcing switch, we observed that pyrolytic carbon deposition can occur here. This slow degradation effect can develop between fixed contacts (interfaces) that often carry the load current, and is similar to the long-term aging of the change-over selector contacts. It shows up in the contact resistance as a disturbance of the linear profile (Figure 6.35) during operation of the arcing switch. In general, the presence of a linear pattern in the plot points to an arcing switch without long-term aging. Two types of arcing switches (those used in selector-switch type OLTCs and in diverter-switch type OLTCs) are discussed in turn below.

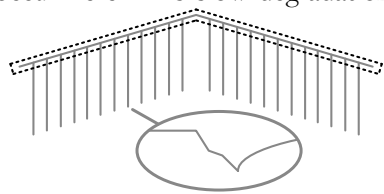


Figure 6.35 The positions where step changes in the current due to the arcing switch are observed.

6.4.1.1 Selector switch type OLTCs

The effect of long-term aging on this type of arcing switch was investigated by plotting the DRM current curve for a separate arcing switch to ensure that contact degradation of the change-over selector did not influence the readings. A selector-switch type OLTC which had been in service for 50 years was used for this trial. Inspection of the contacts showed signs of coking due to long-term aging.

For this experiment, the selector switch was measured separately by disconnecting the arcing switch from the change-over selector and the transformer windings. Figure 6.36 shows the current recorded while the tap changer was switched through all tap positions. It may be clearly seen that the resistance is increased by long-term aging of the contacts of the selector switch. Variations in the resistance occur at the moment when the selector switch operates. The

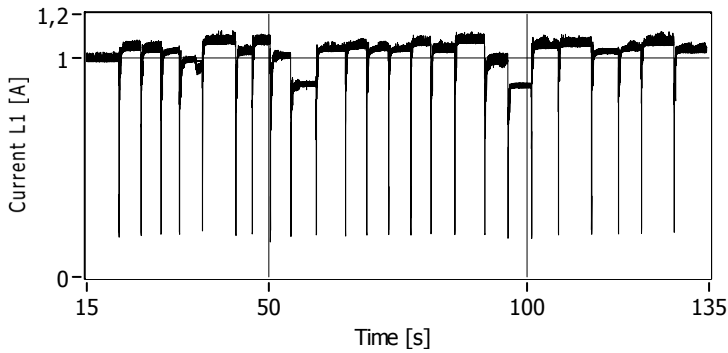


Figure 6.36 Step changes in the resistance are visible in this DRM plot of a separate arcing switch.

resistance remains constant between selector switch operations, because the switch is then motionless.

Figure 6.37 shows a close-up view of the current plot during arcing switch operation. The effect of the transition resistors is measured during the interval 200-300 ms. The spikes caused by moving contacts over degraded fixed contacts are visible before and after the transition resistors are used. It will be recalled that the selector switch contacts can oscillate after each tap change operation (see Figure 3.7) and the spikes in the dynamic resistance are measured during these oscillations.

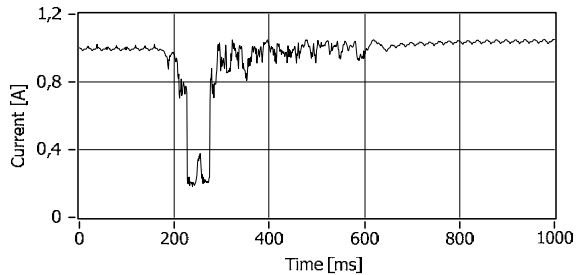


Figure 6.37 Close-up view of Figure 6.36.

The small increase in contact resistance when the arcing switch is installed in the power transformer is also visible in the DRM plots. Figure 6.38 gives an example: the increase in resistance shows up here as a drop in current. This effect is also visible in the DRM plots of circuit breakers [78].

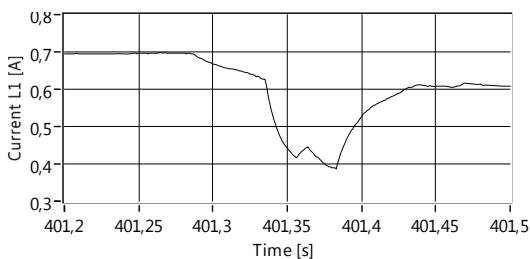


Figure 6.38 Close-up view of the measurement current variation during a dynamic resistance measurement on a selector-switch type OLTC. The contact resistance increased just before the contacts separated.

6.4.1.2 Diverter switch type OLTCs

Unlike a selector-switch type OLTC, a diverter-switch type OLTC has only two sets of contacts available for tap selection. One is selected by the diverter switch and is under load. The second set of contacts is used to select the next tap (pre-selected tap) at zero current. The diverter switch switches from the selected to the pre-selected tap each time the tap changer is operated (see also Appendix A). A typical irregularity of the current appears when one of these contact sets has an increased resistance. The measured resistance will then alternate. An example of such a dynamic resistance measurement is shown in Figure 6.39, which was obtained by measuring a tap changer with a defect that had been artificially applied in order to investigate this effect.

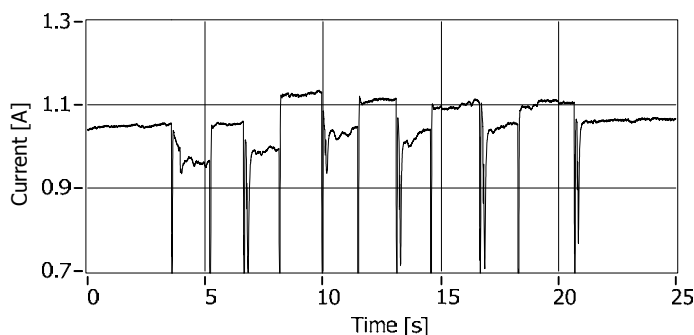


Figure 6.39 Dynamic resistance measurement on a diverter switch type OLTC with one set of deteriorated contacts.

6.4.2 Contact wear of the arcing switch

Wear of arcing switch contacts also changes the DRM plots because it influences the timing of the transition resistors. This effect is short-lived and shows up at throughout the entire cycle of operation where the arcing switch operates (Figure 6.40).

Figure 6.41 shows a typical plot for a service-aged arcing switch (from a diverter-switch type OLTC) which uses one of the transition resistors a little longer. This causes the measurement current to drop to lower values. Trigger points are added to the figure to show up the minima more clearly.

This effect can be caused by contact wear or by an irregular switching speed. Experiments have been designed to show how the contact timing can be affected. The results will be presented in Section 7.2.

Heavily worn contacts can also cause short-lived current interruptions during DRM. These interruptions will be discussed in Section 6.4.5.

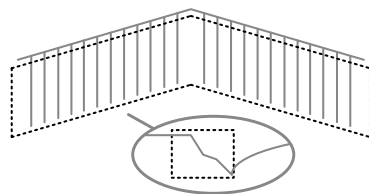


Figure 6.40 The positions where contact wear of the arcing switch shows up.

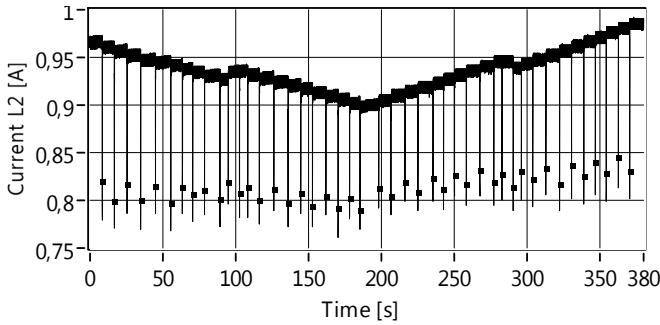


Figure 6.41 The depth of the current drop during the tap change operations alternates due to changes in the switching speed or contact wear in one set of diverter switch contacts.

6.4.3 Timing difference between phases

The three phases of the OLTC are designed to switch at the same time. Defects in the drive mechanism or in the drive shaft can cause loss of synchronism between the phases. The difference in the timing of the transition resistors can be revealed by DRM. When there is a loss of synchronism, the transition resistor is introduced in one phase earlier than in another phase. The measurement current during an OLTC operation will then briefly increase in the path with the lowest resistance (i.e. the phase without transition resistors). Figure 6.44 gives an example: the current through the three phases is shown at the moment when the defective OLTC operates. Two phases switch prematurely, causing the current through the third phase to increase. A simulation of this defect has already been shown in Figure 4.22.

The effect can be seen most clearly when the three phases are measured simultaneously. When only one phase is measured, for example in the case of an tap changer in a delta-connected transformer winding, only the increasing measurement current is observed, thus indicating when the other phases switched. The increasing current typically appears very close to the point of operation of the arcing switch, and can show up throughout the entire cycle of operation, as illustrated in Figure 6.42.

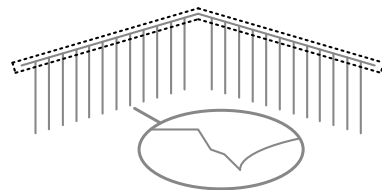


Figure 6.42 The location where contact timing problems are observed.

6.4.4 Maintenance errors

In addition to typical degradation-related DRM results, atypical irregularities in the plot may be caused by errors in the maintenance of the arcing switch. These errors may affect the transition times, cause interruptions of the current or cause irregular contact resistances. An example is shown in Figure 6.43. The irregularities observed in this DRM plot could not be ascribed to severe long-term aging

(contact coking), since they would then appear at several locations in the plot. Nor could they be attributed to other forms of long-term aging or to other contact degradation mechanisms. In fact, they were due to a maintenance-induced problem leading to interruption of the measurement current in one phase. The recorded current was not interrupted because the OLTC was mounted in a delta-connected winding so that an alternative path for the current was still available. A current interruption in a delta-connected transformer leads to a drop of current in another phase. In this case, the defect resulted in incorrect operation of the arcing switch and total loss of the power transformer after it was energised after taking this DRM. It follows that inspection (or re-inspection) of the arcing switch is advisable when atypical irregularities appear in the plot.

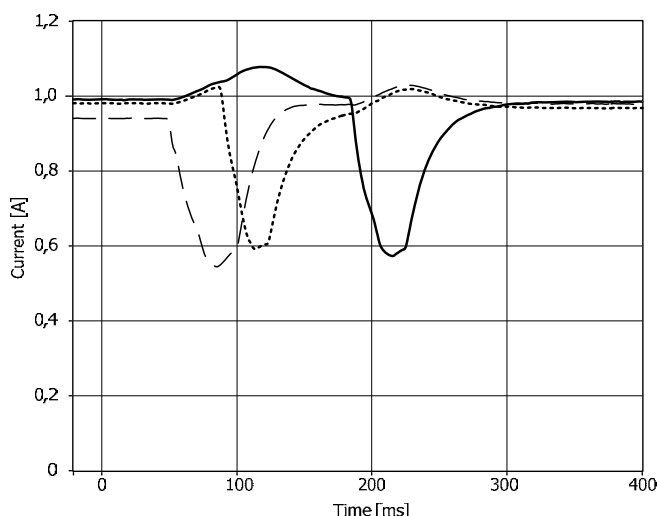


Figure 6.44 Example of a recording of the DRM current in an OLTC with synchronisation problems between the phases.

The example of Figure 6.43 shows clearly that a critical situation can arise due to an irregular dynamic resistance in only one tap position. While a tap position can be used for a long time, a defect on one particular tap position can cause a catastrophic failure of the transformer. Once again, it may be said that a chain is only as strong as its weakest link.

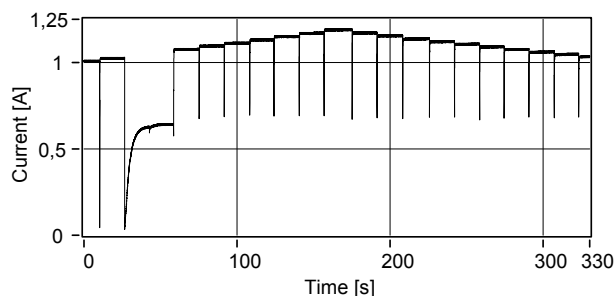


Figure 6.43 Dynamic resistance measurement on a tap changer with a defect in the arcing switch.

6.4.5 Current interruptions due to the arcing switch

Interruptions of the measurement current that originate in the arcing switch are characterized by their short duration – normally only part of the transition time (typically 10-200 ms) or the time corresponding to one complete tap position. Such irregularities in the DRM plot can be attributed to the arcing switch when they appear at moments when the change-over selector is motionless. Longer interruptions are unlikely to originate in the arcing switch because it is operated more frequently than the change-over selector.

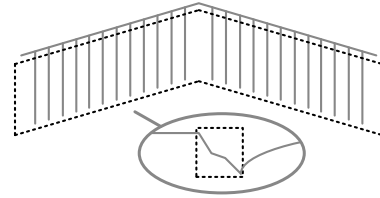


Figure 6.45 Interruptions due to the arcing switch are short and can occur throughout the entire cycle of operation.

All interruptions appear when the arcing switch is operated, as indicated in Figure 6.45. Three causes are discussed in this section: oil between the contacts, contact wear and damaged transition resistors.

6.4.5.1 Short interruptions due to a surface film

Short current interruptions when the arcing switch operates can be caused by a thin layer of oil that has to be pushed away by the moving contacts before a low-resistance contact can be made. This phenomenon occurs at low measurement currents in arcing switches that use contact blocks. The oil layer will not cause current interruptions in normal operation, because the open-circuit voltage is then higher (for instance 300 V instead of 3 V) and the current is also higher. Short interruptions of this type are therefore not critical, but if they occur the OLTC should be checked to ensure that it is indeed subject to this effect.

6.4.5.2 Short interruptions due to wear

Wear of arcing switch contacts can lead to incorrect timing, causing an arcing contact to take over the current too late. This effect accelerates contact wear even more. OLTC types using roller contacts are particularly prone to this effect. Figure 6.46 shows a typical DRM plot for a service-aged selector switch type OLTC with

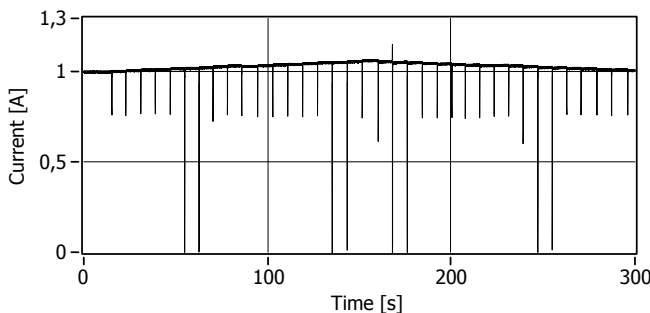


Figure 6.46 DRM plot of an OLTC with roller contacts. Current interruptions are visible due to selector switch contact wear.

roller contacts where current interruptions due to the arcing switch are visible. It may be clearly seen that only specific selector switch contacts are involved. Visual inspection inside the OLTC showed that excessive arcing during normal operation had already damaged the contacts. A close-up view of the relevant portion of this DRM plot reveals one or multiple interruptions in succession (see Figure 6.47). The current expected in the absence of interruptions is shown by a dotted line.

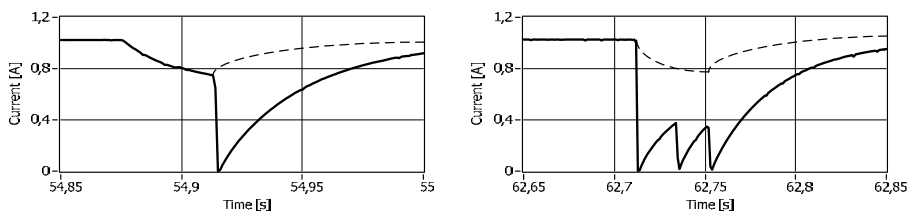


Figure 6.47 Close-up view of a DRM plot of an arcing switch with contact wear. The current is interrupted one or more times in succession.

6.4.5.3 Short interruptions due to damaged transition resistors

The measurement current can also be interrupted due to damaged transition resistors. The resistors are not designed to carry the load current for a long time. Damage to the transition resistors can lead to an open measurement circuit. The pressure relay of the arcing switch immediately switches the transformer off the moment the resistor fails. The open circuit can also be detected with the aid of DRM, and shows up in the plot at locations where the arcing switch normally uses the damaged resistor. An example can be seen in Figure 6.48, where one of the damping resistors caused an open circuit. The total recorded current plot is shown on the left and a close-up view of one operation on the right. The interruption of the measurement current is observed each time the OLTC operates. The current falls to zero at the moment the resistor should take over the current.

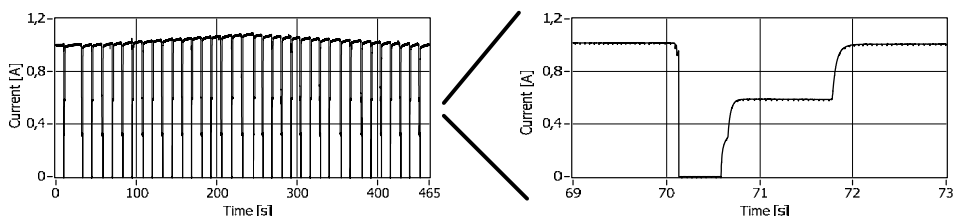


Figure 6.48 DRM plot (left) and close-up view (right) of a slowly-switched OLTC with one damaged transition resistor in the arcing switch. The current falls to zero each time the OLTC operates.

6.4.6 OLTC transition times

The third source of changes in DRM plots that is related to degradation or defects – OLTC transition times – was already mentioned in Figure 6.13C. The transition

time is determined for each operation in the cycle of operation. Mechanical defects or friction can result in longer transition times. This can accelerate arcing contact wear because the switching arc will persist for longer. Irregular transition times can be seen at locations in the DRM plot where the arcing switch operates (Figure 6.49), and may be detected by comparing the results with earlier measurements or with standard transition times for that type of OLTC.

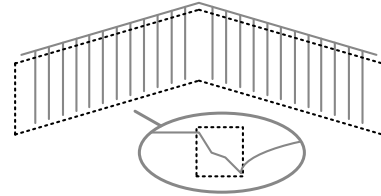


Figure 6.49 Irregular OLTC transition times show up each time the transition resistors are used.

Figure 6.50 shows three examples of the use of DRM to detect irregular transition times due to a defective drive mechanism. In each case, the transition times are shown for all tap change operations in the cycle of operation. The three cases considered are:

1. OLTC with 2 broken energy-accumulation springs in the drive mechanism (transition time between 80 and 90 ms),
2. The same type of OLTC with 1 broken energy-accumulation spring in the drive mechanism (transition time between 50 and 60 ms),
3. The OLTC of example 2 after repair of the defect (transition time between 35 and 40 ms).

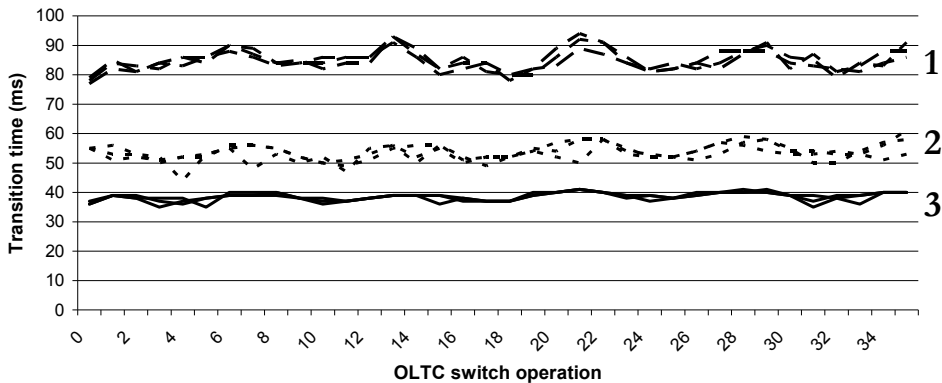


Figure 6.50 Three examples of the use of DRM to measure OLTC transition times. All transition times in the cycle of operation are displayed for the three phases. The cases shown are: an OLTC with two broken energy-accumulating springs (1), an OLTC with one broken energy-accumulating spring (2) and the same OLTC after repair of the drive mechanism (3).

It will be seen that longer transition times are observed when less mechanical energy is available to move the contacts.

Figure 6.51 shows close-up views of the current during the operation of the arcing switch for the examples of Figure 6.50. The transition resistor is used longer due to the slower OLTC operation.

It can be concluded that the transition time can be interpreted by comparing results with earlier measurements. Ref. [89] considers a transition time deviation more than 10 ms as unacceptable and recommends visual inspection.

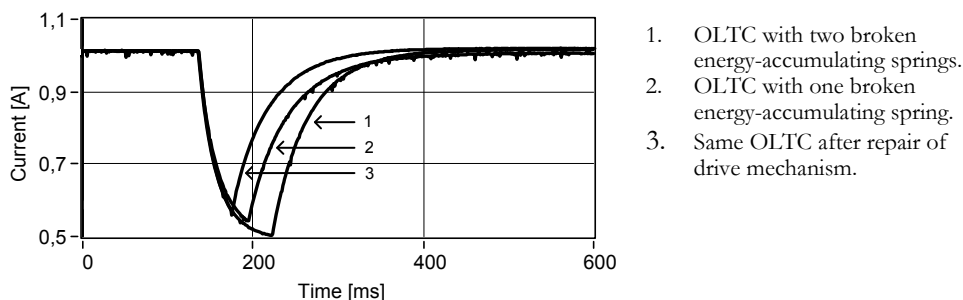


Figure 6.51 Close-up view of the current through the arcing switch for the three examples of Figure 6.50.

6.5 Defects in both parts of the OLTC

Exact localization of the defects and degradation mechanisms can be difficult when long-term aging causes resistance changes in all parts of the DRM plots. An example is given in Figure 6.52. All that can be concluded from this plot is that:

- the long-term aging is severe (thermally degraded contact exist, as described in Section 2.3.3, and the tap changer is in an aging stage where the resistance can increase rapidly, as shown in Figure 2.17.
- the contact resistance of the change-over selector has increased

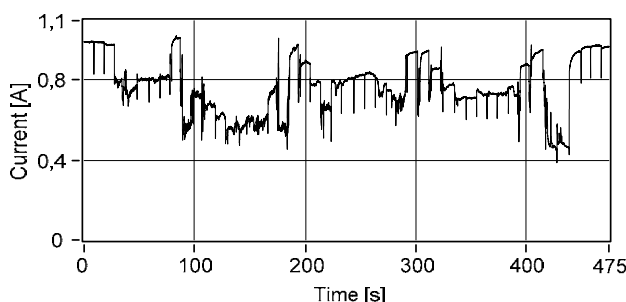


Figure 6.52 Dynamic resistance measurement on an OLTC with different types of long-term aging.

The enormous amount of contact degradation on the change-over selector contacts in this example makes it difficult to say whether the arcing switch also has higher resistance. Inspection of the arcing switch can give the decisive answer here.

A trial of a service-aged selector switch type OLTC provides a good example of this approach (see Figure 6.53). Measurements were first carried out on the OLTC

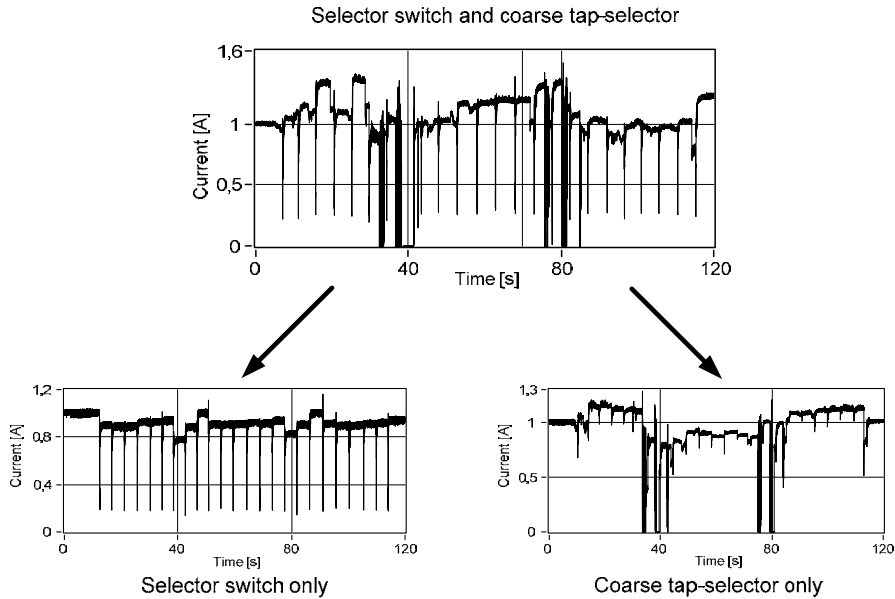


Figure 6.53 DRM plots of a service-aged selector switch type OLTC when the selector switch and the change-over selector were measured in series (top) and separately (bottom)

as a whole (top). The low measurement voltage (0.75 V) in combination with the degraded contacts caused short interruptions of the measurement current. The results of separate measurements on the selector switch and the change-over selector showed clearly that both parts of the OLTC contributed to distortion of the contact resistance. The change-over selector distorts the DRM when its contacts are moved. The selector switch, which uses the same contacts every 9 tap positions, shows the same distortion twice. The degradation of the arcing switch contacts did not show up when both parts were measured in series.

This example shows clearly that increased resistance of change-over selector contacts can mask arcing switch contact degradation in DRM results; the absence of a linear current pattern can be caused by the arcing switch and the change-over selector.

6.6 Conclusions

This chapter dealt with typical DRM results for high-speed resistor-type OLTCs. Firstly, measured plots were subdivided into:

- 1) Plots showing no effects of defects or contact degradation
- 2) Plots showing current interruptions, which can lead to OLTC damage in service. The current interruption may be located:
 - a) on the change-over selector, or

- b) on the arcing switch.
- 3) Plots showing current changes caused by contact resistance, leading to higher local contact temperatures and sometimes ultimately to thermal runaway,
 - a) on the change-over selector, or
 - b) on the arcing switch.
- 4) Plots showing irregular transition times due to mechanical defects.

It follows that the change-over selector, the arcing switch and the drive system can be diagnosed separately with the aid of DRM. The location of the defects can generally be determined on the basis of the moment when the resistance changes.

Secondly, it was shown that many defects and degradation mechanisms lead to changes in resistance, which makes DRM a useful tool for OLTC condition assessment. In particular, it was shown that DRM is sensitive to a variety of defects and degradation such as:

- 1) Long-term contact aging on the contacts
 - a) early (local effects of the surface film)
 - b) advanced (widespread effects of surface film and coking)
- 2) Wear of the arcing switch contacts
- 3) Timing differences between phases
- 4) Maintenance errors
- 5) Irregular transition times

Typical DRM plots revealing these various defects were presented and it was explained how these defects can be recognized in different types of OLTCs. As will be clear from the complicated relationship between the OLTC design, the degradation mechanisms and the DRM method, these results need to be interpreted by a specialist. This specialist needs to have expert knowledge of tap changer operation and aging, and of the DRM method applied. This way, the containing information on the OLTC condition can be extracted from the measurement results.

7

Laboratory verification of selected failure mechanisms

It is important to be able to assess the condition of tap changer parts which are not accessible for inspection during regular maintenance (which only examines the arcing switch). An example being contacts of the change-over selector, at which the long-term aging effect is a major source of contact irregularities observed in the DRM results. However, defects or wear in the arcing switch are also of interest because they may be overlooked during visual inspection. This chapter discusses experiments with typical tap changer degradation, using artificial degraded contacts mounted in a physical tap changer model. The following topics are studied in depth:

- Measurability of the surface film using resistance measurements (§7.1)
- Correlation between DRM and contact degradation (§7.1.1)
- Measurability of arcing contact wear (§7.2)

7.1 Measurability of the surface film using DRM

7.1.1 Correlation between DRM and contact degradation

The exact localisation of contact irregularities provides a better understanding of the stage of development of contact degradation in the OLTC. However, a direct relationship between dynamic contact resistance and the contact condition is not observed.

Chapter 6 revealed that it is possible to determine whether the irregularities in contact resistance originate in the arcing switch or the change-over selector by examining the moment they appear. This section is dedicated to the localization of

contact degradation on the change-over selector contacts. The movement of the change-over selector contacts is related to the physical location and condition of the contacts. The contact status was examined during OLTC overhaul and using overhaul reports. This section will demonstrate that a higher (static or dynamic) resistance does not necessarily mean that the contact surface at that location is in a bad state.

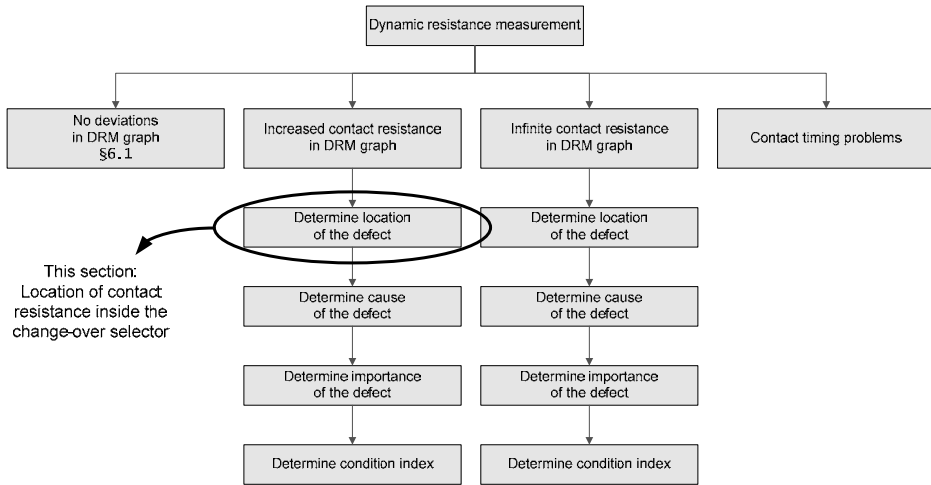


Figure 7.1 *This section elaborates on the location of contact degradation in the change-over selector.*

The change-over selector moves several times for each coarse tap change, thereby using different contact areas. These dynamic movements of the change-over selector can provide valuable information about the stage of development of the long-term aging effect. This section takes a closer look at how these change-over selector contact areas are measured with DRM.

Different types of tap changer are available to study the long-term aging effect using DRM. A typical case study is discussed here, using a selector switch type OLTC with a change-over selector. The type discussed in this section moves its roller contacts while they carry the load current (more information about this type of tap changer can be found in Chapter 2.1.1). The movement of the change-over selector, covering four tap positions, as discussed in Section 6.3.1, can be divided into ten sub-positions, as shown in Figure 7.2. A different DRM result was observed for each sub-position. The mid-position of the change-over selector forms the centre, recognisable by spikes in the current which are observable on both sides of the mid-position (indicated by M). These spikes are caused by the moving roller contacts of the change-over selector. Resistance deviations begin two positions before the mid-position (M-2), in terms of a stepwise change in the current. A stepwise change in the current was also observable one position after the mid-position (M+1).

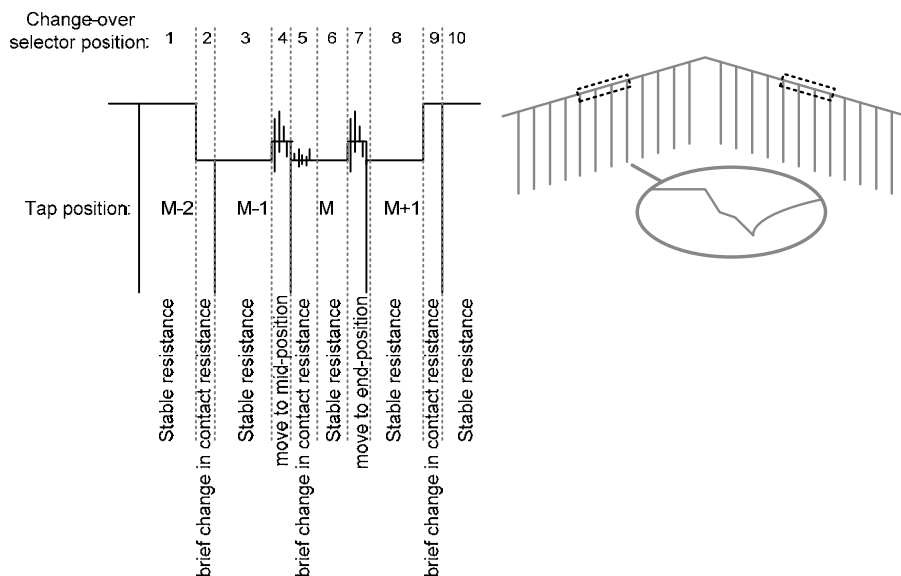


Figure 7.2 A typical deviation originating from the change-over selector covers four tap positions. The change-over selector moves at these tap positions. This movement can be divided into ten parts.

Figure 7.3 shows the stator of a coarse change-over selector with one coarse tap winding, which can be selected by placing the rotor contacts on contact block CT. The load current flows through contact block A, except in the parking position, where block A0 is used. Visual inspection of these contacts revealed an advanced long-term aging effect, see Figure 7.3.

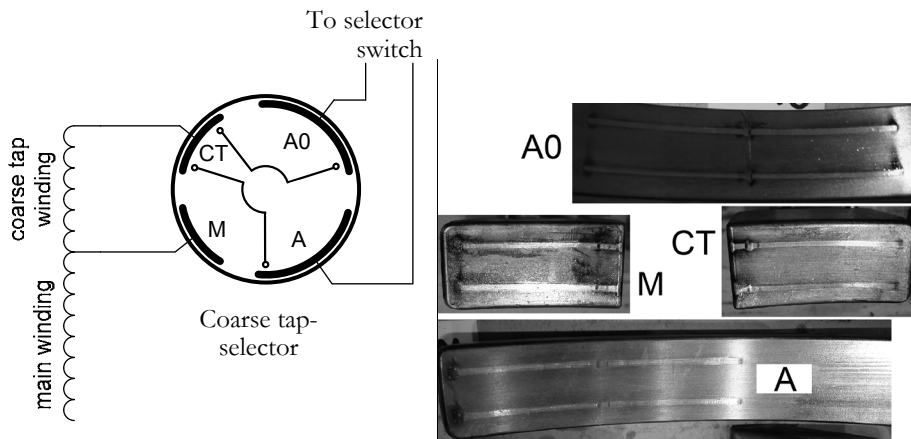


Figure 7.3 Stator contacts of a coarse tap selector. The coarse tap is selected when the rotor selects contact block CT. Block A0 is used in the parking position.

The ten change-over selector positions of Figure 7.2 are related to the position of the rotor. The amount of pitting and carbon is determined for all rotor positions and expressed as a condition index using the condition indices of Table 7.1. Condition indices for the DRM results are also determined on the basis of Table 7.1, resulting in the overview in Figure 7.4, which shows the contact status (stator and rotor average) as seen during inspection and the corresponding dynamic resistance results. All three phases of the transformer and all ten change-over selector positions are considered. Figure 7.4 also shows a linear trend line through these 30 data points. A direct relationship between the contact status and the corresponding irregularity in the DRM plots was expected. Figure 7.4 shows the opposite: an increased contact resistance is measured when the contacts are in good condition, while there is a decrease in resistance when the contacts are in poor condition. The following section investigates this important issue in more detail.

Table 7.1 Overview of condition indices for assessing change-over selector degradation.

Condition code	Contact status	DRM result
0	No pitting and no carbon	No additional contact resistance
1	Light pitting and carbon	Light additional contact resistance
2	Deep pitting and carbon	Considerable additional contact resistance

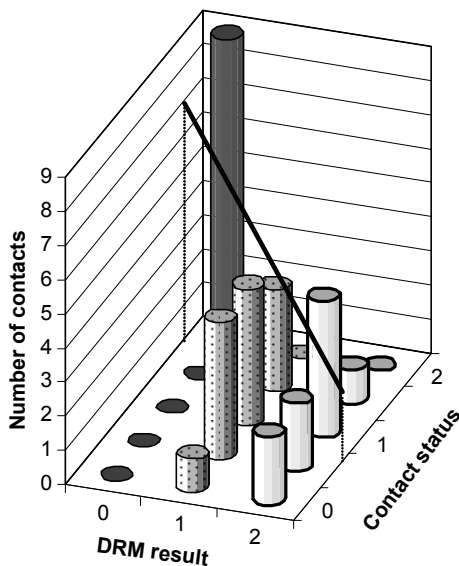


Figure 7.4 Relationship between the condition of 30 contact positions as measured with DRM and as seen by inspection. A linear trend line through these 30 data points is plotted.

7.1.2 Effect of the surface film on DRM

A more detailed investigation shows that the presence of the surface film deviates more clearly the DRM plots than the more dangerous pyrolytic carbon. Figure 7.5 shows our assessment on the relationship between the OLTC contact surface and the contact resistance. The plot shows a decreased measurement current caused by the contact resistance of one of its coarse taps.

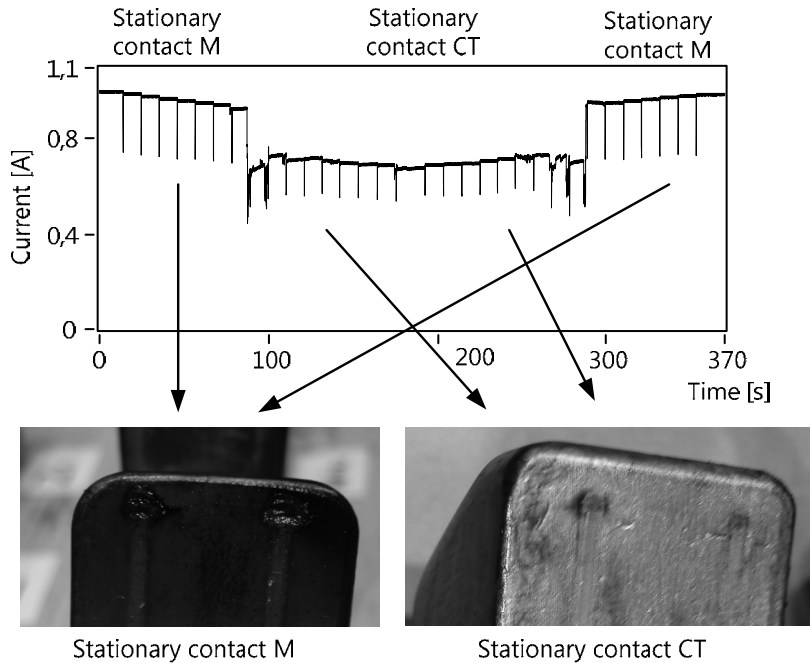


Figure 7.5 Localisation of change-over selector degradation. There is carbon present in the measurement circuit at places where the DRM plots are linear. Irregularities appear in the DRM plots when the slightly aged stationary contacts (right) are used.

It can be observed that the contact resistance of stationary contact CT is higher than the contact resistance of stationary contact M. Visual inspection showed that the contact surface of stationary contact M was affected by coking (as described in Section 2.3.3), while stationary contact CT only showed a thick surface film (due to infrequent use, see Section 2.3.2). When the contact resistance is related to the contact condition, the location with higher contact resistance relates to the surface film on the contacts.

Figure 7.6 shows our assessment of the relationship between the DRM plot and the physical condition of the contacts at the moment the change-over selector moves. Spikes occur in the dynamic resistance when the contacts move over a surface film. This effect is typical for this type of service-aged OLTC. A higher resistance is present at these contact locations which, being less frequently used,

are covered with an insulating surface film. This film layer causes a relatively high contact resistance.

To conclude, this case study, as well as results obtained from other service-aged OLTCs, confirms that DRM at 1 A measures an increased contact resistance due to the surface film. This layer can be measured with a higher amplitude, compared to contact locations subject to coking and pitting. From these observations it follows that the conductivity of pyrolytic carbon is better than the conductivity of contact film.

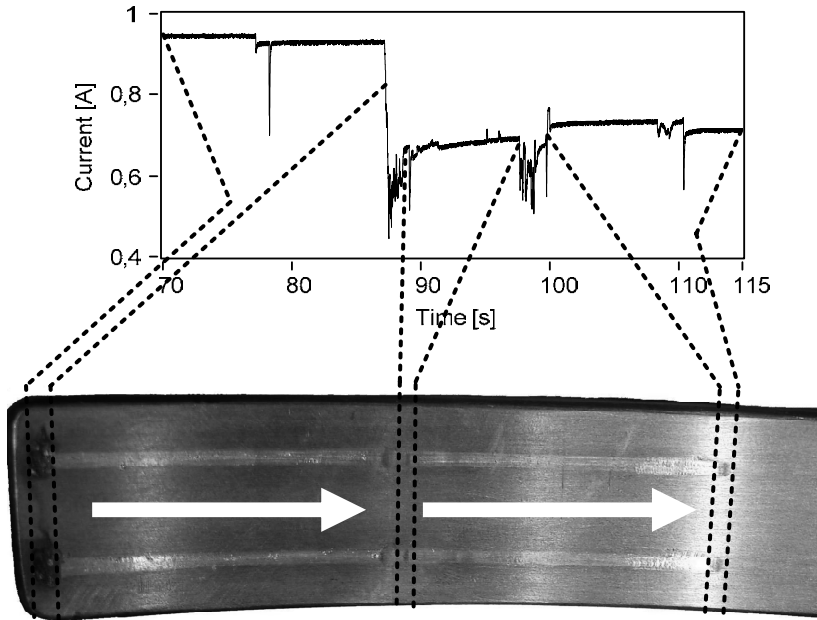


Figure 7.6 Relationship between the DRM plot (top) and the physical condition of the change-over selector contacts. Moving contacts, in combination with a thick surface film, cause spikes in the dynamic resistance.

7.1.3 Accelerated degradation tests

The measurability of the surface film is important because it indicates the onset of the long-term aging effect that leads to coking. In addition to visual inspection of service-aged OLTCs, accelerated degradation tests on a test model [90] can be used to show in a controlled way that the surface film can be measured with DRM.

7.1.3.1 Setup: the test model

Several degraded tap changer contacts were examined in the laboratory to determine the influence of a surface film on their dynamic resistance. A model was developed to test artificially degraded contacts at different stages of degradation. The test model (Figure 7.7) consists of one phase of a 60 kV/630 A selector switch

type OLTC with two $2.4\ \Omega$ transition resistors. The regulation winding was simulated by eight series-connected $43\ \text{m}\Omega$ resistors that can be selected using 9 stationary contacts. The model was connected in series with a power transformer to provide the required circuit inductance. The transformer (three phase 50 kV/14 MVA) was equipped with a tap changer that would not cause irregularities in the dynamic resistance plots and which was not operated during these experiments. The test model was hand-driven and switched in 45-70 ms, a little slower than normal high-speed resistor-type OLTCs. Tap selection was performed with roller contacts using the contact pressure of the original design (108 N). The tap changer model was not submerged in

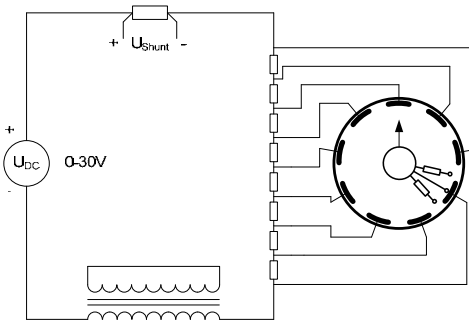


Figure 7.7a Schematic representation of the OLTC test model.

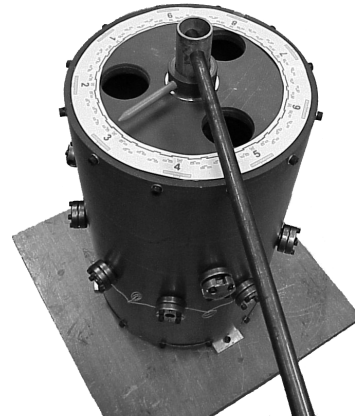


Figure 7.7b The OLTC test model used for experiments with artificial degradation.

transformer oil because the contacts tested already showed the same resistive behaviour as contacts in oil (see [11]). A constant DC measurement voltage was applied to the test model (and the series-connected transformer) and regulated in such a way as to provide 1 A initial measurement current. As soon as the current was stable the test model was switched through all its tap positions and the current was recorded. A sequence of reference DRMs showed that this test model did not cause irregularities in the contact resistance when clean contacts were used, as shown in Figure 7.8. In total, 20 laboratory experiments were performed, each consisting of 3-16 measurements.

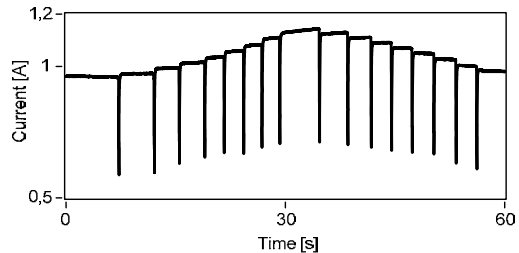


Figure 7.8 The reference current pattern recorded on the test model with clean contacts using the DRM technique. The transition resistors reduce the current when the OLTC moves to the next tap.

7.1.3.2 Accelerated degradation tests

Thermally accelerated degradation tests were carried out on the test model using an artificially grown surface film to investigate its effect on DRM. Service-aged Shell Diala transformer oil was used for accelerated degradation on nine contact blocks of a selector switch. The bulk oil was heated, resulting in a surface film on the entire surface of the contacts. The formulae of [24] were used to calculate the test time (see also Chapter 2): submerging the contacts for 6 hours in oil of 165 °C simulated 40 years of service at 60 °C, which is the average age of the OLTC population evaluated in [11] and tap changer with an age of 25-35 years show increased contact resistances in DRM at 1 A. The thickness of the surface film that is formed during these tests was not verified by ellipsometry or other methods, but visual inspection of the contact surface confirmed the presence of surface film. These accelerated degradation tests caused 300 $\mu\Omega$ additional contact resistance during a static resistance measurement at 100 A, which could not be measured with DRM due to the noise level of the setup. Ref. [11] describes these measurements in more detail, with no increased contact resistance being measured.

Section 7.1.2 showed that a surface film is expected to have a significant effect on contact resistance. Therefore, the accelerated degradation tests as described above were continued, with the objective of generating the plots as measured in the field. During this accelerated degradation test both the contact blocks and the roller contacts were submerged in hot oil, in contrast with [11]. This doubled the thickness of the surface film (note: tap changers in service can have two of such contact sets in series).

The first accelerated degradation test concerned contacts that were aged at 180 °C (temperature controlled between 176-182 °C) for 5.5 hours. Those contacts showed increased contact resistances at only a few of the DRM plots at 1 A. The effect is small and appears only when the contacts are moved. Figure 7.9 provides an example of a plot measured for one of these contacts. In other measurements, the thin film broke and was not detected with DRM.

The final experiments artificially aged the contacts for 14.7 hours at an oil temperature of 201 °C (temperature controlled between 199-202 °C). This time all the contacts tested showed an increased contact resistance in the plots, causing up

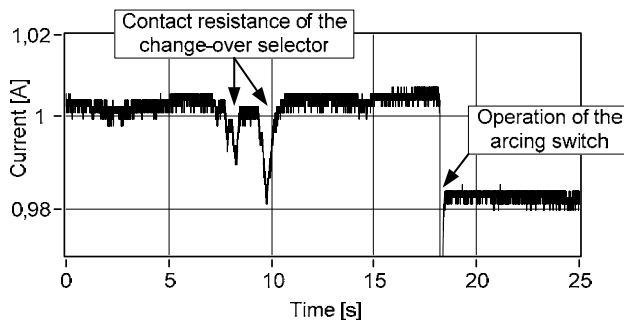


Figure 7.9 DRM plot of an artificially aged OLTC contact (5.5h at 180 °C oil). The contact resistance shows a few spikes when the contacts are moved ($t=7-10$ s) just before the OLTC is switched ($t=18$ s).

to 8% variation in the 1 A measurement current (Figure 7.10). This effect is still small compared to the contact resistances measured during field tests (for example 50% variation in the measurement current). The thin film breaks easily and is quickly wiped away when the contacts are continuously moved for some time (Figure 7.11). However, the typical spikes in the contact resistance correspond with the results of field tests.

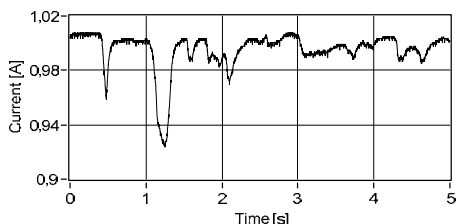


Figure 7.10 DRM plot of artificially aged OLTC contacts (14.7 h at 201 °C oil). The measurement current drops by 8%.

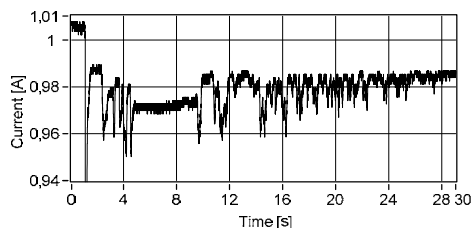


Figure 7.11 The surface film is wiped away when the contacts are continuously moved for 25 s.

Figure 7.12 shows the results of 16 dynamic resistance measurements on the contacts that were aged for 14.7 h at 201 °C. All of the measurements show increased contact resistances above the noise level.

These accelerated degradation tests show that a surface film on contacts can indeed cause a considerable increase in the contact resistance as measured at 1 A. This confirms findings from DRM on service-aged contacts. A thin layer is not detected in every measurement because it often breaks and the conductive path is restored. However, a thick layer is observable as increased contact resistance in every measurement [91]. High local temperatures are needed to grow an insulating layer that is thick enough to be observed in every DRM plot. Service-aged OLTCs

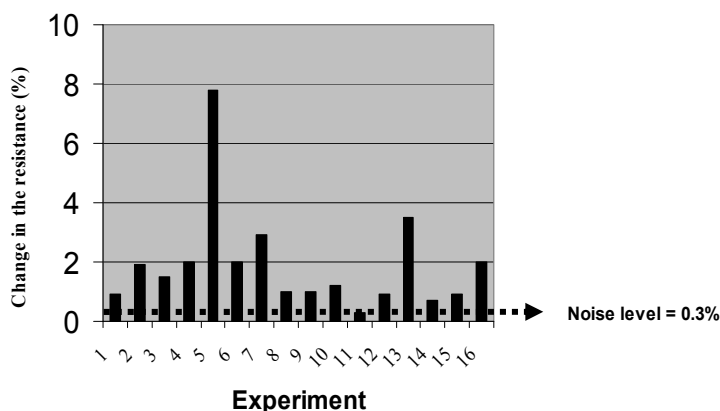


Figure 7.12 Sixteen experiments were performed with degraded OLTC contacts to show that the surface film can be measured. All measurements show increased resistances above the noise level.

in the utility grid can be exposed to such high local temperatures, as suggested by the carbonisation of the oil observed in some service-aged OLTCs.

Therefore, it can be argued that the maximum contact resistance that is measured with DRM can inform us about the thermal degradation stage of the contact surface. DRM may be useful in finding the cause of increased contact resistance: the long-term effect can be recognised due to the current spikes in the plot as shown in Figure 7.6. Static resistance measurements could not have assessed this contact area because it is not used in static situations. A thick surface film on the contacts indicates an advanced long-term aging effect and coking may have occurred on locations where the load current heats the contacts. In order to draw a conclusion about the presence of pyrolytic carbon due to coking, the aging mechanism and the length of time that the thick surface film has been present should be considered. Therefore, previous DRM results for the same OLTC should be considered in order to reach a solid conclusion about the presence of pyrolytic carbon.

7.2 Arcing contact wear

Contact wear can be determined by visual inspection during regular maintenance but can also be measured by DRM because it affects contact timing. Irregularities in the transition time can be measured by DRM when contacts are worn, with even short interruptions of the measurement current appearing in the plots. Section 6.4.5.2 presented an example of DRM where arcing contact wear influenced contact timing. This section discusses two further ways to detect arcing contact wear:

- 1) determine the size of the arcing contact using DRM in combination with a position sensor
- 2) reveal contact timing differences by comparing contact timing with a reference

Figure 7.13 shows how wear of the arcing contact is defined: a new arcing contact has 0% wear, while the contact wear is 100% when the contact material of the arcing contact is abraded until the main contact. The example shown in the picture is therefore 65% worn.

7.2.1 Arcing contact dimensions

Dynamic resistance results provide information about the arcing contact dimensions, in particular when they are combined with a contact position measurement using a position sensor on the remote end of the drive shaft (see also

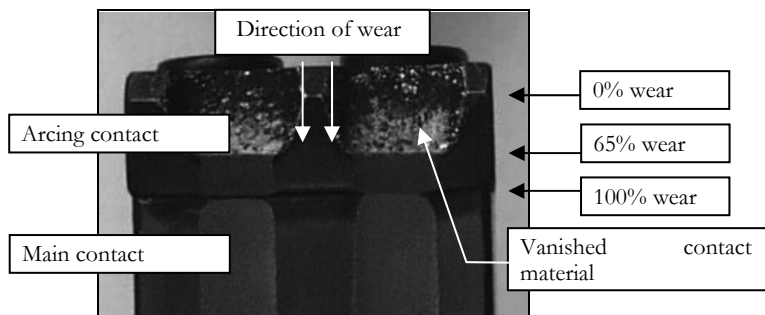


Figure 7.13 An arcing contact about 65% worn.

Figure D.8). Figure 7.14 shows a combination of the measurement current (black line) and the position measurement (grey line) during an arcing switch operation. The contacts of the arcing switch start moving at T_1 and the main contact moves to the end of the stator contact (X_2). During this movement, the main contact (without transition resistor) carries the measurement current, with the latter (black line) indicating an increase in contact resistance. The main contact leaves the contact block at T_2 , thereby introducing a transition resistor. The main contact

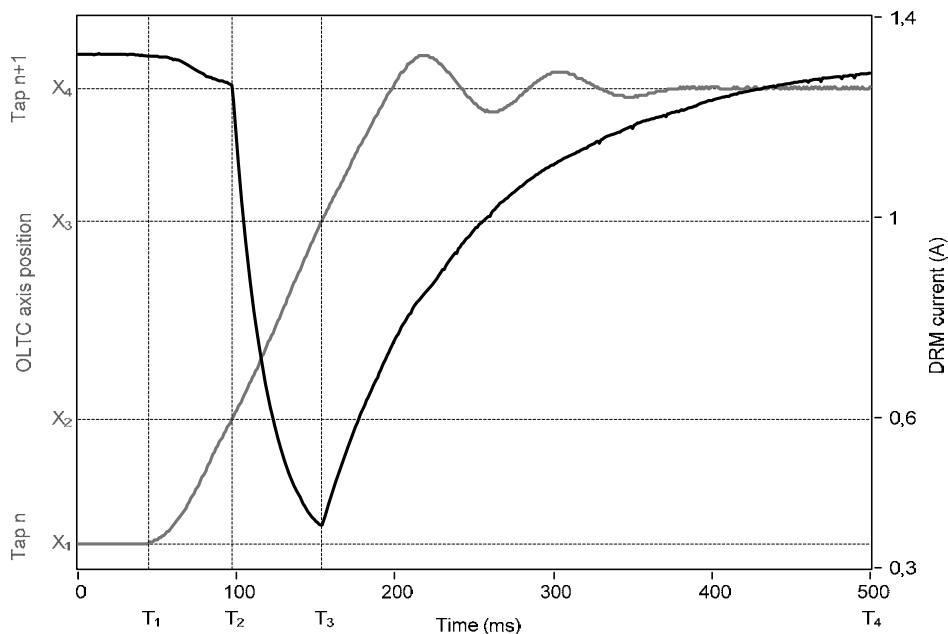


Figure 7.14 The combination of dynamic resistance measurements (black line) and the position measurements of the OLTC contacts (gray line) during an arcing switch operation. The rotor starts moving at T_1 and the transition resistor is used at T_2 . The main contact reaches the next tap at T_3 .

then moves to the next tap, reaching it at T_3 and comes to a standstill at position X_4 , after some mechanical oscillations. Comparing these two measurements provides information about:

- X_2-X_1 : the size of the arcing contact before the main contact disconnects
- X_3-X_2 : the distance between the contacts
- X_4-X_3 : the size of the arcing contact after the main contact connects

The degree of contact wear of an arcing contact can then be determined in terms of the total distance that the main contact travels over the contact block, which can be read from the combined plots. The width of the main contact and the length of a new arcing contact should be considered in this case. Figure 7.15 shows that the moment the main contact arrives at the stationary contact of the diverter switch (indicated by T_3) and the moment it leaves (T_4) can be read from the current curve. In this example, this yields a contact length of ' X_{DRM} '. Contact wear is then calculated as $X_{NEW}-X_{DRM}$. This example demonstrates that contact wear does not affect the results of the position measurement, but the timing T_3 and T_4 of the transition resistors does change. Contact wear can then be determined with an accuracy of a few millimetres when DRM is performed with a 1 ms resolution. Visual inspection will be more accurate.

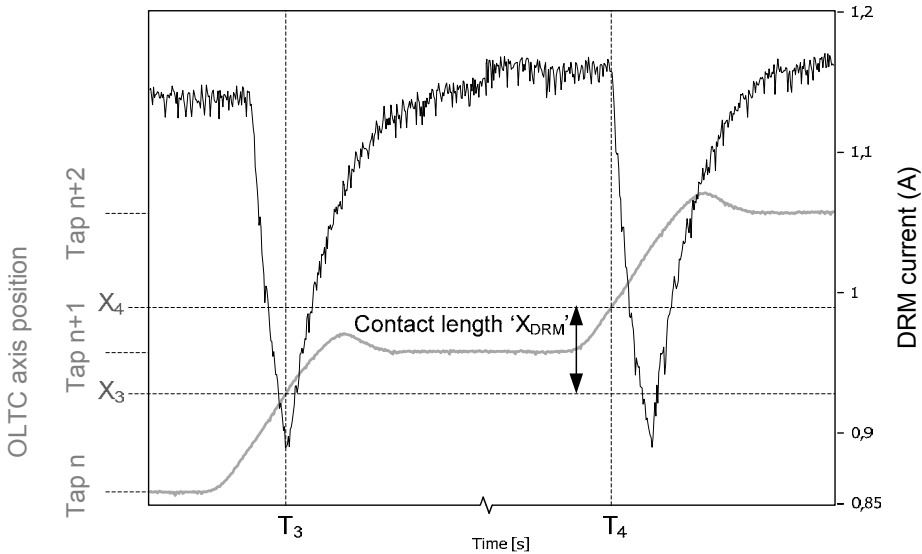


Figure 7.15 The length of the OLTC contact can be determined when the dynamic resistance and the shaft angular position measurements are combined. The main contact of the diverter switch arrives at moment T_3 and leaves the contact again at T_4 , resulting in a contact length of $X_{DRM}=X_4-X_3$.

7.2.2 Arcing contact timing

Contact wear can be revealed without determining the exact contact dimensions if the timing of the arcing switch contacts is compared with a reference. A previous DRM result for the OLTC in question or a typical result for that type of OLTC can be used as a reference. The effect of contact wear on the transition time is small. However, these small variations change the shape and depth of the DRM plot when the arcing switch operates, due to the large dI/dt of the measurement current (as already demonstrated in Figure 6.41).

Measurements of artificially worn arcing contacts were performed with the test model (as described earlier in this chapter) to confirm the effect of contact wear on DRM. Figure 7.16 provides a typical example of the results of these experiments. Figure 7.16a shows a close-up view of the OLTC operation using arcing contacts with 0% wear. The plots change significantly when arcing contacts that were 80% worn are used (Figure 7.16b). The length of time that both transition resistors are used in parallel (T_P) is shortened, while the length of time that only one transition resistor is used is extended (T_{R1} and T_{R2}). The current will drop (from 0.6 A to 0.55 A in Figure 7.16) because one resistor causes a higher dI/dt than two parallel resistors.

To eliminate variations in the transition time of the test model, measurement results are displayed as the percentage of the transition time in which only one transition resistor is used:

$$C_W = \frac{T_{R1} + T_{R2}}{T_{R1} + T_P + T_{R2}} * 100\% \quad 7-1$$

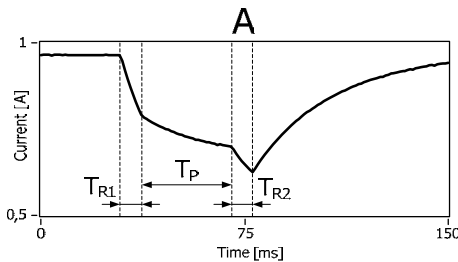


Figure 7.16a Close-up view of a DRM plot at the moment the OLTC switches. The arcing contacts are 0% worn.

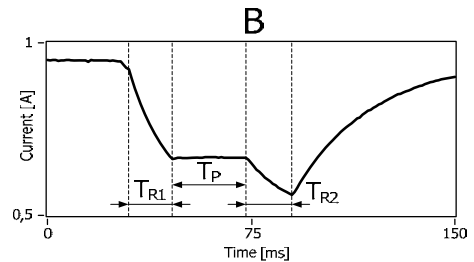


Figure 7.16b Close-up view of a DRM plot at the moment the OLTC switches. The arcing contacts are 80% worn.

Figure 7.17 shows this percentage for each tap change operation in the OLTC's cycle of operation. Contact 3 was 80% worn, which is clearly indicated at each tap change operation involving contact 3. This example demonstrates that small changes of the contact timing at worn arcing contacts can be measured with DRM.

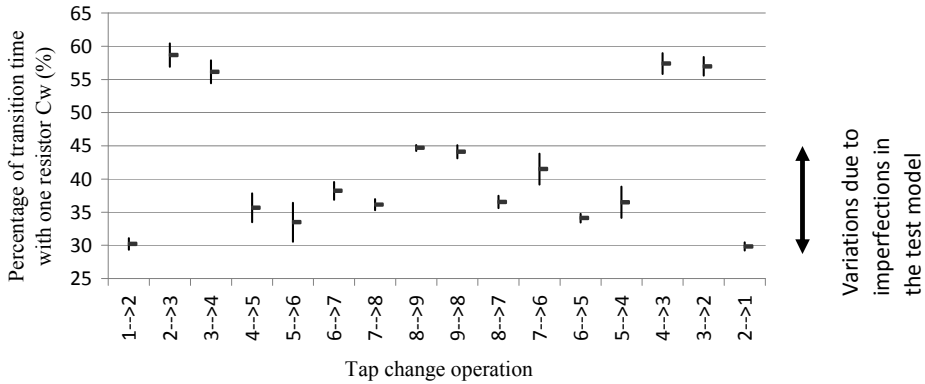


Figure 7.17 Graph of the percentage of the transition time in which only one transition resistor is used. The average and standard deviation of 6 measurements are displayed for every tap change operation in the cycle of operation. The contact of tap 3 is 80% worn, which is clearly indicated in the graph.

Equivalent effects were also observed in service-aged OLTCs. Three examples are provided in Figure 7.18.

Another experiment revealed the effect of extremely worn arcing contacts. Figure 7.19 shows an example of a roller contact from a selector switch about to leave a stator contact block. At this moment, two contacts are on the stator block: the main roller contact (which is about to leave) and the arcing roller contact (which has just arrived at the stator block). The stator contact block is wide enough for both roller contacts. When the arcing contacts are heavily worn, this contact is endangered. This can result in a short interruption of the measurement current due to the main roller contact leaving the contact block too early.

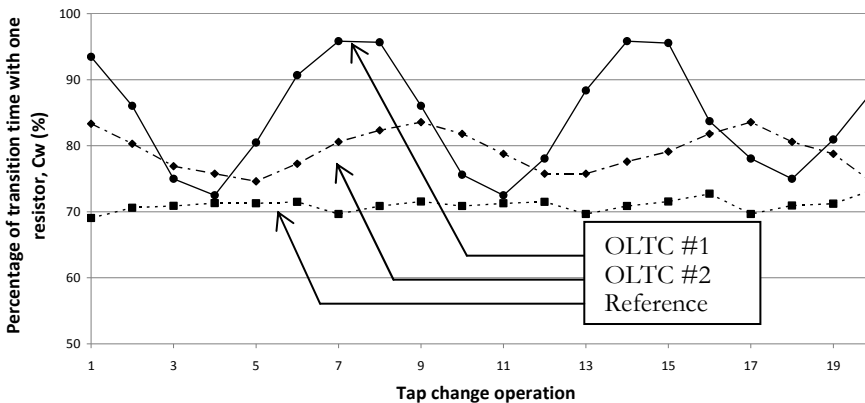


Figure 7.18 Three examples of the transition resistor timing in service-aged OLTCs: the percentage of the transition time in which only one transition resistor is used is plotted. The transformer windings have two coarse taps, therefore in this example the selector switch uses the same arcing contacts three times.

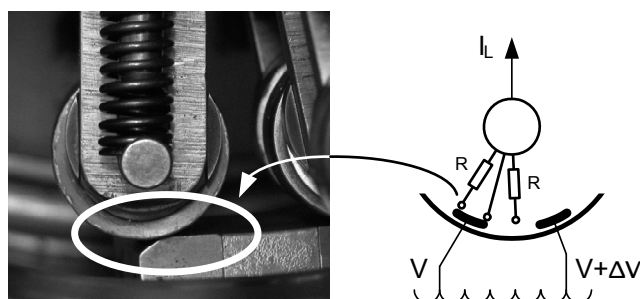


Figure 7.19 A roller contact at the moment it leaves the stator contact block. The contact block is wide enough for both roller contacts, but contact wear can endanger good contact timing.

Experiments with 100% worn arcing contacts mounted in the tap changer test model generated such interruptions of the measurement current. Figure 7.20 shows a recorded current plot of such an experiment. The arcing contact of tap 3 was artificially worn, resulting in short current interruptions when that contact was involved in the tap change operation. Figure 7.20b provides a close-up view of the current interruption.

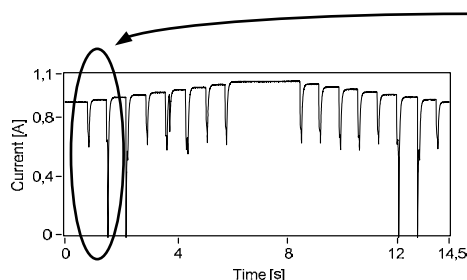


Figure 7.20a DRM plot of the OLTC test model. The arcing contacts of tap position 3 are 100% worn.

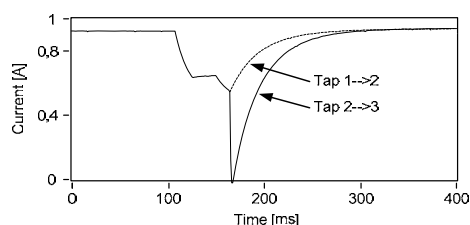


Figure 7.20b Close-up view of a DRM plot at the moment the OLTC switches. The arcing contacts are 100% worn.

Another experiment shows that there is no significant effect of the measurement current on the transition time, see Figure 7.21. DRM can be used at any current to determine the timing of the transition resistors.

It should be noted that the wear of the arcing contacts is a slow process which can be recognised in an early stage during normal inspection of the arcing switch. There is no specific need for arcing contact diagnosis with DRM for the current generation of OLTCs; however, the effect of wear may be indicated by DRM and should be recognised in order to determine the condition of the tap changer.

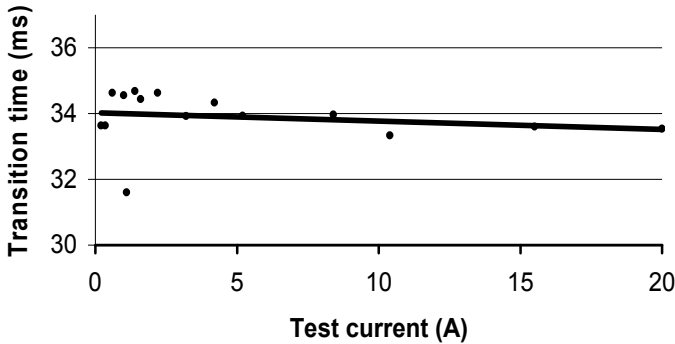


Figure 7.21 OLTC transition times are determined for an OLTC in good condition, using different measurement currents. A trend line is added. No significant change in the OLTC transition time was seen.

7.3 Conclusions

Firstly, this chapter closely examined the relationship between DRM and the physical condition of tap changer contacts. Dynamic contact resistance was shown to increase significantly when contacts move over a surface film. This can conceal more significant contact degradation.

Secondly, this chapter discussed experiments on a tap changer test model with worn arcing contacts and with a surface film. A measurement current of 1 A was used. Experiments with surface film on the contacts showed that the early stage of the long-term effect sometimes causes small irregularities in the contact resistance, but may not always appear, because a thin layer of oil associated with the early stage of the long-term effect often breaks down. However, the effect of the surface film is observed in all measurements when the layer grows thicker. The artificially grown surface film only causes increased contact resistances when the OLTC is operated. Service-aged OLTCs with a more advanced long-term effect show that the static contact resistance also changes significantly when the tap changer is motionless. From experiments it can be concluded that the long-term aging effect influences the dynamic resistance. The surface film is measurable with DRM at 1 A and can be recognised by spikes in the plots when the current-carrying contacts move over it (which is not the case in every type of OLTC). It was also shown that a thin surface film can be wiped away when the contacts move over it, reducing contact resistance. For that reason, reproducible irregularities in plots are more severe than irregularities whose resistance decreases when the OLTC is switched a few times though its cycle of operation. It was demonstrated that the maximum contact resistance measured with DRM can indicate the stage of development of the surface film. A thick surface film on the contacts indicates an advanced long-term aging effect, while coking may have occurred on locations where the load

current has heated the contacts. Previous results measured on the same tap changer should be considered in order to estimate the length of time that the advanced long-term effect has been present, leading to the development of pyrolytic carbon on the contacts. Historical information of the OLTC's tap positions being used can also be used to estimate the amount of carbon and film on the contacts, using the experience that infrequently used contacts are likely to have a contact film and that frequently used contacts are sensitive to contact coking. Further study may include research into the effect of coking on contact resistance.

Thirdly, the experiments confirmed that arcing contact wear influences contact timing, changing the shape and amplitude of the effect of the transition resistors in the DRM plots. The timing of the transition resistors showed no significant dependency on the amplitude of the measurement current. Interruptions of the current can appear in the plots when excessively worn contacts are tested. Contact wear of the arcing contacts can also be detected by:

- 1 comparing the timing of the transition resistor during DRM with earlier measurements on the same OLTC
- 2 DRM in combination with a shaft angular position measurement

8

DRM knowledge rules for decision support

Tap changers which are in critical condition and will best profit from efforts to reduce failure (e.g. maintenance) can be selected on the basis of the dynamic resistance measurement results. DRM is particularly suitable for assessing OLTC degradation processes and defects that potentially lead to failure, and therefore on this basis can be used to reduce the failure rate.

Such huge amounts of diagnostic data are acquired with the aid of DRM that it is difficult to pick out relevant information about the condition of the tap changer. The diagnostic data must therefore be transformed into a statement about the condition which can be done using derived quantities and boundary values. In other words, these results require interpretation before they can be used for the strategic prioritisation of maintenance or the overhaul of the OLTC. For that purpose, a simple way of expressing the results of DRM will be beneficial. An example of the application of this process will also be presented.

8.1 Condition assessment

This chapter elaborates on the technical aspects of a specific class of asset management decisions, namely condition assessment based on DRM at the component level. Selecting the optimal maintenance strategy on the basis of information about the reliability of the tap changer and its life-cycle costs involves more than implementing the diagnostic method described in this chapter, as information about an OLTC's technical condition is only one input in the maintenance decision process. Figure 8.1 shows that an OLTC which is subject to degradation mechanisms and defects can be diagnosed by performing measurements with a diagnostic instrument. A selection of diagnostic methods can be applied in such a way that the symptoms of degradation which occur most frequently are diagnosed (see Chapter 5).

OLTCs in critical condition can be selected for overhaul or repair using the results of a single measurement or from successive measurements over time. In this way, the transformer population can be maintained cost effectively and with a certain reliability.

Economical, societal and safety aspects are not considered in this chapter. In particular, additional information such as operational data (temperature, load profile), failure statistics and the results of visual inspection must also be considered, see Figure 8.1. Furthermore, the cost of failure, the consequence of this failure for the surrounding power transformer and the continuity of power delivery should also play an important role.

8.2 DRM knowledge rules

Residual life estimation and decisions for intrusive maintenance actions are often based on fuzzy information [92]. The interpretation of diagnostic data, as introduced in Figure 6.1, can be structured by using knowledge rules to extract information about degradation and defects from the diagnostic data (see Figure 8.1). Criteria for interpretation are described as knowledge rules [93], which are derived in order to support the condition-based maintenance process [93]. Parameters from the DRM plots that reflect the OLTC condition (see Figure 8.2) are used as the basis for this process. Boundary values can then be

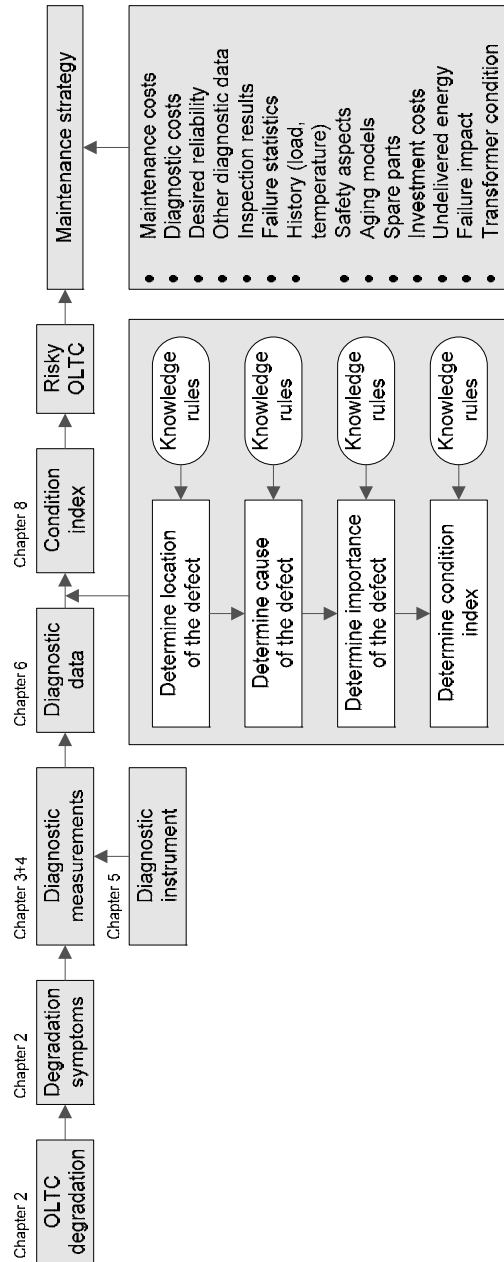


Figure 8.1 Assessment of OLTC degradation for the determination of an optimal maintenance strategy. Symptoms of degradation are measured and interpreted, which results in a selection of higher risk OLTCs. Knowledge rules are used during the localisation of the defect to find its cause and determine its significance.

applied to categorize results in a condition index.

In general, knowledge rules are based on degradation mechanisms on the different OLTC parts and the effect of these failure modes on the DRM results. Knowledge rules are based on the following facts:

- findings from visual inspection and DRM on service-aged OLTCs during regular on-site maintenance
- laboratory studies with artificial degraded OLTC components
- post-mortem investigation of tap changer degradation processes

All these sources of knowledge were considered in this thesis, resulting in the application example of Section 8.5. In particular, collecting and analyzing measurement data is important in the process of knowledge rule generation.

In order to determine the parameters that reflect the OLTC's condition, the overview of Table 8.1 is generated, which summarises the directives for interpretation that were discussed in this thesis and the pages where they were introduced or discussed, structured according to the condition assessment flowchart of Figure 6.1.

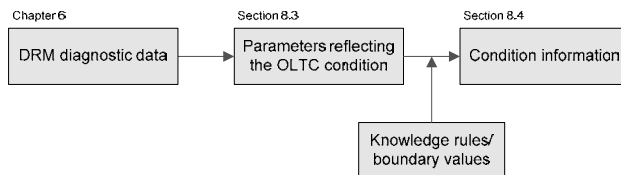


Figure 8.2 Parameters that reflect the OLTC condition can be used to extract condition information from dynamic resistance measurement results. Boundary values are needed for this purpose.

Table 8.1 Overview of major DRM knowledge rules from this thesis and the page where they are discussed.

Directives for DRM interpretation		
General		
1.1	Deviation from the standard plots can be related to degradation or defects and should be investigated before re-energising the transformer. <i>OLTC failure can be prevented this way.</i>	Page 93
1.2	The interpretation of results should not only consider the maximum resistance: the location and nature of the resistance variation should also be taken into account. The location and shape of the irregularity can be used to determine the cause and importance of the defect. <i>Degradation mechanisms have different effects on contact resistance; separate boundary values should be used.</i>	Page 85
1.3	The current pattern can be read backwards to recognise tap change operations. <i>This helps to determine the defective tap position(s).</i>	Page 97
Localization		
2.1	The change-over selector, the arcing switch and the drive system can be diagnosed separately. <i>Because DRM provides information about transition times, contact timing, contact resistance, open contacts and location (based on the location in the DRM plot).</i>	Page 85

2.2	Irregularities in the plots that are caused by the change-over selector appear, change or disappear when it is operated.	Page 95
2.3	Irregularities in the plots that are caused by the arcing switch appear, change or disappear when it is operated.	Page 106
2.4	The change-over selector is likely to cause changes in the plots that are less frequent but persist longer than those caused by the arcing switch. <i>Because the change-over selector is used less frequently.</i>	Page 106
2.5	The absence of a linear current pattern can be caused by the arcing switch and the change-over selector. <i>Because the arcing switch is used during every tap change, which can influence the resistor of the change-over selector due to mechanical vibrations.</i>	Page 116
2.6	The interruption time and its location in the cycle of operation provide information about the location of the interruption. <i>Each contact is used at particular locations in the OLTC cycle of operation and is used a particular time.</i>	Page 105
2.7	The arcing switch is likely to cause problems if the irregularities in the plot that occur when the change-over selector is motionless are out of proportion compared to the irregularities that occur when the change-over selector is operated.	Page 103
2.8	A current interruption at a delta-connected transformer can manifest as a decreasing measurement current in another phase. <i>Because delta-connected windings offer an alternative path for the current if one phase is interrupted.</i>	Page 111
Cause (degradation and defects)		
3.1	The presence of a linear pattern in the plot points to an arcing switch with no long-term aging effect. <i>The arcing switch is operated every tap change, so it will change the contact resistance during the entire DRM.</i>	Page 107
3.2	Change-over selector contact areas that are only used briefly during OLTC operation will not be pitted and are not covered with pyrolytic carbon. <i>See the following knowledge rule.</i>	Page 99
3.3	Frequently used contacts that carry the load current can be subject to contact coking. <i>Contact pitting and coking occurs when the load current flows through the contacts for an extended period.</i>	Page 100
3.4	The surface film is measurable at 1 A and can be recognised by spikes in the resistance when the current-carrying contacts move over it. <i>See page 134.</i>	Page 134
3.5	Carbonised oil on the contacts is measurable. <i>As observed during on-site measurements.</i>	Page 35
3.6	Contact resistance can decrease during the long-term aging effect: the surface film breaks and pitting can occur. <i>A low contact resistance is not enough to conclude that the OLTC is in good condition: the location of the defect and the degradation mechanism should also be taken into account.</i>	Page 23
3.7	A thin surface film can be wiped away when the contacts move over it, reducing the contact resistance. <i>This can be used for testing the development stage of contact degradation and to clean the contact surface.</i>	Page 134
3.8	The surface film grows thicker as the contacts age and this oil-film growth rate is strongly dependent on the surface temperature of the contacts. <i>Therefore a thick film with high resistance indicates a medium or advanced stage of contact degradation.</i>	Page 181
3.9	A thin surface film is not detected in every DRM, because the thin layer breaks and the conductive path is restored, while a thick layer will be detected. <i>Therefore a thick film appearing in every DRM indicates a medium or advanced stage of contact degradation.</i>	Page 127

3.10	Low measurement voltages and low currents will allow a very thick surface film to interrupt the current. The interruptions disappear when the current is increased. <i>This can be used for testing the development stage of contact degradation.</i>	Page 57
3.11	A short increase in the measurement current during OLTC operation can be caused by asynchronous operation of the OLTC phases.	Page 110
Importance		
4.1	The distinction between increased contact resistance and open contacts is important: in general interruptions are more critical. <i>Because an OLTC with open contacts during its cycle of operation may not be able to select some taps, an interruption of the load current may be destructive.</i>	Page 93
4.2	Single peaks in the measurement current are caused by noise in the measurement circuit. <i>Rapid current changes cannot flow through the windings due to the high inductance.</i>	Page 64
4.3	The worst tap position of all phases determines the condition index of the tap changer. <i>Because one tap can be used for a long time and one defective tap can cause failure of the OLTC.</i>	Page 111
4.4	The importance of contact degradation can be investigated by performing DRM with different measurement currents. <i>Contact resistance becomes smaller when the current is increased and sensitivity to surface film on the contacts increases when the measurement current is decreased. A low current may be desired if one wants to assess the importance of the long-term effect.</i>	Page 59
4.5	Short measurement current interruptions when the arcing switch operates are not always critical. <i>They can be caused by a thin layer of oil that has to be pushed away by the moving contacts before a low-resistance contact can be made. The oil layer will not cause current interruptions in normal operation.</i>	Page 112
4.6	The way in which measured results change with time can provide valuable additional information about the importance of contact degradation. <i>A lower condition index can be assigned when the irregularity in the DRM plots increases in time.</i>	Page 151
4.7	Reproducible irregularities in plots are more severe than irregularities whose resistance decreases when the OLTC is switched a few times though its cycle of operation. <i>Because light contact degradation can be wiped away by moving contacts.</i>	Page 134
4.8	An advanced long-term effect on the OLTC contacts will appear in every DRM. <i>Because advanced contact degradation cannot be easily wiped away by moving contacts.</i>	Page 127

8.3 Quantities reflecting the OLTC condition

In general, diagnosing the condition of high-voltage components can be done using characteristic quantities which reflect the condition of the component, thereby reducing the complex measurement result to a set of numbers. For example, discharge measurements on insulating systems use a partial discharge inception voltage (PDIV) as a quantifier, and dissolved gas analysis on insulation oil uses gas ratios to summarise the results of gas analysis. Boundary values can be applied to these quantities, see also Figure 8.2. These quantities should be carefully selected because defects that do not influence these quantities will no longer be revealed after quantification. In the case of DRM, the following quantities will cover the most typical OLTC defects and degradation mechanisms (see also Table 8.2):

- 1 OLTC transition time
Measured as the time that the transition resistors are used. This quantity is sensitive to contact misalignment, mechanical defects and friction, see also Section 6.4.6.
- 2 Timing of the transition resistors
This quantity expresses the timing of the transition resistors in relation to the transition time and is therefore also sensitive to contact timing differences (for example due to contact wear, see also page 131).
- 3 Timing difference between phases
This quantity can be used to check synchronism between the three phases. The final time of the OLTC operation can be used because it is easy to recognize in dynamic resistance plots.
- 4 Time that the measurement current is interrupted
This quantity is defined as the time that the measurement current is below 10% of its initial value, see also Section 8.5.1. It is sensitive to misaligned contacts, defective transition resistors, a thick film on the contacts, advanced long-term aging, mechanical defects and to contact wear that causes incorrect contact timing.
- 5 Maximum contact resistance when using infrequently used contacts
An example of such a contact occurs when the change-over selector is in operation. A film can develop on these contact locations, as described in Section 2.3.2, but thermal degradation described in Section 2.3.3 is not present here; this parameter represents the thickness of this layer and therefore the stage of development of long-term aging, in particular for light contact degradation.
- 6 Maximum contact resistance when OLTC is using frequently used contacts
Contacts through which the load current flows are more sensitive to contact coking and less subject to the development of a surface film. Therefore these contact locations provide information about the advanced stage of the long-term aging effect, which involves pyrolytic carbon, as described in Section 2.3.3.

Table 8.2 shows how these quantities are calculated and which knowledge rules from Table 8.1 should be considered. In addition, Figure 8.3 shows how the quantities can be calculated from a DRM plot. These quantities can be used as input for condition assessment to reveal typical OLTC defects, as depicted in Figure 8.4. DRM results can be checked for problems that affect the transition time, contact timing, phase synchronisation, contact resistance or that interrupt the current. This way, the condition of the tap changer can be determined using boundary values, as will be discussed in the next section.

Table 8.2 Quantities derived from DRM which represent the OLTC condition, including the OLTC defects to which they are sensitive, the way they are calculated and the knowledge rules from Table 8.1 that must be considered.

Quantity:		Sensitive to:	Calculated by (see Figure 8.3):	Knowledge rules:
1	Transition time	Contact misalignment Defective drive mechanism Friction	T_{TR} (ms)	1.1 1.3 2.3 2.4 2.8 3.10 4.2 4.3
	Timing of the transition resistors	Contact wear Contact misalignment Damaged transition resistors	$\frac{T_{R1} + T_{R2}}{T_{TR}} * 100$ (%)	1.1 1.3 2.3 2.4 2.8 4.1-4.3 3.10 3.11
	Timing difference between phases A, B and C	Contact misalignment between phases	$\max \{T_{END-A}, T_{END-B}, T_{END-C}\} - \min \{T_{END-A}, T_{END-B}, T_{END-C}\}$ (ms)	
	Time that the measurement current is interrupted	Contact wear Contact misalignment Damaged transition resistors Advanced long-term aging effect	$T_{I<10\%}$ (ms)	1.1 2.1-2.4 2.8 3.4 3.10 4.1-4.5 4.7 4.8
	Maximum contact resistance when the OLTC uses infrequently used contacts	Long-term aging effect: surface film	$\frac{I_{exp} - I_{min}}{I_{exp}} * 100$ (%)	1.1-1.3 2.1 2.2 2.4-2.7 3.1 3.2 3.4 3.6 3.7 3.9 3.10 4.1-4.4 4.6-4.8
	Maximum contact resistance when the OLTC uses frequently used contacts	Long-term aging effect: pyrolytic carbon	$\frac{I_{high} - I_{low}}{I_{high}} * 100$ (%)	1.1-1.3 2.1 2.3-2.7 3.1-3.6 3.8 4.1-4.3 4.6-4.8

8.4 Condition indexing

It is important that condition assessment is as objective and consistently applied as possible. Ideally, a scoring system would be used [40] to model the continuous degradation process as a discrete process. Condition indexing can be used for this purpose, based on the derived quantities described in the previous section. Condition indexing is the process of assigning limited index numbers to the condition of the tap changer. These condition indices provide fast, simple and systematic information about the condition to the asset manager. For example, the OLTC subsystem condition can be described in terms of ‘Good’, ‘Aged’ and ‘Bad’. Ref. [94] uses the categories ‘Not aged, not worn out’, ‘Aged’ and ‘Worn out (noticeably)’ to classify the condition.

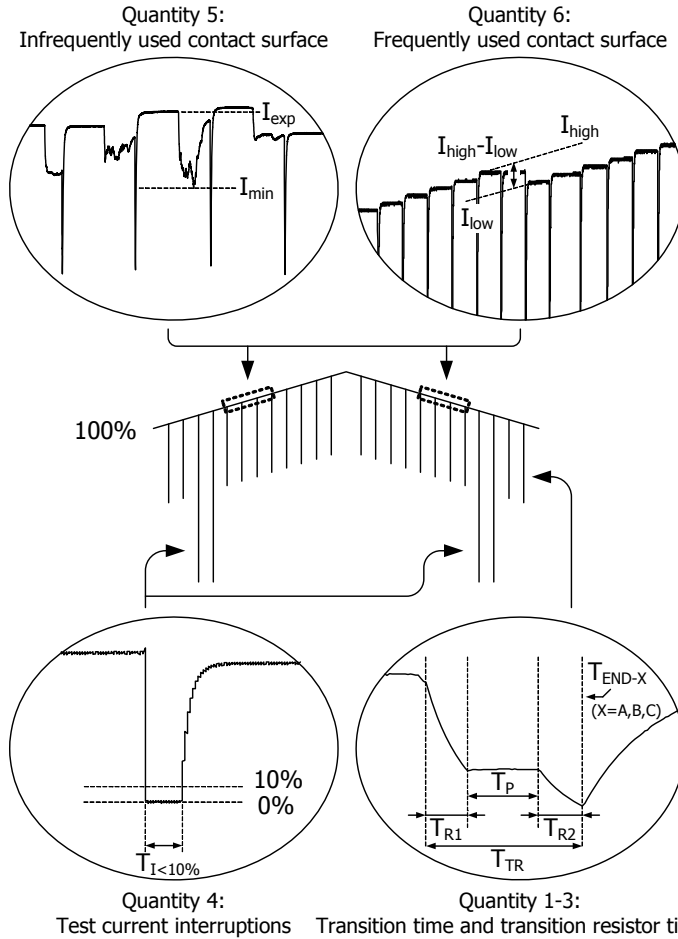


Figure 8.3 Quantities that reflect the OLTC condition can be used to extract condition information from DRM results. This figure shows a set of quantities that can be used to reveal the most common OLTC defects.

To apply condition indexing, boundary values are needed to convert the selected continuous parameters from DRM (see Section 8.3) into a few categories. Section 8.5 describes an application example of these boundary values, based on the relationship between DRM results and visual inspection of the OLTC contacts. Statistical analysis on derived quantities could also be used to derive norm values, see [95]. If the boundaries are too conservative, more false positive conclusions will be drawn, unnecessarily high maintenance expenditure may result and the early replacement of the OLTC components may occur. However, if the boundaries are too tight, unreliable tap changers may remain undetected (false negative conclusions), which can result in serious damage to the transformer. It is very difficult to decide when a fault is serious enough to justify radical action [40].

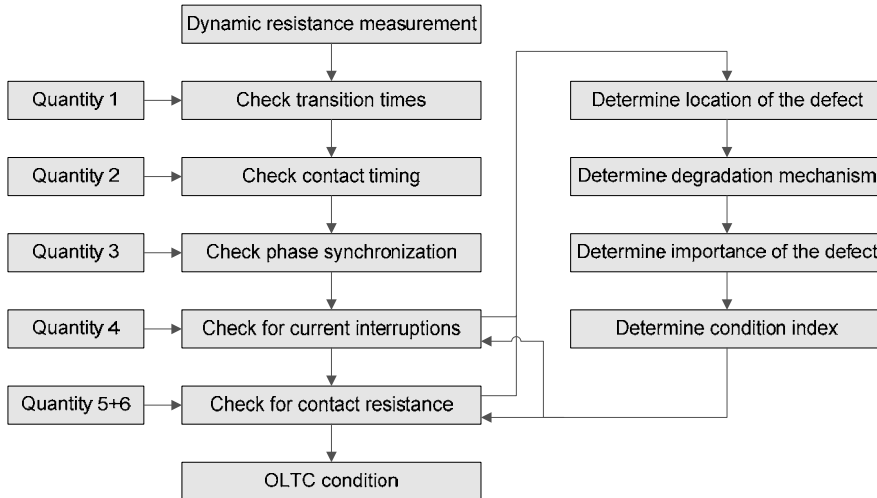


Figure 8.4 The quantities from Table 8.2 can be used to check DRM results for typical irregularities in a structured way. Transition times, contact timing, phase synchronism, open contacts and contact resistance can be checked this way.

Information about condition is lost during the process of condition indexing. However, this final step of condition assessment is advantageous because of its simplicity: the condition index allows different OLTCs to be easily compared, critical OLTCs to be selected and decisions about the maintenance strategy to be made.

The relationship between DRM results and condition indices can be expressed as a membership function. Membership functions have a value between 0 and 1 that expresses the degree that a continuous parameter from the diagnostic data is a member of a linguistic variable. This value is called the degree of truth. The linguistic variables that assess the condition are by definition vague, for example 'Good', 'Aged' and 'Bad'. This allows the condition of the OLTC to be described by a more human classification system, which makes it suitable to present the results to an expert. Figure 8.5 shows an example in which numerical condition indices are used. The condition is described by condition 'Good', 'Aged' and 'Bad'. Fixed boundaries are used, based on the deviation of the measurement current in the DRM results. Limits for condition indexing can be obtained by:

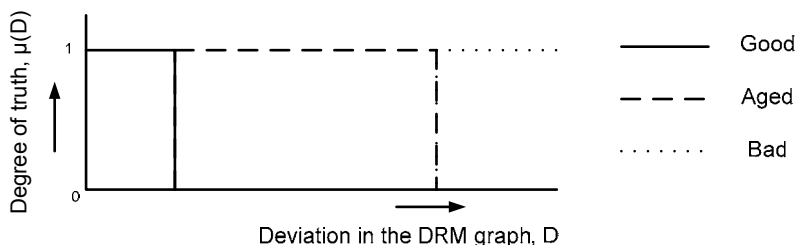


Figure 8.5 Example of deriving condition indices from the deviation in the DRM plots, using fixed boundaries for the membership function.

- A study of service-aged components (see Section 8.5)
 - during overhaul
 - after failure
- A statistical analysis of historical diagnostic data (see [95])

Less information is lost during condition indexing when the result is expressed as a fuzzy membership function. Another advantage of fuzzy membership functions is apparent when DRM is performed on large populations of OLTCs. Many engineers are involved in the process of taking these measurements, and therefore different interpretations of measurement data are inevitable when no strict flowcharts for condition indexing are used. If a comparison of condition indices is required, these decision flowcharts should be based on precisely prescribed quantities.

Figure 8.6 provides an example of a fuzzy membership function, where the condition is defined by fuzzy logic using trapezoidal membership functions. It gives the degree of truth of the deviation in dynamic resistance results for the three linguistic variables (in this example 'Good', 'Aged' and 'Bad'). For example, a measurement result plot with a certain irregularity can have a degree of truth of 0.7 to the variable 'Aged' and 0.3 to 'Bad'.

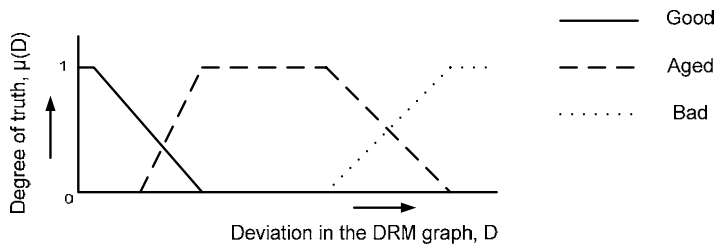


Figure 8.6 Example of a membership function of the deviation in DRM plots for the linguistic variables 'Good', 'Aged' and 'Bad'.

8.5 Application example

The condition indexing of DRM results for OLTCs is type dependent, as each type has a different sensitivity to degradation mechanisms. In general, a faulty condition is expected when the contact resistance is increased 5-10 times the initial value of contact resistance [40].

This section describes the application of DRM at a Dutch utility [96], where condition indexing was used to assess the contact condition of a large number of OLTCs. In this example, parameters from DRM which reflect the tap changer condition are combined with experience from laboratory experiments, failure studies and knowledge about the degradation processes (as shown in Figure 8.2). The condition indices 'A', 'B' and 'C' are used to indicate the condition, corresponding with 'Bad', 'Aged' and 'Good' as described earlier. To begin with, a distinction is made between:

- 1) OLTCs with open contacts (8.5.1)
- 2) OLTCs with an increased contact resistance (8.5.2)

8.5.1 Open contacts

The tap changer has open contacts when the measurement current is interrupted during DRM. The duration of the interruption and the location in the plot are used to determine its source (see Section 8.3). The boundaries from Table 8.3 are set as follows:

- 200 ms is the maximum transition time of the OLTCs in the population
- Short interruptions as observed in this population are normally less than 3 ms, 10 ms is taken as the boundary
- 20 s is the maximum expected time between two operations and depends on the motor operation time of the drive mechanism and time delay relays
- An open contact is defined here as a measurement current that drops below 10% of the initial current. This limit is required because the zero current of short interruptions is not always sampled at a 1 kHz sampling rate. The slowly increasing current will be sampled before it reaches the 10% limit again.

Condition indexing is uncomplicated in the case of open contacts: all contacts which remain open for longer than 10 ms are given condition index 'A' (bad/critical). Shorter interruptions of the measurement current are given condition index 'B' (aged) when roller contacts are used and condition index 'C' (good) when contact blocks are used. Figure 8.7 can be used in the case that fuzzy logic is preferred.

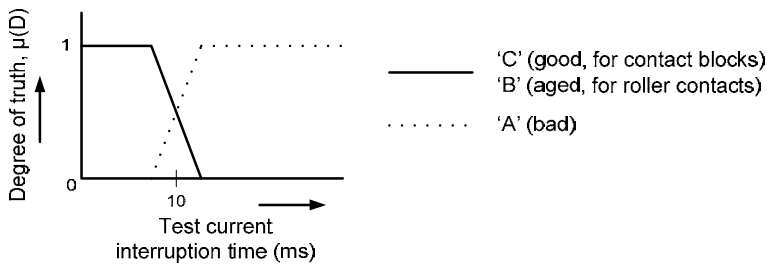


Figure 8.7 The relationship between the interruption time of the DRM measurement current and the OLTC's condition can be displayed as a fuzzy membership function.

Table 8.3 *The interruption time measured with DRM versus the location of the interruption. Boundary values are applied to find the cause of the interruption.*

Interruption time	Location of the interruption	
	Arcing switch operates	Change-over selector moves
$t_{I<10\%} < 10 \text{ ms}$	A harmless layer of oil can be measured when the arcing switch uses contact blocks to establish a connection. When roller contacts are used, the arcing contacts of the stator can be worn.	The long-term effect is measured; most likely a thick surface film.
$10 \text{ ms} \leq t_{I<10\%} < 200 \text{ ms}$	Defective transition resistors.	The long-term effect is measured; most likely a thick surface film.
$200 \text{ ms} \leq t_{I<10\%} < 20 \text{ s}$	-	Change-over selector problems are measured covering a single tap position.
$T_{I<10\%} \geq 20 \text{ s}$	-	Open contacts inside the change-over selector are measured covering multiple tap positions.

8.5.2 Contact resistance

Tap changers with an increased contact resistance can show irregularities in the dynamic resistance results; the location of the degradation or defect is determined by observing the moment the irregularity does (or does not) occur. The timing of resistance changes can be related to the operation of specific contacts, a process requiring knowledge of the OLTC construction and mechanical operation. Answering the following questions can determine the location:

- A. Does the resistance change when the change-over selector moves?
- B. Does the OLTC have higher contact resistance when the change-over selector is motionless?
- C. Is there a linear pattern in the dynamic resistance plot?

Table 8.4 shows the relationship between contact resistance and the location and type of defect. Again, answering three questions can help:

- Do the contacts on that location carry current during normal service conditions and are therefore prone to contact coking?
- Are the contacts on that location switched often and therefore less prone to contact coking?
- Is the resistance constant for the duration of the tap position, or are spikes present in the measured resistance?

Table 8.4 *Irregularities in the DRM current pattern can be localised by 1) examining at which moment it occurs and 2) whether there is a linear section in the DRM plot.*

A Resistance deviation when change-over selector moves?	B Resistance deviation when change-over selector is motionless?	Resistance deviation $B \geq A$?	C Linear pattern present?	Indication of the location
No	Yes	-	-	Arcing switch
Yes	Yes	Yes	No	
Yes	Yes	Yes	Yes	Change-over selector
Yes	Yes	No	-	
Yes	No	-	-	

Depending on the location of the defect, the aging mechanisms and the type of OLTC, different boundary values are required. As an example, a flowchart for the condition indexing of change-over selector contact degradation has been made, see Figure 8.8. Table 8.4 should be used prior to this flowchart, thereby taking into account the location of the defect. This example uses condition indexing based on the deviation from the expected value, using the maximum of parameters five and six from Table 8.2. The four questions from Table 8.4 are included in this flowchart (top). The expected value in a DRM plot cannot be determined when the results are extremely distorted. In such cases maximum and minimum values are used as an approximation. Figure 8.8 shows the flowchart for the condition indexing of the change-over selector using DRM at 1 A. Boundaries are determined on the basis of the selector's physical condition as seen during overhaul or after failure [11], when the contact condition can be compared with the measurement results.

The 10% boundary is used to exclude noise, and the 40% limit to distinguish between aged and critical contacts. This 40% boundary is based on observations made during the overhaul of the OLTC or after failure: coking and critical pitting are present in the population under consideration when the deviation due to the long-term effect exceeds 40%. To determine this boundary value, eight case studies were selected, see Table 8.5. These boundary values were used for all contact materials: silver-plated contacts were diagnosed

Table 8.5 *Eight case studies of OLTCs at an advanced stage of development of the long-term aging effect. The maximum deviation of the DRM measurement current with respect to the expected value is given, together with the contact status as observed during visual inspection of the change-over selector contacts.*

	DRM current deviation	Visual inspection of OLTC contacts
Case 1	25%	About to be critical
Case 2	35%	Not critical
Case 3	40%	Critical
Case 4	45%	About to be critical
Case 5	50%	Critical
Case 6	60%	Critical
Case 7	80%	Critical
Case 8	100%	Failed

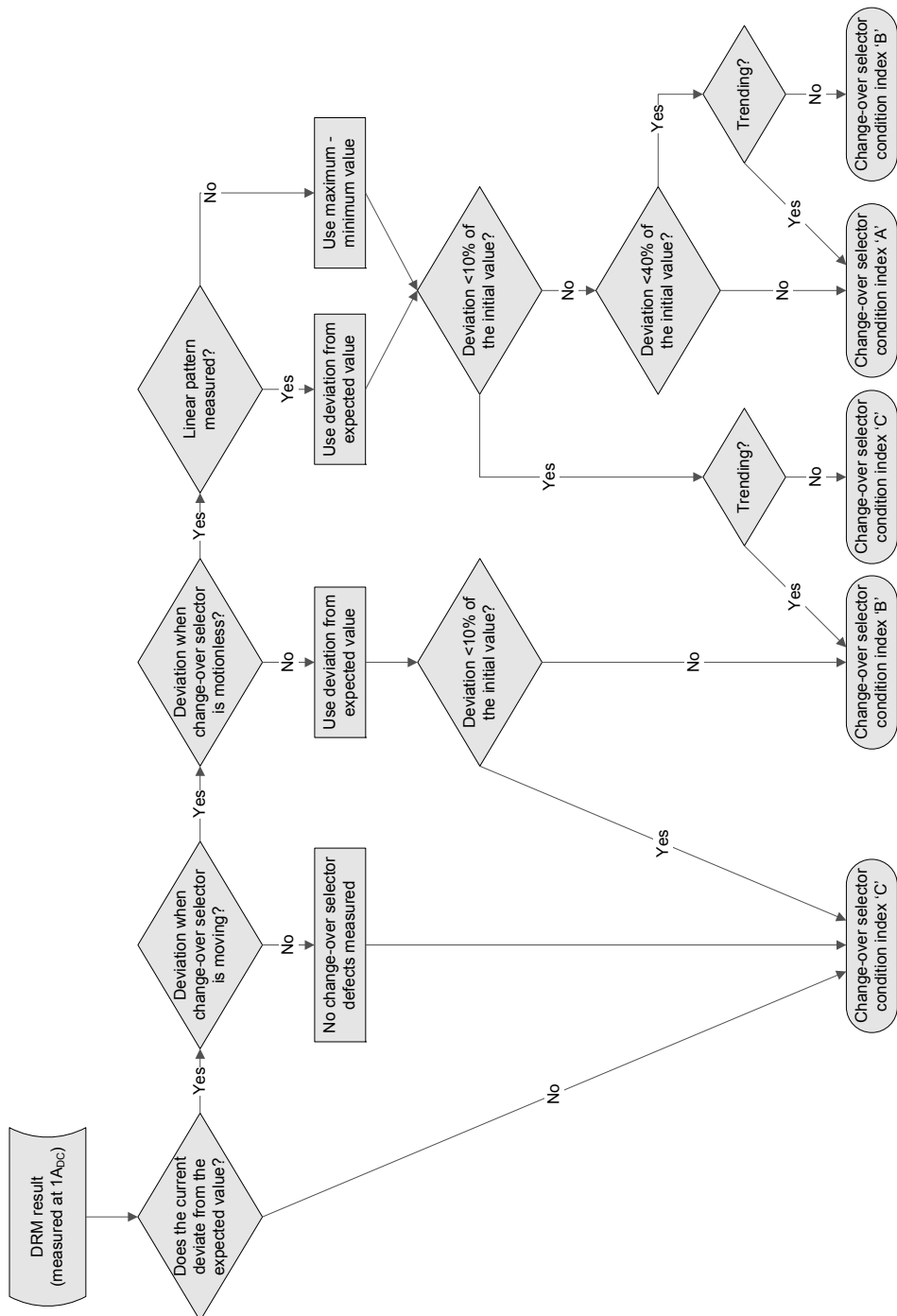


Figure 8.8 Example of the derivation of condition indices for the change-over selector from the irregularities in the DRM plots at 1A, based on the questions and boundaries discussed in this section.

using the same decision rules as non-silver-plated contacts. The way in which the results change over time can also provide valuable additional information [40]. Therefore, the contact deterioration was compared with previous results and a lower condition index was assigned when the irregularity in the plots increased over time.

Condition indexing based on fuzzy membership functions can be applied to this application example as well, using the same boundary values; in that case contact degradation in the change-over selector can be assessed by the membership function of Figure 8.9 for degradation that is not changing over time. The membership function shifts when degradation increases over time, see Figure 8.10.

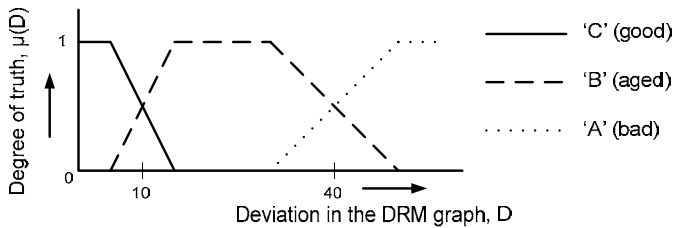


Figure 8.9 Example of a fuzzy membership function for assessing the condition of the change-over selector in case the degradation is not increasing over time, based on DRM at 1A.

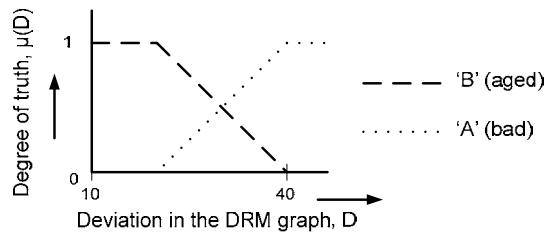


Figure 8.10 The membership function of Figure 8.9 shifts when the degradation increases over time.

If there is insufficient failure data available for a particular type of OLTC, it is impossible to make a good prediction of its end-of-life [97]. In such cases, a statistical analysis using the DRM database can be used to determine boundary values [95], because degradation and aging mechanisms are statistical in nature [97]. If the cause of irregularities in the DRM results is not immediately clear, additional measurements can be performed:

- to determine if the results are reproducible
- to determine if the contact degradation in the form of a surface film can be wiped away, by switching the OLTC through its cycle of operation a few times
- to determine whether the resistance due to degradation is dependent on the current (attention should be paid to not heating the contacts), by using different measurement current amplitudes

8.5.3 Flowchart verification

To verify the flowchart of Figure 8.8, it was applied to the OLTCs of a Dutch utility. The utility used DRM as a method to pre-select critical tap changers, which would then undergo additional measurements, and to detect maintenance errors. This population of tap changer, 455 in total, consisted of 33% diverter switch type OLTCs from manufacturer A and 52% selector switch type OLTCs from manufacturer B (the remaining 15% is from different producers, mostly diverter switch type OLTCs). Most of the transformers were 50/10 kV and the average power rating of the population was 39 MVA. Figure 8.11 shows the condition indices of the total population in relation to the year of installation. It shows that the flowchart of Figure 8.8 correctly does not classify the relatively new OLTCs as 'B' (aged) while tap changers older than 20 years did show irregularities in the DRM plots and were assigned a condition index 'B' (aged) or 'A' (bad).

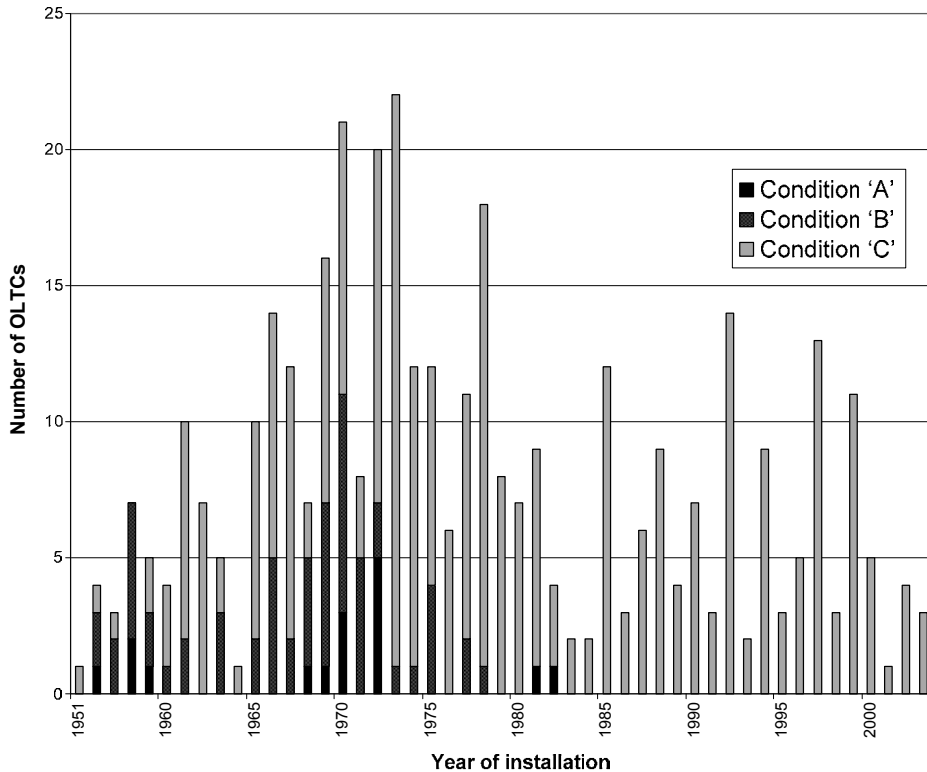


Figure 8.11 DRM results (after condition indexing using the flowchart of Figure 8.8) for the total population of OLTCs, sorted by the year of installation.

Figure 8.12 shows the subpopulations selected and their average ages. OLTCs are grouped according to their condition, their type of contact and contact material. A special subpopulation was created to compare OLTCs with roller contacts to OLTCs using snap contacts ('old snap contacts'), ensuring that the average age of

both subpopulations was equal. Differences in design are seen when the flowchart of Figure 8.8 is applied to the DRM results from this population, see Figure 8.13. It can be seen that tap changers using roller contacts at the change-over selector show more effects of long-term aging than tap changers using snap contacts at the same location. Change-over selectors using roller contacts also have the highest number of critical condition indices.

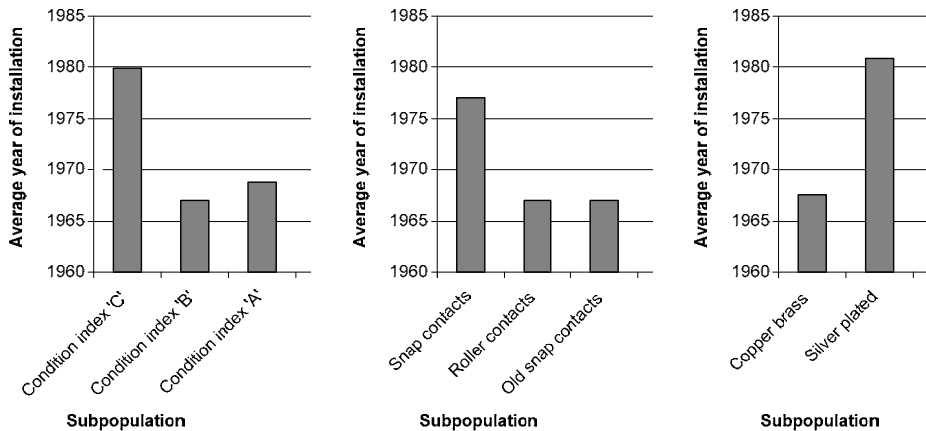


Figure 8.12 Overview of the year of installation of each selected OLTC subpopulation.

The most striking contrast is seen in Figure 8.13 when comparing the type of contact material used at the change-over selector. According to the flowchart of Figure 8.8, the copper-brass contacts had aged to an extreme degree compared with the silver-plated contacts. The flowchart successfully assessed this effect because:

- OLTCs using copper-brass contacts were older (average year of construction 1968 as opposed to 1981)
- OLTCs using copper-brass contacts had no overhaul, while some tap changers with silver-plated change-over selector contacts were silver-plated during their service life (and therefore contact degradation was removed)
- OLTCs using copper-brass contacts are subject to a more rapid long-term aging effect on the change-over selector [24]

The flowchart from Figure 8.8 takes into account contact deterioration over time by looking at the difference between latest measurements and those taken previously. It was seen that about 50% of the tap changers had degraded since the previous measurement and on this basis were assigned a lower condition index.

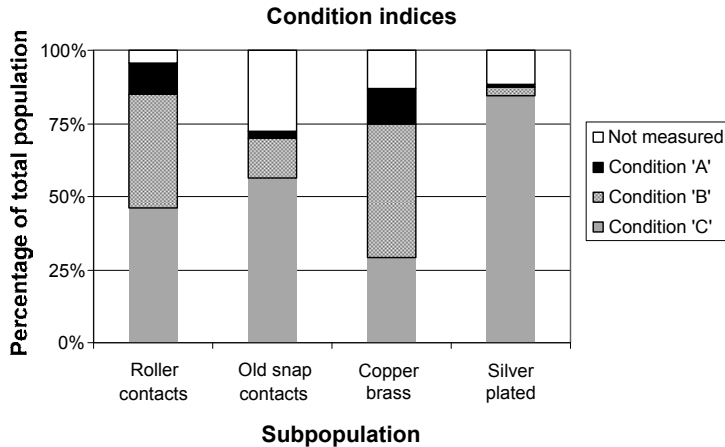


Figure 8.13 Overview of the condition index as determined by the flowchart of Figure 8.8 for each OLTC subpopulation selected from the population studied.

When the flowchart of Figure 8.8 is applied to the OLTCs of Table 8.5 it can be seen that 7 out of 8 cases is categorised according to results from visual inspection. Only case 4 is categorised as 'A' (bad) because it has a measurement current deviation of 45% while the boundary value of Figure 8.8 is 40%, which is incorrect because visual inspection showed that the contacts were about to be critical, but the OLTC could remain in service for some more years (a false positive conclusion). The fuzzy logic approach of Figure 8.9 and Figure 8.10 circumvents this issue when relating DRM results to visual inspection results.

The flowchart of Figure 8.8 was verified in more detail by selecting:

- one OLTC that was categorised as 'C' (good, 0% measurement current deviation)
- one categorised as 'B' (aged, 24% measurement current deviation, not trending)
- one of category 'A' (bad, 48% measurement current deviation, not trending)

The contact resistance of the change-over selector was determined at 100 A for each position of the change-over selector. DRM was performed and the deviation of the current from the expected value was calculated at the same tap positions as for the static measurement. Figure 8.14 shows the static resistance versus the dynamic resistance for the investigated tap position of these OLTCs. The trend line is added, including 80% confidence bounds. It can be seen that the flowchart assesses the good OLTC correctly: the contacts with no irregularities in the DRM results also have a low static contact resistance ($\sim 5 \text{ m}\Omega$) and group nicely near zero. Good contacts are also easily distinguished from aged and bad contacts, which have higher static and dynamic contact resistance. Finally, the trend line shows a light statistical relationship between static and dynamic resistance, but this

relationship is too weak to predict the static resistance based on the dynamic resistance and vice versa.

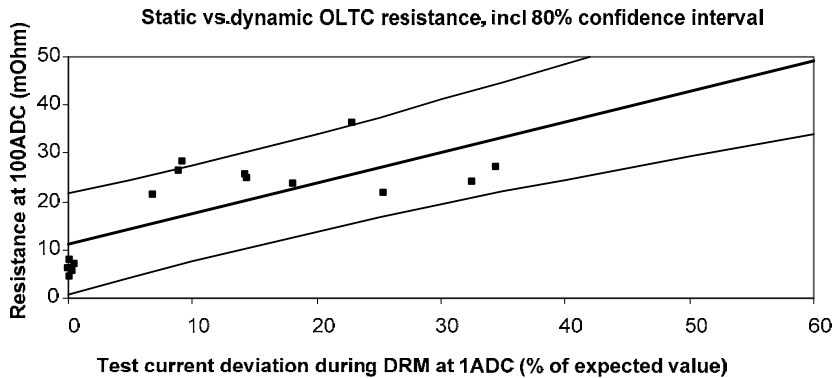


Figure 8.14 Static resistance at 100 A versus dynamic resistance at 1 A. Five tap positions were measured at three OLTCs in different aging staged. The trend line and the 80% confidence interval are drawn.

8.6 Conclusions

This chapter discussed how to deal with dynamic resistance measurement results from OLTCs and demonstrated how these results can be represented as condition indices using a flowchart that categorises them using boundary values. It was shown how the technical condition can be determined by applying boundary values to derived parameters from DRM graphs. By doing so, a set of critical tap changers can be selected that will benefit from failure-reducing efforts (e.g. maintenance). This chapter also concluded that DRM alone does not provide enough information to determine an optimal maintenance strategy for a population of OLTCs, other sources of information, such as results from visual inspection, should be considered as well.

Firstly, knowledge rules were derived from different sources, such as field measurements, laboratory experiments and failure investigation. On this basis a list of DRM knowledge rules was provided.

Secondly, the chapter explained which quantities that are determined from dynamic resistance results will cover the most common defects.

Thirdly, it was shown that with the use of a condition indexing flowchart it is possible to convert complex diagnostic information into simple condition indices, which depends on the type of tap changer being measured. The categories resulting from a condition indexing flowchart can be expressed in vague linguistic variables or as clear numbers using fixed boundaries. Information is lost during this process of condition indexing, but the simplified representation can be an advantage for the asset manager when making decisions about OLTC maintenance or replacement.

An example of a condition indexing flowchart was also presented and its application to a population of OLTCs discussed. Clear differences between tap changer contact materials and transformer age were seen; it was shown that type of contact under consideration has a relationship with the condition indices.

9

Conclusions & recommendations

This thesis has explored contact resistance measurements for the diagnosis of high-speed resistor-type on-load tap changers (OLTCs), extensively used in high-voltage power transformers. The feasibility of using dynamic resistance measurements (DRM) for the pre-failure detection of frequently observed degradation mechanisms and defects has been investigated. Also, the additional value of performing DRM after maintenance has been demonstrated in relation to its capacity to detect the different defects.

9.1 Conclusions

In line with the research goals, the conclusions of this thesis are summarised as follows:

1. Tap changer degradation

- The on-load tap changer showed to be responsible for a major part of the transformer failures. Dominant failure modes include contact degradation, mechanical defects and maintenance errors.
- Contact resistance models from literature have been discussed and corrected to make them suitable for resistance measurements on tap changers, thereby compensating for the contact operation and for the amplitude of the measurement current.

2. Diagnostic methodology for on-load tap changers

- No relationship between the electrical condition of the change-over selector contacts and dissolved gas-in-oil amount (or gas ratios) has been found for the dataset selected.

- A transformer diagnostic system has been derived by combining several diagnostic measurements for power transformers, i.e. measurement of the transformer turn ratio, static and dynamic resistance, drive motor power and drive axis rotation. The proposed measurements are advised in combination with visual inspection and dissolved gas analysis.
- Dynamic resistance measurements assess a larger contact area than static measurements and more degradation mechanisms are detected, e.g. mechanical defects and contact wear.
- This thesis discussed dynamic resistance measurements on the transformer windings with OLTCs (a direct measurement) and on the windings without OLTC (an indirect measurement). Indirect measurements are more sensitive to rapid changes in the contact resistance but the results are dependent on the transformer ratio. Direct measurements are safer because a secondary short-circuit is applied.

3. Sensitivity verification

- DRM has been found to be a dedicated method for :
 - i. Assessing the basic function of an OLTC in a direct and non-destructive way, because it is sensitive to current interruptions that may lead to failure.
 - ii. Discovering contact resistance caused by different kinds of contact degradation that may reduce the reliability of operation.
 - iii. Assessing the condition of parts which are not accessible for inspection during regular maintenance.

Therefore, this method can be used to detect a large variety of defects and degradation mechanisms before failure can occur, in particular in combination with regular tap changer maintenance.

- DRM can also be used for localisation of defects. Localisation is important for risk assessment.
- Laboratory experiments with artificially degraded tap changer contacts show no sensitivity for non-critical thin contact films at 1 A. A thick film can be detected. The measurement of medium contact degradation is inconsistent at 1 A and the film may be wiped away by the moving contacts.

4. Dynamic resistance measurement parameters

- Resistance measurements are more sensitive to surface film and light contact degradation if a low measurement current is used. The initial stage of long-term contact degradation, leading to contact coking, is then revealed, which makes DRM suitable for pre-failure diagnostics. Results measured at low

current can vary due to the tendency of the contact film to break. Therefore, a trade-off should be made.

- Contact resistance measured at different current amplitudes should be corrected before they are compared, due to the non-linear relationship between current and resistance, in particular at degraded contacts. Contact resistance does not resemble the values at nominal current. A correction factor has been introduced to compensate for this effect.
- The measurement current at a tap changer in a delta-connected winding configuration also flows through the parallel phases. A 50% higher measurement current should be used to compensate for this effect in cases where results must be compared with, for example, star-connected tap changers.
- A measurement circuit with higher circuit resistance results in smaller changes in the measured current, and therefore a lower signal-to-noise ratio, but a higher sensitivity to rapid resistance changes is obtained.
- International standards for power transformer measurements do not specify the exact measurement parameters for resistance measurements: most practical parameters can be freely chosen, but standardisation would be beneficial because contact resistance depends on the amplitude of the measurement current.

5. Interpretation of DRM results

- The measurement results can be subdivided into those showing:
 - i. no irregularities
 - ii. the effects of contact resistance
 - iii. open contacts
 - iv. irregularities in contact timing (e.g. phase synchronisation, transition times or timing differences due to wear).

Due to this categorisation a more systematic interpretation is possible.

- DRM plots can be interpreted by comparing them with reference measurements. The following procedure provides a more advanced interpretation:
 - i. Localisation of the defect – the arcing switch, change-over selector and drive system can be separately diagnosed
 - ii. Determining the cause – the degradation mechanisms on the specific location should be evaluated
 - iii. Determining the importance – interpretation of results is type dependent

- Results can be summarised as a condition index, as is demonstrated in this thesis. On the basis of the dynamic resistance results, criteria which can be used to reveal the most important defects were determined; boundary values can be applied to these quantities during interpretation. These boundary values depend on the type of tap changer and the measurement parameters. Condition indexing using flowcharts is beneficial due to its simplicity and objectivity in supporting management decisions.
- The following characteristics of dynamic resistance results should be interpreted to ensure that the transformer can be re-energised safely:
 - i. A dynamic resistance overview plot of all tap positions
 - ii. A dynamic resistance close-up plot of each tap changer operation
 - iii. The transition times of each tap changer operation

All these characteristics should be in correct state, considering the voltage and current that were used for the measurements
- It is recommended that dynamic resistance measurements should be carried out on all on-load tap changers directly after maintenance and that the results of these measurements should be interpreted before the tap changer is returned into operation.

9.2 Suggestions for future work

- Additional accelerated degradation experiments with tap changer contacts should be performed to confirm the boundary values for the condition indexing of DRM results, as were derived in this thesis using the relation between contact resistance and the observed degree of degradation. Criteria should be derived for each type of tap changer and degradation mechanism.
- The distinction between coked contacts and contacts with a thick contact film should be further investigated to make a better distinction between aged and critical contacts. An overhaul could be used to obtain better insight into the location of excessive contact resistance: the behaviour of contact resistance at different aging stages can be further investigated by cleaning the change-over selector step by step, measuring each phase of degradation separately. A transformer which failed due to a winding defect and having aged tap changer contacts would be most suitable for these tests.
- A correction factor for variations in the measurement current amplitude was determined for 2.5 A and higher (C_{DRM} , as introduced in Section 2.3.5). Additional experiments could be conducted to derive a correction factor for lower values of the measurement current (e.g. from 0.5 A and higher) in order to make more sophisticated corrections for contact resistance at lightly aged

contacts. Furthermore, different correction factors can be derived for tap changers in different aging stages.

- A database with DRM case studies can be used to compare results directly after a measurement with previously measured results; most similar results from the database can then be shown on-site to the test engineer. These case studies provide more detailed information about the tap changer condition.
- An on-line monitoring system can be developed to detect overheated tap changer contacts when the power transformer is in service. Different sensors, for example measuring local contact temperatures in the change-over selector or measuring contact voltages, can be applied to detect severely aged contacts.

References

- [1] R. Moxley, A. Guzmán, “Transformer maintenance interval management”, Schweitzer Engineering Laboratories, Cigre Study Committee B5 Colloquium, paper 118, September 2005.
- [2] F. Roos, S. Lindahl, “Distribution system component failure rates and repair times – an overview”, Nordic Distribution and Asset Management Conference, Espoo, Finland, 23-24 August 2004.
- [3] D.J. Allan, A. White, “Transformer design for high reliability”, Second International Conference on Reliability of Transmission and Distribution Equipment’, Conference Publication No. 406, p. 66-72, 29-31 March 1995.
- [4] Cigré WG 12.05, “An international survey on failures in large power transformers in service”, ELECTRA No. 88, p. 21 – 48, 1983.
- [5] M.S.A. Minhas, J.P. Reynders, P.J. de Klerk, “Failures in power system transformers and appropriate monitoring techniques”, Eleventh International Symposium on High Voltage Engineering, London, UK, Conference Publication No. 467, paper 1.94.S23, p. 94-97, 1999.
- [6] R. Jongen, P.H.F. Morshuis, E. Gulski, J.J. Smit, “A statistical approach to processing power transformer failure data”, 19th CIRED International Conference on Electricity Distribution, Vienna, Austria, paper 546, May 2007.
- [7] G. Spence, A.C. Hall, “Users experience and perspective”, European seminar “on-load tap changers-current experience and future developments”, Regensburg, Germany, 9 November 1995.
- [8] H.F.A. Verhaart, L.J.C. Wakkerman, “Tussenrapport over faaloorzaken van distributie- en koppeltransformatoren op basis van de onvoorziene niet-beschikbaarheid”, KEMA, rapport 43613-T&D 94-102278, 1994 (Dutch).
- [9] H.U. Schellhase, R.G. Pollock, A.S. Rao, E.C. Korolenko, B. Ward, “Load tap changers: investigations of contacts, contact wear and contact coking”, Proceedings of the Forty-Eighth IEEE Holm Conference on Electrical Contacts, p. 259- 272, 2002.

- [10] G. Breen, "Essential requirements to maintain transformers in service", presented at the International Council on Large Electric Systems (CIGRÉ), Paris, France, paper 12-103, August 30–September 5 1992.
- [11] J.J. Erbrink, "Tap changer diagnostics on high voltage power transformers using dynamic resistance measurement", Graduate thesis Delft University of Technology, Delft, the Netherlands, 2007.
- [12] P.P. Seitz, B. Quak, J.J. Erbrink, E. Gulski, R. Leich, "Advanced on-site diagnosis of power transformers", International conference on condition monitoring and diagnosis, Beijing, China, paper 148, April 2008.
- [13] P. Kang, D. Birtwhistle, J. Daley, D. McCulloch, "Non-invasive on-line condition monitoring of on load tap changers", IEEE proceedings on generation, transmission and distribution, Vol. 3, p. 2223-2228, January 2000.
- [14] J.J. Erbrink, E. Gulski, P.P. Seitz, R. Leich, "Advanced on-site diagnosis of transformer on-load tap changer", IEEE International Symposium on Electrical Insulation, Vancouver, Canada, p. 252-256, June 2008.
- [15] A. Krämer, "On-load tap-changers for power transformers; Operation principles, applications and selection", Maschinenfabrik Reinhausen GmbH, Regensburg, Germany, ISBN 3-00-005948-2, 2000.
- [16] A. White, "Tapchanging – the transformer designer's perspective", IEE European Seminar on Developments On-Load Tap Changers: Current Experience and Future", Regensburg, Germany, p. 4/1-4/6, 9 November 1995.
- [17] IEC 60214-1, "International standard, tap changers – Part 1. Performance requirements and test methods", first edition, 2003.
- [18] V.V. Sokolov, "Considerations on power transformer condition-based maintenance", EPRI Substation Equipment Diagnostic Conference VIII, New Orleans, USA, 20-23 February 2000.
- [19] R. Crutcher, D. Hanson, L. Savio, "New equipment and performance design review – LTC management course materials", Report 2-4 in "New Equipment and Performance Design Review – LTC Management Course Materials", EPRI, Palo Alto, USA, Technical Report ID 1012350, December 2006.
- [20] P.J. Hopkinson, "Electrical contacts for off-circuit tap changers for oil immersed transformers", IEEE/PES Transformers Committee, DETC working group, October 11, 2005.

- [21] R. Holm, "Electric contacts: theory and application", 4th edition, Springer Verlag, New York, 1967.
- [22] J. A. Greenwood, "Constriction resistance and the real area of contact", British Journal of Applied Physics, vol. 17, no. 12, p. 1621-1632, 1966.
- [23] T. Sun, "Fundamental study of contact resistance behavior in rsw aluminum", dissertation at the Ohio State University, 2003.
- [24] K. Lemelson, "About the failure of closed heavy current contact pieces in insulating oil at high temperature", IEEE transactions on parts, hybrids, and packaging, Vol. Php-9, No.1, p. 50-52, March 1973.
- [25] EPRI, "Evaluation of load tap changer oil for susceptibility to coking", from www.eprweb.com, viewed June 2010.
- [26] EPRI, "Development of load tap changer monitoring technique: mechanism of coking", EPRI, Palo Alto, USA, Technical Report ID 1001946, 2001.
- [27] A. Erk, M. Schmelzle, "Grundlagen der Schaltgeratetechnik. Kontaktglieder und Lascheinrichtungen Elektrischer Schaltgeräte der Energietechnik", Berlin, Germany, Springer-Verlag, ISBN 3540060758, April 1974 (German).
- [28] T. Tamai, "Growth of oxide films on the surface of Cu contact and its effect on the contact resistance property", Electronics and Communications in Japan, Part 2, vol. 72, no. 7, p. 87-93, 1989.
- [29] J. Kosco, "The effects of electrical conductivity and oxidation resistance on temperature rise of circuit-breaker contact materials", IEEE Transactions on Parts, Materials and Packaging, vol. 5, no. 2, p. 99- 103, June 1969.
- [30] L. Boyer, "Contact resistance calculations: generalizations of Greenwood's formula including interface films", IEEE Transactions on Components and Packaging Technologies, vol. 24, no. 1, p. 50-58, March 2001.
- [31] S. Schoft, J. Kindersberger, H. Löbl, "Joint resistance of busbar-joints with randomly rough surfaces", Proceedings of the 21th International Conference on Electric Contact Phenomena, Zurich, Switzerland, p. 230-237, 9-12 September 2002.
- [32] M. Braunovic, V.V. Izmailov, M.V. Novoselova, "A model for life time evaluation of closed electrical contacts", Proceedings of the Fifty-First IEEE Holm Conference on Electrical Contacts, p. 217-223, 26-28 September 2005.
- [33] E. Takano, K. Mano, "The failure mode and lifetime of static contacts", IEEE Transactions on Parts, Materials and Packaging, vol. 4, no. 2, p. 51-55, June 1968.

- [34] Z. Chen, K. Karasawa, K. Sawa, "Effects on contact resistance of passing electrical current through wiping palladium contacts", IEEE Transaction on Components, Packaging, and Manufacturing Technology, Part A. Vol. 18, No. 3, p. 693-700, September 1995.
- [35] H. Schellhase, N. Dominelli, M. Lau, W. Horn, B. Ward, "Evaluation of a filtration system on onload tap changers – a case study", Report 2-3 in "New Equipment and Performance Design Review – LTC Management Course Materials", EPRI, Palo Alto, USA, Technical Report ID 1012350, December 2006.
- [36] Cigre working group 12.18, "Guidelines for life management techniques for power transformers", draft final report Rev 2, 22 June 2002.
- [37] Z. Wang, Y. Liu, P.J. Griffin, "Artificial intelligence in OLTC fault diagnosis using dissolved gas-in-oil information", IEEE Power Engineering Society Summer Meeting, Seattle, USA, Vol. 4, p. 2422-2427, 16-20 July 2000.
- [38] V. Sokolov, J. Mak, A. Bassetto, D. Hanson, "Transformer risk assessment considerations", Proceedings of the EuroTechCon 2002, Birmingham, UK, 1-3 October 2002.
- [39] EPRI, "Development of a filter using adsorbent technologies for the removal of coking precursors: laboratory evaluation", EPRI, Palo Alto, USA, Technical Report ID 1002048, December 2003.
- [40] Cigre, "Life management techniques for power transformers", Working Group A2.18, Technical Brochure 227, June 2003.
- [41] M. Duval, "The Duval triangle for load tap changers, non-mineral oils and low temperature faults in transformers", IEEE Electrical Insulation Magazine, Vol. 24, No. 6, p. 22-29, November-December 2008.
- [42] M. Duval, "A review of faults detectable by gas in oil analysis in transformers", IEEE Electrical Insulation Magazine, Vol. 18, No. 3, p. 8-17, May-June 2002.
- [43] R. Zuijderduin, J.J. Erbrink, E. Gulski, J.J. Smit, R. Leich, "Condition assessment of power transformers OLTC by DGA and dynamic resistance measurements", Proceedings of the 16th international symposium on high voltage engineering, Johannesburg, South Africa, 2009.
- [44] IEEE Std C57.104-1991, "IEEE Guide for the interpretation of gasses generated in oil-immersed transformers".

- [45] M. Wang, A.J. Vandermaar, K.D. Srivastava, "Review of condition assessment of power transformers in service", IEEE Electrical Insulation Magazine, Vol. 18, No. 6, p. 12-25, November-December 2002.
- [46] L.R. Lewand, P. Griffin, "Condition assessment of oil circuit breakers and load tap-changers by the use of laboratory testing and diagnostics", Doble, published in Neta World, summer 2004.
- [47] Kelman, "Transport X", Portable Dissolved Gas Analysis unit and Moisture in Oil, www.kelman.co.uk, viewed June 2010.
- [48] BPL Global, "Serveron", Online Transformer Monitor Model TM3, www.bplglobal.net, viewed June 2010.
- [49] GE Energy, "Hydran M2", Online Transformer DGA Monitoring, www.gepower.com, viewed June 2010.
- [50] D. Chu, A. Lux, "On-line monitoring of power transformers and components: a review of key parameters", Proceedings of the IEEE Electrical Insulation Conference and Electrical Manufacturing and Coil Winding Conference, Cincinnati, USA, p. 669-675, 26-28 October 1999.
- [51] L.A.L. de Almeida, M. Fontana, F.A. Wegelin, L. Ferreira, "A new approach for condition assessment of on-load tap-changers using discrete wavelet transform", Proceedings of the IEEE Instrumentation and Measurement Technology Conference, p. 653-656, 16-19 May 2005.
- [52] M. Foata, R. Beauchemin, C. Rajotte, "On-line testing of on-load tap changers with a portable acoustic system", Proceedings of the IEEE 9th International Conference on Transmission and Distribution Construction, Operation and Live-Line Maintenance, Montreal, Canada, p. 293-298, 2000.
- [53] P. Kang, D. Birtwhistle, "Condition assessment of power transformer on-load tap-changers using wavelet analysis", IEEE Transactions on Power Delivery, Vol. 16, No. 3, p. 394-400, July 2001.
- [54] P. Kang, D. Birtwhistle, "Condition monitoring of power transformer on-load tap-changers. Part 2: Detection of aging from vibration signatures", IEEE proceedings on Generation, transmission and distribution, Vol. 148, No. 4, p. 307 – 311, July 2001.
- [55] P. Kang, D. Birtwhistle, "Condition monitoring of power transformer on-load tap-changers. Part 1: Automatic condition diagnostics", IEEE proceedings on generation, transmission and distribution, Vol. 148, No. 4, p. 301 – 306, July 2001.

- [56] F. Poza, P. Marino, S. Otero, F. Machado, “Virtual instrument for condition monitoring of on-load tap changers“, Proceedings of the Third IEEE International Workshop on Electronic Design, Test and Applications, p. 214-218, 17-19 January 2006.
- [57] ABB, “Tstat Transformer Monitor”, Advanced monitoring for Transformer Management, www.abb.com, viewed June 2010.
- [58] S. Tenbohlen, D. Uhde, J. Poittevin, H. Matthes, U. Sundermann, P. Werle, H. Borsi, “Enhanced diagnosis of power transformers using on- and off-line methods: results, examples and future trends”, Cigre 2000, paper 12-204, Paris, France, August 2000.
- [59] S. Tenbohlen, T. Stürl, G. Bastos, J. Baldauf, P. Mayer, M. Stach, B. Breitenbach, R. Huber, “Experience-based evaluation of economic benefits of on-line monitoring systems for power transformers”, Cigre Session 2002, paper 12-110, Paris, 2002.
- [60] P.J. Griffin, L.R. Lewand, R.C. Peck, N.A. Letendre, D. Frieze, J.L. Johnson, “Load tap changer diagnostics using oil tests – a key to condition-based maintenance”, Minutes of Doble Engineering Company Conference, 2005.
- [61] EPRI, “Inspection and maintenance guidelines for distribution substations: master-plan for content development”, EPRI, Palo Alto, USA, Technical Report ID 1002629, December 2004.
- [62] Qualitrol, “509 ITM-300 Intelligent Transformer Monitor”, Load Tap Changer Monitor, www.qualitrolcorp.com, viewed June 2010.
- [63] GE Energy, “LTC-MAP 1525”, Load Tap Changer-Maintenance Action Planner, www.ge-energy.com, viewed June 2010.
- [64] B. Turnbull, S. McConnell, “How infrared thermography helps Southern California Edison improve grid reliability”, from www.goinfrared.com, viewed June 2010.
- [65] IEEE C57.12.90 – 1987, “IEEE standard test code for liquid-immersed distribution, power and regulating transformers and IEEE guide for short-circuit testing of distribution and power transformers”.
- [66] Omicron, “CPC 100”, Multifunctional Primary Test System for Substation Commissioning and Maintenance, www.omicron.at, viewed June 2010.
- [67] Megger, “MTO210 Transformer Ohmmeter”, Transformer Winding Resistance and Tap-changer Test Set, www.megger.com, viewed June 2010.

- [68] P. de Graaf, "KEMA off-line regelschakelaardiagnostiek met aanvullende diagnostieken. Handleiding van het bij KEMA ontwikkelde meetsysteem", KEMA, report 44412-T&D 95-103450, 8 December 1995 (Dutch).
English version: P. de Graaf, "Manual for the KEMA off-line tap changer diagnostics", KEMA, report 94460525-TDP 98-02371A, 1998 (non vidi).
- [69] KBK Power Solutions, "TDRCA", Tapchanger Diverter Resistor and Contact Analyzer, www.kbkps.co.za, viewed June 2010.
- [70] DV Power / Ibeko Power AB, "RMO60TC", Winding Ohmmeter & Tap Changer Analyzer, www.dv-power.com, viewed August 2010.
- [71] A. Kramer, J. Ruff, "Transformers for phase angle regulation considering the selection of on-load tap-changers", IEEE Transaction on Power Delivery, Vol. 13, No. 2, p. 518-525, April 1998.
- [72] X. Zhang, E. Gockenbach, "Asset-management of transformers based on condition monitoring and standard diagnosis", IEEE Electrical Insulation Magazine, Vol. 24, No. 4, p. 26-40, July-August 2008.
- [73] Doble Client Committee on Transformers, "Analysis of replies to the 1998 technical questionnaire on power transformer failures and troubles", Proceedings of the 65th Annual International Conference of Doble Clients, p. 8-2.1-8-2.10, March 1998 (non-vidi).
- [74] J.J. Erbrink, E. Gulski, J.J. Smit, R. Leich, P.P. Seitz, B. Quak, "Reproducibility of dynamic resistance measurement results of on-load tap changers – effect of test parameters", International Conference on Condition Monitoring and Diagnosis, Tokyo, Japan, 6-11 September 2010.
- [75] H.F.A. Verhaart, "A diagnostic to determine the condition of the contacts of the tap changer in a power transformer", Proceedings of CIRED, Brussels, Belgium, paper 1.13, 1995.
- [76] J.J. Erbrink, E. Gulski, J.J. Smit, P.P. Seitz, B. Quak, R. Leich, R. Malewski, "Diagnosis of on-load tap changer contact degradation by dynamic resistance measurements", IEEE Transactions on Power Delivery, Vol. 25, No. 4, p. 2121-2131, October 2010.
- [77] M. Landry, O. Turcotte, F. Briki, "A complete strategy for conducting dynamic contact resistance measurements on HV circuit breakers", IEEE Transactions on Power Delivery, Vol. 23, No. 2, p. 710-716, April 2008.
- [78] M. Landry, A. Mercier, G. Ouellet, C. Rajotte, J. Caron, M. Roy, F. Briki, "A new measurement method of the dynamic contact resistance of HV circuit breakers", IEEE PES Transmission and Distribution Conference and Exhibition, Dallas, USA, p. 1002-1009, 21-24 May 2006.

- [79] J.J. Erbrink, E. Gulski, J.J. Smit, J. Aditya, L.A. Chmura, R. Leich, P.P. Seitz, B. Quak, "Test procedure and test circuit considerations for on load tap changer dynamic resistance measurement", International Conference on High Voltage Engineering and Application, New Orleans, USA, 11-14 October 2010.
- [80] J.J. Erbrink, E. Gulski, J.J. Smit, R. Leich, P.P. Seitz, B. Quak, "Effect of test parameters on dynamic resistance measurement results from on-load tap changers", IEEE International Symposium on Electrical Insulation, San Diego, USA, 6-9 June 2010.
- [81] H.F.A. Verhaart, "Diagnostiek voor de toestandsbepaling van de contacten in een omschakelaar van een regelschakelaar", KEMA, report 43151-T&D 93-4615, 24 November 1993 (Dutch).
- [82] Vanguard Instruments Company Inc, "LTCA-10", Load Tap Changer Analyzer, www.vanguard-instruments.com, viewed June 2010.
- [83] H.F.A. Verhaart, "Werkwijze voor het meten van een weerstandswaarde", NL Patent 9400221, 11 February 1994 (Dutch).
- [84] J.J. Erbrink, R.A. Jongen, E. Gulski, J.J. Smit, "Tap changer diagnostics on high voltage power transformers using dynamic resistance measurement", 4th IEEE young researchers symposium in electrical power engineering, Eindhoven, the Netherlands, p. 1-5, February 2008.
- [85] J.J. Erbrink, E. Gulski, J.J. Smit, P.P. Seitz, B. Quak, R. Leich, R. Malewski, "On-load tap changer diagnosis – an off-line method for detecting degradation and defects: part 1", IEEE Electrical Insulation Magazine, Vol. 26, No. 5, p. 49-59, September - October 2010.
- [86] Maschinenfabrik Reinhausen GmbH, "Oiltap M", On-Load Tap-Changer for Regulating Transformers Technical Data, www.reinhausen.com, viewed June 2010.
- [87] J.J. Erbrink, E. Gulski, J.J. Smit, L.A. Chmura, R. Leich, P.P. Seitz, B. Quak, "Condition assessment of on load tap changers using dynamic resistance measurements", International Conference on High Voltage Engineering and Application, New Orleans, USA, 11-14 October 2010.
- [88] J.J. Erbrink, E. Gulski, J.J. Smit, R. Leich, P.P. Seitz, B. Quak, "Interpretation of dynamic resistance results of on-load tap changers", International Conference on Condition Monitoring and Diagnosis, Tokyo, Japan, 6-11 September 2010.

- [89] R. Samsudin, Yogendra, A. Berhanuddin, Y. Zaidey, M. Haneef, "Experience on dynamic contact resistance test on eroded and worn-out tap-changer contacts", World Academy of Science, Engineering and Technology (WASET), Singapore, 25-27 August 2010.
- [90] J.J. Erbrink, E. Gulski, J.J. Smit, P.P. Seitz, R. Leich, "Experimental model of aging mechanisms of on-load tap changer contacts", International conference on condition monitoring and diagnosis, Beijing, China, p. 247-250, April 2008.
- [91] J.J. Erbrink, E. Gulski, J.J. Smit, R. Leich, "Experimental model for diagnosing on-load tap changer contact aging with dynamic resistance measurements", 20th International conference on electricity distribution, Prague, Czech Republic, paper 135, June 2009.
- [92] E. Gulski, S. Meijer, J.J. Smit, F. de Vries, R. Leich, H. Geene, R. Koning, L. Lamballais, T.J.W.H. Hermans, E.R.S. Groot, J. Slangen, M.J.M. Boone, J. Kanters, A. Bun, A. Janssen, "Condition assessment and AM decision support for transmission network components", Proceedings of the 2006 Cigre International Council on Large Electric Systems, Paris, France, paper D1-110, 27 August – 1 September 2006.
- [93] E. Gulski, F.J. Wester, W. Boone, N. van Schaik, E.F. Steennis, E.R.S. Groot, J. Pellis, B.J. Grotenhuis, "Knowledge rules support for CBM of power cable circuits", Cigre Conference Proceedings, Paris, France, Session 15, paper 104, 25-30 August 2002.
- [94] M. Fischer, S. Tenbohlen, M. Schäfer, R. Haug, "Determining power transformers' sequence of maintenance and repair in power grids", IEEE International Symposium on Electrical Insulation, San Diego, USA, 6-9 June 2010.
- [95] E. Gulski, J.J. Smit, F. de Vries, "The use of diagnostics data for condition indexing of HV components", Proceedings of the 8th International Power Engineering Conference IPEC, Singapore, December 2007.
- [96] J.J. Erbrink, E. Gulski, J.J. Smit, R. Leich, P.P. Seitz, B. Quak, "On-load tap changer diagnosis: interpretation of dynamic resistance deviations", IEEE International Symposium on Electrical Insulation, San Diego, USA, 6-9 June 2010.
- [97] E. Gulski, O. Piepers, J.J. Smit, R.A. Jongen, P.P. Seitz, F. Petzold, F. de Vries, "New generation of on-site diagnosis for distribution power cables", Proceedings of the CIRED 19th International Conference on Electricity Distribution, Vienna, Austria, paper 178, 21-24 May 2007.

- [98] Smit Transformers, “On-load tapchanging equipment”, product catalogues T59/01/E.
- [99] V. Sokolov, Z. Berler, V. Rashkes, “Effective methods of assessment of insulation system conditions in power transformers: a view based on practical experience”, Proceedings of the Electrical Insulation Conference and Electrical Manufacturing and Coil Winding Conference, Cincinnati, USA, p. 659–667, 26-28 October 1999.
- [100] R.M. Schomper, “Condition assessment model for power transformers”, Master thesis, Technical University of Delft, December 2004.
- [101] R. James, W. Bartley, “Transformer asset management”, Weidmann-ACTI Inc. Second Annual Conference, New Diagnostic Concepts for Better Asset Management, November 2003.
- [102] IEEE Std 62-1995, “IEEE guide for diagnostic field testing of electric power apparatus. Part 1: oil filled power transformers, regulators, and reactors”.
- [103] ANSI/IEEE C57.12.90-1987, “American national standard / IEEE standard test code for liquid-immersed distribution, power, and regulating transformers”.
- [104] Megger, “Instruction Manual AVTM830280 for Transformer Ohmmeter”, www.megger.com, viewed June 2010.
- [105] Megger, “Instruction Manual AVTM550503, for Three-Phase TTR Transformer Turn Ratio Test Set”, www.megger.com, viewed June 2010.

Appendix A

OLTC technology, degradation and protection

This appendix takes a closer look at a tap change operation of the selector switch and a diverter switch (Section A.1). In addition, OLTC degradation is discussed in detail (Section A.2) and common ways of OLTC protection are discussed (Section A.3).

A.1 OLTC technology

Chapter 2 already gave an introduction to the operation principles of an OLTC. It was discussed that OLTC types can be subdivided into types with a diverter and a selector switch. This section describes how these types of OLTC switch from one winding tap to another by using an arcing switch, tap-selector and change-over selector.

A.1.1 Selector switch type OLTC

The selector switch type OLTC as depicted in Figure A.1 consists of a selector switch on top of the coarse change-over selector. The selector switch is accessible at the top of the transformer, while the coarse change-over selector is mounted deeper within the transformer tank, underneath the selector switch. The selector switch and the coarse change-over selector both consist of a stator on which the static contacts are mounted. These contacts are connected to the taps on the transformer windings, shown in Figure A.1. The rotor is inside the stator and rotates using a drive system. The rotor makes a connection between the stator contacts. The OLTC has now selected the main winding on tap A8. The current is brought to the selector switch stator by the rotor of the coarse change-over selector (using contact A in Figure A.1). The selector switch has selected three fine tap windings using tap A3. The current leaves the tap changer using a slip ring.

Selector switch cycle

A selector switch cycle is passed through when a fine tap winding is (de-)selected. This cycle is built up from a few small steps, shown in Figure A.2. The rotor of the selector switch consists of four sets of roller contacts (Figure A.3) for each phase: the main roller contact, two transition contacts which are in series with a low ohmic transition resistor and a set of roller contacts which connects to a slip ring. The roller contacts of the arcing switch are made from tungsten to prevent extreme wear due to arcing. The stator contacts are also equipped with tungsten edges. These tungsten contacts are called arcing contacts.

When the selector switch moves from contact block A3 to A4, the first transition contact takes over the load current. The main roller contact will leave contact block A3 (Figure A.2-2). When the rotor moves a little further, the second transition roller contact will reach tap A4 (Figure A.2-3). The load current now flows through both transition resistors. The transition resistors are necessary to prevent the short circuit of adjacent fine tapped windings and to provide a non-interrupted current path for the load current during the switching operation. The resulting circulating current is determined by the step voltage and the resistance of the selector switch.

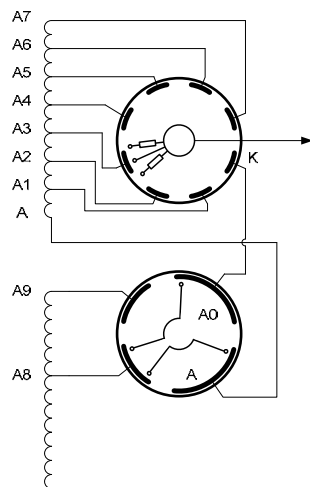


Figure A.1 One phase of a selector switch type OLTC with coarse change-over selector.

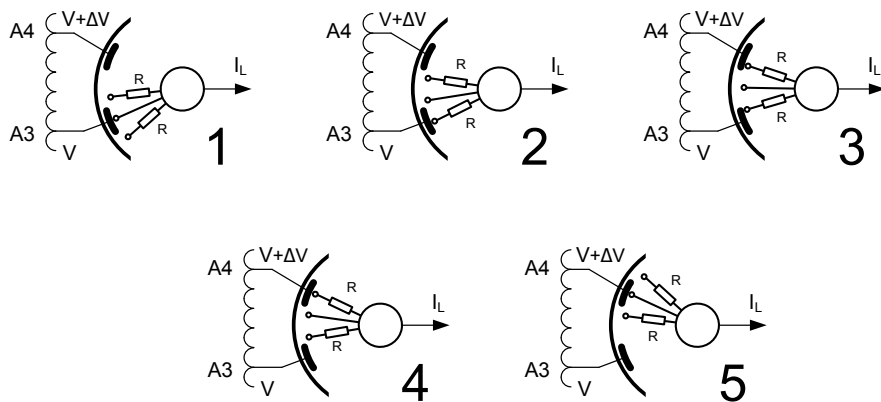


Figure A.2 A selector switch cycle. Normally the load current flows through the main contact (1). When the selector switch moves to the next tap, a transition contact takes the load for a moment (2). Then, the second roller makes contact with the next tap causing a circulating current to flow (3). The rotor moves further and the first roller leaves its contact block (4). The switch cycle is completed when the main contact once again takes over the load current (5).[98]

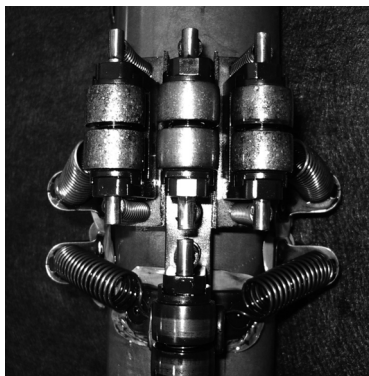


Figure A.3 Roller contacts of a selector switch rotor.

Following this, the main roller contact will move to contact block A4 (Figure A.2-4) and take over the complete load current (Figure A.2-5). The selector switch has now selected another tap and is ready for the next switching cycle. The entire selector switch movement will take about 30-200 ms.

This thesis will focus on a diagnostic method which assesses the timing of this selector switch cycle. The corresponding vector diagram of this tap change operation can be represented as in Figure A.4, with the output voltage and the load current

that flows through the tap changer being depicted. In general the current $I_L \angle \varphi$ will lag the voltage. The OLTC switches the output voltage from V to $V + \Delta V$ using the five steps from Figure A.2. The output voltage drops because of the voltage over the transition resistor. The output vector follows the shape of a flag when switching from step 1 through to 5, which is why this tap change operation is called a flag-cycle operation. All OLTCs that transfer the load current from the main contacts before creating a circulating current show this vector diagram.

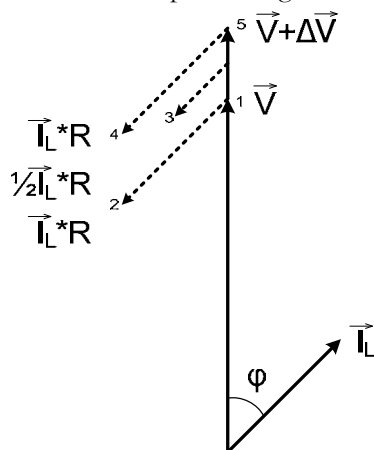


Figure A.4 Vector diagram of a selector switch type OLTC (flag-cycle operation).

Coarse change-over selection

To lower the secondary voltage, the selector switch can select more fine tap windings on the primary side by switching from A1 to A7 (as described in Section A.1.1). When all of the fine tap windings are selected by the selector switch (see Figure A.5A), a coarse tap winding has to be selected before the selector switch can continue. The coarse change-over selector shown at the bottom of Figure A.1 makes a turn for that purpose. The steps of the coarse change-over selector movement are depicted in Figure A.5.

Firstly, one contact of the coarse change-over selector moves to tap A9 (Figure A.5B). Note that the roller contact switches no current because the load current flows through contact A. The voltage on the k-contact is increased with 1 coarse voltage step which is equal to 8 fine voltage steps. The position of the change-over selector in Figure A.5B is called the mid-position. The two contact sets of the change-over selector are on different coarse tap contacts.

Secondly, the selector switch now switches to the k-contact (Figure A.5C). As a result, the selector switch experiences only one voltage step difference. The k-contact of the selector switch is connected directly to the coarse change-over selector. When the selector switch is at the k-contact, the load current flows through coarse change-over selector contact A0. The roller contact which normally carries the load current is now free to move. This tap is called the parking position.

Finally, the second roller contact of the change-over selector is moved to tap A9 (Figure A.5D). As a result, the first roller contact moves over contact A9 while carrying current. After switching the coarse change-over selector, the selector switch is ready to make another rotation.

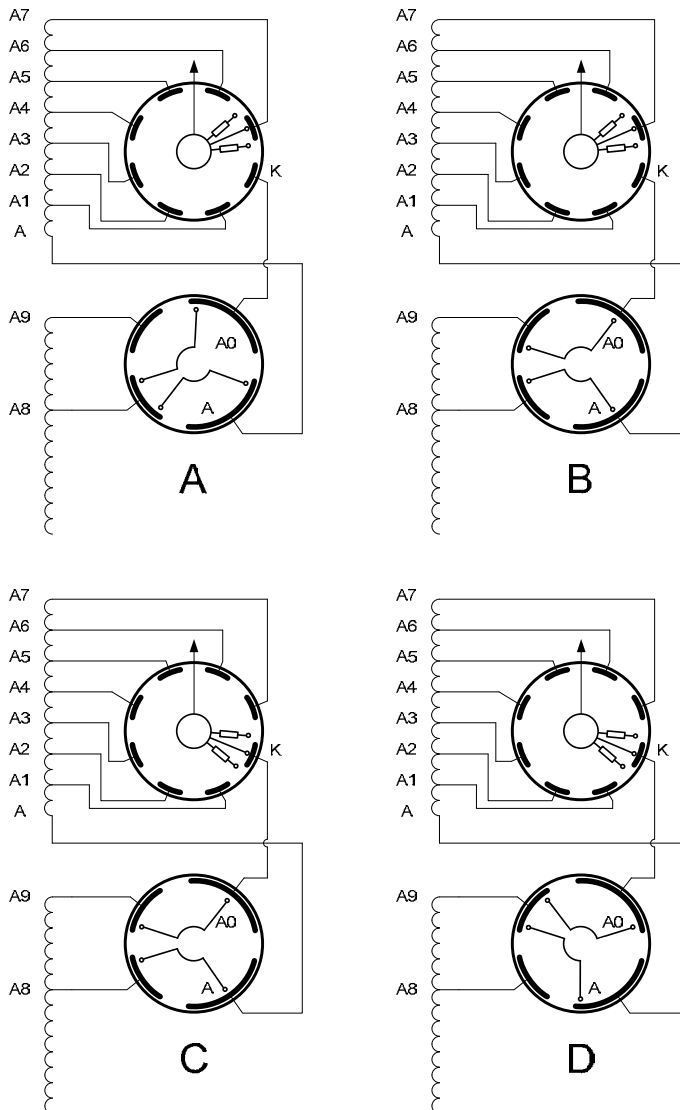


Figure A.5 Switching the coarse change-over selector of a selector switch type OLTC.

A.1.2 Diverter switch type tap changer

A diverter switch type OLTC combines a diverter switch and a tap selector. The tap selector has two sets of contacts available for tap selection. One of the two contacts is selected by the diverter switch and is under load. The other contact selects the next tap (pre-selected tap) without switching current. The diverter switch then switches from the selected to the pre-selected tap. Figure A.6 shows a schematic overview of a tap selector and a diverter switch. The tap selector can be combined with a change-over selector to expand the range of the OLTC. Again, the change-over selector can be designed as a coarse change-over selector (Figure A.7) or a reversing change-over selector (Figure A.8). By switching the reversing change-over selector one can add or subtract the selected transformer windings, thus doubling its range. A coarse change-over selector can add a larger winding to the main winding, in this way changing the voltage of all tap selector contacts.

Diverter switch type OLTCs can also use transition resistors to limit the circulating current in the diverter switch. Over a short period, both taps of a different voltage are connected to the same output, causing a circulating current, as is the case with the selector switch type tap changer. The flag-cycle vector diagram of Figure A.4 also applies to this diverter switch type OLTC.

In contrast to the selector switch type tap changer, most diverter switch type OLTCs have no rotor inside the arcing switch. A stationary insert is used instead. The diverter switch can easily be maintained by removing the diverter switch insert. The dirty oil can be replaced, the diverter switch inspected and its arcing contacts replaced.

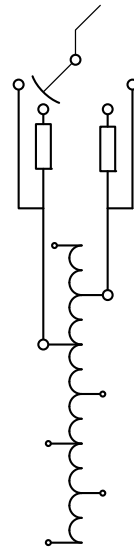


Figure A.6
Diverter switch
with transition
resistors (top) and
a tap selector
(bottom).

A.2 Degradation mechanisms

This section elaborates on OLTC degradation, as introduced in Chapter 2. Mechanical defects and contact degradation on all OLTC contacts show to be especially important and it is discussed in this section that maintenance errors also contribute to a significant part of OLTC failure. Degradation can lead to failure, a situation in which the OLTC cannot perform its primary task, i.e., to select another tap without interrupting the load current.

Degradation and failure modes can be evaluated using a failure mode, effects, and criticality analysis (FMECA). An example of such a FMECA, which is used at a utility, is shown in Figure A.9. A score is assigned to each OLTC failure mode, based on the pre-failure detection chance and the risk. The risk is calculated by multiplying the failure chance and the consequence (which includes the repair time,

repair costs, safety and environmental factors). Using a FMECA, utilities can direct their maintenance expenditure to prevent OLTC failure. In this example, a broken OLTC drive shaft, contact coking by the long term effect and electrical treeing show to be most important, this section discusses these failure modes.

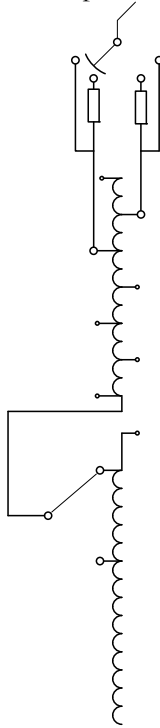


Figure A.7 Diverter switch type OLTC with coarse change-over selector.

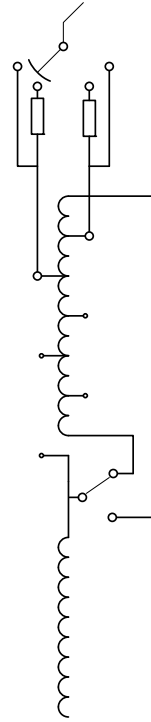


Figure A.8 Diverter switch type OLTC with reversing change-over selector.

A.2.1 Electrical treeing

In-tank tap changers are insulated from the ground by an insulating support cylinder. The high electric field strength that is present over the cylinder can cause partial discharges over the surface of the cylinder. Electrical trees (tracking) can be the result. Electrical treeing is a slow process of creeping surface discharges along the cylinder [99], creating a track that cannot be repaired. These tracks grow slowly, weaken the insulating properties and can cause flashover. Tap changers installed in wye-connected windings can be located at the neutral point and are able to insulate only a part of the line-to-neutral voltage. Tap changers installed in delta-connected windings have to cope with higher electrical stress, for they have to insulate the line-to-line voltage. Tap changers that are installed in delta-connected windings are therefore more prone to electrical treeing than tap changers located at the neutral point of the transformer [100].

System	Sub-system	Part	Sort of failure	Cause of failure	Possible consequences of failure	Detection possibility	A Repair time	B Corrective costs	C Safety	D Environment	E=A+B+C+D	F Failure chance	G=E*F Risk	H Detection chance	H*G Total score
OLTC	Primary	Arching contacts	Low contact pressure	Contact wear	Open contact, transformer de-energised by pressure/flow relay	Visual inspection	1	1	1	1	4	4	16	1	16
OLTC		Change-over selector / tap-selector	Contact interruption	Contact degradation (long term effect)	Catastrophic failure of transformer	Dynamic resistance measurement	5	5	3	2	15	3	45	3	135
OLTC		Transition resistors	Interrupted	Low switch speed, blocked half-way	Transformer de-energised by pressure/flow relay	None	3	3	1	1	8	2	16	5	80
OLTC		Stator	Phase-to-phase fault	Electrical treeing	Catastrophic failure of transformer	Visual inspection	5	5	3	2	15	3	45	1	45
OLTC		Rotor (inside)	Phase-to-phase fault	Electrical treeing	Catastrophic failure of transformer	Visual inspection	5	5	3	2	15	3	45	1	45
OLTC	Dielectric	Rotor (outside)	Phase-to-phase fault	Electrical treeing	Catastrophic failure of transformer	Visual inspection	5	5	3	2	15	3	45	3	135
OLTC		Insulation oil	Contamination	Switching arcs	Accelerated wear and carbon deposition on insulation	Visual inspection	1	1	1	1	4	4	16	1	16
OLTC		Drive axis arcing switch	Rupture	Mechanical load/fatigue	Catastrophic failure of transformer	None	5	5	3	2	15	2	30	5	150
OLTC	Mechanical	Mounting of contacts	Loose	Mechanical load/fatigue	Blocked arcing switch, transformer de-energised by pressure/flow relay	Visual inspection	3	3	1	1	8	2	16	3	48
Drive		Springs	Low switch speed	Weakening / Broken	Failure of transformer	Dynamic resistance measurement	1	1	1	1	4	2	8	1	8
Drive		Brake	Blocked	Broken	Tap change not finished	None	2	1	1	1	5	2	10	5	50
Drive		Drive axis	Leakage	Low seal quality	Accelerated wear due to mechanical oscillation	Visual inspection	1	2	1	3	7	3	21	3	63
Drive		Gear (perpendicular)	No tap change possible	Wear	Too high or too low voltage	None	2	1	1	1	5	2	10	5	50
Drive		Motor	Defective	Wear / aging	No tap change possible	Visual inspection	2	1	1	1	5	2	10	3	30
Protection	Protection	Flow/pressure relay arcing switch	No or limited functioning	Defective	Transformer de-energised by Buchholz protection, heavy damage when the arcing switch fails	Functional check	5	5	3	3	16	2	32	3	96
Protection		Flow/pressure relay arcing switch	Too sensitive	Settings out of range	Unnecessary de-energised transformer	Functional check	1	1	1	1	4	2	8	3	24
Protection		Pressure relay change-over selector	No or limited functioning	Defective	Transformer de-energised by Buchholz protection, heavy damage when the change-over selector fails	Functional check	5	5	3	3	16	2	32	3	96

Figure A.9 Example of an OLTC Failure Mode, Effects, and Criticality Analysis (FMECA).

A.2.2 Contact degradation

Chapter 2 already discussed that the arcing switch and the change-over selector wear differently, because the operation frequency and the amplitude of the current that is switched are different. Normally, an OLTC that is installed in a power transformer in the utility grid will switch a few times a day to compensate for voltage changes in the network. Therefore, the OLTC will stay in one position for several hours and usually only a limited number of tap positions are used. In cases where this limited number of tap positions involves the operation of the change-over selector, the latter may be used every day. However, the change-over selector is not necessarily used on a daily basis and can be motionless for extremely long periods.

Change-over selector contact degradation

Change-over selector contacts (including tap selector contacts) do not wear as fast as arcing switch contacts that wear due to the switching of load currents. These contacts will not switch significant currents, but can show pitting of the contacts and the development of pyrolytic carbon [18-19]. This contact degradation is not due to the arcs caused by switching the current but is caused by two other degradation mechanisms.

Floating windings

The first cause of change-over selector contact degradation discussed here is the small capacitive current that is switched off when the change-over selector operates. The fine tapped windings are temporarily disconnected from the main windings when the tap changer is on the k-contact [15]. Figure A.10 shows this situation for a selector switch type tap changer with a coarse change-over selector. The floating windings take a potential based on the capacitive coupling between the transformer windings and earth [71]. A small capacitive current in the order of tens of milliamps is switched at a recovery voltage of tens of kilovolts [15]. The change-over selector contacts can be slightly damaged by the discharges that occur.

Long-term effect

The long-term effect can be initiated on infrequently operated OLTC contacts. Three basic stages of the long-term effect can be distinguished and are shown in Figure A.11. Section 2.3 already elaborated on this long term aging effect.

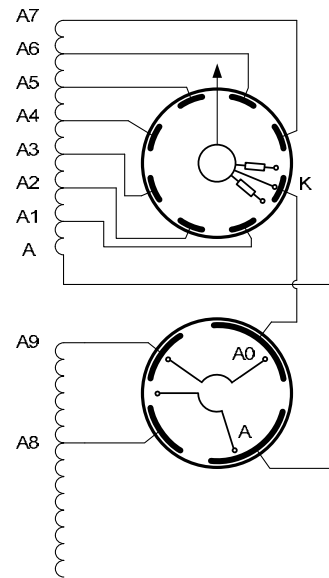


Figure A.10 Floating fine tapped windings (A-A7) in a selector switch type OLTC.

The long-term effect starts with the formation of a thin layer of oil deposited on the contacts [20][24], which reduces conductivity.

Literature describes experiments [18][27] showing that the surface film grows thicker as the contacts age and that the growth rate of this layer is strongly dependent on the surface temperature of the contacts. It can be described as:

$$s = k_0 * \theta_0^{3.862} * t^{0.3559} \quad A-1$$

where s is the thickness in Å of the film layer on copper contacts under Shell Diala insulation oil, θ_0 the surface temperature in °C at which the surface film grows, t the duration of the aging test in hours and $k_0 = 1.883 \cdot 10^{-6}$ with an appropriate unit to balance the equation.

The surface film can be reduced by switching the tap changer through all its tap positions. By doing so, the film layer is partially wiped off and the long-term effect is slowed.



Figure A.11 *The long-term effect starts with the formation of a surface film on the contacts. The increased resistance can cause coking. Thermal runaway can finally cause failure of the OLTC due to open contacts.*

Contact resistance and power losses on the contact increase as a result of the surface film. At this early stage of the long-term effect, the surface film can be wiped away by switching the OLTC through its cycle of operation: the structure of the contact contamination is changed due to the moving contacts [20][34-35].

Due to the temperature dependence of the surface film growth rate, the long-term effect accelerates. The insulation oil dissociates because of discharges and the high contact temperatures. This is the advanced stage of the long-term aging effect. Decomposed transformer insulation oil results in carbon between the contacts (Figure A.11B, [20][37]). This formation of pyrolytic carbon is called coking [19]. Oil cracking occurs at local temperatures over 300 °C [20]. In addition to coking, the contact material wears off locally and pitted spots become visible on the contacts. The contacts are now damaged and cannot be repaired by switching the OLTC through all its tap positions. An overhaul is needed to undo the pitting of the contacts. Because of the infrequent movement of the change-over selector, coking can occur on all stator contacts, rotor contacts and other movable parts that carry the load current.

The coking accelerates due to increased contact resistance and the thermal resistance characteristics of the carbon [9]. Coking between moving parts of the contacts and around the springs that provide the contact pressure can cause the contacts to lose pressure. Finally, a considerable amount of contact material vanishes and excessive arcing activates the tap changer protection mechanisms. Figure A.12 shows an example of change-over selector stator roller contacts damaged in the advanced stage of the long-term effect.

The long-term effect is accelerated by [24]:

- Infrequent movement
 - The surface film is not wiped off the contacts when the change-over selector is not operated.
- High temperatures
 - The formation of the surface film is highly temperature dependent.
- High load
 - Power losses on the contact interface increase exponentially with the load current and heat the contacts.
- Low contact pressure
 - Coking and pitting of the contacts will cause jammed contact more easily when the contact pressure is low. The layer of contamination on the contact surface is also more easily damaged at high contact pressure.
- Copper or brass contacts
 - The growth rate of the surface film is higher on copper and brass contacts compared to silver contacts [24]. Pitting and coking is reduced by silver-coating of the contact surface; however, older OLTC designs may use bare copper contacts.



Figure A.12 Change-over selector stator roller contacts are damaged in the advanced stage of the long-term effect.

Three examples of failed OLTCs due to the long-term effect are discussed below. Damaged contacts can be compared with contacts from another phase of the OLTC, because it can be assumed that they are used and loaded equally but have worn differently (one set of contacts failed in the following examples).

Example 1

One of the results of the long-term aging effect is that the spring system loses resilience. The roller contacts may remain pressed in, see Figure A.13. This breaks the contact and results in an electrical arc. Inspection of the change-over selector during several OLTC overhauls shows that the sliders (and holders) and the stationary contacts are both degraded.

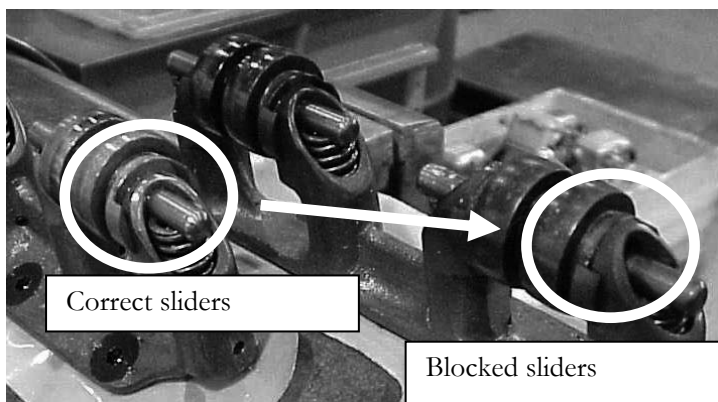


Figure A.13 Example of sliders which are blocked. Normally, the sliders reach beyond the holders, as can be seen left (correct sliders). At blocked sliders (right), the sliders and holders are at the same position. Contact pressure is threatened.

Example 2

Figure A.14 shows an example of a change-over selector contact with pitting and carbon due to the long-term effect. The contact shown on the right already exhibits the effect of extreme arcing. The left contact is from another phase and represents the condition of the contact just before arcing occurred. In this case the Buchholz protection relay detected the development of gas, the transformer was switched off and further damage was prevented.

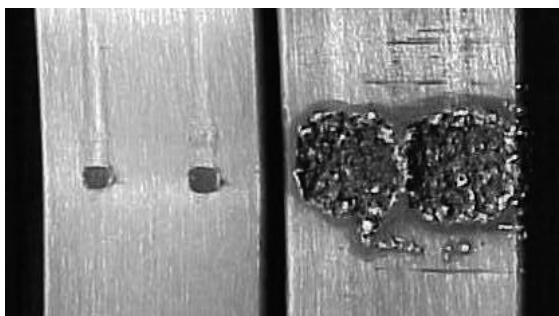


Figure A.14 Change-over selector stator contact blocks before and after failure. Gas development due to arcing was detected by the Buchholz protection relay and the transformer was switched off.

Example 3

When the Buchholz protection relay does not detect gas development from the change-over selector in time, flashover occurs and the transformer can be switched off by the Buchholz or the differential protection mechanism. Figure A.15 shows an example of a change-over selector after a flashover. Again, a contact from an undamaged phase was taken as a reference and is shown on the left. The long-term effect which caused this failure, was diagnosed using dynamic resistance

measurements (pre-failure), and displayed considerable current interruptions. The decision rules found in Chapter 8 will diagnose these last two examples as critical.

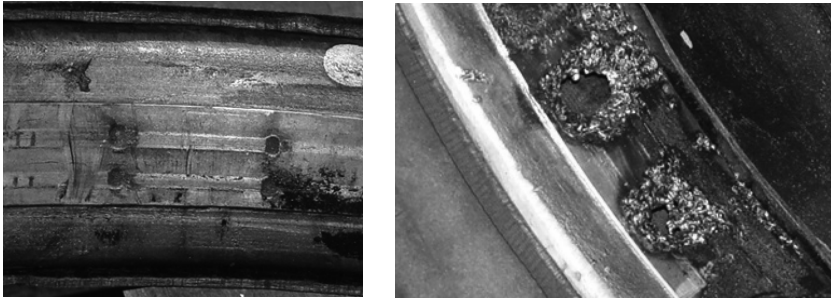


Figure A.15 Example of stator contact blocks before (left) and after (right) flashover. The transformer was switched off by the differential protection and the Buchholz protection relay.

Arcing switch contact degradation

Basically, the arcing switch has two different modes of contact degradation. Contacts that switch the current can wear due to arcing, while contacts that never switch current are liable to the long-term effect.

The circulating current can increase or reduce the current that is interrupted by the arcing switch contacts depending on the direction of operation. This results in different wear of the arcing contacts on both sides of the main contacts, but this effect is largely compensated for by the bidirectional movement of the tap changer rotor.

Before the current is switched to another winding tap, it is transferred from the main contacts to the transition contacts that switch off the current. Both the main contacts and the transition contacts will be pitted due to arcing. The arc is normally quenched at the first zero current.

The arcing switch contacts are normally roller contacts or contact blocks. The tungsten arcing roller contacts and accompanying stator contacts normally do not show carbon on the contacts due to coking.

The long-term effect is also active at the arcing switch, especially on contacts that carry the load current and that are not subject to arcing or wiping. The long-term effect at the arcing switch does not develop as fast as the long-term effect at the change-over selector because of the more frequent movement of the arcing switch contacts.

A.2.3 Mechanical degradation and failure

In addition to the electrical contacts of the tap changer, the mechanical components of an OLTC are also liable to wear and are responsible for a substantial number of OLTC failures [13]. Some frequently reported mechanical problems are:

- Loss of synchronism between the arcing switch and the change-over selector due to a broken or damaged shaft, see Figure A.16.
- Operating too slowly or stopping when the main contacts are not on a contact block, resulting in damage to the transition resistors.
- Leakage of the arcing switch oil onto the change-over selector and into the transformer tank.
- Insufficient contact pressure due to broken or damaged springs or due to excessive carbon build-up between the sliders.
- Defective braking mechanism of the Geneva wheel or a broken lock system.
- Too much play or broken components in the drive mechanism due to wear and vibrations.
- The spring energy accumulator may lose its elasticity.



Figure A.16 Broken drive shaft of the selector switch.

A.2.4 Maintenance-induced failures

Finally, another cause of OLTC failures can occur during normal maintenance. The arcing switch compartment is opened, cleaned and provided with new insulation oil. Incorrect maintenance is a key contributor to OLTC failure [13] due to the mechanical complexity of the tap changer and the stringent requirements that have to be met during and after maintenance. Several failure studies [13][52][101] conclude that maintenance and reassembly-induced failures can certainly not be overlooked. Figure A.17 shows an example of a study of the causes of OLTC failures, where 33% of the failures are related to incorrect or inadequate maintenance or reassembly. Therefore, diagnostic measurements that check the quality of maintenance could significantly reduce OLTC failure [13].

A.3 On-load tap changer protection

When the OLTC fails, for instance due to a defect in the drive mechanism or through the long-term effect, protective relays can switch off the transformer to prevent damage. In addition to local damage to the OLTC, an OLTC failure can also cause damage to the associated transformer. This section discusses protective devices that are used to detect OLTC defects and limit the consequences of OLTC failure.

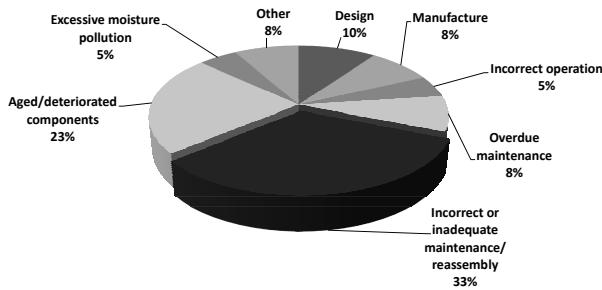


Figure A.17 Poor maintenance and reassembly are responsible for a considerable number of OLTC failures [13].

When a failure occurs within the arcing switch compartment, gas can be generated by an electrical arc. Due to this gas, a flow is generated in the oil pipe connecting the tap changer to the conservator (see Figure A.18). To deal with this, a flow relay is mounted in the oil pipe to protect the arcing switch compartment. The change-over selector and, when present, also the tap selector, is indirectly protected by the Buchholz relay of the transformer main tank, in the case of the change-over selector sharing its oil with the transformer tank (see Figure A.19). This configuration is called a two-compartment system. In a three-compartment

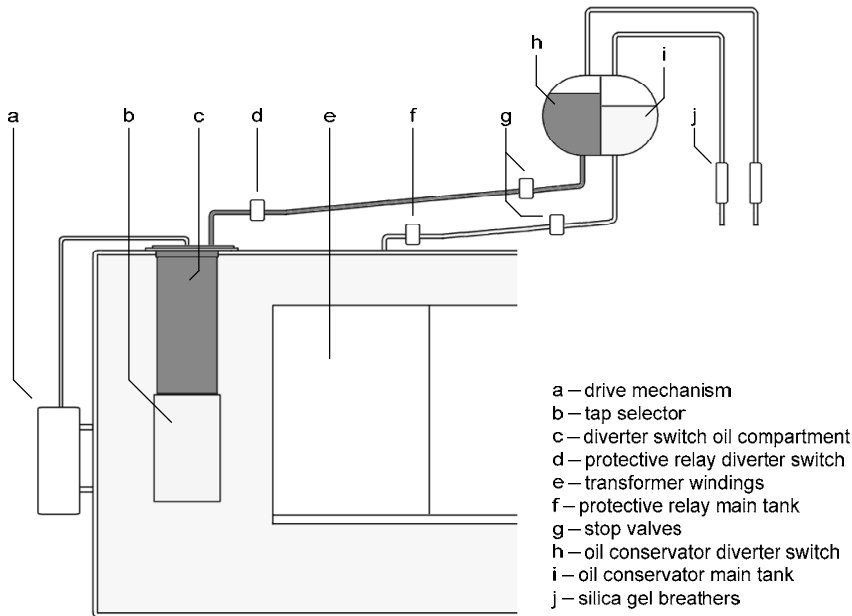


Figure A.18 The oil of the arcing switch (in this case a diverter switch) is separated from the main tank. Flow relay 'd' protects the diverter switch compartment. The change-over selector shares its oil with the main tank (two-compartment configuration), thus Buchholz relay 'f' also protects the change-over selector.

configuration, the change-over selector also has a separate oil tank. In this case, the change-over selector can be protected by a separate protective relay, as is the arcing switch (see Figure A.19).

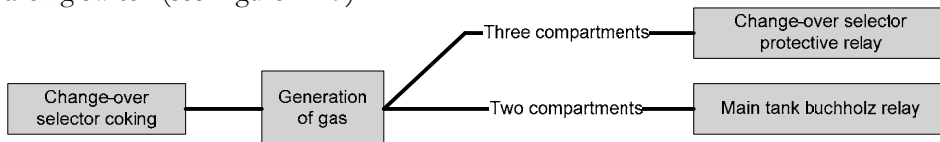


Figure A.19 Defects in the change-over selector can lead to the generation of gas, which can be detected by a protective relay. The change-over selector can have its own relay (three-compartment configuration) or share with the main tank (two-compartment configuration).

As discussed earlier, the mechanical drive system of the OLTC is also a significant source of tap changer failures. To detect problems in moving the rotor (Figure A.20), the OLTC can be protected with a switching-time control relay (tap change incomplete protection). If the switching procedure takes too long, the switching-time control relay will switch off the transformer to prevent arcing inside the OLTC or burnout from the transition resistors. For this purpose, a contactor for switching-time control is mounted inside the drive mechanism to detect the switching (also called the tap change in progress or tap change incomplete contactor). This contactor activates the switching-time control relay. This relay will operate the power switch and turn off the transformer. In the case of arcing, the resulting oil flow can trigger a flow relay.

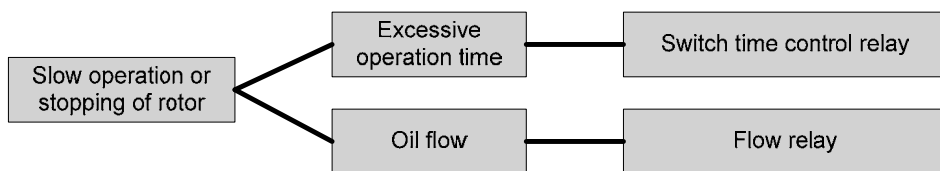


Figure A.20 Defects in the OLTC drive can cause slow operation or stop the operation of the contacts. The switch-time protective relay can detect excessive operation times. Oil flow due to heated insulation oil or short circuits can trigger a flow relay.

Other OLTC protection mechanisms are also used to protect against failure, for instance systems that block the drive mechanism in the case of excessive load currents, out-of-step protection in the case of parallel transformers being in a different tap position, protection against an undesirable oil level, running-through protection, limit switches to detect the end of the cycle of operation or switches that block the drive motor when the OLTC is operated manually.

In addition, transformer protection relays can also detect OLTC failures, as can a differential protection relay or an over current relay. Figure A.21 shows examples that can cause failure of the arcing switch and trigger protection through an oil flow or short circuit current.

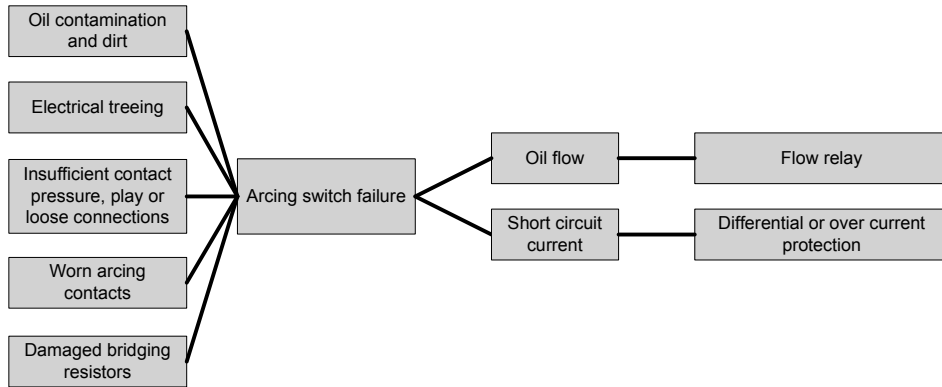


Figure A.21 Examples that can lead to failure of the arcing switch. A resulting oil flow can trigger the flow relay or a short circuit current can be detected by transformer differential protection or over current protection.

The protective devices described above cannot guarantee the prevention of heavy damage to the tap changer or pollution and damage to the adjacent transformer windings in the case of a failure. Transformer protection mechanisms are used to switch off the transformer in the case of failure, but pre-failure detection of OLTC degradation can be useful in the prevention of damage. An example of damaged transformer windings caused by an OLTC defect is shown in Figure A.22. In this particular case, the OLTC switch operation was not completed due to a mechanical failure, causing the transition resistors to heat the surrounding insulation oil. A short circuit finally triggered the protective devices, but the transformer was destroyed. Pre-failure detection of OLTC degradation using diagnostic measurements could thus be useful here.

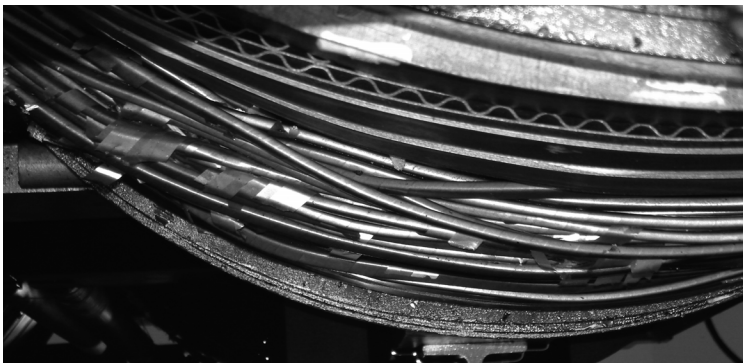


Figure A.22 Example of transformer windings that are destroyed due to OLTC failure, showing that protective mechanisms do not always react quickly enough to prevent transformer damage.

Appendix B

Indirect measurement of the OLTC dynamic resistance

This appendix deals with the measurement of the voltage on the secondary side of the transformer when the OLTC switches a DC current. In this way, the OLTC resistance is measured indirectly.

B.1 Introduction

The resistance of an OLTC changes abruptly when the transition resistors are switched in the circuit. Results of a dynamic resistance measurement should show this change in resistance directly. However, Figure 6.5 showed that the inductance of the transformer windings prevents rapid changes in the current. The result is that the dynamic resistance graphs also show effects of the inductance.

The first way to improve the response of the measurement current is discussed in Chapter 4.3: connecting an extra resistor in series with the OLTC. This improves the response time of the system (which is described by $\tau=L/R$). A disadvantage is that the amplitude of the signal is reduced, resulting in an insufficient degree of accuracy (as shown in Figure 4.17).

A second way to reduce the effect of the winding inductance was introduced in Section 4.1.1: the voltage over the transformer windings can change quickly when the transition resistors are switched in contradiction to the current through the windings. Measuring this voltage on the secondary side of the transformer at the moment the OLTC switches a DC current will indicate the OLTC resistance indirectly. The effect of the inductance is reduced while the signal-to-noise ratio is kept high. This allows the OLTC resistance to be analysed with a high degree of time accuracy.

B.2 Dynamic resistance measured on the secondary side

As discussed in the previous section, the advantage of performing a dynamic resistance measurement on the secondary side of the transformer is the fast response to changes in the circuit resistance. There is also a drawback of this method: a DC current through the transformer windings is dangerous when it is interrupted. There is no alternative path available for the current due to the open secondary side. An attempt to interrupt the DC current will result in a high voltage. These interruptions can be caused by defects in the OLTC or by operation errors. To prevent these situations, the OLTC should firstly be checked for open circuits before performing this measurement. This can be done by a dynamic resistance measurement with the secondary side of the transformer short circuited. Secondly, the measurement circuit should be completely discharged after the measurement. Figure B.1 shows the procedure to perform this measurement in a safe way.

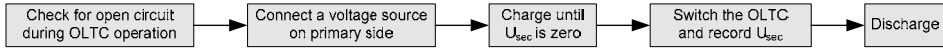


Figure B.1 Procedure for a dynamic resistance measurement with an open circuit on the secondary side of the transformer. The circuit should be checked for open contacts during OLTC operation before the measurement is performed.

A simple setup is used to measure the secondary voltage when the OLTC is in operation (Figure B.2). A measurement voltage is applied to the primary side of the transformer and a current begins to flow. The voltage over the inductances will be zero during DC conditions. Therefore, no voltage is measured on the secondary side when the measurement circuit is stable. In this case the applied voltage U_{test} equals the voltage over the circuit resistance U_R .

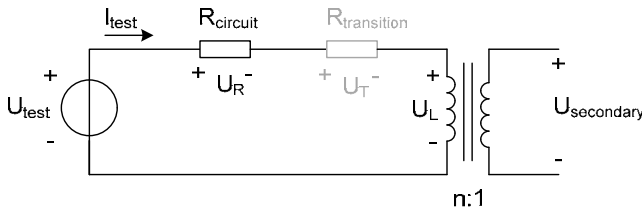


Figure B.2 Simple representation of the measurement setup for measuring the dynamic resistance of the OLTC on the secondary side of the transformer.

The transition resistor ($R_{\text{transition}}$) is added to the circuit when the OLTC is in operation. This causes a change in the voltage on the transformer inductance that can be measured on the secondary side of the transformer. Because the measurement current through the transformer windings is not able to change quickly, it can be assumed that the measurement current will not change as long as the OLTC transition time remains less than the time constant of this LR-circuit.

Therefore the voltage over R_{circuit} remains at U_{test} (and U_{test} has a fixed value). The voltage $U_T = I_{\text{test}} \cdot R_{\text{transition}}$ will appear on the primary transformer inductance (so $U_L = U_T$). This can be measured on the secondary side; however, the amplitude will be different for each tap position due to the changing transformer turn ratio.

Figure B.3 shows an example of the secondary voltage that is recorded when the OLTC on the primary side switches to another winding tap. The measurement was performed on a 50/10 kV Ynd7 power transformer equipped with an OLTC with one transition resistor of 2.4Ω (pennant-cycle operation). Figure B.3 shows the effect of this transition resistor, which is used for about 35 ms. The measurement was performed with 1 A and a series resistor of 23Ω .

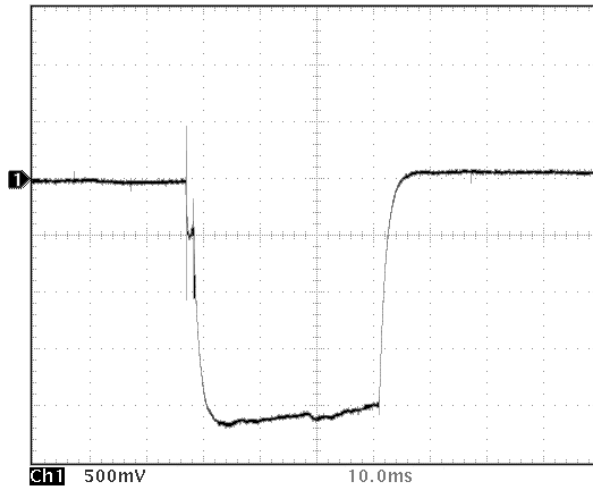


Figure B.3 Example of a secondary voltage measurement of an OLTC operation. The transition resistor is measured directly.

B.3 Effect of the circuit resistance

In the previous section it was assumed that the current through the measurement circuit will not change due to the quick OLTC transition time. In practice, the measurement current will change in reaction to the extra resistance during the OLTC operation. The voltage that is measured on the secondary side will decrease. This effect can be seen in Figure B.3 as a small decrease in the amplitude of the secondary voltage during the OLTC operation.

Changes in the primary current can be reduced by using a series resistor or by adjusting the measurement voltage during the measurement. The measurement circuit can be calibrated for each position of the OLTC by briefly adding a resistor with a known value in series with the voltage source and reading the change in the secondary voltage.

The effect of permanently adding an additional series resistor in the measurement circuit affects the time constant of the system. The time constant is

proportional to $L_{\text{total}}/R_{\text{total}}$. Figure B.4 shows an example of a secondary voltage measurement of the same tap change operation: the deepest curve was measured with a series resistor of $15\ \Omega$ and the upper curve with $23\ \Omega$. The secondary voltage returns to zero faster when the primary circuit resistance is higher. In contrast, a small circuit resistance results in a slow system, so the inductance has no chance to affect the results during the OLTC operation. This is desirable because the inductance should not be measured; only the OLTC resistance is of interest.

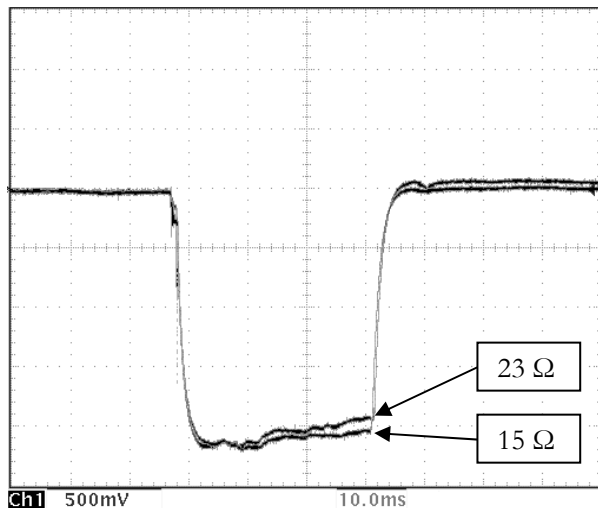


Figure B.4 Example of a secondary voltage measurement of an OLTC operation: the deepest curve is measured with a series resistor of $15\ \Omega$ and the upper curve with $23\ \Omega$.

B.4 Effect of the transformer ratio

A second variation in the secondary voltage measured is caused by the transformer ratio. The value of the transition resistor is equal for each tap position, but on the secondary side of the transformer it is measured with different amplitudes due to a different transformer ratio. The effect of the transformer ratio on the amplitude of the secondary voltage is dependent on the regulating range of the transformer and is typically around 20%. Figure B.5 gives an example of a secondary voltage measurement of an OLTC operation: three tap change operations are shown. The different transformer ratio at these tap positions caused a variation of 25% in the amplitude of the secondary voltage.

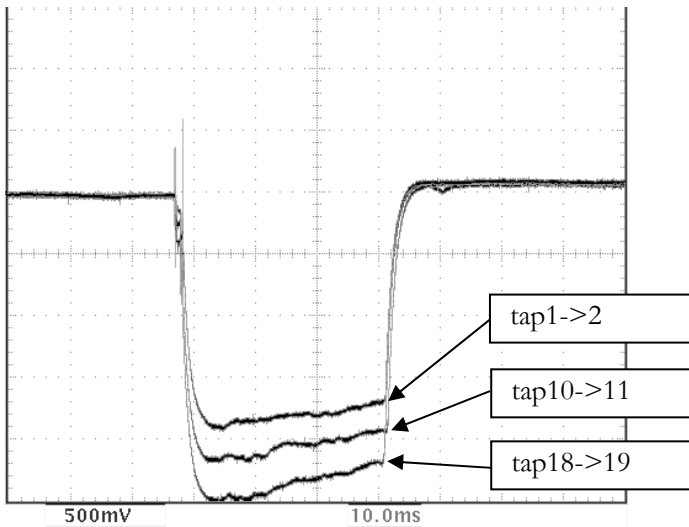


Figure B.5 Example of a secondary voltage measurement of an OLTC operation: three tap change operations are shown. The different transformer ratio caused a variation of 25% in the amplitude of the secondary voltage.

B.5 Discussion

This appendix discussed the secondary voltage at the moment the OLTC switches a DC current. An advantage of this method is the fast response to changes in the resistance on the primary side of the transformer. In this way, the effect of inductance on the measurement is minimal. A disadvantage is the danger of interrupting the DC current.

Two effects were discussed: the effect of the transformer turn ratio and the effect of the primary circuit resistance (which determines the time constant of the circuit). A high resistance is desired on the primary side to keep the changes in the measurement current low. However, a low resistance is desired to keep the LR-system slow (the time constant L/R is then large compared to the OLTC transition time).

Appendix C

Examples of static resistance measurements with increasing current on service-aged OLTC contacts

This appendix presents examples of static resistance measurements on service-aged change-over selector contacts. It is shown how degraded contacts react to different amplitudes of the measurement current. The contact resistance memory effect and the power losses on the contacts are also shown. Typical values of static resistance measured on clean and service-aged OLTC contacts are plotted as a function of measurement current intensity. It can be seen that:

- Resistance of clean silver-plated contacts is approximately constant and stays within the hundreds of micro-ohm range (see the example of Figure C.2)
- Resistance of degraded contacts measured at a low current of 2.5 A may be as high as hundreds of milliohms (see the example of Figure C.3)

The difference between the clean and degraded contacts can be readily detected when resistance is measured at a low current. However, such differences in contact resistance become smaller when the current is increased.

Measurement at a low current allows for distinguishing between the contact and winding resistance. The change of winding resistance caused by temperature variations is negligible at a low current and does not mask the contact resistance of degraded contacts.

Section 2.3.5 uses measurement results from static resistance measurements to derive a correction factor C_{DRM} to account for the effects described in this appendix.

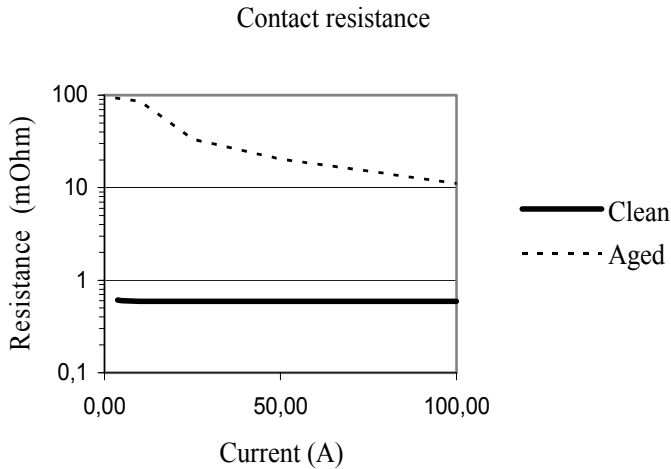


Figure C.1 Example of static resistance measurements on service-aged and silver-plated change-over selector contacts.

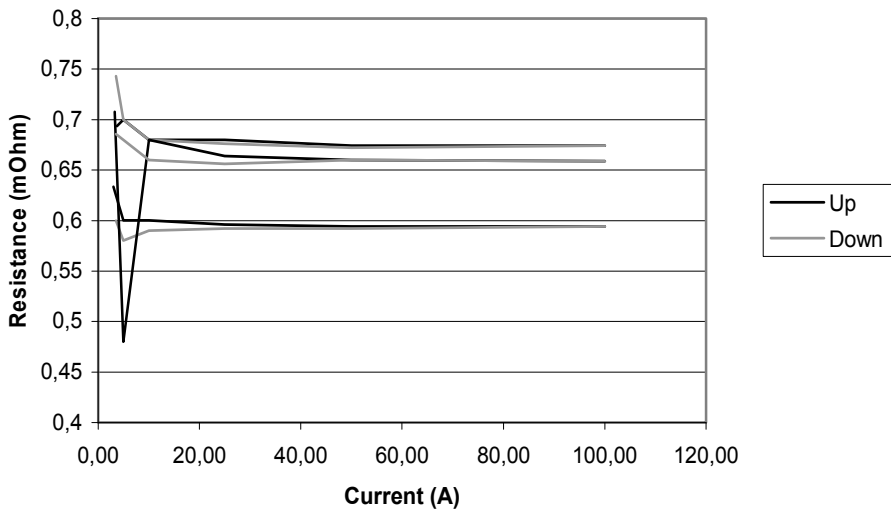


Figure C.2 Example of static resistance measurements on silver-plated change-over selector contacts. The resistance is about 600-700 $\mu\Omega$.

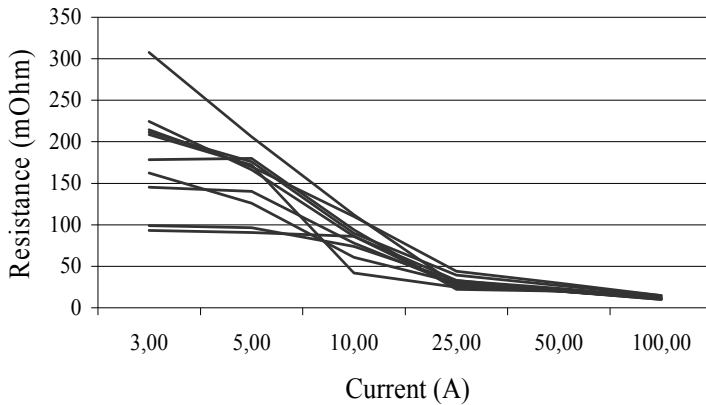


Figure C.3 Typical example of static resistance measurements on service-aged change-over selector contacts with a severe long-term aging effect. The initial resistance can be high, but decreases when the current is increased.

Similar resistance variations in degraded circuit breaker contacts measured with a current up to 2800 A were reported in [77]. Figure C.4 shows the breaker contact resistance as a function of the measurement current, Figure C.5 on its main contacts. The main circuit breaker contact resistance behaves similarly to clean OLTC contacts, while arcing contacts of a circuit breaker are comparable with OLTC contacts that suffer from the long-term effect. The current was increased to 875 A but the resistance readings remained current dependent ([77] shows that this effect is still present at 2800 A).

Resistance measurement of windings and an OLTC without movable contacts shows a very small resistance variation (in this case 0.6 m Ω) when the current is increased to 100 A (see Figure C.6). The changes in contact resistance discussed in this appendix are therefore caused by movable change-over selector contacts (the arcing switch is not measured).

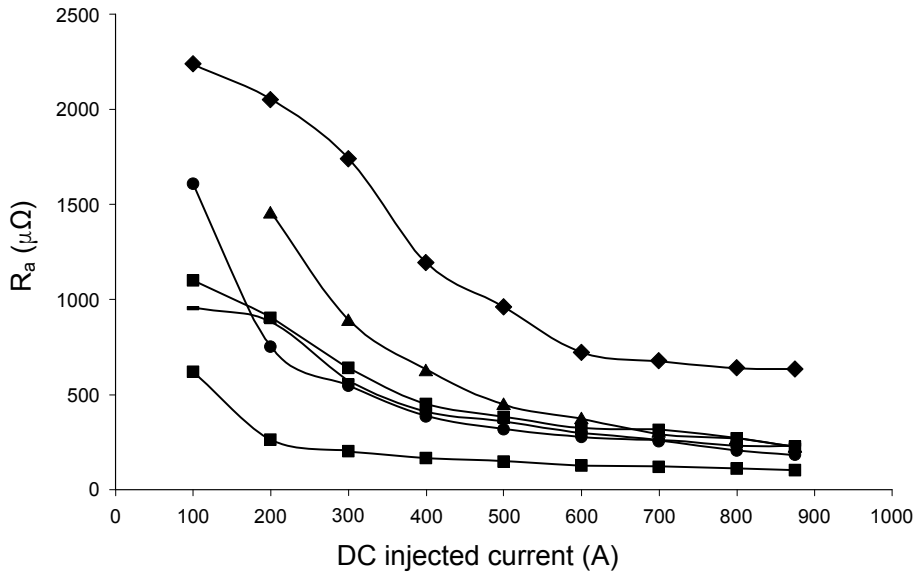


Figure C.4 Example of static resistance on circuit breaker arcing contacts, as discussed in [77].

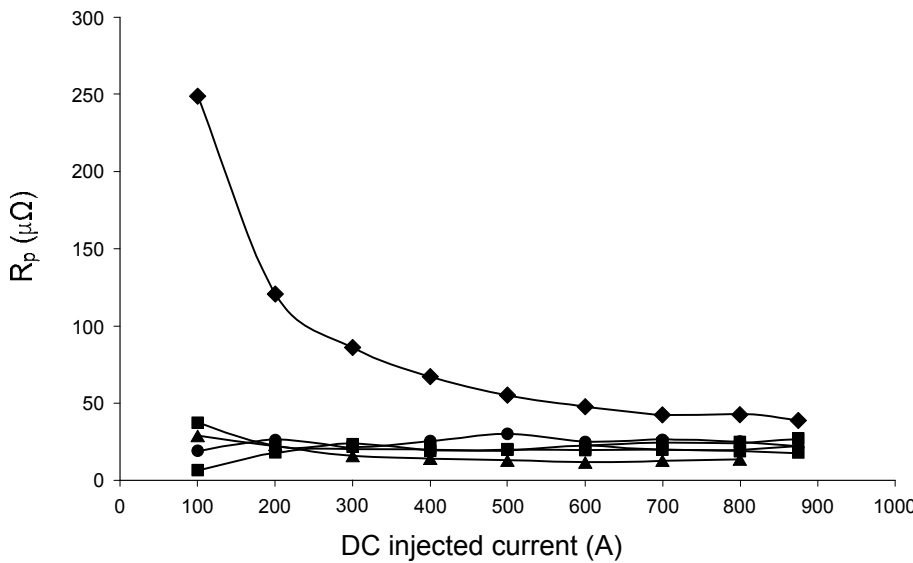


Figure C.5 Example of static resistance on circuit breaker main contacts, as discussed in [77].

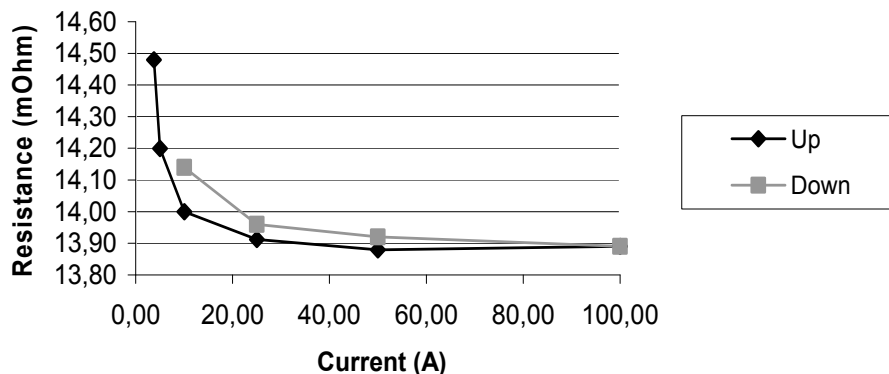


Figure C.6 Example of static resistance measurement on parts of the OLTC and tapped windings without movable contacts. The resistance only changes $0.6\text{ m}\Omega$ when the current is increased to 100 A.

Static resistance measurements on service-aged change-over selector contacts can show a memory effect. Resistance decreases when the current is increased to 100 A but remains low when the current is reduced again. A typical result is shown in Figure C.7 and an example of DRM results for all change-over selector contact positions is shown in Figure C.8.

Clean silver-plated contacts show very little memory effect, with the resistance following almost the same line when the current is increased or decreased.

Figure C.9 gives a typical example of the power loss on change-over selector contacts that suffer from the long-term effect. These losses were measured during a static resistance measurement when the current was increased to 100 A. During these measurements, the power loss on the contact can be as high as 150 W for each phase. Power losses during normal operation can be much higher, resulting in higher contact temperatures.

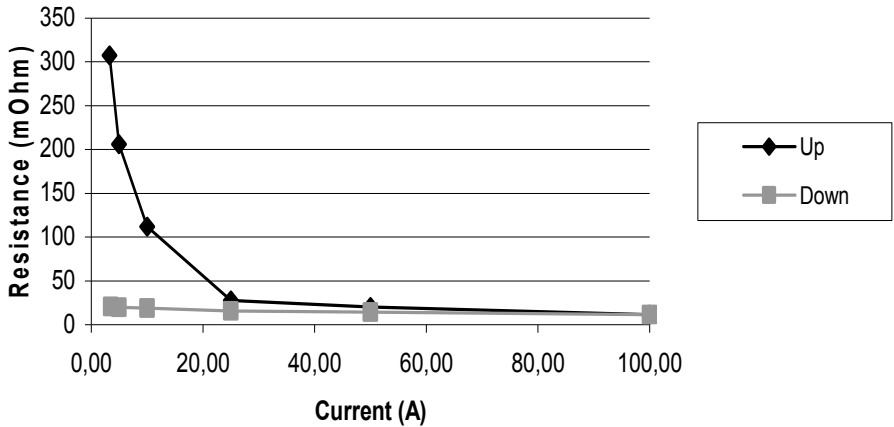


Figure C.7 Typical example of static resistance measurements on service-aged change-over selector contacts with a severe long-term aging effect. The initial resistance can be high, but decreases when the current is increased and remains low when the current is reduced.

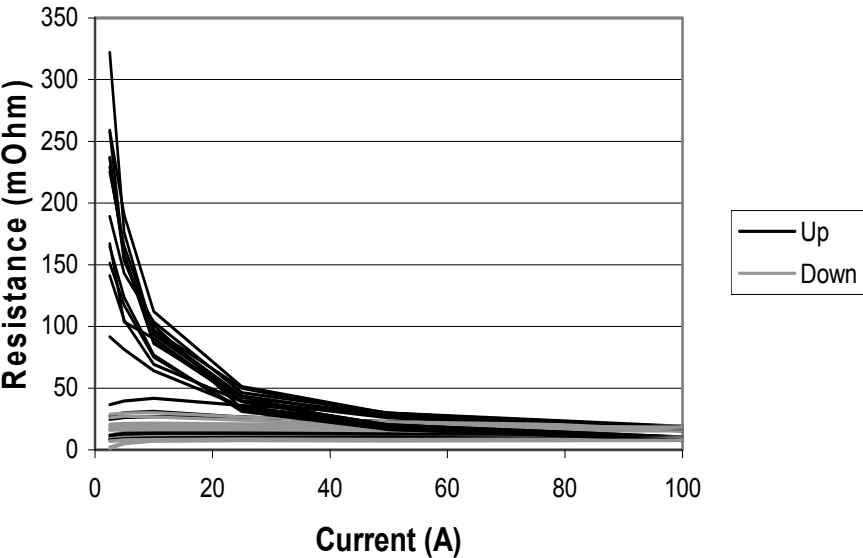


Figure C.8 Typical example of static resistance measurements on all contact positions of a service-aged change-over selector contacts with a severe long-term aging effect. The initial resistance can be high, but decreases when the current is increased and remains low when the current is reduced.

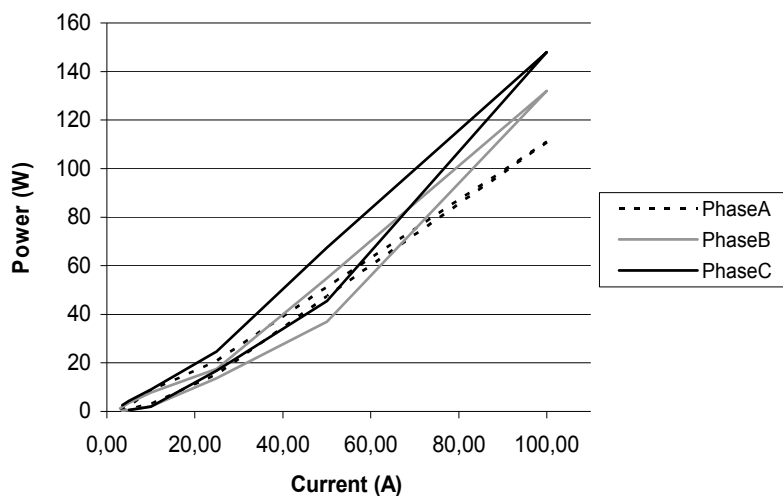


Figure C.9 Example of power loss on change-over selector contacts during static resistance measurements when the current is increased to 100 A. The contacts suffered from the long-term effect.

Appendix D

Design considerations of a transformer diagnostic system

This appendix gives a more detailed description of the transformer diagnostic system proposed in Chapter 5.

Firstly, some examples are given of a user interface that presents key aspects of the DRM results to the user. Secondly, the method used to test the transformer's winding resistance and turn ratio is briefly described. Thirdly, the hardware design of such a transformer diagnostic system is discussed in detail; and finally, ways of processing the measurement data before it is presented to the user are explained.

D.1 Examples of a DRM user interface

It was mentioned in Section 5.3.1 that DRM measurement results should be displayed in such a way that critical defects should be recognisable. An example of one simple DRM user interface for presenting relevant measurement results has already been shown in Figure 5.9. Three further examples of such user interfaces are given below.

1. Figure D.1 shows an example of an overview plot for a delta-connected OLTC with contact degradation (with the three phases measured on different time scales).
2. Figure D.2 shows the same measurement data in the form of an impedance overview plot. The voltage was held constant during the measurement so the impedance graph looks like the current graph, only upside down.
3. Figure D.3 gives an example of a user interface that shows DRM close-up plots for each OLTC operation, the timing of the excessive transition time protection and a plot of the estimated resistance for each tap position.

The transition times of each OLTC operation are shown on the right of the user interface, in the form of a Table (Figure D.1) or a graph (Figure D.2).

APPENDIX D – DESIGN CONSIDERATIONS OF A TRANSFORMER DIAGNOSTIC SYSTEM

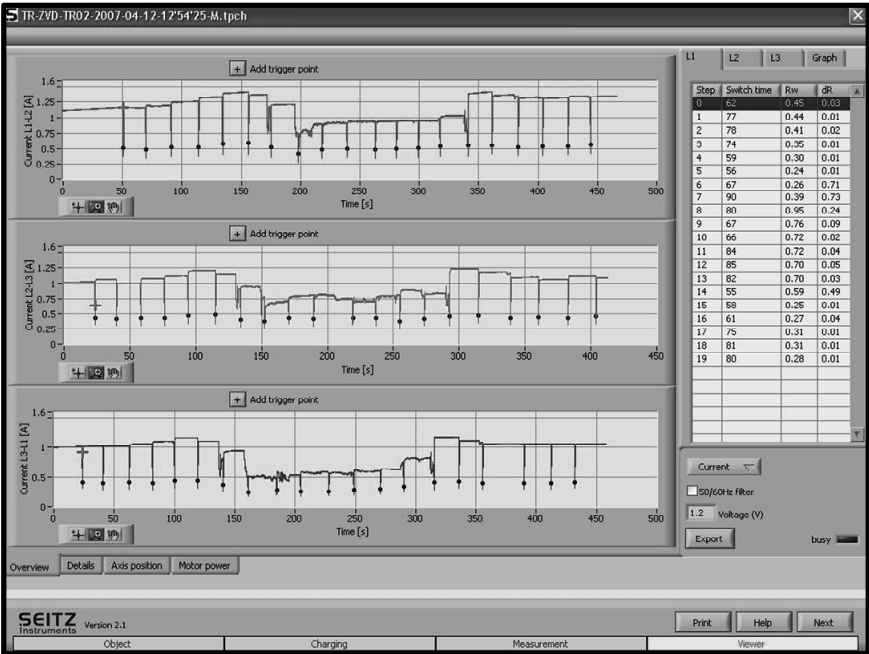


Figure D.1 DRM results for the phases of delta-connected OLTCs are recorded on a different timescale. Results can be displayed as current.

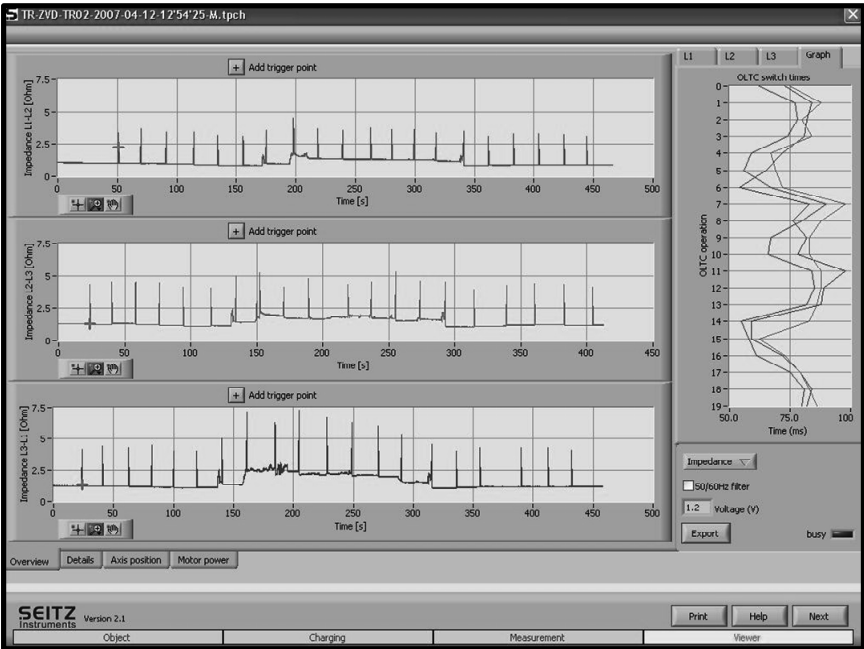


Figure D.2 Signals for mechanical diagnosis can be checked prior to the measurement to reveal erroneous connections. Motor voltage is shown in this example.

D.2 Procedure for OLTC drive system measurements

The measurement procedure for DRM has already been discussed in Chapter 5. This section deals with the mechanical diagnosis of the OLTC and OLTC drive mechanism, which depends on the diagnostic methods selected, the local situation in the substation and the transformer type used. The transformer type and implementation determine which diagnostic methods are technically possible. For example, if the drive shaft is inaccessible the angular position of the shaft cannot be measured and the OLTC drive may not be equipped with excessive OLTC switch-time protection. In general, the procedure illustrated in Figure 5.4 applies.

Firstly, the transformer is de-energised (Figure 5.4.1) and the clamps and sensors are connected to the test object (Figure 5.4.2). Secondly, a short signal check, by switching the OLTC once, can reveal erroneous connections before the measurement begins (Figure 5.4.3c). Figure D.4 shows a signal check screen for motor power signals (motor voltage is displayed), and Figure D.5 a signal check of the excessive switch-time contact voltage.

No charging or discharging is necessary when the OLTC drive system condition is assessed separately from DRM, for example in the case of a drive motor power measurement when the transformer is energised, because no DC

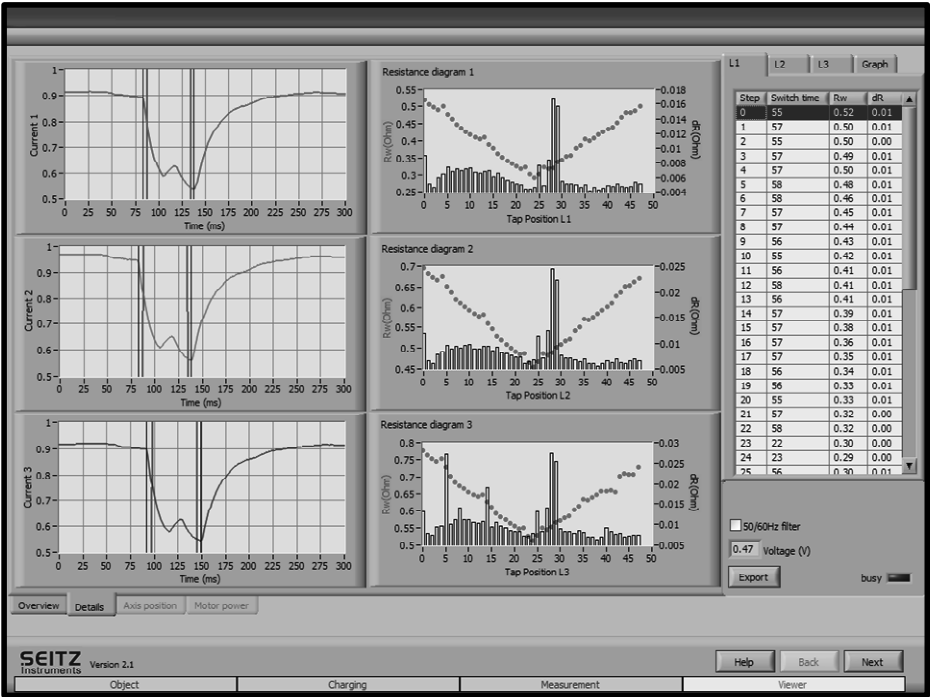


Figure D.3 Signals for mechanical diagnosis can be checked prior to the measurement to reveal erroneous connections. Excessive switch-time contact voltage is shown in this example.

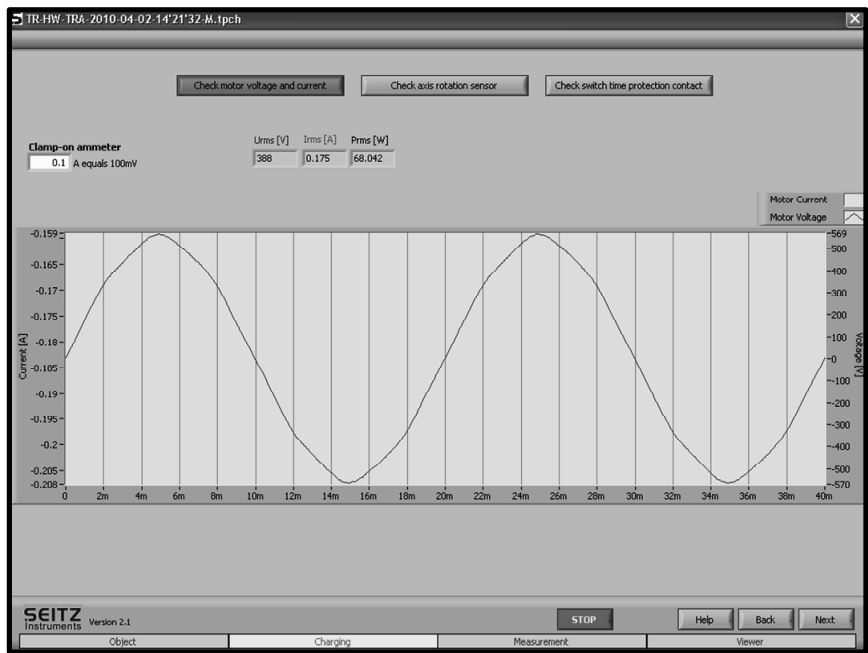


Figure D.4 Signals for mechanical diagnosis can be checked prior to the measurement to reveal erroneous connections. Motor voltage is shown in this example.

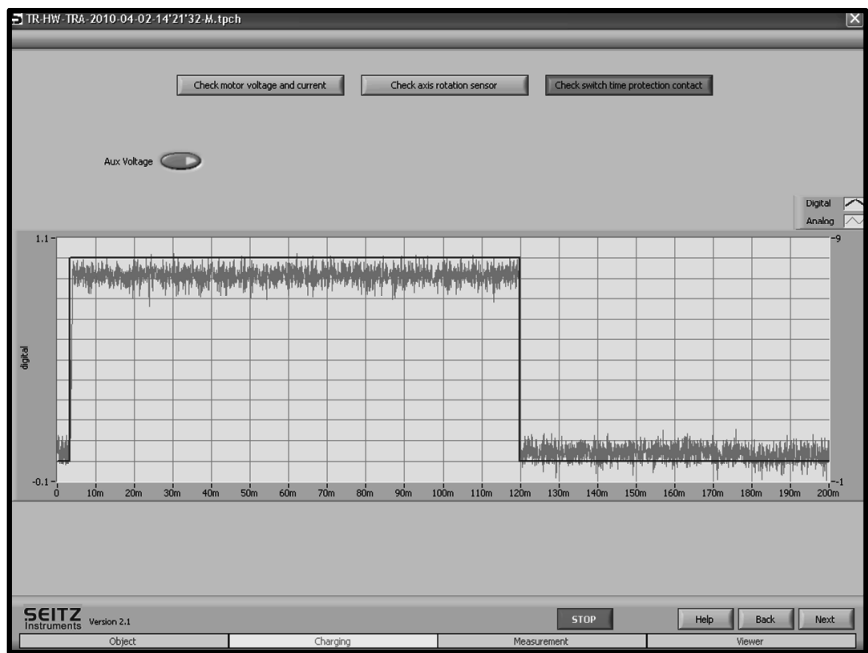


Figure D.5 Signals for mechanical diagnosis can be checked prior to the measurement to reveal erroneous connections. Excessive switch-time contact voltage is shown here.

current is applied to the transformer windings in such a case. As discussed in Section 3.2, measurements of the OLTC drive system can also be performed in combination with DRM. If all of the methods proposed in Section 5.2 are selected, simultaneously recorded signals can be related to each other on the same timescale. Although the mechanical properties of the drive system and drive shaft can be seen when one tap change operation is recorded, friction may occur at specific tap change operations. Therefore, measuring the complete cycle of operation is advisable.

D.3 Winding resistance and turn ratio measurement procedure

The procedure and transformer connection used in DRM can also be used in winding resistance measurements (as showed in Figure 5.4 and Figure 5.5). Both methods could also be combined into a single measurement. The primary and secondary transformer terminals are connected to the diagnostic system and the system configures the measurement circuit. Compared to DRM, the charging process is prolonged and a longer period between OLTC operations must be maintained because the current needs to be stable so that a high level of accuracy can be attained. The stability of the resistance reading can be used to determine when a pure DC situation has been reached. Each tap position should be measured while discharging between measurements on the same phase is unnecessary.

Discharging is identical to DRM: a resistor is switched in added to the circuit until the energy from the windings is dissipated.

The turn ratio is measured by applying a low AC voltage to the high-voltage windings of the transformer using the output stage. Again the measurement procedure of Figure 5.4 applies and all taps should be measured. A short measurement time is sufficient to obtain high accuracy and a discharge process is not needed when using AC voltages.

D.4 Hardware configuration

The hardware which is schematically depicted in Figure D.6 can be used to facilitate the diagnostic measurements described in the previous sections. The diagnostic system (Figure D.6B) forms the interface between the user (Figure D.6A) and the transformer under test (Figure D.6C). Inside the diagnostic system, the embedded control (Figure D.6.4) converts the demands of the user into control signals for the power source (Figure D.6.1) and the output stage (Figure D.6.2). The power source is needed to energise the windings during the off-line resistance and ratio measurements.

The main function of the output stage is to configure the measurement circuit by connecting the power source to the test object and to apply a secondary short circuit. Meanwhile, the embedded control converts the diagnostic parameters, as

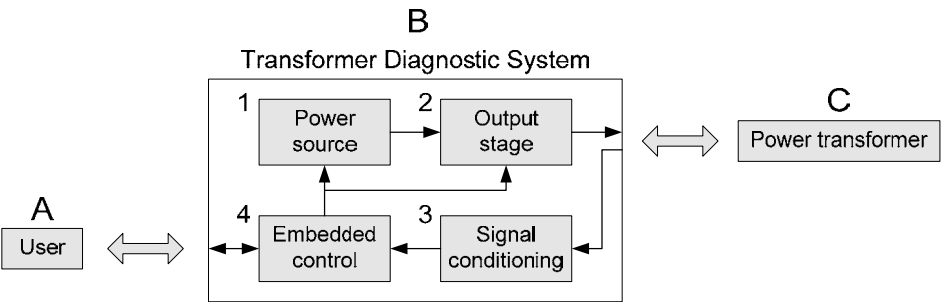
measured by the signal conditioning block (Figure D.6.3), in such a way that they can be displayed to the user (for example by scaling and filtering the signals). Its four basic building blocks are discussed in this section for each of the selected diagnostic measurements. Figure D.7 provides a more detailed schematic of the output stage, which forms the interface between the voltage sources and the power transformer. Its basic functions include configuration of the measurement circuit, discharging and current measurements. The specific demands for this block diagram are also discussed in this section.

D.4.1 Dynamic resistance of the OLTC

For each building block of Figure D.6.1-4, technical demands for performing DRM are set up and summarized in Table D.1.

Power source

As a power source (Table D.1.1), a controllable DC voltage source is necessary to supply a DC current. Due to the short circuit on the secondary windings, the current rises quickly and a low source voltage can be used (for example, a few volts are sufficient when measuring with currents ≤ 5 A). The diagnostic system used for the work of this thesis is designed to take resistance measurements up to 8 A and 30 V, ratio measurements are performed with 20 V at 0-300 mA magnetizing current.



1	Power source	Energize the test object
2	Output Stage	Configure the test circuit: - connect the power source to the test object - apply secondary short circuit
3	Signal conditioning	Scale measured signals
4	Embedded control	Converts user demands into control signals for the power source and the output stage Scale and filter measured signals for display to the user

Figure D.6 Simple block representation of the proposed transformer diagnostic system and the main function of the four building blocks.

Output stage

The main functions of the output stage (Table D.1.2) during DRM include configuration of the measurement circuit, discharging and overvoltage protection:

1. The output stage configures the measurement circuit using relays (Figure D.7D).
2. During the discharge process, the discharge resistor is added to the circuit by the output stage (Figure D.7B) to dissipate the energy stored in the transformer windings safely. During discharge, the voltage on the transformer bushings is dependent on the total measurement current and the value of the discharge resistor. This voltage can exceed the maximum range of DC power supply and the signal conditioning. The value of the discharge resistor should be selected based on this discharge voltage.
3. The output stage also offers overvoltage protection (Figure D.7E). An overvoltage is shunted to ground by overvoltage diodes or spark gaps, for example in the case of a current interruption, thereby reducing the stress on the signal conditioning block.

Table D.1 Hardware demands for DRM with the proposed transformer diagnostic system. Demands for the basic building blocks of Figure D.6 are listed and discussed in this section.

1	Power source	Stable DC source, controllable by embedded control for automatic accurate charging
2	Output Stage	Three current measurements
		Relays to connect power source to primary transformer connection
		Relays to short-circuit transformer secondary side
		Overvoltage protection
		Discharge resistor
3	Signal conditioning	Voltage measurement on primary transformer connection
4	Embedded control	Digital outputs for relay control of the output stage
		Analogue output for voltage source control
		Analogue inputs for voltage and current measurement
		OLTC control relay contacts
5	Transformer connection	Four-point measurement to measure the voltage separately from the injected current

Signal conditioning

The signal conditioning block (Table D.1.3) is responsible for the scaling of the measured signals, filtering and for the electrical insulation between the embedded control and the transformer.

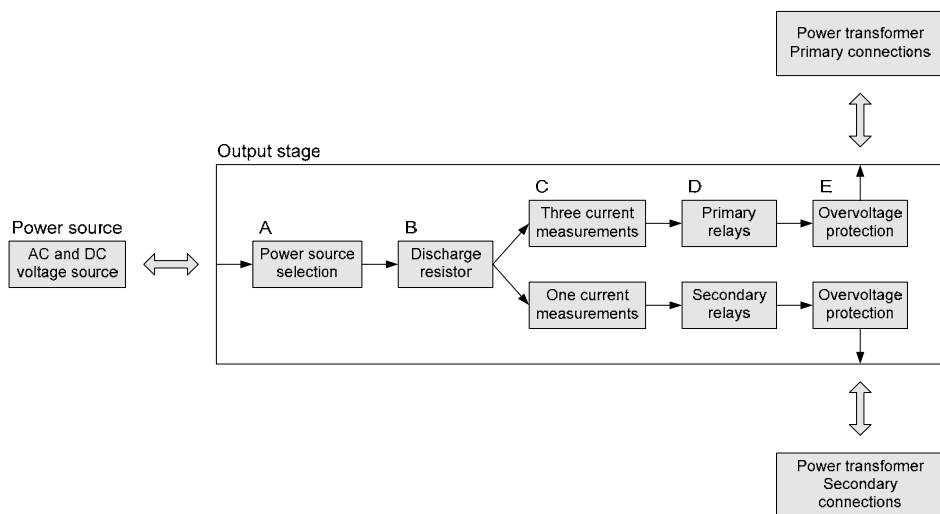


Figure D.7 Detailed schematic of the output stage, as shown in Figure C.6, for the proposed transformer diagnostic system.

A voltage and current measurement are needed to record the dynamic resistance. Three phase measurements can be supported when three current and voltage measurements are implemented. These DC currents, for example in the range of 0-10 A, can simply be measured by means of a current shunt (Figure D.7C). Voltage measurements, by means of voltage dividers, are needed on all terminals on the OLTC side of the transformer. The maximum range is determined by the maximum voltage of the DC voltage source or by the maximum current multiplied by the value of the circuit resistance, including the discharge resistor.

Embedded control

The embedded control (Table D.1.4) selects the voltages and currents that are used for the calculation based on the transformer vector group, the winding configuration and the tested phase. Analogue measurement channels are included to measure these signals at 1 kS/s (or higher when oversampling is desired). OLTC control is added to the proposed transformer diagnostic system, which gives an OLTC operation command in case the next tap can be measured. Relay contacts are included to bridge the OLTC control buttons in the OLTC drive control box. In this way, the results are easier to interpret because the OLTC is switched at regular intervals.

Transformer connection

Four-point measurement must be used according to international test standards to measure the voltage on the transformer terminals [102-103] (Table D.1.5).

D.4.2 OLTC drive system condition

The hardware configuration for the diagnosis of the mechanical condition consists of signal conditioning with filtering, amplitude adjustment and electrical insulation. Its hardware demands for the building blocks of Figure D.6 are discussed in this section and are summarized in Table D.2.

The proposed transformer diagnostic system is equipped with a multi-purpose connector which can be configured to support the diagnostic measurements described in Section 3.2.

Power source

As is standard, the transformer diagnostic system measures the active drive motor power, the remote end drive shaft rotation and the timing of a protective contact (see Section 5.2). Only an auxiliary power source is necessary (Table D.2.1). This low-voltage auxiliary power source is available for measurement of the contact voltage of de-energised protective contacts.

Output stage

Overvoltage protection of the output stage (Table D.2.2) should be designed to manage the incorrect connection of this auxiliary voltage.

Signal conditioning

Inside the signal conditioning block (Table D.2.3), active motor power is measured by recording the motor voltage (phase-to-neutral, see Section 5.4) and motor current (of one phase, see also Section 5.4). Motor current is measured using a standard current probe, and motor voltage by an electrical insulated voltage divider. The remote end drive shaft rotation is measured using a position sensor connected to a 0-10 V analogue input without specific hardware demands.

The timing of a protective contact is measured by recording the contact voltage, for example at an OLTC-in-operation contact.

Embedded control

The embedded control (Table D.2.4) has analogue measurement channels available to digitize the analogue signals from the signal conditioning block (at 1 kS/s or higher when oversampling is desired). Control signals are sent to the power source and output stage using digital outputs.

Transformer connection

An example of transformer connections (Table D.2.5) is depicted in Figure D.8. Clamps for the motor voltage and the excessive switch-time contact are connected to the drive mechanism and a current probe is used to measure the motor current (Figure D.8A). A rotation sensor for the drive shaft rotation is connected to the remote end of the drive shaft (Figure D.8B).

Table D.2 Hardware demands for diagnosis of the mechanical condition of the OLTC and OLTC drive using the proposed transformer diagnostic system. Demands for the basic building blocks of Figure D.6 are listed.

1	Power source	Auxilliary voltage source to measure protective contacts
2	Output Stage	Overvoltage protection
3	Signal conditioning	Insulated line voltage measurements of drive motor voltage and protective contacts Noise reduction on drive motor current and axis rotation signal
4	Embedded control	Digital output for relay control of auxilliary voltage Analogue inputs for signal measurement from signal conditioning
5	Transformer connection	Current probe to measure drive motor current 360° rotation sensor for axis rotation

D.4.3 Winding resistance and turn ratio

Table D.3 lists the hardware demands for the building blocks of Figure D.6 for the measurement of DC winding resistance, in addition to the demands for DRM. The same voltage and current are measured: differences include a higher accuracy and an extra current measurement of the DC current on the secondary side of the transformer.

The winding resistance is relatively low compared to the inductance; values of 0.1-2 Ω are typical for power transformers in the high-voltage distribution and transmission network. Compared to dynamic resistance measurements, DC

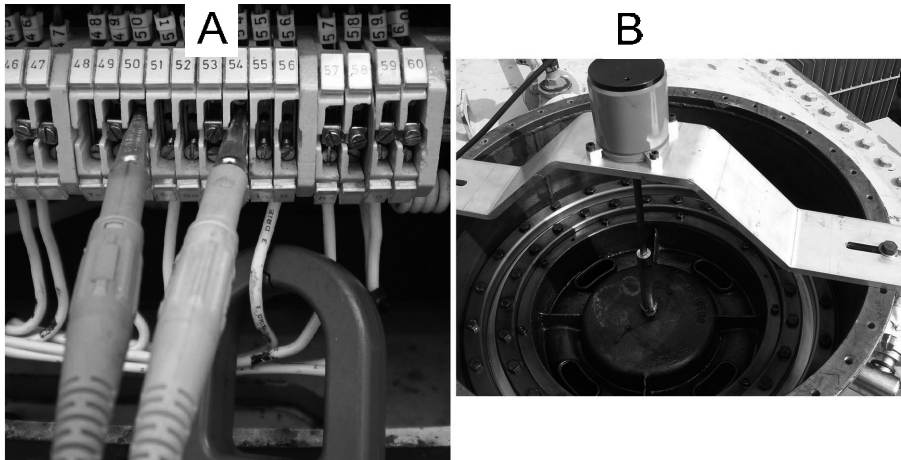


Figure D.8 Example of a connection for motor voltage and current measurement, using clamps and a clamp-on current probe (A), and an example of a rotation sensor connection on the remote end of a selector switch rotor (B).

winding resistance measurements can use a high output DC voltage to saturate the transformer core faster, thereby achieving a DC situation more quickly.

Power source

The transformer turn ratio can be measured by adding an AC voltage source. Using the same output stage as defined in Figure D.7, this low AC voltage is applied to the high-voltage windings of the power transformer. Voltage is measured on the primary and secondary transformer terminals and the voltage difference between two terminals is used for ratio calculation.

Typical power transformer ratios are in the range of 1:2 to 1:15. The proposed diagnostic system should be accurate in this range (a deviation in the turn ratio of maximum 0.5% is considered acceptable).

Table D.3 Hardware demands for winding resistance testing and transformer turn ratio measurements with the proposed transformer diagnostic system. Additional demands not found in Table D.1 are listed for the basic building blocks of Figure D.6.

1	Power source	low AC voltage, line frequency, 3 phase
2	Output Stage	1 more current measurement for secondary side
3	Signal conditioning	no additional demands
4	Embedded control	no additional demands
5	Transformer connection	no additional demands

Output stage

In the output stage, the primary excitation current is also measured. This current is in the range of milliamps and can be measured with the same hardware as is used for winding resistance measurements.

D.5 Data processing and analysis

Measurement data must be analyzed immediately after each measurement or when the stored measurement data is being opened. This section is dedicated to filtering, processing and selection of relevant measurement data by the proposed transformer diagnostic system, whereupon it is displayed to the user. Each of the diagnostic methods of the transformer diagnostic system faces different issues, which this section elaborates on.

D.5.1 Dynamic resistance of the OLTC

The measurement current during DRM has a typical time constant in the order of tens of milliseconds. Dynamic resistance results can therefore be processed and shown in 1ms resolution without losing information about the OLTC condition.

In order to generate the results displayed in Figure D.1-3, the recorded voltages and currents are filtered. In this way, undesired signals that are superimposed on the recorded voltages and currents can be removed. In addition to hardware noise filters, digital signal processing (e.g. low pass filters and sample averaging) and oversampling can be used to optimize the accuracy.

Figure D.9 gives two examples of the most common noises in the DRM signals. Firstly, spikes can be visible on the recorded signals (Figure D.9A, at 1100 ms), for example due to switching transients that are generated when operating the OLTC motor drive. These current spikes cannot flow through the transformer windings due to the slow time constant and must therefore be caused by noise. A spike filter can be applied to the recorded measurement current to remove these spikes.

Secondly, net frequency noise (Figure D.9B) can occur, especially when using unshielded measurement cables, which makes the determination of the OLTC transition time impossible and reduces the sensitivity of DRM to low-resistive defects. Digital net frequency filters can be applied to reduce this noise, but care should be taken, as excessive filtering can affect the determined OLTC transition times.

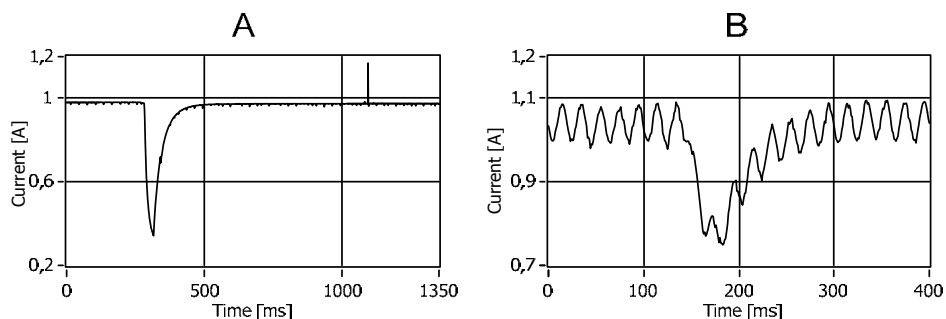


Figure D.9 Example of a DRM current with A) a spike on the recorded current at 1100 ms and B) net frequency noise during OLTC operation.

After filtering, the filtered signals can be used to calculate the impedance and to determine the moments of OLTC operation. Close-up views of the plots of the tap change operations are made (see Figure D.10A) to study defects in the arcing switch in more detail. A close-up period of 300 ms is sufficient, because OLTCs typically have operating times of ≤ 200 ms. Graphic presentation of tap position characteristics can give a clear indication of irregular taps. The proposed diagnostic system graphically presents:

- A median of the measurement current or impedance of each tap position and for each phase (Figure D.10B).
- The fluctuation of the measurement current or impedance (maximum minus minimum value) in each tap position and for each phase (Figure D.10C).

- c. OLTC transition times for each phase and for each tap transition (Figure D.10D), based on the moment the main contact of the arcing switch breaks and restores the contact.

Chapter 6 elaborated further on the analysis of DRM results.

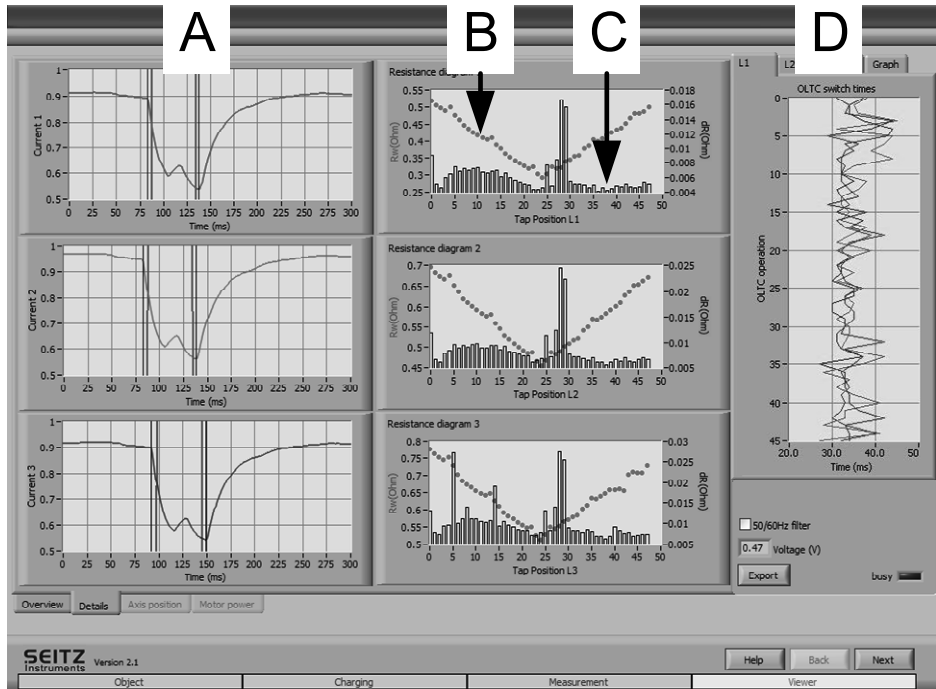


Figure D.10 Analysis of a DRM file results in close-up plots of the current or impedance during OLTC operation (A), plots of the median values (B) and fluctuation (C) of the current or impedance for each tap position and a transition time plot (D).

D.5.2 Winding resistance and turn ratio

For winding resistance measurements, the proposed transformer diagnostic system averages the measured current and voltage over multiple seconds to increase the accuracy of the measurement. These average values are used to calculate the resistance and should be stable before final resistance values can be determined.

In the case of a wye-connected transformer winding without a neutral point, the current can flow from one phase to another while measuring the voltage on the third phase. Values read from delta-connected transformer windings can be multiplied by 1.5 to obtain the one-phase winding resistance in the case of equal winding resistances, because the two other windings are measured in parallel. Values obtained from delta-connected windings with unequal winding resistance can be corrected using the formulae found in [104]. After this calculation and

correction, values for each phase and tap position are displayed, together with the accuracy that was reached by the diagnostic system.

Average values can also be used during turn ratio testing: the proposed transformer diagnostic system averages the measured primary and secondary voltages until the desired accuracy is reached. Ratio measurements on some transformer vector groups are also subject to correction factors to convert the measured ratio to the transformer turn ratio. A factor of $\sqrt{3}$ should be used when line-to-line values are compared with line-to-neutral values. For example, an Yyn0 transformer indicates the turn ratio directly while the measured turn ratio at an Ynd7 transformer needs a factor of $\sqrt{3}$ to obtain the line-to-line voltage ratio. In cases where there is no accessible neutral, a factor of $0.5*\sqrt{3}$ can be applied [105].

In addition to the turn ratio, information about the presence of winding and core defects is also obtained by the proposed diagnostic system through the measurement of:

- a. The primary excitation current
- b. The phase angle between the primary measurement voltage and secondary voltage
- c. The phase angle between the primary measurement voltage and primary current

Lists

List of abbreviations

AC	Alternating Current
ANSI	American National Standards Institute
DC	Direct Current
DETC	De-Energised Tap Changer
DGA	Dissolved Gas Analysis
DRM	Dynamic Resistance Measurement
HV	High Voltage
IEC	International Electrotechnical Commission
IEEE	Institute of Electrical and Electronics Engineers
KEMA	NV tot Keuring van Elektronische Materialen te Arnhem
LV	Low Voltage
OLTC	On-Load Tap Changer
RMS	Root Mean Square

List of gasses

C_2H_2	Acetylene
C_2H_4	Ethylene
C_2H_6	Ethane
C_3H_6	Propene
C_3H_8	Propane
CH_4	Methane
H_2	Hydrogen
T	Total amount of $CH_4 + C_2H_4 + C_2H_2$

List of units

°	Degree
°C	Degree Celsius
$\mu\Omega$	Micro Ohm
Ω	Ohm
A	Ampere
Å	Ångström
F	Farad

H	Henry
Hz	Hertz
kg	Kilogram
kS/s	Kilo samples per second
kV	Kilo Volt
m Ω	Milli Ohm
mA	Milli Ampere
MVA	Megavolt Ampere
N	Newton
s	Second
V	Volt
W	Watt

List of symbols

\angle	Angle
α	Apparent contact radius (meter)
β	Bulk contact resistivity factor
γ	Contact area correction factor
δ	Film thickness (Ångström)
δ_c	Critical film thickness (Ångström)
δ_m	Maximum film thickness (Ångström)
$\Delta E, \Delta V$	Electric potential difference (Volt)
ΔT	Temperature difference (degree Kelvin)
θ	Homologous temperature in relation to the melting point
θ_0	Contact surface temperature (degree Celsius)
$\lambda, \lambda_i, \lambda_j$	Surface resistivity of contact film (Ohm-square meter) at spot i and j
λ_{eff}	Effective thermal conductivity of contact film (Watt/Kelvin)
$\mu(D)$	Degree of truth
ρ	Specific electric resistivity (Ohm-meter)
τ, τ_1, τ_2	Time constant (Seconds)
τ_{i1}, τ_{i2}	Constants used to describe the effect of the current amplitude
Φ, φ	Phase angle (Degree)
φ_{eff}	Effective electrical resistivity of contact film (Ohm-meter)
A	Cross sectional contact area (square meter)
a	Contact radius (meter), amount of coke precursor (g/cm ³)
a_c	Critical contact spot radius (meter)
a_i, a_j	Contact spot radius of spot i of j (meter)
a_m	Initial maximum contact spot radius (meter)
An	Winding tap ($n = 1, 2, \dots$)
B	Temperature dependent diffusion parameter
$\cos \varphi$	Power factor
$\cos \varphi_N$	Power factor of phase N ($N = A..C$)
C, C_1, C_2	Constant
C_{DRM}	Correction factor for the contact resistance
C_{OLTC}	Correction factor for the contact resistance

CT	Stator contact of a change-over selector (connected to the coarse tap)
C_W	Coefficient of contact wear
D	Deviation in the DRM graph (% of expected value), distance (meter), diameter (meter), diffusion coefficient of contact film (m^2/s)
D_0	Frequency factor of contact film growth (m^2/s)
d_i	Current difference due to changes in circuit resistance (Ampere)
dI/dt	Derivative of the current (A/s)
d_{ij}	Distance between centres of contact spots i and j (meter)
dR	Dynamic resistance variation (Ohm)
E	Electric potential (Volt)
E_a	Activation energy of the coke deposition process (Joule per mol)
f	Frequency (Hertz)
$f(x)$	Contact spot radius distribution
I, I_0, I_n, i	Current (Ampere)
I_{exp}	Expected current in DRM plot (Ampere)
I_{high}	Trend line of the DRM current of a coarse tap with highest current (Ampere)
I_i	Injected current (Ampere), current through contact spot I (Ampere)
I_j	Current through contact spot j (Ampere)
I_L	Load current (Ampere)
I_{low}	Trend line of the DRM current of a coarse tap with lowest current (Ampere)
I_{min}	Minimum current in DRM within a tap position (Ampere)
I_N	RMS current of phase N ($N = A..C$) (Ampere)
$i_{N(t)}$	Current of phase N ($N = A..C$) as function of time (Ampere)
i_{offset}	Constant used to describe the effect of the current amplitude
I_{Phase}	RMS current in balanced operation (Ampere)
$i_{(t=x)}$	Current at time x (Ampere)
I_{test}	Test current (Ampere)
K	Coke deposition rate (cm/day)
k	Coupling factor, critical contact resistance increment
k_0, k_1, k_2, k_3	Coefficients
K_δ	Coefficient of approximation derived by [32]
k_{dyn1}, k_{dyn2}	Constant used to describe the effect of the current amplitude
L	Inductance (Henry), Lorenz constant (Volt ² /degree Kelvin ²)
L_1	Primary inductance (Henry)
L1	First transformer connection
L2	Second transformer connection
L3	Third transformer connection
M	Mid-position of the change-over selector contacts, stator contact of a change-over selector (connected to the main winding)
N, n	Transformer ratio, transformer neutral connection, number
$n, n(t)$	Number of contact spots, as a function of time
n_0	Initial number of contact spots

n_y	Number of OLTC operations per year
$P_{3\phi}$	Three-phase RMS power (Watt)
$P_{3\phi(t)}$	Three-phase instantaneous power (Watt)
ppm	Parts per million
R	Resistance (Ohm), gas constant (Joule per mol · Kelvin)
$R_{(t)}$	Resistance as a function of time (Ohm)
r	Effective contact radius (meter)
R_0	Initial contact resistance (Ohm)
R_1	Primary resistance (Ohm)
R_2	Secondary resistance (Ohm)
$R_{2.5}$	Contact resistance measured at 2.5 Ampere (Ohm)
$r_{(t)}$	Effective average contact radius as a function of time (meter)
R_a	Contact resistance of a circuit breaker (Ohm)
R_B	Bulk resistance (Ohm)
R_c	Contact resistance (Ohm)
$R_{c(t)}$	Contact resistance as a function of time (Ohm)
$R_{circuit}$	Circuit resistance (Ohm)
R_{clean}	Contact resistance of a clean metal-to-metal contact (Ohm)
R_{film}	Resistance of a thick film (Ohm)
R_i	Contact resistance measured at i Ampere (Ohm)
$R_{interaction}$	Contact resistance due to interaction between contact spots (Ohm)
R_M	Measured resistance (Ohm)
$R_{measure}$	Measurement resistance (Ohm)
$R_{ny=0}$	Contact resistance when the OLTC is not operated (Ohm)
R_p	Contact resistance of a circuit breaker (Ohm)
$R_{parallel}$	Contact resistance due to parallel contact spots (Ohm)
R_s	Resistance at reference temperature T_s (Ohm)
R_t	Transition resistance of the OLTC (Ohm)
R_{tunnel}	Tunnelling resistance of a thin film (Ohm)
R_{tw}	Resistance of a tapped winding (Ohm)
R_w	Winding resistance (Ohm)
S	Contact surface area (square meter)
s	Thickness of the contact film layer (Ångström)
T	Temperature (degree Kelvin)
T, t_1, t_n	Time, duration (Seconds)
T_b, T_B	Bulk temperature (degree Kelvin)
T_c	Super temperature increment over the bulk temperature (degree Kelvin)
T_{END-X}	End time, with $X = A..C$ (Seconds)
$T_{I<10\%}$	Time that the current is below 10% of its expected value (Seconds)
T_K	Winding material constant
t_l	Contact lifetime (Seconds)
T_m	Melting point of the contact material (degree Kelvin)
T_M	Temperature at which resistance was measured (degree Celsius)
t_m	Maximum contact lifetime (Seconds)
T_n	Time ($n = 1, 2, \dots$) (Seconds)

T_P	Time with two transition resistors in parallel (Seconds)
T_{R1}, T_{R2}	Time with one transition resistor in use (Seconds)
T_S	Reference temperature (degree Celsius)
T_{TR}	OLTC transition time (milliseconds)
U	Voltage (Volts), first transformer connection
U_L	Voltage over winding inductance (Volt)
U_R	Voltage over a resistor (Volt)
U_T	Voltage over transition resistor (Volt)
U_{test}	Test voltage (Volt)
V	Second transformer connection, voltage (Volt)
V_N	RMS line-to-neutral voltage of phase N ($N = A..C$) (Volt)
$v_{N(t)}$	Line-to-neutral voltage of phase N ($N = A..C$) as function of time (Volt)
V_{Phase}	RMS line-to-neutral voltage in balanced operation (Volt)
W	Third transformer connection
Wa	Stator contact of a change-over selector
$Wa0$	Stator contact of a change-over selector
X, X'	Length (meter)
X_n	Position ($n = 1,2,...$) (millimetre)
YNd	Transformer vector group: primary star with neutral, secondary delta
$Yyn0$	Transformer vector group: primary star, secondary star with neutral, zero phase shift
Z	Stator contact of a change-over selector
$Z1$	Stator contact of a change-over selector

List of publications

- [1] J.J. Erbrink, "Tap changer diagnostics on high voltage power transformers using dynamic resistance measurement", Graduate thesis Delft University of Technology, Delft, the Netherlands, 2007.
- [2] J.J. Erbrink, R.A. Jongen, E. Gulski, J.J. Smit, "Tap changer diagnostics on high voltage power transformers using dynamic resistance measurement", 4th IEEE young researchers symposium in electrical power engineering, Eindhoven, the Netherlands, p. 1-5, February 2008.
- [3] P.P. Seitz, B. Quak, J.J. Erbrink, E. Gulski, R. Leich, "Advanced on-site diagnosis of power transformers", International conference on condition monitoring and diagnosis, Beijing, China, paper 148, April 2008.
- [4] J.J. Erbrink, E. Gulski, J.J. Smit, P.P. Seitz, R. Leich, "Experimental model of aging mechanisms of on-load tap changer contacts", International conference on condition monitoring and diagnosis, Beijing, China, p. 247-250, April 2008.

- [5] J.J. Erbrink, E. Gulski, P.P. Seitz, R. Leich, "Advanced on-site diagnosis of transformer on-load tap changer", IEEE International Symposium on Electrical Insulation, Vancouver, Canada, p. 252-256, June 2008.
- [6] J.J. Erbrink, E. Gulski, J.J. Smit, R. Leich, "Experimental model for diagnosing on-load tap changer contact aging with dynamic resistance measurements", 20th International conference on electricity distribution, Prague, Czech Republic, paper 135, June 2009.
- [7] R. Zuijderduin, J.J. Erbrink, E. Gulski, J.J. Smit, R. Leich, "Condition assessment of power transformers OLTC by DGA and dynamic resistance measurements", Proceedings of the 16th international symposium on high voltage engineering, Johannesburg, South Africa, 2009.
- [8] J.J. Erbrink, E. Gulski, J.J. Smit, R. Leich, P.P. Seitz, B. Quak, "Effect of test parameters on dynamic resistance measurement results from on-load tap changers", IEEE International Symposium on Electrical Insulation, San Diego, USA, 6-9 June 2010.
- [9] J.J. Erbrink, E. Gulski, J.J. Smit, R. Leich, P.P. Seitz, B. Quak, "On-load tap changer diagnosis: interpretation of dynamic resistance deviations", IEEE International Symposium on Electrical Insulation, San Diego, USA, 6-9 June 2010.
- [10] J.J. Erbrink, E. Gulski, J.J. Smit, R. Leich, P.P. Seitz, B. Quak, "Reproducibility of dynamic resistance measurement results of on-load tap changers – effect of test parameters", International Conference on Condition Monitoring and Diagnosis, Tokyo, Japan, 6-11 September 2010.
- [11] J.J. Erbrink, E. Gulski, J.J. Smit, R. Leich, P.P. Seitz, B. Quak, "Interpretation of dynamic resistance results of on-load tap changers", International Conference on Condition Monitoring and Diagnosis, Tokyo, Japan, 6-11 September 2010.
- [12] J.J. Erbrink, E. Gulski, J.J. Smit, P.P. Seitz, B. Quak, R. Leich, R. Malewski, "On-load tap changer diagnosis – an off-line method for detecting degradation and defects: part 1", IEEE Electrical Insulation Magazine, Vol. 26, No. 5, p. 49-59, September - October 2010.
- [13] J.J. Erbrink, E. Gulski, J.J. Smit, P.P. Seitz, B. Quak, R. Leich, R. Malewski, "Diagnosis of onload tap changer contact degradation by dynamic resistance measurements", IEEE Transactions on Power Delivery, Vol. 25, No. 4, p. 2121-2131, October 2010.
- [14] J.J. Erbrink, E. Gulski, J.J. Smit, J. Aditya, L.A. Chmura, R. Leich, P.P. Seitz, B. Quak, "Test procedure and test circuit considerations for on load tap changer dynamic resistance measurement", International Conference on

- [15] J.J. Erbrink, E. Golski, J.J. Smit, L.A. Chmura, R. Leich, P.P. Seitz, B. Quak, "Condition assessment of on load tap changers using dynamic resistance measurements", International Conference on High Voltage Engineering and Application, New Orleans, USA, 11-14 October 2010.

Acknowledgements

Writing this PhD thesis and performing the accompanying research was not something I could have done alone; the book you have in your hand would not be there without you! Thank you!

If this is the first page you read (and perhaps the only page you plan to read) I would like to invite you to read some of the chapters and find out what was achieved with your help.

Firstly, I would very much like to thank Professor Johan Smit, my supervisor, for the opportunity to work in the Department of High Voltage Technology and Management, which is a wonderful and unique place to work!

Special thanks to my daily supervisor Edward Gulski for his enthusiasm and trust, constructive criticism and coaching during this project.

Thanks to my former colleagues at Seitz Instruments AG, I really enjoyed working with you all. I would like to thank Paul Seitz for giving me the opportunity to spend time writing my thesis and for his trust in dynamic resistance measurements as a diagnostic tool for tap changers. Ben, thank you also for critically thinking through the issues with me, for your valuable comments on my papers and for your assistance with LabView. Your ideas really inspired me.

I warmly thank the highly experienced people at Liandon for their hospitality and for giving me the opportunity to explore the on-site activities there. The practical aspects and on-site measurement experience were indispensable for this research. The work would never have been completed by simulations and laboratory studies alone. In particular, I would like to express my gratitude to Nico Sinnige, Ad van der Giessen, Jur Beemer, Piet van der Gulik, Martin Snel and Bob Koene for broadening my view of OLTC maintenance. Rory Leich, thank you for sharing your thoughts with me and Philip Salverda, thank you for sharing your experience!

In addition, I'm also very thankful to:

- Ryszard Malewski, thank you very much for your editorial support; your experience and opinion as an expert in transformer testing were crucial to me, my professor and my daily supervisor
- Roy Zuijderduin and Julian Aditya for your role in this research project as MSc students and for your assistance during on-site testing
- Frank Wester at TenneT, for allowing us to perform OLTC diagnosis in the TenneT grid

- Singapore Power Grid Ltd, for their hospitality and for their interest in dynamic resistance measurements
- Tim Noonan and Brendan Diggin from ESB International, as it was of valuable assistance to also perform measurements in Ireland
- Mr Wiesinger from Maschinenfabrik Reinhausen for his valuable comments and for sharing his extensive experience in servicing OLTCs
- Smit Transformers for offering me material to assist in the building of an OLTC experimental model

Thanks to René Orler and colleagues from Spital Schwyz for their excellent diagnostics and ‘repair’ after I enjoyed Switzerland a bit too much; I’m very happy that I was able to continue my PhD work again.

My fellow MSc students must also be mentioned here. I have had a wonderful time in Delft and would not have decided to stay there to work on this thesis otherwise. Therefore, I want to express my particular appreciation to Rookmeijer, Lisse, Putter, LH Groenewoud, triple thanks to Bertus, Friesland, Zuijderduin, Bleeker, Victor Charlie, Pernis and Rotterdam. Thanks not only for the great time, but also for your trust in my capabilities as a PhD researcher, even before I decided to start my PhD research.

At the University of Delft, I want to thank Paul van Nes, Bertus Naagen and Wim Termorshuizen for their support, patience and ideas during my experiments in the High Voltage Laboratory, and Aad van der Graaff for his extremely accurate mechanical engineering. And of course I want to thank my fellow PhD students with whom I worked day in, day out. Rick vKessel, mijn complimenten and my sincere thanks for your inspiring advice.

Als laatste, maar zeker niet het minste, wil ik graag mijn hartelijke dank uiten aan mijn familie en vrienden: jullie voortdurende interesse in mijn voortgang, het luisterend oor dat jullie me boden of gewoon de gezellige afleiding buiten werktijd! Anneke, jij liet me de drukte op mijn werk direct vergeten zodra we bij elkaar waren, ontzettend bedankt daarvoor! Dank je voor de tijd die je me gaf om rustig aan dit proefschrift te werken en voor je geduld tot ik eindelijk dit boekje afgerond had.

Last, but certainly not least, it’s my pleasure to express my thankfulness to my family and friends: your continued interest in my progress, the hours that you spent listening or the entertaining distractions you supplied at the end of a hard day’s work! Anneke, you enabled me to forget the pressure at work as soon as we were together, and I am immensely grateful! Thanks for giving me the time to focus on my dissertation and for your patience until the end product was finally complete.

Jur Erbrink

Samenvatting

Regelschakelaardiagnose aan hoogspannings vermogenstransformatoren gebruikmakend van dynamische weerstandsmetingen

Het is een moderne tendens om toestandsafhankelijk onderhoud in plaats van periodiek onderhoud uit te voeren. Op deze manier proberen nutsbedrijven onderhoudskosten te reduceren, de levensduur van materieel te verlengen en mogelijk catastrofale storingen te voorkomen. Toestandsafhankelijk regelschakelaaronderhoud benodigd diagnostische metingen om de conditie van de regelschakelaar (on-load tap changer, OLTC) te bepalen, om daarmee vast te stellen wanneer en welk onderhoud nodig is. Daarnaast kunnen diagnostische metingen gebruikt worden voor het detecteren van defecten die niet tijdens onderhoud gezien zijn voordat ze een storing veroorzaken en om de conditie te beoordelen van onderdelen die niet gemakkelijk voor visuele inspectie toegankelijk zijn. Ondanks dat er veel verouderde regelschakelaars in bedrijf zijn en ondanks dat de literatuur laat zien dat het verantwoordelijk is voor een groot deel van de transformatorstoringen, is het ongebruikelijk om na onderhoud de conditie te bepalen alvorens de transformator weer in bedrijf te nemen. Onderhoudsfouten, contactdegradatie en mechanische defecten kunnen dus onopgemerkt blijven.

Dit proefschrift weidt uit over de conditiebepaling van elektrische contacten in regelschakelaars met schakelweerstand gebruikmakende van dynamische weerstandsmetingen (DRM). Van oorsprong is het toegepast op vermogensschakelaars maar het is ook geschikt om de weerstand te meten terwijl de regelschakelaar schakelt. Dit proefschrift beschrijft hoe DRM uitgevoerd kan worden en hoe de resultaten geïnterpreteerd kunnen worden.

Volgend op de introductie geeft Hoofdstuk 2 een overzicht van OLTC technologie, veroudering en storing. Verschillende modellen voor contactweerstand uit de literatuur worden besproken en de toepasbaarheid op DRM is toegelicht. Vervolgens worden in Hoofdstuk 3 de mogelijke methoden besproken die beschikbaar zijn om de technische conditie van regelschakelaars te diagnosticeren. Het verband tussen gas-in-olie analyse (DGA) en contactweerstand is verder onderzocht om te kijken of beide methoden overlappen. Een statistische analyse is uitgevoerd op DGA en DRM resultaten van een onderzoekspopulatie transformatoren maar er was geen relatie gevonden tussen de geselecteerde gegevensverzamelingen.

Hoofdstuk 4 laat zien dat conditiebepaling op verschillende typen regelschakelaars toegepast kan worden en dat DRM een grote variatie aan defecten

en verouderingsmechanismen kan detecteren door gebruik te maken van een lage meetstroom. Extra informatie over de conditie van de regelschakelaar is verkregen ten opzichte van statische weerstandsmetingen en belangrijke informatie over de ernst en locatie van verschillende verouderingsmechanismen kan uit de resultaten gehaald worden. Dynamische weerstandsmetingen worden in detail besproken, waaronder het effect van de meetstroom en circuitweerstand.

Omdat elke diagnostische methode gevoelig is voor bepaalde defecten is er een set methoden geselecteerd en geïmplementeerd (Hoofdstuk 5) met een diagnostisch meetsysteem als resultaat. De bouwstenen van een dergelijk diagnostisch systeem zijn besproken en hardware-eisen voor elk deel vastgesteld. Het hoofdstuk bespreekt welke resultaten na een meting duidelijk zullen worden gepresenteerd zodat de transformator in bedrijf genomen kan worden zonder het risico van een storing.

De verouderingsmechanismen die door DRM ontdekt kunnen worden zijn geordend in Hoofdstuk 6. De verschillende onderzochte verouderingsmechanismen zijn: filmvorming op het contactoppervlakte, koolvorming op plaatsen met hoge temperatuur veroorzaakt door de belastingstroom, putvorming en contacterosie door vlambogen. DRM resultaten van ongeveer 450 regelschakelaars zijn gedurende dit project onderzocht en meetdata van een aantal van deze regelschakelaars was vergeleken met bevindingen van visuele inspecties. Een substantieel deel binnen deze onderzoekspopulatie blijkt gedegradeerde contacten te hebben. Hoofdstuk 6 bewijst dat DRM een effectief hulpmiddel is om de technische conditie van regelschakelaars te toetsen, het blijkt hoogst gevoelig voor de dominante defecten, in het bijzonder voor contactveroudering door het lange termijn verouderingseffect in de grofkiezer, omschakelaar of voorkiezer, en voor defecten die conflicteren met de hoofdtaak van de regelschakelaar (schakelen tussen aftakkingen zonder de laststroom te onderbreken). Typische DRM grafieken die deze gevarieerde defecten onthullen zijn gepresenteerd met uitleg over hoe deze defecten kunnen worden herkend in verschillende soorten regelschakelaars, in het bijzonder in delen van de transformator die tijdens regelmatig onderhoud niet toegankelijk zijn voor visuele inspectie omdat ze zijn ingesloten in de transformatorbak.

Laboratoriumexperimenten (Hoofdstuk 7) en verschillende testcases zijn vervolgens gebruikt om te verifiëren voor welke verouderingsmechanismen DRM gevoelig is. Naast DRM met 1 A zijn ook andere meetstroom niveaus gebruikt tijdens experimenten (bijlage B). Het effect van kunstmatig verouderde contacten op de meetresultaten was bestudeerd met een testmodel. Het onderzoek laat zien dat filmvorming op het contactoppervlakte meetbaar is; de contactweerstand bleek significant toe te nemen als de contacten over een oppervlaktefilm bewegen, wat ernstigere contactdegradatie kan verbergen. Slijtage van de afbrandcontacten beïnvloedt de timing van contacten en verandert daardoor de vorm en amplitude van de weerstand grafieken. Stroomonderbrekingen kunnen in de grafieken verschijnen wanneer buitensporig versleten contacten gemeten worden.

Dit proefschrift demonstreert ook hoe DRM resultaten gerepresenteerd kunnen worden door conditie-indices gebruikmakende van een interpretatiediagram die ze categoriseert door toepassing van grenswaarden (Hoofdstuk 8). Complexe diagnostische informatie is omgezet in simpele conditie-indices. Dit proces is afhankelijk van het gemeten type regelschakelaar.

Afwijkingen kunnen worden toegewezen aan de lastschakelaar, de voorkiezer, grofkiezer of omschakelaar, en de aandrijving. Kwantiteiten waren afgeleid uit DRM resultaten die gebruikt kunnen worden om de meeste gebruikelijke defecten te ontdekken. In principe kunnen zes situaties ongescheiden worden: contacten in goede conditie, contacten met een verhoogde contactweerstand, regelschakelaars met open contacten, schakeltijd afwijkingen, versleten contacten of fase synchronisatieproblemen. Een voorbeeld van een interpretatiediagram voor beslissingsondersteuning was ontwikkeld en geverifieerd voor praktische toepassing op een grote populatie van regelschakelaars. De afwijking van de DRM stroom ten opzichte van de verwachte waarde was gebruikt en limieten waren vastgesteld voor het maken van beslissingen. De technische conditie kan hierdoor vastgesteld worden, wat het mogelijk maakt een selectie te maken van kritische regelschakelaars die voordeel hebben van storingreducerende maatregelen.

Curriculum Vitae

Jur J. Erbrink was born in Arnhem, the Netherlands, on July 20, 1982. He studied electrical engineering at the HAN University of Applied Sciences in Arnhem from 2000 to 2004. In 2007 he was awarded an MSc in electrical power engineering from the Delft University of Technology, Delft, the Netherlands. He continued to work as a researcher at TU Delft and from 2008-2009 worked as a product specialist at Seitz Instruments AG, Niederrohrdorf, Switzerland. In 2007 he also began working on his PhD thesis at the Delft University of Technology in the Department of High Voltage Technology and Management, focusing on tap changer diagnosis with dynamic resistance measurements, leading to this thesis.



Switching the OLTC during a dynamic resistance measurement